

**SSC -249**

**SHIP VIBRATION PREDICTION METHODS  
AND EVALUATION OF INFLUENCE  
OF HULL STIFFNESS VARIATION  
ON VIBRATORY RESPONSE**

**This document has been approved for  
public release and sale; its  
distribution is unlimited.**

**SHIP STRUCTURE COMMITTEE**

**1975**

# SHIP STRUCTURE COMMITTEE

AN INTERAGENCY ADVISORY  
COMMITTEE DEDICATED TO IMPROVING  
THE STRUCTURE OF SHIPS

## MEMBER AGENCIES:

United States Coast Guard  
Naval Sea Systems Command  
Military Sealift Command  
Maritime Administration  
American Bureau of Shipping

## ADDRESS CORRESPONDENCE TO:

Secretary  
Ship Structure Committee  
U.S. Coast Guard Headquarters  
Washington, D.C. 20590

SR-214

6 MAR 1975

With the increasingly powerful propulsion plants in modern ships frequently exciting the first and possibly second modes of vibration of the ship's hull, and today's larger ships being built with lighter scantlings, new loading criteria are needed to overcome arbitrary limits imposed on the ship's length to draft ratio. The Ship Structure Committee has initiated and completed a project to review the literature in detail and suggest what must be done to alleviate the limits imposed in order to make full use of higher strength steels and other emerging materials.

The attached report presents the results of the analysis and also recommends additional areas of research.

Comments on this report and suggestions for additional research topics or problem areas will be most welcome.



W. M. BENKERT  
Rear Admiral, U. S. Coast Guard  
Chairman, Ship Structure Committee

SSC-249

FINAL REPORT

on

Project SR-214, "Hull Flexibility Criteria Study"

SHIP VIBRATION PREDICTION METHODS AND EVALUATION OF INFLUENCE  
OF HULL STIFFNESS VARIATION ON VIBRATORY RESPONSE

by

R. G. Kline  
U. S. Steel Corporation

and

J. C. Daidola  
M. Rosenblatt & Son, Inc.

under

Department of the Navy  
Naval Ship Engineering Center  
Contract No. N00024-73-C-5206

*This document has been approved for public release and sale;  
its distribution is unlimited.*

U. S. Coast Guard Headquarters  
Washington, D.C.  
1974

## ABSTRACT

Research is conducted to obtain a greater understanding of induced hull vibrations and, more specifically, to define the role of hull stiffness in such phenomena.

Available methods for the prediction of vibratory response to propeller, slam and wave excitations are evaluated. The methods embrace the formulation and solutions of the equations of vibratory motions, computer programs for the dynamic problem, and the computations of the excitation forces and the structural and hydrodynamic characteristics of the ship. The work scope is limited essentially to the vertical vibration of the main hull.

Parametric analyses are presented which include the calculations of the propeller, slam- and wave-induced vibrations of three ships with their hull stiffness varying from 40 percent below to 40 percent above the as-built stiffness. The three ships are a 249,300 DWT tank ship, the Great Lakes ore carrier "STR. EDWARD L. RYERSON" and the 544 ft. general cargo ship "S. S. MICHIGAN." Design trends are developed with respect to characteristics that influence ship stiffness and vibratory response.

Propeller-induced main hull vibrations for all three ships do not appear to be effected by variations in hull stiffness. Slam-induced vibrations seem to increase and decrease as stiffness increases and decreases. The tank ship and the Great Lakes ore carrier appear to be prone to wave-induced vibration, and increased hull stiffness has a beneficial effect on limiting the response.

Further research is required which would lead to engineering methods for the estimation of propeller excitation forces and slam loads which can be used to predict vibration during the design stages.

Literature on wave-induced vibration is limited and the subject deserves significant research effort. Both vertical and lateral vibration must be covered. Particular attention should be paid to the effects of forebody and afterbody shapes and damping.

An evaluation is required of the existing methods for the estimation of added mass and damping to assess their validity over the complete range of frequency.

## CONTENTS

	<u>Page</u>
1. INTRODUCTION	1-1
1.1 Background and Objectives	1-1
1.2 Work Scope	1-2
2. LITERATURE SURVEY AND DESCRIPTION OF METHODS	2-1
2.1 General	2-1
2.2 Mathematical Methods	2-1
2.3 Computer Programs for Dynamic Structural Analysis	2-7
2.4 Calculation of Input Data	2-8
2.5 Empirical Methods	2-19
2.6 Design Criteria	2-20
3. SELECTION OF ANALYTICAL METHOD	3-1
3.1 Selected Method of Analysis	3-1
3.2 Modifications and Additions	3-8
4. PARAMETRIC ANALYSES	4-1
4.1 General	4-1
4.2 Input Data for Parametric Analyses	4-5
4.3 Results of the Parametric Analyses	4-15
5. DISCUSSION OF RESULTS AND TRENDS	5-1
5.1 General	5-1
5.2 Propeller-Excited Vibration	5-1
5.3 Slam-Excited Vibration	5-8
5.4 Wave-Excited Vibration	5-9
5.5 Design Trends	5-13
6. CONCLUSIONS	6-1
7. RECOMMENDATIONS	7-1
8. REFERENCES	8-1
9. APPENDICES	
A. Parametric Analyses Input Data	A-1 - A-16
B. Parametric Analyses Results	B-1 - B-65
C. Trends	C-1 - C-18

## List of Figures

<u>Figure</u>		<u>Page</u>
3-1	Complete Ship Idealization	3-2
4-1	Tank Ship	4-2
4-2	Great Lakes Ore Carrier STR. EDWARD L. RYERSON	4-3
4-3	General Cargo Ship S. S. MICHIGAN	4-4
5-1	ISO Guide for Evaluating Human Exposure to Whole-Body Vertical Vibration (Acceleration)	5-2
5-2	ISO Guide for Evaluating Human Exposure to Whole-Body Vertical Vibration (Velocity)	5-2
5-3	ISO Guide for Evaluating Human Exposure to Whole-Body Vertical Vibration (Displacement)	5-3

### Appendices

A-1 through A-8	Added Mass and $\bar{A}$
B-1 through B-51	Propeller Computer Output
B-52 through B-69	Slam Response
B-70 through B-105	Slam Computer Output
B-106 through B-116	Wave-Excited Response
C-1 through C-14	Tanker Trends
C-15 through C-34	Containership Trends
C-35 through C-46	Great Lakes Ore Carrier Trends

## List of Tables

<u>Table</u>		<u>Page</u>
4-I	Ship Models	4-6
4-II	Summary of Parametric Analyses Variations	4-7 and 4-8
 <u>Appendices</u>		
A-I through A-III	Properties of Main Hull and Double Bottom	A-2 - A-4
A-IV through A-VI	Data for Propulsion System and Superstructure	A-5 - A-7
A-VII through A-XI	ABAR	A-8 - A-12
B-0	Conversion Table for Metric Units	B-1
B-I through B-X	Peak Propeller Response	B-2 - B-6
B-XI	Cumulative Damage	B-7
B-XII	Special Studies	B-7

## SHIP STRUCTURE COMMITTEE

The SHIP STRUCTURE COMMITTEE is constituted to prosecute a research program to improve the hull structures of ships by an extension of knowledge pertaining to design, materials and methods of fabrication.

RADM W. M. Benkert, USCG  
Chief, Office of Merchant Marine Safety  
U.S. Coast Guard Headquarters

CAPT J. E. Rasmussen, USN  
Head, Ship Systems Engineering  
and Design Department  
Naval Ship Engineering Center  
Naval Ship Systems Command

Mr. M. Pitkin  
Asst. Administrator for  
Commercial Development  
Maritime Administration

Mr. K. Morland  
Vice President  
American Bureau of Shipping

CAPT L. L. Jackson, USN  
Maintenance and Repair Officer  
Military Sealift Command

## SHIP STRUCTURE SUBCOMMITTEE

The SHIP STRUCTURE SUBCOMMITTEE acts for the Ship Structure Committee on technical matters by providing technical coordination for the determination of goals and objectives of the program, and by evaluating and interpreting the results in terms of ship structural design, construction and operation.

### NAVAL SHIP SYSTEMS COMMAND

Mr. P. M. Palermo - Member  
Mr. J. B. O'Brien - Contract Administrator  
Mr. G. Sorkin - Member

### U.S. COAST GUARD

LCDR E. A. Chazal - Secretary  
CAPT D. J. Linde - Member  
LCDR D. L. Folsom - Member  
CDR W. M. Devlin - Member

### MARITIME ADMINISTRATION

Mr. J. Nachtsheim - Chairman  
Mr. F. Dashnaw - Member  
Mr. F. Seibold - Member  
Mr. R. K. Kiss - Member

### MILITARY SEALIFT COMMAND

Mr. T. W. Chapman - Member  
Mr. A. B. Stavovy - Member  
Mr. J. G. Tuttle - Member

### NATIONAL ACADEMY OF SCIENCES SHIP RESEARCH COMMITTEE

Mr. R. W. Rumke - Liaison  
Prof. J. E. Goldberg - Liaison

### AMERICAN BUREAU OF SHIPPING

Mr. S. G. Stiansen - Member  
Mr. I. L. Stern - Member

### SOCIETY OF NAVAL ARCHITECTS & MARINE ENGINEERS

Mr. A. B. Stavovy - Liaison

### WELDING RESEARCH COUNCIL

Mr. K. H. Koopman - Liaison

### INTERNATIONAL SHIP STRUCTURES CONGRESS

Prof. J. H. Evans - Liaison

### U.S. COAST GUARD ACADEMY

CAPT C. R. Thompson - Liaison

### U.S. MERCHANT MARINE ACADEMY

CAPT W. M. Maclean - Liaison

### U.S. NAVAL ACADEMY

Dr. R. Bhattacharyya - Liaison

## 1. INTRODUCTION

### 1.1 Background and Objectives

The structure of a ship hull is most complex and must absorb a variety of static and dynamic loads. Further, much uncertainty prevails with respect to the nature (location, frequency of occurrence, periodicity, magnitude) of these loads. Under these conditions, it has been natural for designers of ship structure to rely heavily on semi-empirical methods rooted in past experience. This approach has been possible because the evolution of ships (including types, size, proportion, materials, power machinery) has been gradual, requiring extrapolation from the data base in small steps only.

However, within the last decade, these methods are beginning to prove inadequate due to the relatively sudden demand for much larger, faster and different types of ships. The lack of past design data and experience with these ships has made it necessary to develop and refine analytical design procedures. The new trends in ships are, of course, a result of the changes in the economics of marine transportation, the emergence of new types of cargo (containers, LPG, LNG, etc.) and the availability of high-powered machinery, and a wider variety of structural materials. In addition to the changes in size, form, speed and type, we must add the trends to lighter scantlings brought about by improved coatings, high-strength steels, better knowledge of loads, etc.

These trends have resulted in structural and hydrodynamic characteristics of the ships that are beyond the range of past experience. This in turn has resulted in unexpected changes in their response to both static and dynamic loads (waves, slamming, propulsion-system machinery). As can be surmised, all this has brought about new problems, or more correctly, problems that were not so important in the past have now become more important. The implications to the designer are that he must have a much greater understanding of the phenomena that determine both the dynamic loadings and the structural response of the ship.

The various aspects of the changing trends have directly or indirectly influenced the basic stiffness of the ship's main hull - the knowledge of which is vital to so many considerations in ship design such as hull deflection, stress, metal fatigue, human comfort, and loads applied to nonstructural components such as piping and joiner bulkheads. A most important consequence of the trends in hull stiffness is the change of the vibratory response of the primary structure. This applies to Great Lakes ore carriers, to tank ships as well as container ships and other vessels.

These prevailing trends in ship designs have provided the background to the Ship Structure Committee's Project SR 214, "Hull Flexibility Criteria Study" reported here. Its main objectives were to evaluate the currently available methods for predicting ship vibrations and to conduct research to obtain a greater understanding of induced hull vibrations and, more specifically, to define the role of hull stiffness in such phenomena. The induced vibrations referred to are the result of the following types of excitation:

1. The steady excitation by propulsion system machinery
2. The transient excitation of the hull by slam loads
3. The random excitation of the hull by waves

The problem of ship hull and propulsion-system vibration has been the subject of extensive research since the latter part of the 19th century. As ship propulsion plant size and power have grown over the years, the hull vibration induced by the propulsion system has also increased and the problems associated with this excitation source have become more pronounced. In addition, the higher propulsive powers have enabled ships to maintain moderate speeds in adverse weather, thus encountering a higher incidence of slamming and slamming damage.

Another factor that has influenced the dynamic behavior of ship structures is the trend to larger and longer ships. In general, the trend to larger ships has resulted in a lowering of the natural frequencies of vibration of the ship, sometimes bringing the fundamental frequency of vertical vibration into the range of wave-encounter frequency for waves with significant energy, and thus subjecting the ship to an additional source of dynamic excitation. This situation, too, is aggravated by additional ship speed since a higher ship speed will allow resonant-encounter frequencies to occur with longer and larger waves, which possess greater potential for dynamic excitation.

## 1.2 Work Scope

Ship vibration may involve only local structure or the main hull girder. Local vibration may be excited by the main-hull-girder vibration, and the presence of local vibration can alter the vibratory response of the main hull girder. The main hull can experience vertical, transverse and torsional vibrations.

Rotating machinery and marine shafting systems are subject to torsional, lateral (whirling) and longitudinal vibration. These vibrations can be excited by the engine, propeller, or main hull vibration.

The investigation of all types of vibration for both the main hull girder and the propulsion system is a monumental task, greater than intended herein. In addition, the modeling techniques and calculations for the exciting forces and coefficients in the equations of motion are similar for both the propulsion system and main-hull-girder analyses. Therefore, the discussions to follow will be limited to main hull vibration only. However, most propulsion system analyses procedures can be assumed similar.

Although the main hull may experience vertical, transverse and torsional vibrations, only the vertical vibrations will be considered here. This has been done for several reasons. First, it was necessary to put some limits on the scope of the work. Second, the procedures for vibratory analysis are similar enough in all cases so that parallel conclusions frequently can be drawn. Third, the torsional and horizontal vibrations, which are coupled in reality, have not lent themselves very well to empirical or analytical investigation. Finally, the vertical vibration is generally of greater interest and most theoretical development has been done in this area. Local structure will only be analyzed where it is felt that its contribution to main-hull-girder vibrations may be significant.

The ultimate practical value of investigations such as those described herein is in the influence that may be exerted on the design rules and procedures currently in existence. For the most part, these current rules and procedures pertain to the longitudinal strength and stiffness of the hull in vertical bending. Thus, the emphasis has been placed on the vertical bending stiffness of the ship's main hull in this study.

The initial task of the project was to perform a literature survey and the evaluation of the available analytical methods for the calculation of propeller-, slam- and wave-induced vibrations of the main hull girder. In addition to the structural analysis methods, of course, this includes the methods for the estimation of the excitation, ship's hydrodynamic and structural properties. Evaluation required looking into several aspects of the methods, such as applicability of the physical principles utilized, assumptions, simplifications, computational effort required and the degree to which the predictive capabilities were verified.

The next task was to select a method for performing parametric analysis of three ship types; namely, a tank ship, Great Lakes ore carrier and a general cargo ship. The analysis consisted of calculating the vibratory responses for three ships whose hull bending stiffness was varied from 60 to 140 percent of the as-built bending stiffness. The shear stiffness was varied from 77 to 118 percent in conjunction with the above bending stiffness variations.

Concurrent with the parametric analysis, a study was conducted to determine ship design trends with respect to characteristics that influence ship-main-hull-girder stiffness and vibratory response. These characteristics include dimensional proportions, scantlings, hull-girder-section properties, speed and power.

The results of the parametric analysis have been examined to determine the influence of the variation of the main-hull-girder stiffness on vibratory response. Further, interpretations have been attempted to shed light on how the design trends are influencing vibratory response.

A special effort was made to generate a comprehensive bibliography which has been submitted to the Ship Structure Committee under a separate cover, and which will be published as SSC-250.

## 2. LITERATURE SURVEY AND DESCRIPTION OF METHODS

### 2.1 General

The prediction and analysis of the vibratory response of a ship's main hull girder to various excitation sources involves technical inputs from many disciplines. The study of the problem requires knowledge of structural modeling, sources and types of damping, propulsion system and seaway-induced loads, and criteria for acceptable levels of vibration based on structural behavior, machinery performance, and human tolerance of noise and vibratory motions.

A mathematical analysis of the problem requires that an idealization of the physical system must be synthesized, the equations of motion written, the inputs to the equations of motion developed, and the equations of motion solved. A large portion of this work is of a general nature and has been developed and refined in many separate technical disciplines. In addition, development work in ship vibrations has been underway for many years. Thus, the amount of development work accomplished in these areas over the years has been voluminous and the task of conducting a complete survey is a formidable one.

Thus, the literature survey has yielded an extensive list of references on this subject and, because of the large number of references available, only the most pertinent have been reviewed.

The information derived from the literature survey has been broken down into several categories. First, vibration-analysis techniques will be summarized with regard to the formulation of the equations of motion and their solution. Secondly, the computer programs that are currently being used in solving the dynamic problem will be summarized. Thirdly, the methods used in determining the computer inputs will be described. Fourthly, empirical methods and fifthly, existing design criteria concerning vibrations will be discussed.

### 2.2 Mathematical Methods

#### 2.2.1 Equations of Motion

The basis for most analytical solutions to the equations of motion of ship vibrations is the vibrating uniform beam. To obtain the equations of motion of a uniform beam, the procedure used is to isolate an elemental length of the beam and

indicate the externally applied forces, the inertia forces, and the internal elastic forces. Then by summing the vertical forces and moments about the element center of gravity the following equation may be derived<sup>1,2)</sup>\* for free vibration of a uniform beam:

$$m \frac{\partial^2 v}{\partial t^2} - \left( \frac{EI_m}{KAG} + I_r \right) \frac{\partial^4 v}{\partial t^2 \partial x^2} + \frac{I_r m}{KAG} \frac{\partial^4 v}{\partial t^4} + EI \frac{\partial^4 v}{\partial x^4} = 0 \quad (2-1)$$

where:

- m = Mass of beam element.
- I = Moment of inertia of beam element.
- $I_r$  = Rotatory inertia of beam element.
- KA = Shear area of beam element.
- x = Distance along longitudinal axis of beam.
- v = Beam deflection (composed of both bending and shear deformation).
- E = Young's modulus.
- G = Shear modulus.

It should be noted that the effects of damping are small and have been neglected in equation (2-1).

If the rotation of the beam element and the deflection due to shear are neglected then all terms involving rotatory inertia and shear vanish and the well known Euler equation (2-2) for the free vibration of long slender beams results.

$$m \frac{\partial^2 v}{\partial t^2} + EI \frac{\partial^4 v}{\partial x^4} = 0 \quad (2-2)$$

In general, equation (2-1) is solved by first assuming the bar to be uniform, ignoring shear deformations and the rotatory inertia terms, and solving the homogeneous problem. With the appropriate boundary and initial conditions, the solution yields an infinite number of frequencies and a corresponding number of orthogonal mode shapes.

---

\* See references which are given in the Reference Section at the end of the report.

Alternatively, the equations of motion may be expressed in terms of an integral equation. Making use of the influence-function concept, the deflection and slope of the beam are expressed as integrals of the distributed force and moment on the beam times the appropriate force-deflection, force-slope, moment-deflection, or moment-slope influence function. Each influence function is derived on the basis of the boundary conditions on the beam. Again, the integral equations are readily solved only after making simplifying assumptions with regard to rotatory inertia and shear distortion effects, and their solution results in an infinite number of the same natural frequencies and orthogonal mode shapes as does the solution of the differential equations of motion.

Bisplinghoff, et.al.<sup>3)</sup> provide an excellent summary of the derivation and solution of both the differential equations of motion and the integral equations of motion of restrained and unrestrained beams.

Another procedure for arriving at the equations of motion of a dynamically loaded beam is through the use of energy methods<sup>3)</sup>. The principle of virtual work can be employed to develop the equations of motion simply by including the virtual work done by the inertia forces with that done by the externally applied forces on the structure. A specialized form of this method results in what is termed Lagrange's equation. Lagrange's equation is applicable to structural systems in which the deformed shape of the structure can be described by a system of generalized coordinates and where the generalized coordinates are a function of time.

The beam differs from the ship in two important respects. One is that significant internal damping may exist in the ship. The other relates to the fact that the normal and shear stress distributions for a ship can differ significantly from those in the beam.<sup>4)</sup>

Much information and insight into the ship hull vibration problem has been obtained from the study of uniform and nonuniform beam vibration characteristics. However, it has become increasingly apparent that the study of propeller-induced hull vibration requires more accurate and complete information on the higher order frequencies and mode shapes than can be obtained from a study of beam-like vibratory behavior as applied to a ship hull. For this reason, there has been a trend towards a more and more complex idealization of the ship hull structure so that important subsystems of hull vibration can be modeled and analyzed.

It has been shown,<sup>5,6,7,8,9,10,11)</sup> for instance, that large areas of double-bottom structure and the associated mass of cargo and added mass of water can be undergoing vibratory movement that affects the main-hull-girder vibration. Other portions of the ship that form important subsystems are tall deck houses, large machinery components, individual decks, appendages, and the propulsion system. If sufficient mass is associated with any of these systems, they will couple with and significantly alter the beam-like vibration characteristics of the main hull.

Idealizations of the ship hull more complex than a simple beam have been accomplished in several ways. These more complex schemes may require a direct solution to the eigenvalue-eigenvector problem. In matrix notation the sets of equations to be solved are of the following form:

$$[M]\{\ddot{v}\} + [C]\{\dot{v}\} + [K]\{v\} = \{P\}$$

where:

[M] = Mass matrix.

[C] = Damping matrix.

[K] = Stiffness matrix.

{v} = Deflection vector.

{P} = Vector of externally applied forces.

In this equation the first term represents the inertia forces of the system, the second term represents the damping forces, the third term represents the internal elastic forces, and on the right hand side of the equation are the externally applied forces.

One type of the more elaborate ship idealizations uses an assemblage of discretized beams and individual sprung masses all of which may be connected to a rigid base with springs to simulate buoyancy effects,<sup>5,20)</sup> and linear viscous dampers to simulate hydrodynamic damping (see Section 3 of this report).

Another idealization models the ship as a lumped mass, double elastic-axis system for the main hull and double-bottom structure, with the deck house and propulsion system being represented as additional mass, spring, and elastic-axis systems coupled to the main hull.<sup>6)</sup>

Ultimately the ship can be modeled as an assemblage of various types of finite elements. This technique allows a very complete representation of the ship to be analyzed.

### 2.2.2 Solutions of the Equations of Motions

In each of the idealizations of the ship hull and associated secondary vibrational systems mentioned above, the equations of motion are constructed by expressing in equation form (either differential or integral) the dynamic equilibrium of each discretized element and generalizing the solution of these equations by numerical solution techniques, usually matrix methods. These solutions may involve the construction of a "dynamic matrix" which is then solved for its eigenvalues and its corresponding eigenvectors, or it may involve the conversion of partial differential equations into finite difference equations which in turn are generalized for matrix computation. Other methods solve the integral equations of motion using various numerical integration schemes such as weighting matrices or through various iteration schemes.

Some of the more commonly used methods of solution of the equation of motion for single-beam idealizations of the hull are the Rayleigh-Ritz method, the lumped-parameter method, the method of Stodola, the Holzer-Myklestad method, and Prohl's method. A detailed description of these methods may be found in the literature.<sup>3,4,12,13)</sup>

The more complex idealization methods use several different types of solution techniques for matrix equations. The solution techniques are not discussed here since they are essentially mathematical procedures employed by the various computer programs for extracting eigenvalues and eigenvectors. Some of the large computer programs do have the capability of limiting the number of degrees of freedom analyzed in the solution of the dynamic equations of motion. This allows more economical use of computer time.

The solution of the equations of motion generally consists of obtaining the natural mode shapes and frequencies of the dynamic structural system. To obtain the response of the structure to various dynamic loadings, additional analysis techniques are needed.

The types of dynamic loading which are considered here are propeller excitation loadings, slam loadings, and wave excitation loadings. Propeller excitation may be considered to be a steady-state excitation, although conditions are never so ideal that this is actually the case. Slam loadings are transient in nature, and analysis techniques different from those used in

calculating steady-state response must be used. Wave-excitation loading is of a random nature and must be evaluated statistically, although the tools used in the statistical analysis are based on the steady-state response of the structure to components of the random sea.

The steady-state response of the ship structure, regardless of complexity, is in principle easily calculated once the natural mode shapes and frequencies of the structure have been determined. The response of the structure to a given steady excitation is simply the linear superposition of the steady response of each individual mode shape to that excitation. The response of individual mode shapes may be obtained as if it were a one-degree-of-freedom spring-mass system.

The transient response of the ship is also obtained as the superposition of the transient response of each individual mode shape, but may be determined in a number of different ways. If each mode shape is treated as a one-degree-of-freedom spring-mass system its transient response to certain well defined transient loads may be determined in a simple, straightforward manner by solution of the differential equation of motion. Two loadings for which a direct solution is known are the unit-impulse and the unit-step-function loading. Duhamel's integral is a method of obtaining the transient response to an arbitrarily shaped impulse that is equivalent to approximating it with a series of unit impulses, each with a different scale factor, stacked side by side or a series of unit-step functions of varying length stacked on top of one another.

An alternate method of obtaining the transient response is by directly integrating the equations of motion, expressed in generalized coordinates, by numerical integration procedures and then converting the response in terms of generalized coordinates back into overall ship response by replacing the generalized coordinates by the individual mode shapes.<sup>12)</sup>

In some analysis procedures the mode shapes and frequencies are obtained by determining for selected frequencies the deflected position of one segment of the ship with respect to its adjoining segment on the basis of assumed free-end conditions and the distributed external loading and internal distribution of bending and shear stiffness.<sup>14,15)</sup> The equations of motion are converted to finite-difference equations and solved by matrix methods in this analysis procedure. A natural frequency and mode shape are obtained when the proper boundary conditions

are satisfied at the extremities of the structure. The transient response can be obtained directly with these analysis procedures, and many nonlinearities may be accommodated.

### 2.3 Computer Programs for Dynamic Structural Analysis

The literature survey has produced computer programs developed specifically for the analysis of ship vibrations, as well as general-purpose programs which can be adapted to analyze these vibrations. Brief descriptions of the programs follow:

2.3.1 NASTRAN - This is a large, commercially available structural analysis system developed by NASA and is continuously being improved and enlarged in scope.<sup>16)</sup>

The system uses a variety of finite elements of the beam, plate and three-dimensional type. Any combination of these elements may be used to represent one-, two-, or three-dimensional structures with up to six degrees of freedom at each nodal point. Also, springs and dashpots may be used to simulate the buoyancy and hydrodynamic damping of the vibrating ship.

The system can perform either real or complex eigenvalue-eigenvector analyses.

Transient, harmonic, and random-response analyses can be performed using the real or complex eigenvalues and eigenvectors.

2.3.2 DYNAL - This large commercially available structural analysis system<sup>17)</sup> has basically the same capabilities as NASTRAN except that only real eigenvalue-eigenvector analyses can be performed in which the damping is specified as a certain percent of critical damping.

2.3.3 STARDYNE - This commercially available system<sup>18)</sup> has similar capabilities to DYNAL.

2.3.4 GBRC 1, 2 and GBRP - These three programs<sup>14,15,19,20)</sup> are specifically intended and written for the analysis of ship vibration. GBRC 1 provides solution to vertical harmonic vibration, GBRC 2 for torsional-horizontal harmonic vibration, and GBRP for vertical transient vibration.

These programs represent the ship as a moderately nonuniform slender beam. The problem is then set up as a set of finite-difference equations in terms of matrices, which are solved subject to free-end conditions for deflection, moment and angular twist at the end of the beam.

Several types of damping can be included in the idealization.

The ship can only be represented as a single beam in these particular programs. Buoyancy forces and hydrodynamic damping can be included.

2.3.5 SHVRS - This particular program<sup>5,21,22</sup>) was written specifically for ship hull vertical vibration with shafting system and super-structure included and is the program that was selected for use in this study. A detailed description of this program may be found in Section 3 of this report.

2.3.6 ANSYS - This commercially available system<sup>23</sup>) has similar capabilities to DYNAL and STARDYNE.

## 2.4 Calculation of Input Data

### 2.4.1 Ship Properties

#### 2.4.1.1 Ship and Cargo Mass Terms

1. Structural Mass - The structural mass consists of all the structure which forms the ship hull girder and all other items which are structurally attached to the hull girder such as deck houses and propulsion systems. The effect of increasing the structural mass is to reduce the natural frequency of vibration and the response to excitation, all other parameters held constant.

2. Cargo and Non-Structural Mass - This consists of all cargo, liquids, outfit, personnel, etc. Where the ship is modeled as a double elastic axis (main hull and double bottom) the cargo must be divided between the double bottom and main hull with care. This becomes particularly difficult when the cargo is a liquid. The effects of this mass on the vibratory characteristics of the ship are identical to those of the structural mass.

3. Rotatory Inertia - For a ship cross section in which cargo and added mass of water are included, it is difficult to determine what part of the cross section is effective in developing rotatory-inertia moments. Consequently, investigations have been made as to its importance<sup>24,25)</sup> and it has been found to be negligible in some cases. Ohtaka et.al<sup>25)</sup> have found the effect of rotatory inertia on the natural frequency to be negligible up to 6~7 noded modes.

#### 2.4.1.2 Damping Terms

There is very little known about the damping associated with ship hull vibration.<sup>26)</sup> The types of damping from within the hull are the cargo and structural damping. There is little theoretical knowledge available for calculating these but there is empirical data available<sup>27)</sup> from full-size ships. Unfortunately, this measured data does not discriminate between types of damping, since all types are measured simultaneously.

1. Structural Damping - When structural material is cyclicly stressed, energy is dissipated internally in the material.<sup>2)</sup> It has been shown by experiment that for most materials, the energy dissipated per cycle of stress is independent of the frequency and proportional to the strain amplitude squared.

For very large structures such as ships the direct calculation of this damping is impossible. Measurements of this damping in large structures can be found in the literature however.

2. Cargo Damping - Cargo damping can occur as three independent phenomena:

a. Vibration absorber type damping which is due to the sprung mass effect of the cargo on the decks and double bottom.

b. Damping within the cargo itself (such as in the shock absorbers of automobiles and internal friction of bulk cargo).

c. Internal friction and movement between the cargo and the ship hull.

### 2.4.1.3 Stiffness Terms

1. Bending Stiffness - The bending stiffness can be calculated directly from the structural and material properties of the hull. Limited superstructures should be disregarded in the moment-of-inertia calculation of the main hull. For vessels with extensive superstructure, a judgment must be made with regard to their effectiveness.

Decreased stiffness will lower the natural frequency and increase the response amplitude of the main hull, all other parameters held constant. Bending stiffness has a primary influence on natural frequency in the lower modes of vibration only.

2. Shear Stiffness - The shear stiffness also can be calculated from the structural and material properties of the hull. It is generally assumed that the shear force is taken by the continuous, vertically oriented plating members such as the side shell and longitudinal bulkheads. More elaborate estimations of shear stiffness can be made using energy methods. The shear stiffness determined by the first method described may give results considerably in error (over-estimated).

Variations in the shear stiffness have the same effect as variations in the bending stiffness but are more pronounced for the higher modes of vibration.

3. Shear Lag - Shear-lag effects are more pronounced in short, wide flanges and thus would seem to become important in the higher modes of vibration in which the distance between nodal points becomes short. This would, in effect, reduce the bending stiffness in the higher modes. However, it is in the higher modes of vibration that the bending stiffness becomes less influential; and it is assumed, therefore, that the effect of shear lag would be to reduce higher-mode frequencies and to increase the amplitude of response, both by a slight amount.

### 2.4.2 Hydrostatic and Hydrodynamic Coefficients

The water surrounding a ship directly influences the vibratory characteristics of the hull. The effects will manifest themselves as terms in the mass, damping and stiffness matrices.

The effects due to the generation of pressure waves in the water and those due to viscosity are normally neglected although Hoffman and Van Hooff<sup>28)</sup> indicate the latter may be considerable in developing damping.

The remaining dynamic effects are those due to the nonviscous fluid motion set up by a ship vibrating in the free surface. By making use of "strip theory" (see Section 2.4.3.1 Wave-Excitation Forces), these phenomena may be described by the fluid motion set up around a 2-dimensional section of the ship with the total effect equal to that from the lengthwise integration of the 2-D problem along the ship length. The resultant effects of the fluid motion about the hull are resolved into the "added mass" and "hydrodynamic damping."

The hydrostatic effects are those due to the buoyancy of the ship.

#### 2.4.2.1 Added Mass

A vibrating ship imparts kinetic energy to the surrounding water. That mass of water which, if vibrating at the same amplitude and frequency as the ship, would possess that same amount of kinetic energy is termed the "added mass" of water. Thus, in determining the vibratory characteristics of the ship, the surrounding water is ignored, and the "added mass" is added directly to the structural and cargo masses in the equations of motion.

As discussed previously it is calculated by considering the kinetic energy in the 2-dimensional flow about a ship section oscillating in the free surface.

Over the years various methods have been developed for estimating this quantity for ship hulls. One of the most important differences in the various methods is their ability to include the effect of frequency of oscillation. Frequency dependence of added mass only exists at lower oscillation frequencies. In the past, the prediction of hull vibratory response has mainly been associated with propeller-induced vibration. This phenomena occurs at the higher modes of hull vibration where frequency dependence of added mass is small. However, the field of rigid-body ship motion has been concerned with the lower end of the frequency spectrum where frequency dependence of added mass is important. As a consequence, methods have been developed to calculate added mass for all frequencies.

It should be noted that, for the vibratory response to wave excitation with less stiff ships of today, the vibratory response has taken place in frequency ranges where frequency dependence of added mass is important.

The other important difference between the various methods available is their ability to represent the hull shape accurately. Lewis<sup>29)</sup> presented the first method of calculating added mass for a series of 2-dimensional forms which closely resemble the sections of many ship types (except notably bulbous bows, multi-hulls, or a shape with some discontinuity). These have become known as Lewis Forms. Later researchers have developed methods which can calculate added mass for more arbitrary variations in hull forms.<sup>30,31,32)</sup>

The various methods of calculating the sectional added mass will now be discussed in detail. It should be noted the added mass is not a negligible quantity regardless of the frequency of vibration.

#### 1. Lewis Form Method

Since Lewis presented his famous paper on the calculation of added mass there have been extensions to the capability of this method. The direction has been to either compute the added mass independent of frequency for high-frequency propeller-excited hull vibration or to calculate frequency-dependent added mass for rigid-body ship motions use.

With any Lewis Form method the ship section is mathematically represented by a Lewis-Form geometric shape which has the same beam, draft and sectional area as the ship section, but not necessarily the same shape. This method is fast and inexpensive and gives good results for many common ship forms.

Landweber and Macagno<sup>33,34)</sup> discuss the Lewis Form and an extension of the Lewis Form to increase its accuracy for frequency-independent added-mass calculations.

Loukakis<sup>35)</sup> gives a computer program of the Grim method for calculating the frequency-dependent added mass of Lewis Forms. According to Grim<sup>36)</sup> the method is accurate at any frequency.

Loukakis<sup>35)</sup> gives an extension of Lewis Forms to include bulbous bow forms also.

## 2. The Close-Fit Mapping Method

In this method the ship sections are conformally mapped into a circle by applying a mapping function with as many coefficients as necessary in order to get the desired accuracy.

Porter<sup>30)</sup> and Tasai<sup>32)</sup> first presented this method. In theory any form of ship section can be described and results obtained for any frequency.

Landweber and Macagno<sup>37,38)</sup> present a conformal mapping technique for the calculation of frequency-independent added mass only.

The Close-Fit mapping technique requires significantly increased computational time, as compared to the Lewis Form method, for the possible additional accuracy. Of course, sections which cannot be described by Lewis Forms can be described by the Close-Fit technique.

## 3. The Frank Close-Fit Source Distribution Method

In this method, which was developed by Frank,<sup>33)</sup> the shape of the ship section is represented by a given number of offset points and pulsating sources are then distributed over the section in order to calculate the hydrodynamic quantities. This method in the original form gave very accurate results over the entire frequency range except for certain "irregular" frequencies in the higher frequency range. This can now be avoided by using the numerical fairing technique of Faltinsen.<sup>39)</sup>

This method gives accurate results for any shape hull but like the close-fit mapping technique, the additional computational time involved is significant.

Faltinsen<sup>40)</sup> gives a comparison between the Frank method and others for various hull shapes.

## 4. J-Correction Factor

The added mass discussed above has been shown to vary for different modes of vibration.<sup>29,41,42)</sup> This is due to the difference in kinetic energy of the surrounding fluid between the actual 3-dimensional motion and the 2-dimensional

motion assumed in conjunction with strip theory. The J-Correction Factor is the ratio of these energies. As the mode of vibration increases exact 3-dimensional calculations have shown that the added mass decreases, so that the values of added mass from the 2-dimensional strip theory should be reduced.

However, these researchers have found no evidence in the literature that the procedures now available for determining the correction factor give better results than assuming the correction factor equal to 1.0.

#### 5. Division of Added Mass Between the Main Hull and the Double Bottom

As indicated in Section 2.2.1, the ship can be modeled as a double elastic axis, one representing the main hull and the other the double bottom. Additionally, in the case of very wide ships such as large tankers, it is also indicated that division of the hull into beams representing the sides and the longitudinal bulkheads should be considered.

Methods of determining the amount of added mass to be considered with the double bottom, main hull, sideshell, or longitudinal bulkhead may be found in the references cited in Section 2.2.1.

#### 2.4.2.2 Hydrodynamic Damping

Although pressure wave generation and viscous resistance do exist, as mentioned previously they are generally considered small and neglected. Therefore, the only hydrodynamic damping which remains is that due to surface-wave generation as the ship vibrates in the fluid surface. This damping may be calculated by the same procedure as the added mass providing that the methods can account for frequency effects, since at an infinite frequency of oscillation the damping will approach zero. The methods of Grim, Frank, Porter and Tasai discussed above are suitable for the calculation of hydrodynamic damping.

Generally hydrodynamic damping need only be considered for very low frequencies of vibration since, as previously mentioned, its value approaches zero as the frequency of vibration is increased.

### 2.4.2.3 Buoyancy

As the ship vibrates it will experience changes in draft along its length which will induce buoyancy forces. McGoldrick<sup>43)</sup> has indicated that the buoyancy effects may become significant for ships with very low fundamental frequencies.

### 2.4.3 Excitation Forces

#### 2.4.3.1 Wave-Excitation Forces

In recent years the area of rigid-body ship motion has received great attention and the theory which is considered most complete is that by Salvesen, Tuck and Faltinsen.<sup>44)</sup> These authors have used this along with latest modifications of the strip theory<sup>45,46)</sup> in determining wave-excitation forces.

The main assumptions of the theory are as follows:

1. Viscous effects can be disregarded, therefore, the only hydrodynamic damping considered is that due to the energy loss in creating free-surface waves.
2. The potential problem can be linearized, therefore, it is assumed that the wave-resistance perturbation potential and all its derivatives are small enough to be ignored. This means that the free-surface waves created by the ship advancing at constant speed have no effect on the motion. This is reasonable for fine slender hull forms.
3. The 3-dimensional problem can be reduced to a summation of 2-dimensional problems (strip theory assumption). This requires that the wave length be approximately of the same order as the ship beam.

Further details of the theory of wave-excitation forces can be found in Section 3.2, Method Modification.

#### 2.4.3.2 Propeller-Excitation Forces

The propeller develops alternating forces which can excite vibration in the ship hull. These forces fall into two groups namely bearing forces and surface forces.

The bearing forces are those which are transmitted to the hull through the bearings. If the propeller is balanced, the only bearing forces will be those due to thrust and torque fluctuations of the propeller blades. These arise from the propeller operating in a nonuniform and nonsteady wake in the proximity of a boundary, namely the hull and appendages.

The surface forces are caused by the pressure field surrounding each propeller blade. As the propeller blades sweep by the stern frame, rudder, and other adjacent parts of the hull structure, they cause alternating pressure perturbations at the hull. These pressure disturbances are caused by both the thickness and loading of the propeller blades.

#### 1. Propeller-Induced Bearing Forces

The propeller-induced bearing forces acting on a ship can be of two types. These are the torque and thrust variations which can excite vibration in the machinery, and the vertical and transverse forces and thrust eccentricity which can excite the ship hull.

The torque and thrust variations are generated by harmonic components of the wake having blade frequency and multiple blade frequency fluctuation. Some typical experimental results of these forces for a tanker are as follows:<sup>47,48)</sup>

a) 4-bladed propeller (even number of blades generate large thrust and torque fluctuation) - Torque fluctuation (first harmonic) = 6.5 percent of average total torque. Thrust fluctuation (first harmonic) about 10 percent of average total thrust. Another source<sup>49)</sup> gives torque fluctuation for single-screw vessels as 10-15 percent and thrust variations as 3-8 percent of mean torque and mean thrust, respectively.

b) 5-bladed propeller - Torque fluctuations vary between 1.5 percent and 1.0 percent of average torque while thrust variations are between 1.5 percent to 2 percent of average thrust. Another reference<sup>49)</sup> gives 4-5 percent for torque and 3-8 percent for thrust.

The vertical and transverse forces and thrust eccentricity developed by the propeller are caused by blade frequency harmonic components and their multiples plus and minus one.

Again, some results for a tanker are of interest.<sup>47,48)</sup> The transverse force fluctuations of a 5-bladed propeller are twice as large as those for a 4-bladed propeller (4-blade: horizontal 7.3 percent, vertical 7.6 percent of mean thrust; 5-blade: horizontal 15 percent, vertical 13 percent). The higher harmonic components of a 5-bladed propeller are the same as those of a 4-bladed propeller while the fluctuations in thrust eccentricity for a 5-bladed propeller are considerably larger than those for a 4-bladed propeller.

Other experimental findings for both types of bearing forces<sup>47,48)</sup> indicated that there was no systematic correlation between the amplitudes of the force fluctuation and important hull parameters. Also, fine and high-speed ships gave rise to higher fluctuations.

Usually theoretical methods for predicting bearing forces<sup>47,48,49,50,51)</sup> rely on 2-dimensional or quasi-steady theories using measured wake data. A rational theory<sup>51)</sup> which includes 3-dimensional unsteady flow, blade and helical wake geometry and the distribution of ship wake or inflow to the propeller has been developed and gives computational results which correlate well with the limited experimental results presented. There has recently been a further refinement of the method.<sup>52)</sup>

Most information regarding the magnitude of thrust and torque excitations is given for the full-power operating point. Since the propeller thrust and torque vary approximately as the RPM<sup>2</sup> it seems reasonable to scale the fluctuating forces in this manner for other RPM's.

## 2. Propeller-Induced Surface Forces

Although much experimental and theoretical work had been done in this area less has been accomplished than with bearing forces because of the increased difficulty of the problem.

Breslin,<sup>53)</sup> Tsakonas and Jacobs<sup>54)</sup> give solutions for very idealized ship forms which can be used for establishing trends but cannot give results for an actual stern configuration.

Breslin and Eng<sup>55)</sup> give a procedure which should be capable of giving good results but at the expense of long computational time.

Vorus<sup>50</sup>) presents a method which gives hull-surface components of the propeller-generated force and which takes into account the vibratory response of the ship.

Huse<sup>56</sup>) indicates that measuring of surface forces may be impossible during experiments when pressure transducers are fitted in hull plates of the afterbody of a ship. This is due to vibratory motion of the afterbody and hull plates in the vicinity of the transducer interfering with the propeller-induced pressure.

Huse<sup>57</sup>) also presents a method for determining the hull-surface forces by calculating the free-space pressure field due to the propeller and then using a correction factor to take into account the "solid boundary" of the hull in the actual case, thereby eliminating much of the involved mathematics. Some of his main conclusions are particularly interesting. He finds skeg pressure amplitudes decrease rapidly with increasing propeller clearance and these amplitudes can be greater than those induced on the hull. Also, the total surface force in the vertical direction obtained by integration of the pressure over the afterbody is of the same magnitude as the vertical bearing force. In addition, the phase of the vertical bearing force and vertical surface force can be such that the two cancel each other. This depends on the tip clearance and for other tip clearances the phases will vary.

Cavitating propellers can seriously increase the vibratory excitation described above.<sup>58,59,60</sup>)

#### 2.4.3.3 Slam-Excitation Forces

Ship slamming refers to the phenomena which occurs when a portion of the hull impacts the sea surface creating large forces of short duration.

Various types of ship slamming have been described. When the bow of a ship emerges from the water and subsequently re-enters such that the angle between the ship bottom and water is small, large forces of short duration are produced. This phenomena is called bottom slamming. If the bow of a ship with significant bow flare rapidly submerges into the sea surface large forces of short duration are also produced although of less severity than those of a bottom slam. Finally, the slapping of waves on the bow of a ship may also be considered a form of slamming. Very little reference to stern slamming was found in the literature by these researchers.

The magnitude, duration, and shape of the slam-pulse-excitation force has eluded accurate prediction in both the experimental and theoretical fields. Most experimental efforts have been aimed at predicting pressures to aid in the design of bottom plating, but little has been done to determine force-time histories for slams. Records of experimental data on full-scale slams exist, and many theories of the slamming phenomena have been developed.<sup>61,62,63)</sup>

## 2.5 Empirical Methods

In the study of ship vibrations, there are many uncertainties in the theoretical calculation of the ship's mass and stiffness properties, in the nature and magnitude of the various damping mechanisms in the estimation of hydrodynamic coefficients, in the prediction of excitation forces, and in the calculation of the response. It is natural, therefore, that a large amount of experimental data (both model and full scale) have been compiled in an effort to confirm estimation and calculation procedures for the various parameters of interest.

These empirical methods have taken the form of model tests on ship motions, ship slamming, propeller-excitation forces, wave-excitation forces, and dynamic response. Full-scale tests have been conducted to confirm response-prediction calculations for propeller excitation, to measure slam pressures and responses, to investigate shafting vibration, and to obtain data on the structural response to wave excitation.

Because of the complexity of the ship-dynamic-response problem and the problem of scaling the structure in reasonable-size models, the empirical methods have not lent themselves to becoming analysis tools for the complete ship-vibration problem, but have proved useful in the determination of various quantities in the equations of motion, the most valuable being the exciting forces. Applications of empirical techniques have been noted in previous sections.

Several semi-empirical equations for the estimation of hull natural frequencies have been in existence that require only a few significant ship parameters and coefficients that are estimated from experience with similar ships. The most famous of these are the formulas of Schlick, Todd, Marwood and Burrill.<sup>4,64)</sup> The general form of these equations is as follows:

$$N = C' \sqrt{\frac{I}{\Delta' L^3}}$$

where:

- N = Natural frequency.
- C' = Coefficient based on ship type and mode of vibration.
- I = Moment of inertia of midship section.
- $\Delta'$  = Effective ship weight.
- L = Ship length.

These empirical formulas can only be used for similar ships for which coefficients (C') can be determined and usually can only account for the lower modes of vibration.

## 2.6 Design Criteria

Design criteria that are explicitly identifiable with vibration and which can be actually employed in the course of executing a commercial design are nearly non-existent. They are indirectly assimilated in the primary and secondary strength and the shafting design requirements found in the classification society rules.

Most ship specifications do not have any numerical values for unacceptable vibration. Generally they call for shafting calculations and calculations for the natural frequency of the 2; 3; 4- and 5-noded vertical vibration. This is merely to compare the hull-vibration frequency with the blade frequency.

For unusual designs, owners have model tests performed to detect adverse flow in the afterbody area, and poor wake or cavitation which could result in unacceptable propeller-induced vibration.

The det Norske Veritas Rules, 1974, provide limited guidelines regarding external dynamic loading on the hull and local-panel vibration. The rules have a method involving ship length, depth and draft which permits estimating the dynamic load at any point along the length of the ship, above and below the waterline. A method is provided to estimate the fundamental-mode vibration frequency of panels to insure that it will be above the exciting frequency due to the main engine and the propellers. The method corrects for the added mass when the panel is partially or fully immersed in a liquid.

### 3. SELECTION OF ANALYTICAL METHOD

#### 3.1 Selected Method of Analysis

The method of analysis selected for conducting the parametric study of stiffness effects on dynamic response is that embodied in the computer program SHVRS. The SHVRS program\* was initially developed to study the effects of stiffness and configuration variations in various types of dry cargo ships on the overall response of the ship structure to both propeller- and slam-excitation forces. For this study, its capability was extended to include wave-excited response.

A review of the available programs indicated that many were capable of performing the desired evaluation, particularly for slam- and propeller-excited vibration.

SHVRS was chosen because of a) its availability, b) the researchers' familiarity with its format and the consequent ease of modification, c) the ease of input and parameter variation, and d) the fact that it offered the simplest idealization of the structure consistent with the analysis needs and the state-of-the-art of developing input information.

The analysis procedures used by SHVRS for the calculation of vibratory response to propeller, slam, and wave excitation are essentially those described in References (1) and (2), with the analysis procedure for wave-excited vibration being an adaptation of the procedure for calculating steady-state response to propeller excitation.

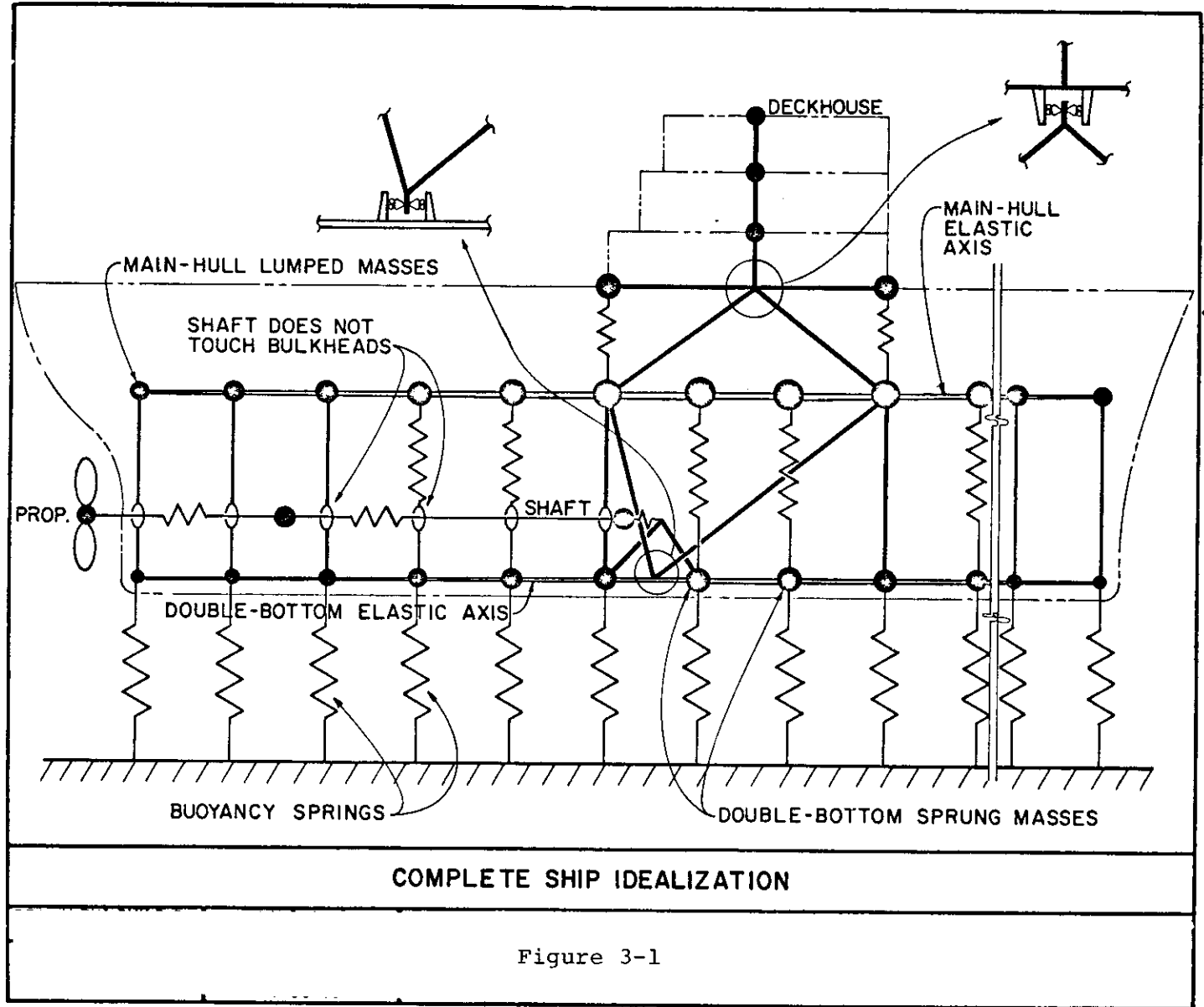
##### 3.1.1 Ship Idealization

The ship idealization used is that shown in Figure 3-1. It consists of a double elastic axis representation of main-hull and bottom-structure that reflects the bending and shear stiffness properties of the ship along its length. In addition, evenly spaced lumped masses on each axis represent both the ship mass and the added mass of water at the mass-point in question. The bottom-structure elastic axis is connected to the main-hull elastic axis by rigid bulkhead links as well as by

---

\* The purchase or use of the computer program, SHVRS, may be arranged by contacting USS Engineers and Consultants, Inc., - a subsidiary of U. S. Steel Corporation

3-2



flexible bottom-structure springs representative of the transverse stiffness properties of the double bottom. This elastic-axis, lumped-mass idealization rests on buoyancy springs with spring constants determined by the waterplane area of the ship at each station. Each mass point of hull and bottom structure has one-degree-of-freedom translation in the vertical direction.

In addition to the idealization of the ship's main hull and bottom structure, the ship idealization shown in Figure 3-1 includes the propulsion system and a short (with regard to fore and aft length), tall deckhouse or superstructure. The idealization of the propulsion system is intended to represent the mass and stiffness properties of the propeller, shafting, thrust bearing foundation, and reduction gear that are influential in transmitting the oscillating longitudinal thrust forces generated at the propeller to the main hull and bottom structure. The inertial effects of the propulsion system are represented by three lumped masses: one at the propeller that includes propeller mass and added mass of water along with a portion of the mass of the shaft, a second mass for the mid-portion of shaft, and the third mass that includes the forward portion of the shaft along with the effective mass of the thrust bearing and attached gear wheel. The elastic properties of the system are idealized by three springs, two of which are representative of shafting stiffness and a third one that combines the stiffness of the thrust bearing and its foundation. The remainder of the propulsion system idealization consists of rigid bar links that couple the propulsion system to the double-axis-hull-girder model. The attachment of the thrust block to the bottom structure is so arranged that any longitudinal motion of the thrust block results in vertical bending of the double bottom. The other pair of rigid bars similarly couples the longitudinal motions of the thrust block with vertical deformation of the main hull girder. This mechanism therefore accounts for the eccentricity of the propulsion system relative to the two elastic axes.

The deckhouse idealization is a vertical cantilever beam, as shown in Figure 3-1. This vertical elastic axis is supported by a rigid base, which is attached to adjacent bulkhead stations on the hull-girder axis by two springs. In addition, a pair of rigid bars are attached to a special coupling on the rigid base, and are used to transmit inertia forces in the fore-and-aft direction to the main-hull elastic axis while allowing free motion in vertical translation and rotation. The two springs at the base represent the stiffness of the main-deck structure and may have widely differing properties, depending on whether the deckhouse extends over transverse bulkheads or whether its sides are continuous with the ship sides or longitudinal bulkheads.

Above the rigid base, the deckhouse is treated as a typical lumped-mass idealization. The deckhouse masses are assumed to be concentrated at the deck levels, and the elastic properties are evaluated by a standard-beam-stiffness analysis, including the influence of the shear distortion. The two masses at the ends of the rigid base account for all vertical inertia forces developed in the deckhouse, the distance between them being chosen to represent the rotatory inertial effect associated with the longitudinal distribution of mass in the deckhouse. These vertical and rotatory inertia forces are transmitted to the main-hull axis by the springs representative of the stiffness of the connection between main-deck structure and the deckhouse, and by rigid-bar links that function in a manner similar to those connecting the thrust-bearing foundation to the main-hull elastic axis.

### 3.1.2 Equations of Motion

The objective of any dynamic-analysis procedure is to obtain the displacement of mass points of the structure to the dynamic loading. This is accomplished by solving the equations of motion of the ship structure idealization. The equations of motion express the dynamic equilibrium of forces acting on the structure, both externally and internally. The internal forces are inertial, elastic, and damping; and the external forces are those imposed by the environment, primarily hydrodynamic in nature.

The dynamic equilibrium of the ship structure may be expressed by the matrix equation:<sup>1)</sup>

$$[M]\{\ddot{v}\} + [C]\{\dot{v}\} + [K]\{v\} = \{P\} \quad (3-1)$$

where the terms on the left side of the equation represent the internal forces previously mentioned and the right side represents the externally applied dynamic loading.

In these investigations, the dynamic response of the ship structure was evaluated by the mode-superposition method using mode shapes that were derived for the undamped structure. These mode shapes have been derived by solving the characteristic-value problem

$$[K]\{v\} = \omega^2 [M]\{v\} \quad (3-2)$$

under the assumption that they possess certain orthogonality properties: namely, that the mode shapes are orthogonal with respect to the mass distribution in the structure and also with respect to the stiffness distribution in the structure. In equation form, these characteristics may be expressed as follows:

$$\begin{aligned} \{\phi_m\}^T [M] \{\phi_n\} &= 0 \\ \{\phi_m\}^T [K] \{\phi_n\} &= 0 \end{aligned} \quad m \neq n \quad (3-3)$$

where  $\{\phi\}$  are the mode shapes and  $[M]$  and  $[K]$  are the mass and stiffness matrices, respectively.

It has also been assumed that the damping matrix is a linear combination of the mass and stiffness matrices, and consequently that the mode shapes are also orthogonal with respect to the damping distribution in the structure. If the damping matrix is expressed as follows:

$$[C] = \alpha[M] + \gamma[K] \quad (3-4)$$

where  $[C]$  is the damping matrix, and  $\alpha$  and  $\gamma$  are constants, then the modal damping coefficient,  $\lambda_n$ , may be expressed as follows:

$$\lambda_n = \frac{\alpha + \gamma\omega_n^2}{2\omega_n} \quad (3-5)$$

where  $\lambda_n$  is the fraction of critical damping in the  $n^{\text{th}}$  mode and  $\omega_n$  is the natural frequency of the undamped  $n^{\text{th}}$  mode in radians per second.

The above assumptions permit the equations of motion to be solved in a valid manner in terms of the mode shapes and frequencies derived for the undamped system.

If the displacements of the structure are expressed in terms of "normal coordinates", as follows:

$$\{v\} = [\phi]\{Y\} \quad (3-6)$$

where  $\{Y\}$  is the modal-amplitude vector, the coupled equations of motion, equation (3-1), may be transformed into a set of uncoupled equations by virtue of the orthogonality relations, equation (3-3). The equation of motion for each normal coordinate is then

$$\ddot{Y}_n + 2\omega_n \lambda_n \dot{Y}_n + \omega_n^2 Y_n = \frac{P_n^*(t)}{M_n^*} \quad (3-7)$$

in which the following notation is used:

$$M_n^* = \{\phi_n\}^T [M] \{\phi_n\} \quad (3-8a)$$

$$\omega_n^2 M_n^* = \{\phi_n\}^T [K] \{\phi_n\} \quad (3-8b)$$

$$2\lambda_n \omega_n M_n^* = \{\phi_n\}^T [C] \{\phi_n\} \quad (3-8c)$$

$$P_n^*(t) = \{\phi_n\}^T \{P(t)\} \quad (3-8d)$$

Thus the dynamic response problem is reduced to the solution of a set of independent, single-degree-of-freedom equations for the time history of modal response, which may then be transformed back to the original ship geometry through the reapplication of equation (3-6).

For excitation sources such as assumed point loadings of propeller excitation, either the alternating-thrust load on the propeller or the vertical combined-surface-and-bearing-force load, a simplified form of the generalized force may be used:

$$P_n^*(t) = \phi_{pn} P(t) \quad (3-8e)$$

In this case,  $\phi_{pn}$  represents the  $n^{\text{th}}$  mode shape amplitude at the point of loading.

### 3.1.3 Solution of Equations of Motion

The computer program, SHVRS, was set up to obtain the dynamic response of ship structure to two types of

dynamic loadings - steady-state propeller-excitation and transient-slam forces. Each type of response requires a different solution technique.

The general propeller-excitation input was assumed to be of the form

$$P(t) = P_0 \sin pt \quad (3-9)$$

and the steady-state response of the  $n^{\text{th}}$  mode to this excitation may be written

$$Y_n(t) = \frac{P_n^*(t)}{M_n^* \omega_n^2} \{A_n \sin pt - B_n \cos pt\} \quad (3-10)$$

where  $A_n$  and  $B_n$  are the amplitude of in-phase and out-of-phase response components, respectively. They may be expressed in terms of the frequency ratio,  $\beta_n$ , and the damping ratio,  $\lambda_n$ , as follows:

$$A_n = \frac{1 - \beta_n^2}{(1 - \beta_n^2)^2 + (2\lambda_n \beta_n)^2} \quad (3-11a)$$

$$B_n = \frac{2\lambda_n \beta_n}{(1 - \beta_n^2)^2 + (2\lambda_n \beta_n)^2} \quad (3-11b)$$

The total in-phase and out-of-phase response of all pertinent modes are obtained by superimposing the corresponding modal components of the response. Since SHVRS calculates the response to both vertical excitation forces of blade frequency on the main hull in the vicinity of the propeller as well as longitudinal excitation forces of blade frequency acting on the propulsion system at the propeller, it is necessary to sum up two sets of modal in-phase and out-of-phase response components. If there is a phase difference between the vertical excitation force and the longitudinal alternating thrust force, the second set of modal response components is resolved into components that are in phase with the first set of components and then summed. This aspect of the program proved to be very useful in in-putting the wave-excitation forces for the study of the dynamic response to wave excitation.

The bow-slam input is a general class of dynamic loading for which the response of each mode was evaluated numerically. The modal responses were not evaluated separately,

however, but were obtained by numerically integrating the equations of motion as expressed in normal coordinates. The numerical integration was performed over a series of very small time increments by first assuming a linear variation of acceleration from one time increment to the next and obtaining relationships between amplitude, velocity, and acceleration of the system in terms of their value during the preceding time increment. Initial conditions were chosen and the integration carried out over a time period considerably exceeding the slam duration. Again, the final values of ship response were obtained by replacing the normal coordinates by the natural mode shapes of the ship idealization.

### 3.2 Modifications and Additions

#### 3.2.1 General

The basic modification made to SHVRS was that which was necessary to enable the calculation of wave-excited hull vibration. At first this modification consisted of merely altering the program to accept distributed steady-state excitation forces rather than the point loadings that were assumed for the propeller excitation. This simply meant reverting to the more general form of the expression for generalized force:

$$P_n^*(t) = \{\phi_n\}^T \{P(t)\} \quad (3-12)$$

where  $\{P(t)\}$  is a force vector for the distributed loading instead of a point load.

Following this modification, it was necessary to establish a frequency range over which the response to the wave-excitation forces should be evaluated. The validity of the statistical-analysis procedure requires that this range be large enough to cover all of the significant response, while the validity of the SHVRS dynamic-analysis procedure requires that the range be small enough that the hydrodynamic coefficients of the equations of motion do not display large variations in magnitude due to frequency dependence. This is necessary because values of these coefficients are kept constant and equal to those of the fundamental-mode frequency of the hull.

The last significant modification made to SHVRS was the incorporation of the necessary calculation procedures to carry out the statistical analysis of the bending moment

response to random wave excitation as well as the equations for calculating accumulative damage in fatigue.

### 3.2.2 Basic Approach to Problem

From a review of the literature, it appears that most wave-excited-vibratory-response-calculation procedures determine the space-time variation of wave-induced loads on a rigid, non-heaving, non-pitching ship and then determine the first-flexural-mode response of that ship to those forces over a range of wave-encounter frequencies in the vicinity of the first-mode natural frequency. In general then, these procedures ignore the heave and pitch motions of the ship, the higher flexural modes of response, and most of the hydrodynamic forces (inertia forces being the exception) generated by the response of the ship. In some calculation procedures the hydrodynamic damping associated with the generation of surface waves is ignored, while in others the various damping terms are rationalized to suit the calculation procedure.

The basis for the wave-excited vibratory-response-calculation procedure incorporated into the SHVRS computer program is that a lumped-mass idealization of the ship exists which is capable of comprehending distributed excitation forces that are dependent on the relative movement between ship section and the wave surface, and that this relative movement of ship section and wave surface may be broken down into two components: (1) the relative movement between the wave and the still-water ship waterline and (2) the relative movement between the still-water surface and the ship. Thus, the wave forces due to the wave motions alone may be treated as the excitation forces while the forces generated by the flexural and rigid-body response of the ship are accommodated by the ship idealization. In this way, the modification of the hydrodynamic-force computation due to the orbital motion in the wave (Smith Effect) can be confined to the wave motions (excitation forces) while the hydrodynamic forces generated by the response are unaffected by this phenomena. The major shortcoming in the existing version of the computer program with regard to the wave-excited vibratory-response-calculation procedure is that the hydrodynamic-damping forces are not properly represented in the ship response (i.e., ship idealization) portion of the computation procedure. This is discussed further in Section 3.2.4.

### 3.2.3 Wave-Excitation Forces

For use in SHVRS, the vertical force on a ship segment resulting from relative movement between ship segment and wave surface was derived from the expression for the total heaving force on a ship hull as presented by Salvesen, et. al.<sup>3)</sup>:

$$F_3 = \alpha \int e^{ikx} e^{-kd^*} \left\{ \rho g b - \omega (\omega_e m' - i N') \right\} dx \quad (3-13)$$

$$- \frac{\alpha V}{i \omega_e} e^{ikx_A} e^{-kd^*} \omega (\omega_e m'_A - i N'_A)$$

where  $x_A$ ,  $m'_A$ , and  $N'_A$  are values of ordinate, added mass, and damping associated with a transom stern or similar discontinuity along the length of the ship - apparently a correction to thin-ship theory. As interpreted for our calculation purposes, differentiation of the above equation yields the following expression for the ship segment force per unit wave height:

$$\frac{dF}{dx} \cdot \frac{1}{\alpha} = e^{ikx} e^{-kd^*} \left\{ \frac{\omega}{\omega_e} \left( \frac{\rho g b}{\omega/\omega_e} - V \frac{dN'}{dx} \right) \right. \quad (3-14)$$

$$\left. + i \omega_e \left( N' - V \frac{dm'}{dx} \right) - \omega_e^2 m' \right\}$$

where:

- dx = station spacing
- $\alpha$  = wave amplitude
- $k = 2\pi/\lambda$
- $\rho g b$  = buoyant force
- $\omega$  = wave frequency
- $\omega_e$  = encounter frequency
- V = ship speed,  $V = -U$  for head seas
- $m'$  = added mass
- $N' = \frac{\rho g^2 \bar{A}^2}{\omega_e^3}$  damping due to surface wave generation
- $\bar{A}$  = ratio of generated wave amplitude to heave amplitude
- $\lambda$  = wave length

The " $e^{ikx}$ " term in the above equation provides the traveling wave nature of the excitation and can be replaced by a cosine-wave form of unit amplitude and a sine-wave form of unit amplitude which when properly phased will provide the equivalent excitation. Thus, the two phased propeller-excitation inputs in the SHVRS program may be replaced by a distributed cosine-wave-form excitation function and a distributed sine-wave-form excitation

function that lags the former in the phase plane by  $90^\circ$ . Thus, the traveling-wave excitation is represented by two stationary-wave forms.

These two wave forms are modified by the term  $e^{-kd^*}$ , the "Smith Effect", where  $d^*$  is the effective draft of the ship at the station in question.

The wave profile thus corrected for "Smith Effect" is used to obtain the wave force acting on the ship section based on the relative amplitude, velocity, and acceleration between the wave surface and still-water plane by taking into account the wave frequency and the encounter frequency between ship and wave system.

The buoyancy force, as indicated in equation (3-13) is unaffected by encounter or wave frequency and is obtained simply by multiplying the effective wave amplitude at each station along the length of the ship by the corresponding buoyancy per foot of immersion at that station. Since the computer program is written to apply the wave excitation in terms of the excitation or encounter frequency, the term  $\omega/\omega_e$  was factored out of the damping and inertia terms in equation (3-14) to appear as a correction factor along with  $e^{-kd^*}$ . Thus, the buoyancy term is divided by this fraction.

The speed correction term applied to the buoyancy is a result of differentiation of the last term in equation (3-13) which, it is assumed, will apply to any section of the ship over which the gradient of  $N'$  is significant.

The hydrodynamic damping,  $N'$ , and the associated speed-correction term,  $v \frac{dm'}{dx}$ , which is derived under the same assumptions as for the buoyancy correction, are preceded by the coefficient,  $i\omega_e$ , which indicates that the wave-surface velocity relative to the still-water surface precedes the buoyancy force or wave amplitude by 90 degrees in phase. Thus the damping force associated with the cosine-wave form is subtracted from and applied in phase with the buoyancy and inertia forces associated with the sine-wave form and vice versa.

The inertia-force term of equation (3-14) has no associated speed-correction term; however, segmented-model tests run in a towing tank<sup>4,5)</sup> have shown that the sectional added mass is affected by ship speed. Since buoyancy and inertial

forces are 180 degrees out-of-phase it is assumed that the recorded influences of speed on added mass can just as correctly be termed buoyancy-force corrections and are assumed to be accounted for in the  $v \frac{dN'}{dx}$  term of equation (3-14)

#### 3.2.4 Response Forces

The SHVRS computer program computes the individual components of wave-excitation force in each of two phase planes at each excitation frequency and then determines the steady-state amplitudes of response of the ship in much the same way as it does for propeller excitation. These amplitudes of response are then modified by a force-transformation matrix to obtain the bending-moment response along the length of the ship.

Since the ship added mass is included in the ship idealization as are the sectional buoyancy forces, the inertia and buoyancy forces generated by the response (i.e., the forces generated by relative movement between the ship and the still-water plane) are automatically accounted for by this type of solution. The distributed hydrodynamic-damping forces due to relative movement between ship and still-water plane are not explicitly accounted for, however.

It should be noted that most solutions proposed to date<sup>6,7)</sup> for the response to wave-excited vibration assume that the heave and pitch motions of the response are negligible, that the flexural response is only of the 2-noded mode, and that no buoyancy or damping forces are generated by the response. The bow amplitude of response at resonance, however, may be of the same order of magnitude as the wave height that induced it.

The damping forces to be included in the ship idealization as representative of those generated by ship motion relative to the still-water plane should theoretically include all internal structural and cargo damping associated with the ship vibratory motions as well as the hydrodynamic-damping forces generated by the ship response. For the hydrodynamic damping associated with the response to be represented in a manner consistent with that in the excitation forces, viscous dampers in parallel with the buoyancy springs should be included in the ship idealization. The damping constant for each would have to be determined in accordance with the frequency of excitation ( $N'$  is frequency dependent) and the ship speed (for the  $v \frac{dN'}{dx}$  term).

The resulting distribution of damping would violate the assumption stated by equation (3-4), and would make equation (3-5) invalid. In fact, the proper solution of the dynamic matrix would be in terms of complex eigenvalues and eigenvectors. The significance of this situation is that the damping distribution is such that it tends to couple the undamped modes of response. Thus pitching motion would tend to induce heaving motions and flexural response; and likewise, the flexural response would tend to be coupled and also induce heaving and pitching motions. The degree to which this coupling would take place would depend on the amount of damping, how badly it violates the assumptions of equation (3-4), and the relative amplitude of the response. Because of the complications in the solution procedure that would have been introduced by the proper incorporation of damping into the ship idealization, a more approximate representation of the response damping forces was utilized.

Equation (3-5) can be rewritten as:

$$\lambda_n = \frac{\alpha}{2\omega_n} + \frac{\gamma\omega_n}{2} \quad (3-15)$$

where  $\alpha$  and  $\gamma$  are constants that determine the fraction of critical damping in each mode of the response. If the  $\alpha$  and the  $\gamma$  factors in this equation are plotted separately, each as a function of  $\omega$ , the  $\gamma$  portion will increase linearly with  $\omega$  while the  $\alpha$  portion will be inversely proportional to  $\omega$ . These two variations can be assumed to correspond to the variation of structural damping with frequency and the variation of hydrodynamic damping with frequency respectively, and the values of  $\alpha$  and  $\gamma$  can be chosen in accordance with experimentally determined damping values.

It is difficult to evaluate the error introduced into the calculations by this simplification except to observe that heave and pitch motions can be negligibly small during the wave-excited vibratory response and that experimental investigations into the overall system damping<sup>7)</sup>, derived under the assumption that the response is linear, indicate a similar trend in damping values as a function of frequency.

The values of  $\alpha$  and  $\gamma$  used in this investigation, 0.04 and 0.0004 respectively, were derived to approximate the

structural damping data summarized by Goodman<sup>6)</sup> for the higher frequencies and to provide a minimum value of 0.4% of critical for the combined damping. The minimum value for modal damping as calculated by equation (3-5) occurs at a frequency of

$$\omega = \left(\frac{\alpha}{\gamma}\right)^{1/2} \quad (3-16)$$

and has a value of

$$\lambda_{\min} = (\alpha\gamma)^{1/2} \quad (3-17)$$

The lowest value of damping cited by McGoldrick<sup>8)</sup> was 0.3% of critical for the ore carrier C. A. PAUL, and the destroyer CHARLES R. WARE recorded a minimum of 0.5% of critical at a frequency of about 12 radians per second. The above values of  $\alpha$  and  $\gamma$  cited above give a minimum of 0.4% of critical damping at 10.0 radians per second.

### 3.2.5 Statistical Analysis of Response

The statistical analysis procedure used to evaluate the response of the ship to wave excitation is intended to provide a measure of the maximum bending moment induced by random excitation from a specified sea state<sup>9)</sup>. It is also intended to measure the accumulative damage in fatigue that results from the additional stress excursions.

The chosen analysis procedure assumes the wave-excited bending response to be a zero-mean, stationary Gaussian process  $M(t)$  with a computed power spectral-density function,  $S_M(\omega)$ , where

$$S_M(\omega) = S(\omega) M^2(\omega) \quad (3-18)$$

and where  $S(\omega)$  is the power spectral-density function of a representative sea state, and  $M(\omega)$  is the bending-moment response to unit wave height over the applicable range of wave frequency,  $\omega$ .

If we define

$$m_n = \int_{-\infty}^{\infty} \omega^n S_M(\omega) d\omega \quad (3-19)$$

it can be shown that the mean frequency of occurrence of positive or negative maxima over the complete range of  $M(t)$  is given by

$$N_1 = \frac{1}{2\pi} \left( \frac{m_4}{m_2} \right)^{1/2} \quad (3-20)$$

If the bending moment is expressed nondimensionally as

$$\eta = \frac{M}{m_0^{1/2}} \quad (3-21)$$

then the probability function for maxima can be expressed as

$$p(\eta) = \frac{1}{\sqrt{2\pi}} \left[ \epsilon e^{-\eta^2/2\epsilon^2} + (1-\epsilon^2)^{1/2} \int_{-\infty}^{\eta(1-\epsilon^2)^{1/2}/\epsilon} e^{-x^2/2} dx \right] \quad (3-22)$$

where

$$\epsilon^2 = \frac{m_0 m_4 - m_2^2}{m_0 m_4} = \frac{\Delta}{m_0 m_4} \quad (3-23)$$

If  $M(t)$  approaches a narrow band process,  $\epsilon$  approaches 0, in which case equation (3-22) becomes

$$p(\eta) = \eta e^{-\eta^2/2} \quad (3-24)$$

i.e. a Rayleigh distribution.

If we assume that the  $N$  consecutively observed maxima are independent and have the probability-density function  $p(\eta)$  given by (3-24), then the probability that all  $N$  maxima will be less than  $\eta$  is given by

$$\text{Pr} [\text{all } N \text{ maxima } < \eta] = P(\eta)^N \quad (3-25)$$

where  $P(\eta)$  is the probability-distribution function for maxima as defined by

$$P(\eta) = \int_{-\infty}^{\eta} p(\eta) d\eta \quad (3-26)$$

From this the probability-distribution function for the largest maxima,  $P_e(\eta)$ , can be obtained, and the derivative of this gives the probability-density function for the largest maxima (i.e., the extreme value) in the form

$$P_e(n) = NP(n)^{N-1} p(n) \quad (3-27)$$

The number of maxima,  $N$ , occurring in a sample function  $M_r(t)$  over a time  $T$  is found to be

$$N = \frac{1}{2\pi} \left( \frac{m_4}{m_2} \right)^{1/2} T \quad (3-28)$$

Thus,

$$P_e(n) = e^{-vT} e^{(-n^2/2)} \quad (3-29)$$

where

$$v = \frac{1}{2\pi} \left( \frac{m_2}{m_0} \right)^{1/2} \quad (3-30)$$

From equation (3-29) it can be shown that the mean extreme-value is given by the approximate relation

$$\bar{n}_e = (2 \ln vT)^{1/2} + \frac{\gamma}{(2 \ln vT)^{1/2}} \quad (3-31)$$

where  $\gamma = 0.5772$  (Euler's constant), and that the standard deviation of the extreme-values is

$$\sigma_{n_e} = \frac{\pi}{\sqrt{6}} \frac{1}{(2 \ln vT)^{1/2}} \quad (3-32)$$

From Equations (3-31) and (3-21), the mean extreme value of bending moment is

$$\bar{M}_e = \bar{n}_e \sqrt{m_0} \quad (3-33)$$

$\bar{M}_e$ , the mean extreme-value of bending moment will be used as the primary basis for comparison in evaluating the effect of main hull stiffness on the ship's dynamic response to wave-excitation forces.

### 3.2.6 Evaluation of Fatigue

In the evaluation of the effects of main hull stiffness on the fatigue-related problems of wave-excited hull vibration, it was decided that the cumulative damage in fatigue

as evaluated by Miner's linear-cumulative-damage criteria would be used<sup>9,10</sup>) It is realized that the stresses from hull loadings other than the wave-excited vibratory response are important in the total cumulative-fatigue-damage calculation and that the calculation itself has shortcomings with respect to the prediction of actual hull failures. Miner's linear-cumulative-damage criteria is intended to predict fatigue-crack initiation or failure of small structural components, and the ship-fracture problem is more closely associated with crack propagation from existing flaws. This cumulative-damage criteria is intended only for comparison purposes, and for this purpose it is believed to be a useful and valid tool. However, because of the short time period,  $10^8$  seconds, the arbitrary stress-concentration factor, 3.0, and the assumptions stated above, the results of the computations should not be interpreted as valid design data.

The cumulative damage, AD, can be expressed in the following form:

$$AD = \int_0^{\infty} \frac{n(S)}{N(S)} dS \quad (3-34)$$

where  $n(S)dS$  is the number of stress cycles with amplitudes between  $S$  and  $S+dS$ , and where  $N(S)$  is the number of cycles to failure for a specified material of the same stress level. This assumes that the S-N relationship can be established.

Assuming a narrow band, stationary response process of duration  $T$ , the total number of stress cycles will be  $\nu T$ , in which case

$$n(S)dS = \nu T p(S)dS \quad (3-35)$$

where  $p(S)$  is the probability-density function for stress amplitude  $S$ . Substituting equation (3-35) in equation (3-34) gives

$$AD = \nu T \int_0^{\infty} \frac{p(S)}{N(S)} dS \quad (3-36)$$

Most S-N curves can be expressed in the form

$$N(S) = \left( \frac{S_1}{S} \right)^{b_{N_1}} \quad (3-37)$$

where  $(S_1, N_1)$  is a representative point on the S-N curve. If  $p(S)$  is of the Rayleigh form, equation (3-36) may be expressed in the following form:

$$AD = \frac{vT}{N_1} \left( \frac{\sigma_s}{S_1} \right)^b 2^{b/2} \left( \frac{b}{2} \right)! \quad (3-38)$$

where  $\sigma_s^2$  is the variance of the fatigue-producing stress. For calculation purposes,  $\sigma_s^2$  has been assumed to be equal to the variance of the main-deck stress as produced by  $M(t)$  and multiplied by an assumed stress-concentration factor of 3.0:

$$\sigma_s^2 = \left( \frac{3\sqrt{m_c}}{Z} \right)^2 \quad (3-39)$$

where  $Z$  is the midship section modulus.

For the purpose of evaluating the effect of the ship stiffness on fatigue loadings that result from the response of the ship to dynamic-wave excitation, the cumulative damage was calculated in accordance with equation (3-38) for a time period equal to  $10^8$  seconds in a Pierson-Moskowitz fully-developed sea with a significant wave height of 10 feet.

#### 4. PARAMETRIC ANALYSES

##### 4.1 General

The objective of the parametric analyses was to define trends in dynamic responses due to propeller, slam and wave excitations, as a result of variation in hull stiffness for three representative ship types.

The ship types chosen were a large tank ship, a general cargo ship and a Great Lakes ore carrier. The reason for choosing these were that they are prevalent in U. S. shipping today, have significantly different characteristics, and current trends in their design are likely to alter their hull stiffness and consequently their vibratory response. The specific vessels analyzed were a 249,300 DWT tank ship, the 712 ft. Great Lakes ore carrier STR. EDWARD L. RYERSON and the 544 ft. general cargo ship S. S. MICHIGAN. The inboard profiles of these vessels are shown in Figures 4-1, 4-2 and 4-3. The principal characteristics of the ship are also given in these figures.

The particular tank ship shown was chosen since the vessel is believed to experience wave-excited hull vibration and the owner readily consented to make the design available to the project. Also, full-scale hull-girder stress measurements are being gathered on a similar ship and it is hoped that they will be made available in the future for correlation with calculations presented in this report. This vessel has a high-strength steel deck and bottom structure, and the as-built section modulus was determined considering the reductions accordingly allowed by the classification societies.

The RYERSON was chosen since it is of an advanced design, it has been widely used in U. S. Coast Guard projects, and full-scale data has been obtained and published. The RYERSON has high-strength steel in the tank-top plating. The main hull is of mild steel, however.

The choice of the S. S. MICHIGAN was a compromise since the researchers were unable to secure the design of a modern containership. Full-scale measurements of propeller-induced vibration on this ship are available, however. This vessel has considerable amounts of high-strength steel in the main hull structure and a section modulus which has been determined accordingly.

The analytical models of the ships consist of a double elastic axis representing the main hull and the double bottom, together with the propulsion system and the deckhouse.

# TANK SHIP

## PRINCIPAL CHARACTERISTICS

LOA	----- 1153'-0"	SHP	32 000 @ 80 RPM
LPP	----- 1085'-1"	SPEED	~ 15.7 KNOTS
LWL	----- 1107'-0"	PROP DIA. 6 BLADES	29.19'
BEAM, MLD.	----- 170'-0"		
DEPTH, MLD.	----- 45'-6"	L/B	----- 6.38
DRAFT, FULL LOAD	----- 63'-0"	B/T	----- 2.70
DRAFT, BALLAST AFT 36'-8" FWD 23'-8"		C <sub>B</sub>	----- .89
DISPL., FULL LOAD	----- 286300LT		
DISPL., BALLAST	----- 126000LT		

4-2

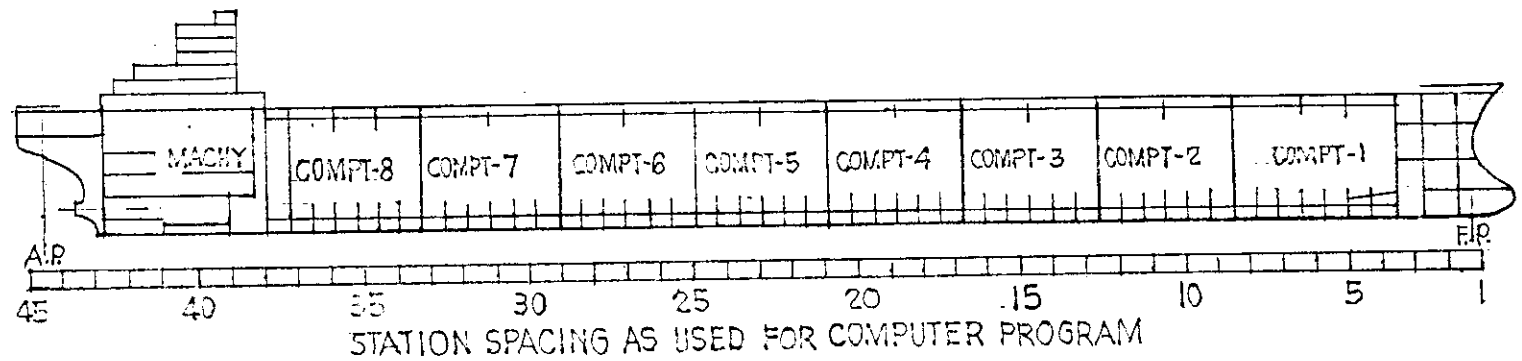


FIGURE 4-1

# ORKLA LAKLS ORE CARRIER SIR. EDWARD L. RYERSON

## PRINCIPAL CHARACTERISTICS

LOA	730'-0"	SHP	9000 @ 105 RPM
LPP	712'-0"	SPEED	14.55 KT
LWL	730'-0"	PROP DIA. (5 BLADES)	20'-0"
BEAM, MLD.	82'-0"	L/B	9.99
DEPTH, MLD.	39'-0"	B/T	2.88
DRAFT, FULL LOAD	26'-0"	C <sub>B</sub>	.89
DRAFT, BALLAST AFT 22'-0" FWD 12'-0"			
DISPL., FULL LOAD	34,135 LT		
DISPL., BALLAST	21,132 LT		

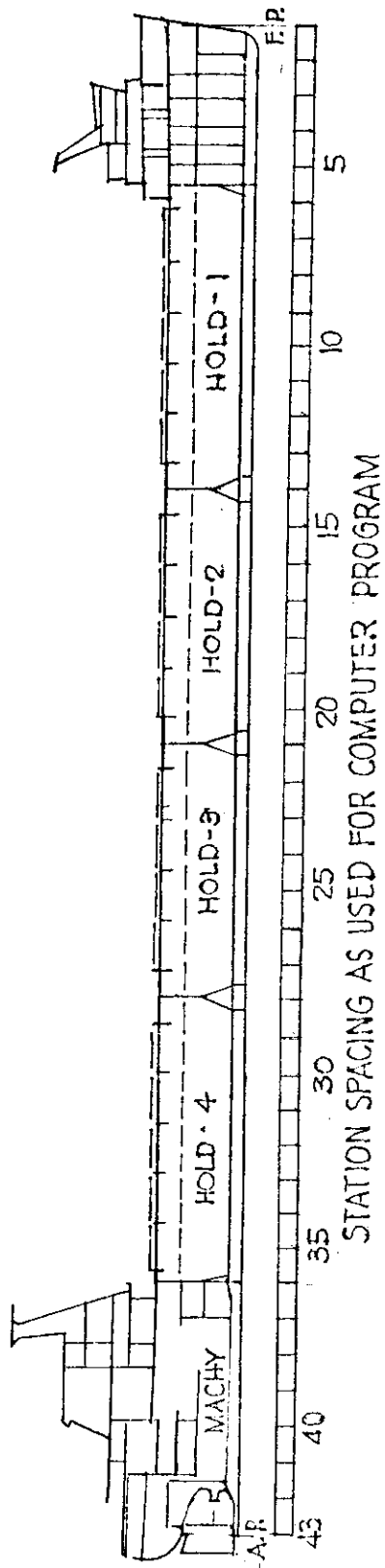


FIGURE 4-2

# GENERAL CARGO SHIP S.S. MICHIGAN

## PRINCIPAL CHARACTERISTICS

LOA	579'-0"	SHR. 24,000	@	RPM
LPP	544'-0"	SPEED		23 KT.
LWL	540'-0"	PROP DIA. (6BLADES)		22'-6"
BEAM, MLD.	82'-0"	L/B		6.59
DEPTH, MLD.	45'-6"	B/T		3.04
DRAFT, FULL LOAD	27'-0"	C <sub>8</sub>		.53
DISPL, FULL LOAD	18,100 LT.			

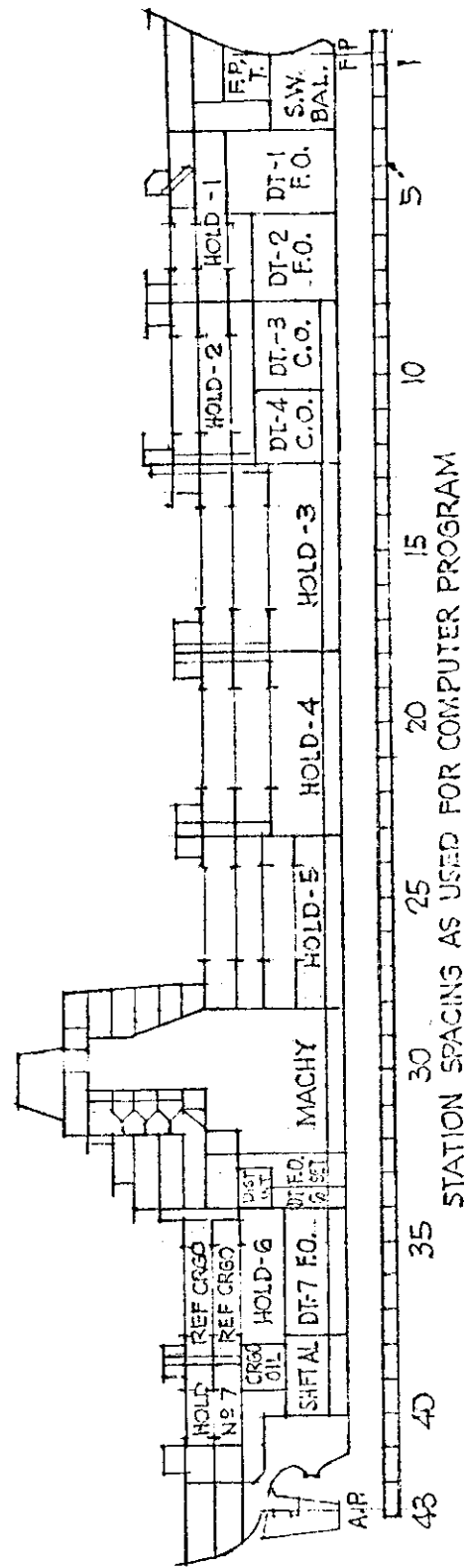


FIGURE 4-3

Table 4-1 summarizes the ship models used in the analysis. Table 4-2 summarizes the variations in the ship characteristics that were incorporated in the parametric analyses.

A detailed description of the program input data and the output follow. The discussion of the results appears in Section 5.

#### 4.2 Input Data for Parametric Analyses

##### 4.2.1 List of Input Data

Listed below is the input data required for each ship in order to perform the various vibratory-response calculations. The list is followed by a discussion of the data that require special consideration.

##### Hull Data:

- a. No. of ship stations (max 45)
- b. Ship length
- c. Displacement
- d. No. of modes of response (max 40)
- e. Young's modulus
- f. Fraction of critical damping
- g. Shear modulus
- h. Main-hull segment moment-of-inertia
- i. Main-hull segment shear area
- j. Double-bottom moment-of-inertia
- k. Double-bottom shear area (propeller- and slam-excited vibration only)
- l. Spring stiffness of connection between main hull and double-bottom girders
- m. Mass of main hull
- n. Mass points of double bottom
- o. Buoyancy per station space

##### Deckhouse Data:

- a. No. of decks in superstructure
- b. Fwd and aft connection points to main-hull girder
- c. Fwd. and aft spring stiffness of connection between superstructure and main hull
- d. Mass of superstructure
- e. Shear area, and moment-of-inertia of sections between decks of superstructure

Table 4-I

Ship Models

<u>Ship</u>	<u>Double-Bottom Computer Representation</u>	<u>Deckhouse Computer Representation</u>	<u>Propulsion-System Computer Representation</u>
Tank Ship (Ballast)	Machinery Space Double Bottom only	6-Deck Superstructure (Condensed to 4 mass points)	Propulsion System Included
Tank Ship (Full load)	Machinery Space Double Bottom only	6-Deck Superstructure (Condensed to 4 mass points)	Propulsion System Included
MICHIGAN (Loaded)	Complete Double Bottom	4-Deck Superstructure (Top of house ignored)	Propulsion System Included
RYERSON (Ballasted)	Complete Double Bottom	Superstructure modeled as part of hull	Propulsion System Included
RYERSON (Loaded)	Complete Double Bottom	Superstructure modeled as part of hull	Propulsion System Included

Table 4-II

Ship Parameter Variations

	<u>Ships</u>		
	<u>RYERSON</u>	<u>MICHIGAN</u>	<u>Tank Ship</u>
Loading Conditions:	Loaded Ballasted	Loaded	Loaded Ballasted

Hull Stiffness Variations

	(1)	(2)	(3)	(4)	(5)
Hull Bending Stiffness, %	60	80	100	120	140
Hull Shear Stiffness, %	77	90	100	110	118

Double Bottom, Propulsion System, and Deckhouse Stiffnesses remained constant throughout all investigations.

Excitation VariationsPropeller Excitation:

$$\text{Vertical Excitation Force: } F_V = K_1 \overline{\text{cpm}}^{n_1}$$

$$\text{Thrust Excitation Force: } F_T = K_2 \overline{\text{cpm}}^{n_2}$$

	<u>K<sub>1</sub></u>	<u>K<sub>2</sub></u>	<u>n<sub>1</sub></u>	<u>n<sub>2</sub></u>	<u>cpm Range</u>
RYERSON (Ballasted & Loaded)	2.68 x 10 <sup>-5</sup>	1.34 x 10 <sup>-5</sup>	2.0	2.0	300-600
MICHIGAN	1.62 x 10 <sup>-5</sup>	0.81 x 10 <sup>-5</sup>	2.0	2.0	300-600
Tank Ship (Ballasted)	6.94 x 10 <sup>-5</sup>	3.47 x 10 <sup>-5</sup>	2.0	2.0	400-700
Tank Ship (Loaded)	8.00 x 10 <sup>-5</sup>	4.00 x 10 <sup>-5</sup>	2.0	2.0	400-700

Excitation Variations (Continued)Slam Excitation:

Impulse = 100 ton-seconds  
 Impulse Shape: half-sine pulse

	<u>Slam Duration, seconds</u>	<u>Slam Location</u>
RYERSON	0.0625, 0.125, 0.25, 0.50, 1.00	Station 1
MICHIGAN	0.04, 0.08, 0.16, 0.32, 0.64	Station 8
Tank Ship	0.0625, 0.125, 0.25, 0.50, 1.00	Station 3

Wave Excitation:

Wave Encounter Frequencies: 60, 80, 90, 95, 98, 100,  
 (as % of first natural frequency) 102, 105, 110, 120, 140

	<u>Ship Speeds, feet per second</u>	
	<u>Head Seas</u>	<u>Beam Seas</u>
RYERSON	0, 10, 20, 30	20
MICHIGAN	10, 20, 30, 40	30
Tank Ship	0, 10, 20, 30	20

$$\text{Sea Spectrum: } S(\omega) = \frac{8.39}{\omega^5} e^{-\frac{33.56}{H^2 \omega^4}}$$

where H = 10 feet.

Propulsion-System Data:

- a. Vertical location of shaft with respect to main hull and double-bottom elastic axes
- b. Stiffness of shaft, thrust collar, bearing, housing and foundation
- c. Mass of propulsion system
- d. Location of thrust-bearing foundation

Propeller-Excitation Forces:

- a. Excitation input location
- b. Frequency range of desired response
- c. Fraction of basic thrust corresponding to max. excitation for both vertical-induced surface and bearing forces and longitudinal alternating thrust
- d. Phase between combined bearing and surface forces and longitudinal alternating thrust excitation
- e. Coefficients for variation of excitation with changes in RPM

Slam Forces:

- a. Type of pulse (half-sine, rectangular, damped-sine)
- b. Slam location station
- c. Slam duration
- d. Impulse

Wave-Excitation Forces:

- a. Fundamental Ship Vibration Frequency
- b. Hydrodynamic damping (frequency dependent)
- c. Hydrodynamic mass (frequency dependent)
- d. Draft and sectional area at each ship station
- e. Sea spectrum
- f. Material S-N curve

4.2.2 Main Hull and Double-Bottom Properties

The double elastic axis idealization used for the ship hull in the calculations requires that bending and shear stiffness values be estimated for the main hull as well as the double bottom. This was done by estimating the portion of ship double bottom that effectively behaves as a secondary vibratory

system coupled to the main hull. Estimations of the amount of cargo and added mass of water that effectively move with that portion of double bottom were also required.

The main hull bending and shear-stiffness values were obtained by calculating section properties for the hull cross section at several points along the length of the ship, fairing curves of moment of inertia and effective shear area through the calculated points, and then picking off individual values at the various ship stations. Similar properties were estimated for the double-bottom structure by estimating the deflected vibratory shape of the bottom, taking into account the boundary conditions at the sides of the bottom structure and then estimating an effective width of bottom structure which if vibrating entirely at the maximum amplitude (the relative amplitude between the CVK and ship sides) would have the same kinetic energy as the real structure. This estimation reflects both the cargo mass and added mass movements associated with that portion of the bottom structure. Once the effective width of bottom structure is estimated, the longitudinal bending and shear stiffness of that portion is assigned to the bottom girder.

Top and bottom girder masses were determined in much the same way (see Section 4.2.5.3 for added-mass input determination).

The support springs that connect the top and bottom girders between transverse bulkheads have their stiffnesses estimated on the basis of the transverse stiffness of the double bottom for each station space. The stiffness values assigned to these support springs include both the bending and shear stiffness of the double bottom.

The stiffness of the buoyancy springs is simply based on the water-plane area between stations at the load waterline.

For the parametric analysis of hull-stiffness effects on dynamic response, the above mentioned main-hull bending stiffness was varied from 60 to 140 percent of the basic bending stiffness (as built) in steps of 20 percent. This is the only bending stiffness that was varied. The stiffness properties of the bottom structure, deckhouse, and propulsion system were maintained constant.

Actual variations in main-hull bending stiffness for a given ship length and capacity can be accomplished in several

ways: (1) by changing the proportions of the cross section, (2) by changing allowable stresses (and therefore reducing scantlings) through application of higher strength steels, or (3) by use of other materials such as aluminum. In each of the above schemes for altering the bending stiffness of the ship, the shear stiffness will bear a different relationship to the bending stiffness. If hull bending stiffness is reduced by either of the first two methods, the reduction in bending stiffness will be more rapid than the reduction in shear stiffness. For this reason the shear stiffness values used in association with the varying bending stiffness values were chosen so the shear stiffness varies approximately as the square-root of the bending stiffness variation.

<u>BENDING STIFFNESS</u> (percent)	<u>SHEAR STIFFNESS</u> (percent)
60	77
80	90
100	100
120	110
140	118

These stiffness variations, for the main hull only, were used throughout all investigations of each type of vibratory excitation - propeller, slam and wave.

The mass and stiffness values discussed above that were used for the three ships, are tabulated in Appendix A, Tables A-1 through A-3. (Added mass has been included in the hull mass.)

#### 4.2.3 Deckhouses

A tall deckhouse is represented on two of the ships, the tank ship and the general cargo ship, and the bending and shear stiffness of the deckhouse in the vertical direction had to be determined, as well as the stiffness of the connection between deckhouse and main hull. For the RYERSON the long superstructure was included as part of the hull.

The mass and stiffness properties of the deckhouse were estimated in much the same way as for the main hull; however, the data on which these estimates were made was very limited. In addition, the lack of vertical continuity of structure in the deckhouses made it very difficult to estimate the effective stiffness values. The most important aspect of

deckhouse stiffness is the house-to-hull connection stiffness and this is possibly the most questionable of all estimated values. The importance of very accurate estimates in the stiffness of the deckhouse to the trends studies in this investigation is believed to be minimal; nevertheless, a serious effort was made to accurately estimate these stiffness values.

The mass and stiffness properties of the deckhouses can be found in Appendix A, in Tables A-4 and A-6.

#### 4.2.4 Propulsion System

Longitudinal degrees of freedom for the propulsion system are represented, and it is necessary to determine the longitudinal stiffness of the shafting as well as the stiffness of the thrust-bearing foundation.

The estimates of the mass and stiffness properties for the propulsion system were based on available propeller and shafting drawings and were rather straightforward except for the estimates of thrust bearing and foundation stiffness and the effective mass of gearing that moves with the forward end of the shaft (1 thru 4). The propulsion system properties can be found in Appendix A in Tables A-4 through A-6.

#### 4.2.5 Excitation Input

##### 4.2.5.1 Propeller Excitation

The representation of the propeller-excitation forces assumes that the hull-surface pressure forces and the stern-tube bearing forces can be combined vectorially into a single harmonically varying vertical force whose phase relationship to the longitudinally oscillating thrust forces on the propeller is known and remains constant throughout the frequency range investigated. This constant phase relationship is an over-simplification but there is little established technical data upon which to base a more elaborate relationship.

In the present investigation, because emphasis has been placed on the effects of varying main-hull stiffness, it was assumed that the phase angle between the vertical propeller-excitation force and the longitudinal thrust-excitation force was zero-degrees. This phase angle has been held constant throughout the investigation.

In addition to the above simplifications with regard to propeller-excitation forces it was assumed that both the vertical and the thrust-excitation forces were a constant percentage of the steady thrust, 7 percent and 3.5 percent respectively (see Section 2 for ranges given in the literature), and that the steady thrust varied parabolically over the range of frequencies studied. The frequency range over which the response was calculated was based on the number of blades on the propeller and a maximum shaft speed of about 120 RPM. For the tank ship this approximately corresponded to 67-117 RPM, for the RYERSON 60-120 RPM and for the general cargo ship 60-120 RPM.

In calculating the response to propeller excitation, 25 mode shapes were used in the majority of the calculations, the first two of which are the rigid-body modes of translation and rotation (heave and pitch). 25 modes proved to be insufficient for the tank ship since the response was calculated over a range from 400 to 700 cycles-per-minute, and the 25th natural frequency ranged from about 430 cpm to 530 cpm for the range of stiffnesses investigated. Therefore, 40 mode shapes (the maximum possible) were used in calculating the response to propeller excitation for the tank ship.

#### 4.2.5.2 Slam Excitation

Various assumptions were made with regard to the slam-excitation forces chosen for this investigation. Because the three ship types chosen for the investigation varied so greatly, it was decided that a different type of slam impact should be simulated in each case. For the general cargo vessel, a bottom slam was simulated; for the tank ship, a bow-flare slam; and for the Great Lakes ore carrier, a wave-slap. These were assumed to be the most typical type of slams for each ship.

For each ship, five separate slams of equal impulse, 100 foot-tons, but of varying duration were applied to the same ship station for all variations of ship stiffness. The duration of the slams applied to the bottom structure of the general cargo vessel at station 8 varied from 0.04 seconds to 0.64 seconds in equal logarithmic increments. In a similar manner, the duration of slams applied to the main hull of the tank ship at station 3 and the main hull of the Great Lakes ore carrier at station 1 varied from 0.0625 seconds to 1.0 second, also in equal logarithmic increments.

The pulse shape used in all cases was a half-sine-wave pulse. The impulse magnitude was 100 tons-seconds and held constant for all slam calculations.

#### 4.2.5.3 Wave Excitation

The ship data required for the calculation of wave-excited vibratory response is considerably in excess of that required for propeller- and slam-excited response. Because the wave-excited vibratory response is centered about the ship's fundamental frequency of vertical vibration and because this frequency can be significantly below the frequency of propeller excitation, a more careful calculation of the frequency-dependent added-mass values must be undertaken. In addition, hydrodynamic-damping forces, which are also frequency dependent, must be calculated and used in constructing the wave-excitation force vectors. The excitation-wave height must be modified for the so-called "Smith Effect" and sectional area coefficients and local drafts are required for this calculation.

The researchers faced a dilemma in choosing between the 2-parameter Lewis form and the close-fit or mapping methods to calculate the added mass and damping, neither having been validated in the relatively low-frequency range of the first-flexural-mode vibration in question. The close-fit method would have been a safer approach but it was too time consuming and costly to use in a relatively small project. Grim's 2-parameter method (see Section 2.4.2.1) which uses the Lewis form was selected after consultation with leading hydrodynamicists. This method cannot be used for bulbous bows and wherever such sections occurred approximate estimates of added mass and damping were made by these researchers. The results of the calculation can be found in Appendix A in Tables A-7 through A-11 and Figures A-1 through A-8.

The fundamental frequency of vertical vibration as determined in the calculation of propeller-excited response was used to calculate added mass and hydrodynamic-damping values for use in the wave-excited vibratory-response calculation. Since the variations in ship stiffness altered the natural frequency significantly, separate added mass and damping values had to be calculated for each value of ship stiffness.

Once these added mass and  $\bar{A}$  (where  $\bar{A}$  = ratio of generated wave amplitude to heave amplitude) values were determined for each ship stiffness, they were held constant

throughout the wave-excitation frequency range. This excitation frequency range varied from  $0.6 \omega_n$  to  $1.4 \omega_n$  in eleven increments, where  $\omega_n$  is the natural frequency of the fundamental mode. The eleven calculation increments were not uniformly spaced throughout the frequency range, but were spaced so as to obtain a good definition of the response peak at the resonant frequency.

For each ship and each ship loading, wave-excited vibratory response was calculated for head seas of unit amplitude and various ship speeds - usually 0 to 30 feet-per-second in 10-feet-per-second increments - however, a range of 10 to 40 feet-per-second was used in the general cargo ship calculations. Additional calculations were made for beam seas at a ship speed of 20 feet-per-second. Although the speed range given is particularly high for actual Great Lakes ore carriers the investigation was still carried out purely to indicate trends with speed for ships of different stiffnesses.

To obtain the variance of the bending-moment response of the ship to wave excitation, it was necessary to specify a representative sea state. The Pierson-Moskowitz spectrum with 10 ft. significant wave height was employed in the analysis. This corresponds to a sea state of 5-6.

#### 4.3 Results of the Parametric Analyses

##### 4.3.1 General

The type of vibratory-response data obtained for each type of vibratory excitation (i.e., propeller, slam and wave) was determined on the basis of which aspect of response was a design concern. Below, each type of response is considered in detail and the graphs and tables developed are described.

##### 4.3.2 Propeller-Excited Vibration

Propeller-excited vibration has historically manifested itself in local vibration and noise problems aboard ship. These problems have resulted in crew discomfort and damage to sensitive equipment. The problems have manifested themselves mainly in the after end of the ship and can be predicted if amplitudes, velocity and acceleration due to the vibration are known. Therefore, the direct output from the computer analysis consisted of vibration amplitude over the operating frequency range considered. From this data corresponding vibratory velocities and accelerations were determined.

The information derived from the computer output is listed below and may be found in Appendix B along with samples of the direct computer output. (Tables B-1 through B-10 and Figures B-1 through B-51)

1. Tabulation of peak stern vibratory amplitude, velocity and acceleration (for all ships and stiffnesses) for the frequency range considered.

2. Tabulation of peak vibratory amplitude of a point on the shafting just before the thrust bearing (for all ships and stiffnesses).

#### 4.3.3 Slam-Excited Vibration

Besides being dependent on the structural properties of the ship, the slam-excited vibration will vary depending on the duration of the slam pulse, its magnitude and shape, and the location at which it is applied.

Slamming can result in both local structural damage and main-hull bending moments and shears. Although the local effects were not generally considered in this study, a severe slam on the main hull will frequently produce local damage. Thus, the computer output consisted of bending moments and shear forces as a function of time at given locations, or as a function of location along the hull.

For the MICHIGAN the double-bottom bending moment and hull-double-bottom connection forces were obtained as additional output. This information was obtained primarily to determine the effects of main-hull stiffness on local response.

Knowledge of the time history of the main-hull bending moment can give an indication of the strain rate, since  $\frac{dM}{dt} \propto \frac{d\varepsilon}{dt}$ , and strain rates may play an important role in the initiation and propagation of brittle fractures.

The plots derived from the computer output are listed below and may be found in Appendix B along with samples of the direct computer output. (Figures B-52 through B-105)

1. Maximum Bending Moment vs Ship Stiffness for all pulse durations (all ships)
2. Max. Midship Bending Moment vs Ship Stiffness for all pulse durations (all ships)

3. Max. Shear Force vs Ship Stiffness for all pulse durations (all ships)
4. Strain Rate vs Ship Stiffness (MICHIGAN (loaded) - shortest pulse only)
5. Max. Double Bottom Bending Moment at Slam Location vs Ship Stiffness (MICHIGAN (loaded) - for all pulse durations)
6. Double Bottom to Hull Connections Forces vs Ship Stiffness (MICHIGAN (loaded) - for all pulse durations)

#### 4.3.4 Wave-Excited Vibration

The vibratory response due to wave-exciting forces occurs in resonance at the fundamental natural ship frequency only. The response of concern for this type of vibration has been both the magnitude of the bending moment and amount of cumulative fatigue damage produced by its repetitive nature, since full scale measurements of this vibratory phenomena have indicated unusually high bending moments occurring at the fundamental frequency of the hull.

Because of the characteristics of wave-excited vibration described above, one measure of response obtained from the computer analysis was the midship bending moment at resonant-wave encounter for various ship speeds, headings, and stiffnesses. In addition, the fundamental ship natural frequency was always obtained. The bending moment associated with regular seas of unit amplitude is not a correct measure of the wave-excited ship response in a random sea. Therefore a statistical analysis employing a Pierson-Moskowitz sea spectrum was performed as described in Section 3.2.5. This analysis gave the mean extreme bending moment in addition to the maximum bending moment, and is more representative of the response of the ship in a random sea.

The graphs and tables developed from the computer output are listed below and may be found in Appendix B. (Figures B-106 through B-116 and Table B-11)

1. Spectral Density and Schlick Number vs Natural Frequency
2. 2-Node Natural Frequency vs Ship Stiffness
3. Mean Extreme Bending Moment vs Ship Stiffness (all ships - random seas)
4. Maximum Bending Moment/Unit Wave Amplitude vs Ship Stiffness (RYERSON, loaded - regular seas)

5. Maximum Bending Moment/Unit Wave Amplitude vs Ship Speed (RYERSON, loaded - regular seas)
6. Maximum Bending Moment/Unit Wave Amplitude vs Heading Angle (RYERSON, loaded - regular seas)
7. Tabulation of Statistical Output (Including Cumulative Fatigue Damage Data)

## 5. DISCUSSION OF RESULTS AND TRENDS

### 5.1 General

The type of response output that has been analyzed for each type of vibratory excitation has been discussed in Section 4, Parametric Analyses. Here, this output is discussed in light of the trends and stiffness parameters presented in Section 5.5, Design Trends. Some additional special investigations were also performed and are presented herein.

It should be noted that in the case of propeller and slam-induced vibration the presence of the double bottom, propulsion system and deckhouse may have had a modifying effect on the level of main-hull response. This would have been due to the vibratory response of these secondary systems and their somewhat random coupling with the main-hull vibration. Although this effect may have at times confused the overall trends of response with changes in main-hull stiffness, it was believed that the elimination of these effects would have oversimplified the results and detracted from their credibility.

It is important to remember, however, that the type of vibratory response considered in this study is that of the main-hull girder, and although some subsystems are included in the computer models, local vibration is not considered.

### 5.2 Propeller-Excited Vibration

#### 5.2.1 General

The propeller-excited vibration calculations for the three ships considered were performed for approximately 50% - 100% of full power, although the ship types studied are intended to be operated at full power whenever possible.

As discussed in Section 4.3.2, if the propeller-excited vibration is significant it will usually cause discomfort to operating personnel and malfunction of sensitive machinery without causing heavy machinery and hull structural damage. The only item of the foregoing that is amenable to quantitative evaluation is that of personnel comfort, since general information regarding machinery-acceptable vibration levels are scarce.

Figures 5-1, 5-2 and 5-3, which have been reproduced from Reference (1), give the "fatigue decreased proficiency limits" for 8-hour exposure of personnel to vertical

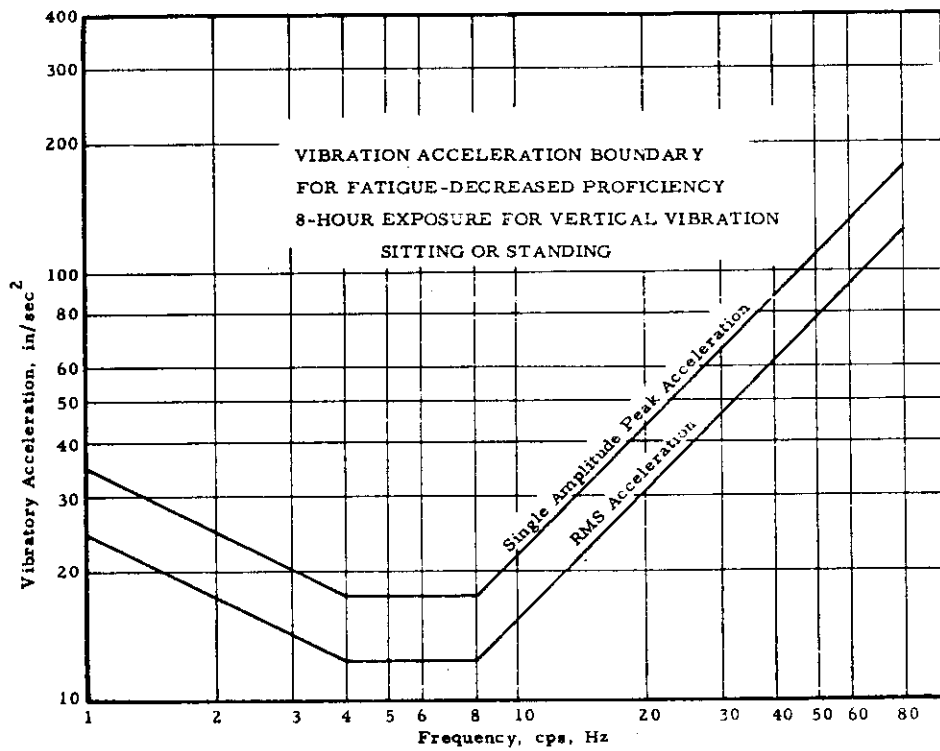


FIG. 5-1 ISO guide for evaluating human exposure to whole-body vertical vibration (acceleration, ips units)

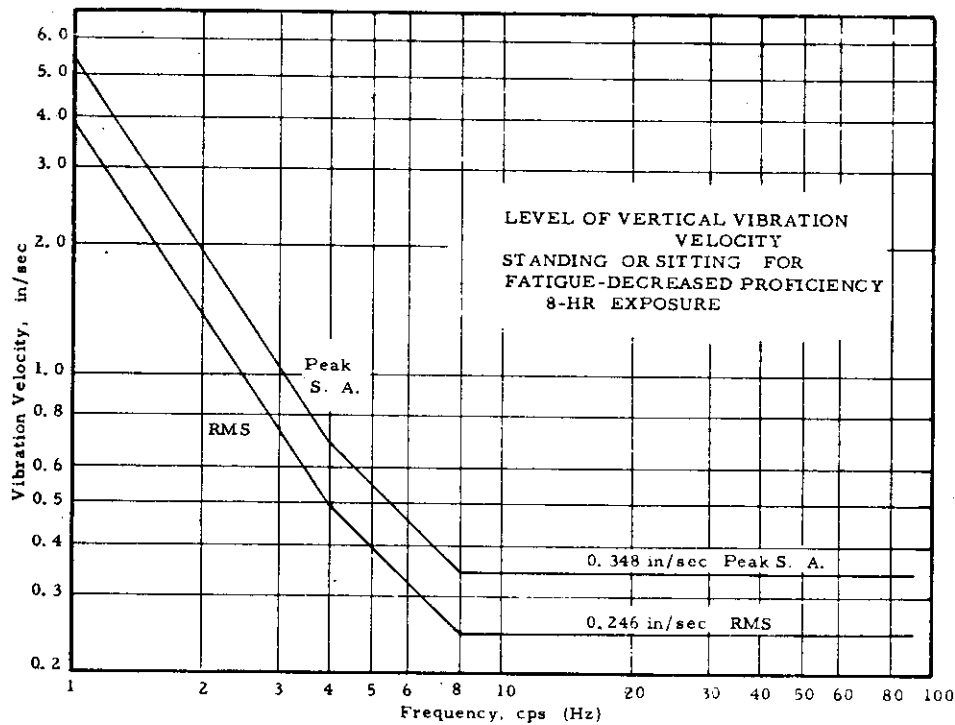


FIG. 5-2 ISO guide for evaluating human exposure to whole-body vertical vibration (velocity, ips units)

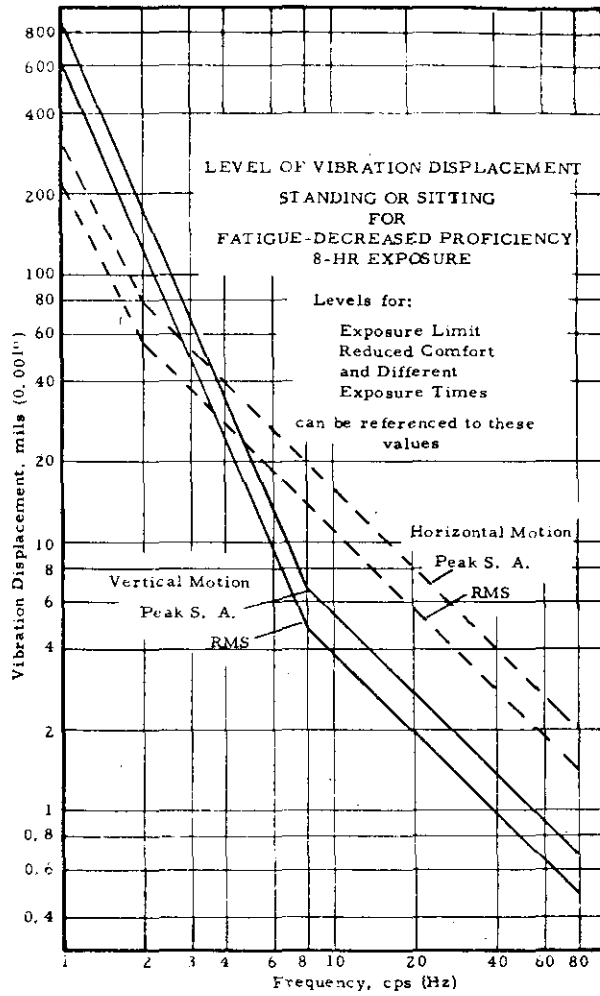


FIG. 5-3 ISO guide for evaluating human exposure to whole-body vibration expressed as displacement in mils (0.001 in.)

vibratory acceleration, velocity and displacement respectively. The exposure limits for other time intervals, the "maximum safe exposure limits" (longer) and "reduced comfort limits" (shorter) can be determined from these<sup>1)</sup>

The trends and the parametric analyses results will be discussed with respect to Figures 5-1, 5-2 and 5.3.

The ship locations where propeller-excited response has been calculated are at the stern, the foreward engine-room bulkhead, the bow, the propeller, and on the shaft at the thrust bearing. The response for the hull is given in the vertical direction while that for the shaft is given in the fore-and-aft direction. It was assumed that the response at the stern and on the shaft would provide the best indication of overall vibratory response and these two locations were used for comparison with human-comfort criteria based on an 8-hour exposure.

#### 5.2.2 Large-Tank Ships

The results of this study indicate that propeller-excited vibration of the main-hull girder for large-tank ships is not very sensitive to changes in main-hull-girder stiffness. In addition, if propeller-excitation forces are essentially of the magnitude assumed in this study the vibration levels should be acceptable. This indicates that a design criteria for the main-hull stiffness of these ships based on propeller-excited vibratory response is not warranted.

Hylarides<sup>2)</sup> also indicates that this is the case for modern tank ships, bulk carriers, and freighters. He states that increased propeller-induced vibration in modern ships is not caused by a hull resonance but by an increase of the excitation forces due to propeller cavitation and propeller-shaft resonance. The fundamental cause of both of these is ascribed to the increase of the propulsion power in modern ships. Hylarides also feels that the solution of present-day propeller vibration problems must be found in reducing the excitation forces.

Although propulsion system resonances were inherently considered in the analyses included herein, the increase in propeller-excitation forces due to cavitation was not

considered because of the lack of available methods for determining magnitudes. Pressure fluctuations have shown magnification due to cavitation of up to 20 times and more<sup>2)</sup>.

Tables B-1 and B-2 of Appendix B indicate that for the tank ship ballasted, the least stiff ship will generally have the greatest or near the greatest vibratory amplitude, velocity and acceleration at low frequencies. However, at higher frequencies (higher RPM) the stiffer ships will have the greater response.

Comparison of Tables B-1 and B-2 indicate that "fatigue-decreased proficiency limits" for 8-hour exposure are not surpassed. In fact, even if the "reduced-comfort limits" are determined by dividing the "fatigue-decreased limits" by 3.15<sup>1)</sup> the new limits are not surpassed although the least stiff ships approach the values at the lower frequencies.

Tables B-3 and B-4 indicate that in the loaded condition the response of the main hull and the shafting has significantly decreased, both still displaying the general trends with stiffness as discussed for the ballasted case. It should be noted that the ship idealization used in this study did not provide accurate modal-response predictions above 600 CPM for the tank ship in the loaded condition because of the limited number of degrees of freedom. Therefore, response comparisons for frequencies higher than 600 CPM are invalid for the loaded condition.

Figure C-3 of Appendix C indicates greatly increasing loaded weight of large tank ships with length so that the beneficial effect of increased weight on reducing hull response noted in the results above should be realized in current ships while in the loaded condition.

Figure C-4 indicates that as tanker length increases so does ship power and therefore the source of excitation. In the case of deep-draft tankers this will partially be offset by increased propeller clearances, but in the case of shallow-draft tankers this will not be the case. It is interesting to note the dual trend line displayed by Figure C-1, which indicates differences between large shallow-draft and deep-draft tank ships.

It is also important to consider Figure C-5 in conjunction with C-4 which indicates that although power is

increasing with size it is increasing at a decelerated rate with ship weight, so that the beneficial weight effect can help offset the increased exciting forces. Of course this does not necessarily apply to the ballasted condition.

Figure C-9 indicates that the longer VLCC's are becoming stiffer on the basis of  $\frac{EI}{L^3}$  as a measure while Figure C-11 indicates rapidly decreasing fundamental vibration frequencies. The latter effect is due to the rapid increase of displacement with length which offsets the increased stiffness as measured by  $\frac{EI}{L^3}$ . In addition it should be noted that particularly for the high-mode propeller-excited vibration of large-tank ships the shear stiffness becomes overwhelmingly important in the bending response and  $\frac{EI}{L^3}$  is not a direct measure of this although it indicates increases in shear stiffness also.

Considering the results of the trends and the parametric analysis simultaneously it may be stated that the apparent tendency towards increasing tanker stiffness with length, increasing weight per foot-of-length and limiting the increase in propulsion power are all steps toward keeping propeller vibration in check, even though these trends may have come about due to different considerations. (Such as maximum available SHP per shaft.) The effect of propeller clearance in shallow draft tankers will partially offset the beneficial results of the above items. It appears that the less stiff the ship the lower its tendency toward significant propeller excitation at higher RPM's.

The lack of trends data for ballasted tankers precludes comparison with the parametric-analysis results. However, it should be noted that the tank ship used in the analysis did not experience excessive vibration in the ballasted condition.

### 5.2.3 General Cargo Ships

As discussed in Section 4 the MICHIGAN was used in this study after attempts to obtain a container ship failed. However, at the time it was decided to use the MICHIGAN the trends study of container ships was already completed. Because of the amount of work involved in the trends study and the fact that both the MICHIGAN and many container ships have the same form, speed, and size although differing structure, it was felt that a comparison of the parametric analyses results of the MICHIGAN to the container ship trends could yield some insight. For these reasons a comparison was made between the two and should be viewed accordingly.

This study indicates that the main-hull stiffness does not have significant effects on the main-hull response to propeller excitation. However, the trend toward higher and higher propulsive powers in current cargo-ship designs may cause levels of propeller excitation that induce significant propeller-excited vibration regardless of main-hull stiffness. A design criteria based on hull stiffness therefore does not seem to be needed. Hylarides<sup>1)</sup> also covers this point as discussed in Section 5.2.2.

Table B-5 of Appendix B shows that increased stiffness causes considerably less response of the main hull even though in no case is the response detrimental to "8-hour comfort". On the other hand Table B-6 indicates that at the thrust bearing location the response is increased with increased main-hull stiffness, however, again, the response is not significant.

The Figures in Appendix C which correspond to cargo ships (C-15 through C-34) indicate a great amount of scatter of data. This is due to the fact that many of the ships considered were conversions from a great range of ship types as particularly emphasized by Figure C-18. For this reason it is difficult to draw conclusions from the trends. However, Figures C-19 and C-20 clearly indicate the rapid increase in power for cargo ships of increased size.

#### 5.2.4 Great Lakes Ore Carriers

The trends indicate that the larger Great Lakes ore carriers are becoming more stiff and are experiencing greater propeller-excitation forces since propulsive powers are increasing while drafts are remaining fairly constant due to restrictions. The parametric analyses indicate that increased stiffness may be detrimental when the ship is in a ballasted condition. Increased power will cause more response in any case and this should be considered in any design. The response of the RYERSON (all stiffnesses) in all cases, however, was not severe. A design criteria based on hull stiffness therefore does not seem to be warranted.

Tables B-7 and B-8 of Appendix B indicate that for the RYERSON (loaded) the vibratory response does not change significantly with changes in main-hull stiffness. In addition the response never exceeds the "8-hour comfort limit" for any stiffness.

Tables B-9 and B-10 indicate that for the RYERSON (ballast) the main-hull response does not change significantly with changes in ship stiffness and is not excessive. However, the response at the thrust bearing is larger for both the two stiffest ships and the least stiff ship.

The tables also indicate that the response of the RYERSON in the loaded condition is considerably less than in the ballasted condition.

Figure C-37 of Appendix C indicates almost an exponential increase in displacement with ship length. Figure C-38 indicates rapid increase in propulsive power with ship size. Figure C-43 shows rapid increase in main hull stiffness as measured by  $\frac{EI}{L^3}$  for increased ship size, while the leveling off of fundamental-mode frequency for increased ship size shown in Figure C-45 also indicates considerably increased structural stiffness when taken in conjunction with Figure C-37.

### 5.3 Slam-Excited Vibration

Decreased ship stiffness has been shown to be generally beneficial (See Figures B-52 through B-69 in Appendix B) with regard to the structural response of the ship to slamming loads. This would be particularly true if it could be shown that, in general, high-slam forces are associated with short-slam durations, since the greatest decrease in bending moment with decreased stiffness was associated with the shortest duration slams. The decreased response with decreased hull stiffness was only significant for short-duration slams and rational-design criteria based on this variation of slam-induced bending moment would require a careful, in-depth statistical study of full-scale slamming data.

The slam-response affects the ultimate hull strength, the possible initiation of fractures, and to a lesser degree the low-cycle fatigue strength of the hull. It should be pointed out that the shear forces associated with slam bending moments are much higher than the shear forces associated with wave bending moments of comparable magnitude and therefore the structural design of the hull to accommodate slam-induced loads should more directly involve the design of the shear strength of the hull than the bending strength of the hull. To put it another way, if the hull strength in both bending and shear is designed on the basis of wave-induced bending and shear loads, then the slam-induced loads are much more likely to overload the hull in shear than in bending.

As shown in Figures B-67 and B-68, the main-hull stiffness variations have an influence on the bottom-structure slam-induced loads. Decreased stiffness of the main hull reduces the loads imposed on the bottom structure.

A measure of the strain rate in the longitudinal direction in either main deck or bottom structure due to slam-induced bending moments is plotted in Figure B-69 as a function of ship stiffness. From this plot it appears that strain rates increase with stiffness, and this increase is most pronounced for short duration slams. However, the absolute strain rate will depend on the severity of the actual stress concentration, and it does not appear that the strain rates are high enough to affect material properties and hence the tendency of the steel to fracture in a brittle manner.

#### 5.4 Wave-Excited Vibration

##### 5.4.1 General

The most simple analysis of the effects of decreased hull stiffness on the response of the hull to wave-excited vibration shows that decreased hull stiffness will decrease the natural frequency of the two-noded mode of vibration and thus cause the natural frequency to fall in the range of wave frequencies corresponding to greater wave heights. This will result in the possibility of greater wave excitation. The picture is complicated however by the fact that a change in natural frequency alters the combination of wave length, ship speed, and ship heading required to produce resonance, and all these factors are influential in determining the level of the response. The change in frequency also changes the magnitude of the added mass and damping and further complicates the situation. Generally a lower frequency will mean less added mass and greater hydrodynamic damping and these two trends tend to cause opposite effects in the level of the response. Therefore, without an extensive analysis of the problem it is difficult to say whether resonance with seaway-wave components of increased energy will generally cause greater response.

If it is assumed that maximum dynamic response to wave excitation will not occur during periods when the quasi-static wave bending moments are near their maximum then the primary design consideration with respect to wave-excited hull vibration may be its contribution to fatigue-type failures. Although the computer calculations of cumulative damage in fatigue were intended to be used for comparison purposes only, the cumulative damage values that were calculated appear to be

unusually small. (See Table 11 of Appendix B). However, the cumulative-damage problem is not linear and a more severe stress concentration than the one assumed, or a smaller value for internal ship damping might significantly alter the apparent seriousness of the problem.

Figure B-106 of Appendix B shows the variation of fundamental vibration frequency for the different ships with changing ship stiffness. In all cases as the stiffness of the ship is reduced the natural frequency behaves likewise.

#### 5.4.2 Tank Ships

The results have shown that decreased main-hull stiffness results in increased vibratory response of the hull to wave excitation.

Figure B-107 of Appendix B indicates that large-tank ships have fundamental vertical vibration frequencies at frequencies where sea states as low or lower than 5 have significant wave energy. Significant heaving and pitching are not characteristic of such sea states.

Figures B-108 and B-109 indicate a general trend to less wave-excited response for increased stiffness for both ballasted and loaded conditions of a large-tank ship. In addition the ballasted response is almost always greater than the loaded response and increased speed results in greater response.

It is of interest to note that the tank ship that was used for the parametric analysis did experience wave-excited vibration in the ballasted condition.

Figures C-11 and C-12 of Appendix C indicate a rapid decrease in the fundamental two-noded vertical ship-vibration frequency with increased ship size for oil tankers of current design. The decrease is particularly rapid up to approximately 900 ft. or 175,000 DWT. This trend is also reflected in Figure B-107 of Appendix B. Figures C-13 and C-14 indicate increased fundamental frequency with ship speed, and tank ships of very different L/B's have nearly identical fundamental mode frequencies. The former is due to the fact that smaller stiffer tankers have faster speeds.

The trends in conjunction with the parametric-analysis output indicate that the decreasing fundamental-mode frequencies of current large-tank ships should be undertaken cautiously in order to avoid wave-excited vibration.

#### 5.4.3 Cargo Ships

In summary it may be stated that the parametric analyses of the general cargo ship in conjunction with the container ship trends do not indicate that cargo ships are likely to be subject to significant wave-excited vibration.

Figure B-110 of Appendix B indicates that only very large container ships ( $\Delta > 50,000$  tons) will experience significant wave energies at frequencies about their fundamental mode frequency.

Figure B-111 shows generally increased response with ship speed but also indicates mean extreme bending moments of only a fraction of those of large-tank ships and Great Lakes ore carriers. It is possible that the erratic nature of the curves of Figure B-111 are due to the fact that the wave-excited response is of small magnitude.

The variation in first-mode natural frequencies indicated in Figures C-30 through C-33 of Appendix C show a significant amount of scatter, probably due to the fact that many of the ships used to make the plots were conversions.

#### 5.4.4 Great Lakes Ore Carriers

The results show that Great Lakes ore carriers are very susceptible to wave-excited vibration and that decreased main-hull stiffness causes greater hull response.

Figure B-112 of Appendix B indicates that Great Lake ore carriers, even those in the 20,000-ton displacement class, can have their fundamental vibration frequency at the same value as waves of significant energy for the lower sea states.

Figures B-113 through B-116 show the great influence of speed and ship heading on the wave-excited response. This is in agreement with the fact that changes in course and lowering of speed have decreased the wave excitation of actual ships on the Great Lakes.

Both Figures B-113 and B-116 indicate that a maximum wave-excited response can possibly occur at the 100% stiffness value. However, because of the many variables involved in determining the wave-excited hull response it is possible that points of equal or greater response exist for ship stiffnesses and speeds intermediate to those considered. Therefore, only tentative conclusions can be drawn based on the trends of bending-moment response with ship stiffness. Considering all ship variations that were investigated, however, the general trends appear to indicate that the response will increase with decreased stiffness.

Figures C-44 and C-45 of Appendix C indicate a linear decrease in the measure of fundamental-mode frequency. Figure C-45 also indicates a possible leveling off for the very largest ships ( $\Delta = 65,000$  tons).

Considering the trends in conjunction with the parametric results it appears that a possible limiting of the ship fundamental frequency is a positive step in reducing wave-excited vibration. It appears from the calculations that Great Lakes ore carriers are extremely prone to wave-excited response. Considering the smaller strength of the Great Lakes ore carrier as compared to the large-tank ships the stresses introduced by the response of each will be closer than the bending-moment response that Figures B-108, B-109 and B-113 indicate.

#### 5.4.5 Special Investigations

In the course of conducting the parametric analysis several interesting sub-topics have manifested themselves. Also, a number of special investigations were conducted in addition to those required for the parametric variations.

##### 5.4.5.1 Hydrodynamic Added Mass and Damping

Tables A-7 through A-11 and Figures A-1 through A-8 of Appendix A give the hydrodynamic "added mass" and  $\bar{A}$  values for the ships used in the parametric analyses. The various curves indicate the variation of "added mass" and  $\bar{A}$  over the length of the ship for a range of oscillation frequencies. 50 rad./sec. can be considered an infinitely large frequency from a practical standpoint. In all cases the "added mass" gives consistent results increasing with increased frequency for the variations of frequency considered. On the other hand the  $\bar{A}$  values show some erratic behavior. Of importance is the high  $\bar{A}$  value at the ship ends which does not vanish even at high

frequency. The greatest amount of scatter is indicated in Figure A-6 for the RYERSON ballast condition but it should be noted that the  $\bar{A}$  values are smaller than those in the other figures. These researchers have not been able to explain the phenomena displayed by the respective  $\bar{A}$  curves.

#### 5.4.5.2 Components of the Wave-Excitation Force

The velocity correction of the buoyancy force,  $V \frac{dN'}{dx}$ , when ignored in calculating the bending-moment response of the RYERSON (loaded) at 20 feet-per-second in head seas resulted in differences of 1.0 to 2.0 percent in the bending-moment response. When  $\bar{A}$  was assumed to be zero, and hence  $N'$  and  $V \frac{dN'}{dx}$  were also zero, a 20 percent difference was noted in the peak bending moment, however, even greater differences were noted in bending-moment response away from resonance. Ignoring the buoyancy term in the exciting force resulted in a 50 percent reduction in the bending moment at resonance with still more extreme variations at other than resonant excitation. These results are presented in Table B-12.

#### 5.4.5.3 Number of Vibratory Modes Considered in the Wave-Excited Response

The number of response modes generally considered in the wave-excited vibration was 25. This number was reduced to 3 for one RYERSON (loaded) calculation. The difference in response between assuming 25 or 3 was very small, which indicates that the wave-excitation force only affects the lower response modes (see Table B-12).

### 5.5 Design Trends

#### 5.5.1 General

The trends that have been chosen for investigation here are those trends in ships proportions, size, and power that relate directly to ship stiffness or to vibration characteristics such as natural frequency or excitation magnitude. The purpose of the trends is to look at them in light of the results of the parametric analyses and to obtain any indications as to which trends, if any, may lead to unacceptable vibrations.

The approach taken has been to plot data on ship proportions and powering with respect to ship size and type in

an effort to indicate trends (See Appendix C). The trends of some ship characteristics such as machinery location and end shapes cannot easily be studied by a graphical approach. However, these characteristics are discussed briefly in Section 5.5.3.

The trends have been taken from data given in the literature on recent buildings, ships on order, and proposed ships. Data for some ships were incomplete and therefore the same plots for all three ship types was not possible. Data points on the figures of trends representing proposed ships are denoted as such on the figures to avoid confusion.

In Section 5.5.2 the characteristics which will be considered as parameters for trends are discussed.

#### 5.5.2 Stiffness Parameters

The ship characteristics considered in this investigation are the length, beam, draft, depth, block coefficient, shaft horsepower, speed, deadweight and displacement. By identifying which of these can directly influence vibratory response, various stiffness parameters based on ship characteristics can be obtained.

Ship vibratory frequency is influenced by bending stiffness, as measured by  $\frac{EI}{L^3}$  and shear stiffness as measured by  $\frac{GA}{L}$ . The midship moment of inertia<sup>1)</sup> is approximately proportional to  $BD^3$ , and  $A$  is approximately proportional to  $D$ . Therefore, plots of  $D$  vs  $L$  and  $B$  vs  $L$  will give an indication of the variation of stiffness and, therefore, indicate changes in vibratory response for certain ship types.

The mass distribution of structure and cargo are functions of the block coefficient, deadweight, displacement and ship type. The vibratory response of the ship is dependent on the manner in which this mass is distributed, so that a plot of one of the foregoing mass descriptions vs length is of interest. It should be noted that the block coefficient also indicates the form of the ship, which in turn, can be related to the hydrodynamic coefficients and wave-excitation forces.

The propeller-excitation forces are dependent on the power delivered to the propeller, as well as on the propeller, rudder and aperture design, therefore, a plot of SHP vs  $L$  and SHP vs  $\Delta$  or  $C_B$  will be of interest.

Ships that are designed in accordance with classification society rules, reflect the strength and stiffness requirements provided by those rules. Longitudinal strength requirements in the ABS rules for ocean-going ships apply to vessels having depths not less than one-fifteenth of their lengths and breadths which do not exceed twice their depth. The basic hull-girder section modulus is  $SM=c \times B \times f (C_B + 0.5)$ , where the value of  $c$  depends on the ship type and the value of  $f$  depends on ship length. The required section moduli to the deck and bottom are determined from the basic  $SM$  and the maximum still-water bending moment. Because the actual  $SM$ 's or still-water bending moments were not known for ships in this study, the basic section modulus,  $SM$ , was used. This was deemed adequate for comparison purposes.

It is evident from the  $SM$  formula that section modulus is a function of  $c$ , which is determined by ship type,  $f$ , which is a function of ship length,  $B$ , ship beam and  $C_B$ , block coefficient. Therefore, plots of  $SM$  vs length, beam and block coefficient might be revealing.  $L/D$ 's varied from 9.5 to 13.0 for large-tank ships (11.0 to 14.0 for smaller tankers) and from 10.0 to 14.0 for container ships.  $B/D$ 's for large tank ships varied from 1.5 to 2.3 (1.6 to 2.0 for other tankers) while for container ships they varied between 1.3 and 1.9.

For Great Lakes vessels, the ABS requirement for section modulus is determined by the equation,  $SM=M_{GL} \times B \times D$ , where  $M_{GL}$  is a factor which varies with ship length,  $B$  is ship beam, and  $D$  is the design draft. If the ship is longer than 712 ft., the Ottawa (1967) Rules must be used. The section modulus is then given by  $(0.01L)^2 BZ'$  where  $L$  is ship length,  $B$  is ship beam and  $Z'$  is a factor which depends on draft, depth, beam and length. The same plots that were important for ocean-going vessels are obviously important for Great Lakes ships.

The empirical formulas of Todd, Burrill, and Schlick for estimating the fundamental frequency of hull vibration are of the form  $N=c \sqrt{\frac{I}{k\Delta L^3}}$  where  $N$  is the frequency of vibration,  $c$  is a constant depending on ship type, and  $k$  is a constant depending on whether or not "added mass" is considered. Therefore, another plot should be  $\frac{I}{\Delta L^3}$  vs  $L$  and also  $\Delta$ . For wave-excited vibration  $\frac{I}{\Delta L^3}$  vs  $V$  should be considered.

In the case of wave-excited vibration the relation of the 2-node natural frequency of vibration (that which is

excited in this type of vibration) to the seaway spectral density is extremely important and plots representing this relation are given in Appendix C.

If the ship is considered as a beam statically loaded by a point force, its bending stiffness can be measured by  $\frac{EI}{L^3}$  and its shear stiffness by  $\frac{GA}{L}$ . In addition, the midship moment-of-inertia,  $I$ , is approximately proportional to  $BD^3$  for a certain ship type and  $L/D$ , and  $A$  is approximately proportional to  $D$ . Therefore, plots of these quantities will give an indication of the variation of static stiffness and therefore may indicate changes in vibratory response for certain ship types.

### 5.5.3 Miscellaneous Trends

Certain design trends and current practices are not amenable to graphical representation due to lack of sufficient data, or because they require exhaustive investigation which could not be accommodated on this project. Some observations of the type of trends and practices alluded to are made here.

#### 1. Forebody and Afterbody Shape

End shapes exert considerable influence on the exciting forces and the hydrodynamic coefficients involved in propeller, slam and wave-induced vibrations. Invariably, the bows of container ships have raked stems with small bulbs, fine entrance and a relatively short transom stern. Modern tankers and bulk carriers tend to have full ends with a bulb and a cut-off cruiser stern. Such end shapes of vessels with high-block coefficients result in added mass and damping coefficient curves with steep slopes at the ship ends.

#### 2. Corrosion Control and Higher Strength Material

Classification societies' rules provide for taking advantage of the application of effective coatings by allowing reduction in scantlings. The ABS reduction allowance varies with structural members, however, generally speaking the reduction is 10 percent of the thickness but not more than 0.125 inch. The reduction allowances are not associated with the required hull-girder moment-of-inertia or the section moduli. Therefore, the affect of corrosion control on stiffness is not appreciable. Also, it is not common for owners to specify corrosion control on the entire top and bottom girders.

The application of higher-strength steels to a point where the entire top and bottom flanges are fabricated from them is common practice today. ABS rules permit reduction in section moduli and the moment-of-inertia when higher strength steels are used as compared to mild steel. Reduction in the section moduli may be as much as 25%. The associated moment-of-inertia is rarely down to the reduced allowance value mainly because the L/D of tankers is generally much lower than the allowable.

### 3. Gas-Turbine Engines and Nuclear Propulsion

Should there be a trend towards the use of gas turbines in the future it could influence the ship's vibratory response. One of the advantages claimed for gas turbines is that due to their compactness they can be located higher up in the ship and then some of the prime space occupied by the conventional engine room can be devoted to cargo. This could alter the structural arrangement and weight distribution aft.

The nuclear-propulsion system with its large concentrated weight, structural support and radiation and collision-protection requirements can also be expected to alter the stiffness and weight distribution. Again, this could result in different vibratory responses.

## 6. CONCLUSIONS

1. No criteria or guidelines which can be identified explicitly with vibrations exist for hull stiffness.
2. The principal weakness of the existing methods for the prediction of propeller- and slam-induced vibrations is the lack of relatively quick and reliable procedures to compute exciting forces.
3. The principal weaknesses of the existing methods for the prediction of wave-induced vibrations are (1) the lack of a validated procedure for computing hydrodynamic coefficients of added mass and damping and (2) the lack of rigor in accounting for the distribution of damping along the hull and its effect in coupling the modes of vibration.
4. Very little data are available to give separate values for cargo, structural, and viscous damping in ships.
5. In ships with low stiffness, the very high modes of hull response needed to determine propeller-excited vibrations indicate that accurate predictions using simplified ship computer models may be difficult. In addition the high frequency and mode character of the response indicates that local vibration problems may be more prevalent than any associated with the main-hull girder.
6. Propeller-excited vibratory response does not appear to be affected appreciably by increases or decreases of as much as 40 percent in the as-built ship stiffness. The responses with the assumed magnitude of excitation for the tank ship, the Great Lakes ore carrier, and the general cargo ship were found to be acceptable from human tolerance considerations throughout the stiffness variation range.
7. Slam-induced vibratory response appears to vary measurably with ship stiffness and the trends are uniform and consistent (i.e., increased stiffness increases response, and decreased stiffness lowers response). In the future, as more becomes known about slam loads, it may be desirable to develop criteria for ship stiffness based on slam vibration.

8. Large-tank ships and the Great Lakes ore carriers appear to be prone to wave-induced vibration and increased hull stiffness seems to have a beneficial affect on limiting the response. However, the response to wave excitation is extremely variable with regard to ship speed, ship-length/wave-length ratio, and the angle of encounter of the ship with the wave system so that the magnitude of the trends are not clearly defined. A stiffness criteria related to first-flexural-mode frequency may be desirable to limit wave-induced vibrations.

## 7. RECOMMENDATIONS

It has been stated previously that the investigation of ship vibration requires knowledge of structural modeling, sources and types of damping, propulsion system and seaway-induced loads, and criteria for acceptable levels of vibration based on structural behavior, machinery performance, and human tolerance of noise and vibratory motions. Of the foregoing, the sources and types of damping and propulsion system and seaway-induced loads are areas where adequate methods and procedures for predicting such quantities are particularly lacking as stated in the conclusions of Section 6.

Also, the parametric study undertaken in this report consisted of a limited scope due to the limited size of the project.

The conclusions of Section 6 and the discussion given above indicate that the work outlined below should be undertaken in the future:

1. Initiate a research project on propeller-excitation forces to obtain a better understanding of these and also reliable engineering design oriented methods for their determination. This project should include, at least, the following:

- a. Determination of the variation of the forces with propeller RPM. This is needed in order to predict propeller-induced response over an operating range.
- b. Determination of higher order blade-frequency components. This will indicate the necessary degree of harmonic analysis required for accurate prediction of the forces.
- c. Determination of relative magnitude and the phase relationships of bearing and surface forces and the location of resultant forces.

2. Initiate a research project on slam loads to obtain a better understanding of these and also reliable engineering design oriented methods for their determination. This project should include, at least, the following:

- a. Description of the space-time history of the loads. This includes the duration and shape of the force-time history of the pulse, and the magnitude of the impulse. Changes in any of these can result in measurably different vibratory response.

- b. Determination of the influence of non-linearities such as large ship motion and large wave amplitude on the hydrodynamic coefficients. Slamming occurs when these non-linearities occur and changes in the hydrodynamic coefficients could significantly alter predicted response.
3. Initiate a research project on wave induced vibration which includes, at least, the following:
    - a. Influence of forebody and afterbody shapes on excitation forces. It has already been shown that these effects are important both in this report and others.
    - b. Proper inclusion of the distribution of damping along the hull in the computer model. The importance of this has been discussed previously and the main effect is that the modes of vibration are coupled.
    - c. Evaluate the existing methods for estimating added mass and damping to assess their validity over the complete range of excitation frequencies. Most methods have not been validated for the range of wave excited vibration.
    - d. Consideration of combined horizontal-torsional vibration as well as vertical vibration. In other than head seas it is possible for this type of vibration to be excited.
  4. Research to obtain greater understanding of and values for cargo, structural and viscous damping. This could consist of a literature survey, theoretical approaches, model, and full scale measurements. The results would hopefully give a better understanding of these phenomena and ways of determining values for them.
  5. Parametric analyses with extensive variations of dimensions, speeds and headings of ships should be conducted. Although knowledge of better prediction methods for loadings, etc., outlined above, would be helpful for this, the work could still be carried out with existing knowledge to get a relative comparison between different stiffnesses. The more extensive parametric analysis would serve to more or less conclusively show the relation between hull stiffness and vibratory response.

## ACKNOWLEDGMENTS

In addition to the authors, several individuals contributed significantly to this study.

At M. Rosenblatt & Son, Inc. the foremost was Mr. Naresh M. Maniar, who provided technical input, advice, and the project management. Mr. Richard Sheffield obtained most of the data for the trends studies and input data for the computer analyses.

At U. S. Steel Corporation Mr. Joseph J. Amma made the modifications to the basic SHVRS computer program to accommodate the calculation of wave-excited hull response, and Mr. Douglas E. Splitstone assisted in the interpretation and implementation of the statistical analysis.

Finally, the members of the Ship Structure Committee reviewing this project and those individuals that were contacted throughout the industry for advice are thanked for their valuable contributions.

8. REFERENCES

Code of Abbreviations for References

DTMB	David Taylor Model Basin
IME	Institute of Marine Engineers
INA	Institute of Naval Architects
JSR	Journal of Ship Research
MIT	Massachusetts Institute of Technology
NASA	National Aeronautical and Space Administration
NSRDC	Naval Ship Research and Development Center
RINA	Royal Institution of Naval Architects
SNAME	Society of Naval Architects and Marine Engineers
SSC	Ship Structure Committee

## Section 2 References

1. TIMOSHENKO, S. and YOUNG, D. H., "Vibration Problems in Engineering," Princeton, N. J., Van Nostrand, 1955.
2. THOMSON, W. T., Vibration Theory and Application, Englewood Cliffs, N. J., Prectice-Hall, 1965.
3. BISPLINGHOFF, R. L. et.al., Aeroelasticity, Cambridge, Massachusetts, Addison-Wesley, 1955.
4. NOWACKI, HORST, "Ship Vibrations: Lecture Notes," Department of Naval Architecture and Marine Engineering, Ann Arbor, University of Michigan, January 1970.
5. KLINE, R. G. et.al., "Propeller-Excited Ship Vibrations," Paper presented at the SNAME Northern California Section Meeting, March 11, 1971.
6. SUETSUGA, I., "The Effects of the Bottom Vibration on the Hull Natural Frequencies," International Shipbuilding Progress, September 1963.
7. OHTAKA, K. et.al., "Higher Mode Vertical Vibration of Giant Tanker," 1st Report, Journal of the Society of Naval Architects of Japan, Vol. 125, June 1969.
8. KAGAWA, K. and OHTAKA, K., "Higher Mode Vertical Vibration of Giant Tanker," 2nd Report, Journal of the Society of Naval Architects of Japan, Vol. 128, December 1970.
9. OHTAKA, K., "Vertical Vibration of Ships Coupled with Bottom Vibration," 2nd Report, Journal of the Society of Naval Architects of Japan, Vol. 131, June 1972.
10. OHTAKA, K. and OHYAMA, T., "Vertical Vibration of Ships Coupled with Bottom Vibration," 1st Report, Journal of the Society of Naval Architects of Japan, Vol. 26, December 1969.
11. YAMAKOSHI, M. and OHNUMA, S., "On the Coupling of Hull Vibration and Bottom Vibration of Ships," Society of Naval Architects of Japan, Vol. 2, 1969.
12. SCANLAN, R. H. and ROSENBAUM, R., Introduction to the Study of Aircraft Vibration and Flutter, New York, MacMillan, 1951.

13. THIEN WAH ed., A Guide for the Analysts of Ship Structures, Washington, D. C., Office of Technical Services, Department of Commerce, 1962.
14. HENDERSON, F. M., "Description and Usage of General Bending Response Code 2," DTMB Applied Mathematics Laboratory Technical Note AML-59-66, August 1966.
15. LEIBOWITZ, R. C. and KENNARD, E. H., "Theory of Freely Vibrating Nonuniform Beams, Including Methods of Solution and Application to Ships," DTMB Report 1317, May 1961.
16. MacNEAL, R. H., The NASTRAN Theoretical Manual, Level 15, a NASA Publication, April 1972.
17. McDONNELL-DOUGLAS Automation Company, ICES DYNAL Users Manual, 1972.
18. ROSEN, R. et.al., STARDYNE: Users Manual, Mechanics Research, Inc., September 1972.
19. HENDERSON, F., "Transient Response Calculations in the Frequency Domain with General Bending Response Program," NSRDC Report 3613, February 1971.
20. CUTHILL, F. H. and HENDERSON, F. M., "Description and Usage of General Bending Response Code 1, DTMB Report 1925, October 1964.
21. KLINE, R. G. and CLOUGH, R. W., "The Dynamic Response of Ships Hull as Influenced by Proportions, Arrangement, Loading, and Structural Stiffness," SNAME Spring Meeting, 1967.
22. KLINE, R. G. and SHIPE, E. U., "SHVRS Computer Program Documentation," United States Steel Publication.
23. DeSALVO, G. and SWANSON, J., ANSYS Engineering System User's Manual, Elizabeth, Pennsylvania, Swanson Analysis System, October 1, 1972.
24. TRAIL-NASH, R. W. and COLLAR, A. R., "The Effects of Shear Flexibility and Inertia on the Bending Vibration of Beams," Quarterly, Journal of Mechanics and Applied Mathematics, Vol. VI, Part 2, 1953.

25. OHTAKA, K., "A Study of Vertical Vibration of Ships,"  
2nd Report, Journal of the Society of Naval Architects  
of Japan, Vol. 119, 1966.
26. GOODMAN, R. A., "Wave-Excited Main Hull Vibrations in Large  
Tankers and Bulk Carriers," Transactions of RINA, 1970.
27. JOHNSON, A. J., "On the Amplitudes of Ship's Hulls,"  
Transactions of the Institute of Engineers and Shipbuilders  
in Scotland, 1962.
28. HOFFMAN, D. and VAN HOOFF, R. W., "Experimental and Theoretical  
Evaluation of Springing on a Great Lakes Bulk Carrier,"  
Glen Cove, New York, Webb Institute of Naval Architecture,  
November 1972.
29. LEWIS, F. M., "The Inertia of Water Surrounding a Vibrating  
Ship," Transactions of SNAME, 1929.
30. PORTER, W. R., "Pressure Distribution, Added Mass and Damping  
Coefficients for Cylinders Oscillating in a Free Surface,"  
Institute of Engineering Research, University of California  
Report, 1960.
31. FRANK, W., "Oscillation of Cylinders in or Below the Free  
Surface of Deep Fluids," NSRDC Report 2375, 1957.
32. TASAI, F., "On the Damping Force and Added Mass of Ships  
Heaving and Pitching," Report of Research Institute for  
Applied Mechanics, Kyuchu University, 1960.
33. LANDWEBER, L. and MACAGNO, M. C., "Added Mass of Two-  
Dimensional Forms Oscillating in a Free Surface,"  
JSR, November 1957, p. 20.
34. LANDWEBER, L. and MACAGNO, M.C., "Added Mass of a Three-  
Parameter Family of Two-Dimensional Forms Oscillating in  
a Free Surface," JSR, March 1959, p. 36.
35. LOUKAKIS, T. A., "Computer Aided Prediction of Seakeeping  
Performance in Ship Design," MIT Report, August 1970.
36. Discussion of Paper "A New Appraisal of Strip Theory,"  
by L. Vassilopoulos and P. Mandel, In Fifth Symposium  
on Naval Hydrodynamics, edited by J. K. Lunde and S. W.  
Doroff, 1964.

37. LANDWEBER, L. and MACAGNO, M. C., "Added Masses of Two-Dimensional Forms by Conformal Mapping," JSR, June 1967, p. 109.
38. MACAGNO, C. M., "A Comparison of Three Methods for Computing the Added Mass of Ship Sections," JSR, December 1968, p. 279.
39. FALTINSEN, O., "A Study of the Two-Dimensional Added-Mass and Damping Coefficients by the Frank Close-Fit Method," Report 69-10-S, Oslo, Norway, Det Norske Veritas, 1969.
40. FALTINSEN, O., "A Comparison of Frank Close-Fit Method with Some Other Method Used to Find Two-Dimensional Hydrodynamical Forces and Moments for Bodies which are Oscillating Harmonically in an Ideal Fluid," Report 69-43-S, Oslo, Norway, Det Norske Veritas, 1969.
41. TAYLOR, J. L., "Some Hydrodynamic Inertia Coefficients," Transactions of INA, 1930.
42. DUTTON, G. W. and LEIBOWITZ, R. C., "A Procedure for Determining the Virtual Mass J-Factors for the Flexural Modes of a Vibrating Beam," DTMB Report 1623, August 1962.
43. MCGOLDRICK, R. T., "Buoyancy Effect on Natural Frequency of Vertical Modes of Hull Vibration," JSR, July 1957, p. 47.
44. SALVESEN, N., TUCK, E. O., and FALTINSEN, O., "Ships Motions and Sea Loads," Transactions of SNAME 1970.
45. TASAI, F., "Improvements in the Theory of Ships Motions in the Longitudinal Waves," Appendix II to the Report of the Seakeeping Committee, 12th International Towing Tank Conference, Rome, 1969.
46. GERRITSMA, J., GLINDORP, C. G., and PIJERS, J. G. L., "A Note on Damping and Added Mass from Vertical Motions," Report of the Seakeeping Committee, 13th International Towing Tank Conference, Hamburg, 1972.
47. WERELDSMA, R., "Propeller-Excited Shaft and Hull Vibrations of Single Screw Ships," International Shipbuilding Progress, December 1964, pp. 547-553.
48. VAN MANEN, J. D. and WERELDSMA, R., "Propeller-Excited Vibratory Forces in the Shaft of a Single Screw Tanker," International Shipbuilding Progress, September 1960, pp. 371-389.

49. HARRINGTON, R. ed., Marine Engineering, New York, SNAME, 1971, Chapter XI.
50. VORUS, W. S., "An Integrated Approach to the Determination of Propeller-Generated Vibrating Forces Acting on a Ship Hull," Ann Arbor: University of Michigan, Report 072, March 1971.
51. BRESLIN, J. P., "Theoretical and Experimental Techniques in Practical Estimation of Propeller-Induced Vibratory Forces," Symposium on Ship Vibration, February 17, 1970.
52. TSAKONIS, S., JACOBS, W. R., and ALI, M. R., "An 'Exact' Linear-Surface Theory for a Marine Propeller in a Non-uniform Flow Field," JSR, December 1973, p. 196.
53. BRESLIN, J. P., "A Theory in the Vibratory Effects Produced by a Propeller on a Large Plate," JSR, December 1959, p. 1.
54. TSAKONIS, S., BRESLIN, J., and JACOBS, W., "The Vibratory Force and Moment Produced by a Marine Propeller on a Long Rigid Strip," JSR, March 1972, p. 21.
55. BRESLIN, J. P. and ENG, K. S., "A Method in Computing Propeller-Induced Vibratory Forces of Ships," First Conference on Ship Vibration, Stevens Institute, Hoboken, N. J., January 1965.
56. HUSE, E., "Hull Vibration and Measurements of Propeller-Induced Pressure Fluctuation," Norwegian Ship Model Experiment Tank Publication 103, March 1970.
57. HUSE, E., "The Magnitude and Distribution of Propeller-Induced Surface Forces on a Single-Screw Ship Model," Norwegian Ship Model Experiment Tank Publication 100, December 1968.
58. HUSE, E., "Propeller-Hull Vortex Cavitation," Norwegian Ship Model Experiment Tank Publication 106, May 1971.
59. HUSE, E., "Pressure Fluctuations on the Hull Induced by Cavitating Propellers," Norwegian Ship Model Experiment Tank Publication 111, March 1972.
60. HYLARIDES, S., "Hull Resonance No Explanation of Excessive Vibrations," International Shipbuilding Progress, April 1974, pp. 89-99.

61. HENRY, J. R. and BAILEY, F. C., "Slamming of Ships: A Critical Review of the Current State of Knowledge," SSC-208, 1970.
62. OCHI, M. K. AND MOTTER, L. E., "Prediction of Slamming Characteristics and Hull Responses for Ship Design," SNAME Annual Meeting in New York, November 1973.
63. HUANG, R. T. and SIBUL, O. J., "Slamming Pressures on a Barge Model," SNAME Technical and Research Report R-14, 1971.

### Section 3 References

1. KLINE, R. G. and CLOUGH, R. W., "The Dynamic Response of Ships' Hulls as Influenced by Proportions, Arrangement, Loading, and Structural Stiffness," SNAME Spring Meeting 1967.
2. KLINE, R. G., CLOUGH, R. W., and KAVLIE, D., "Propeller-Excited Ship Vibrations," Paper presented at the SNAME Northern California Section Meeting, March 11, 1971.
3. SALVESEN, N. TUCK, E. O., and FALTINSEN, O., "Ship Motions and Sea Loads," Transactions of SNAME 1920.
4. GERRITSMAN, J. and BEUKELMAN, W., "Distribution of Damping and Added Mass Along the Length of a Shipmodel," Research Center TNO for Shipbuilding and Navigation, Delft Report 49S, March 1963.
5. GERRITSMAN, J. and BEUKELMAN, W., "The Distribution of the Hydrodynamic Forces on a Heaving and Pitching Ship Model, with Zero Forward Speed in Still Water," Shipbuilding Laboratory, Technological University of Delft, Publication 124, February 1965.
6. GOODMAN, R. A., "Wave-Excited Main Hull Vibrations in Large Tankers and Bulk Carriers," Transactions of RINA, 1970.
7. HOFFMAN, D. and VAN HOOFF, R. W., "Experimental and Theoretical Evaluation of Springing on a Great Lakes Bulk Carrier," Glen Cove, New York, Webb Institute of Naval Architecture, November 1972.
8. MCGOLDRICK, R. T., "Ship Vibration," DTMB Report 1451, December 1960.
9. Letter from Joseph Penzien, January 7, 1974.
10. BOLOTIN, V. V., "Statistical Method in Structural Mechanics," translated by Samuel Aroni, Holden-Day, 1969.

#### Section 4 References

1. KLINE, R. G., CLOUGH, R. W., and KAVLIE, D., "Propeller-Excited Ship Vibrations," Paper presented at the SNAME Northern California Section Meeting, March 11, 1971.
2. COUCHMAN, A. J., "Axial Shaft Vibration in Large Turbine-Powered Merchant Ships," Transactions of IME, Vol. 77, No. 3, March 1965.
3. KANE, J. R. and MCGOLDRICK, R. T., "Longitudinal Vibration of Marine Propulsion-Shafting System," Transactions of SNAME, Vol. 57, 1949.
4. "Longitudinal Stiffness of Main Thrust-Bearing Foundation," SNAME Technical and Research Report R-15, September 1972.

## Section 5 References

1. REED, F. E., "Acceptable Levels of Vibration on Ships," Marine Technology, April 1973, p. 105.
2. HYLARIDES, S., "Hull Resonance No Explanation of Excessive Vibrations," International Shipbuilding Progress, April 1974, pp. 89-99.

APPENDIX A - PARAMETRIC ANALYSES INPUT DATA

Glossary of Symbols for Hull Input Data

- B = Buoyancy, in tons per foot of immersion per station space.
- $I_B$  = Double-bottom-girder inertia, in feet<sup>4</sup>.
- $I_H$  = Main-hull-girder inertia, in feet<sup>4</sup>.
- $KA_B$  = Double-bottom-girder shear area, in feet<sup>2</sup>.
- $KA_H$  = Main-hull-girder shear area, in feet<sup>2</sup>.
- $M_B$  = Double-bottom mass, in tons per second<sup>2</sup> per foot.
- $M_H$  = Main-hull mass, in tons per second<sup>2</sup> per foot.
- S = Support-spring stiffness, in tons per foot per station space.

Table A-I

## Properties of Main Hull and Double Bottom, Tank Ship, Loaded\*

Station	Main-Hull-Girder Stiffness		Double-Bottom-Girder Stiffness			Buoyancy	Main-Hull Mass	Double-Bottom Mass
	$I_H$	$K_{A_H}$	$I_B$	$K_{A_B}$	S	B	$M_H$	$M_B$
1					0	12.200	52.371	0
2	55,000	18.20	10.000	2.000	0	28.170	85.885	0
3	59,000	18.40	10.000	2.000	0	48.440	132.880	0
4	63,500	18.55	10.000	2.000	0	71.410	127.680	0
5	66,800	18.70	10.000	2.000	0	92.220	181.250	0
6	71,000	18.90	10.000	2.000	0	106.930	263.970	0
7	75,000	19.05	10.000	2.000	0	116.260	302.960	0
8	79,500	19.30	10.000	2.000	0	120.890	328.250	0
9	84,300	19.60	10.000	2.000	0	121.930	378.400	0
10	89,500	19.90	10.000	2.000	0	121.930	419.010	0
11	94,000	20.20	10.000	2.000	0	121.930	456.180	0
12	99,300	20.70	10.000	2.000	0	121.930	494.280	0
13	100,500	21.20	10.000	2.000	0	121.930	512.710	0
14	110,400	21.70	10.000	2.000	0	121.930	513.020	0
15	114,500	22.13	10.000	2.000	0	121.930	513.220	0
16	117,000	22.00	10.000	2.000	0	121.930	394.710	0
17	118,000	22.00	10.000	2.000	0	121.930	321.720	0
18	118,000	22.00	10.000	2.000	0	121.930	321.860	0
19	118,000	22.00	10.000	2.000	0	121.930	322.200	0
20	118,000	22.00	10.000	2.000	0	121.930	385.770	0
21	118,000	22.00	10.000	2.000	0	121.930	501.570	0
22	118,000	22.00	10.000	2.000	0	121.930	502.240	0
23	118,000	22.00	10.000	2.000	0	121.930	503.070	0
24	118,000	22.00	10.000	2.000	0	121.930	392.380	0
25	118,000	22.00	10.000	2.000	0	121.930	324.090	0
26	118,000	22.00	10.000	2.000	0	121.930	324.670	0
27	118,000	22.00	10.000	2.000	0	121.930	325.610	0
28	118,000	22.00	10.000	2.000	0	121.930	335.260	0
29	117,800	22.00	10.000	2.000	0	121.930	396.190	0
30	117,000	22.00	10.000	2.000	0	121.930	392.790	0
31	114,800	22.00	10.000	2.000	0	121.930	389.490	0
32	112,000	22.13	10.000	2.000	0	121.610	384.230	0
33	107,000	21.70	10.000	2.000	0	120.570	375.870	0
34	100,500	21.20	10.000	2.000	0	118.600	360.980	0
35	91,000	20.70	10.000	2.000	0	115.010	341.390	0
36	82,500	19.70	10.000	2.000	0	109.090	268.890	0
37	75,000	15.20	10.000	2.000	0	101.190	280.790	0
38	68,000	10.80	10.000	2.000	0	92.04	241.100	0
39	62,500	11.00	50.000	2.000	160,500	80.56	155.920	44.044
40	56,000	11.20	105.830	2.113	237,300	67.10	122.630	34.850
41	53,000	11.45	77.890	2.274	384,000	53.10	65.490	17.447
42	49,000	11.80	63.700	2.449	1,000,000	37.32	36.600	10.044
43	43,500	12.65	64.280	2.740	0	14.35	30.030	0
44	36,500	12.65	65.000	2.800	0	0	24.430	0
45	25,000	12.65	65.000	2.800	0	0	19.520	0

\* Units are in tons, feet, and seconds.

Table A-II

Table A-II

Properties of Main Hull and Double Bottom, RYERSON Ballast

Station	<u>Main-Hull-Girder Stiffness</u>		<u>Double-Bottom-Girder Stiffness</u>			<u>Buoyancy</u>		<u>Main-Hull Mass</u>	<u>Double-Bottom Mass</u>
	$I_H$	$KA_H$	$I_B$	$KA_B$	$S$	$B$	$M_H$	$M_B$	
1									
2	5729	3.270	13.180	0.410	0	13.510	3.180	0	
3	6875	4.290	13.180	0.410	0	23.570	7.082	1.651	
4	8417	6.800	13.180	0.410	0	30.620	16.880	3.418	
5	9917	8.080	13.180	0.410	0	34.020	26.616	6.453	
6	6371	10.740	13.180	0.410	0	35.190	33.743	8.647	
7	6371	10.740	13.180	0.410	28,500	35.870	36.667	9.669	
8	6371	10.740	13.180	0.410	28,500	36.110	38.754	10.576	
9	6371	10.740	13.180	0.410	28,500	36.450	40.171	11.168	
10	6371	10.740	13.180	0.410	28,500	36.550	42.920	12.227	
11	6371	10.740	13.180	0.410	28,500	36.550	44.000	12.682	
12	6371	10.740	13.180	0.410	28,500	36.550	44.025	12.690	
13	6371	10.740	13.180	0.410	28,500	36.550	44.142	12.719	
14	6371	10.740	13.180	0.410	28,500	36.550	44.193	12.723	
15	6371	10.740	13.180	0.410	0	36.550	44.215	12.722	
16	6371	10.740	13.180	0.410	30,750	36.550	44.363	12.770	
17	6371	10.740	13.050	0.410	30,750	36.550	44.545	12.828	
18	6371	10.740	13.050	0.410	30,750	36.550	45.090	13.033	
19	6371	10.740	13.050	0.410	30,750	36.550	46.043	13.393	
20	6371	10.740	13.050	0.410	30,750	36.550	46.099	13.407	
21	6371	10.740	13.050	0.410	30,750	36.550	46.155	13.421	
22	6371	10.740	13.050	0.410	30,750	36.550	46.230	13.439	
23	6371	10.740	13.050	0.410	30,750	36.550	47.352	13.860	
24	6371	10.740	13.050	0.410	30,750	36.550	47.908	14.073	
25	6371	10.740	13.050	0.410	30,750	36.550	48.023	14.107	
26	6371	10.740	13.050	0.410	30,750	36.550	48.132	14.138	
27	6371	10.740	13.050	0.410	30,750	36.550	48.135	14.124	
28	6371	10.740	13.050	0.410	30,750	36.550	48.134	14.121	
29	6371	10.740	13.050	0.410	0	36.550	48.246	14.157	
30	6371	10.740	13.050	0.410	30,750	36.550	48.382	14.198	
31	6371	10.740	13.270	0.410	30,750	36.550	48.503	14.235	
32	6371	10.740	13.270	0.410	30,750	36.550	45.893	13.213	
33	6371	10.740	13.270	0.410	30,750	36.550	44.672	12.730	
34	6371	10.740	13.270	0.410	30,750	36.450	44.773	12.765	
35	6371	10.740	13.270	0.410	30,750	36.110	44.267	12.632	
36	6371	10.740	13.270	0.410	30,750	35.870	43.194	18.850	
37	9257	7.580	13.270	1.430	0	35.090	41.092	10.994	
38	9056	7.200	17.490	1.430	29,850	33.920	34.743	8.756	
39	7951	6.890	10.400	1.430	23,700	31.100	28.274	6.658	
40	5382	6.600	7.950	1.430	36,650	26.880	22.129	5.005	
41	3410	6.250	7.950	1.430	75,000	21.380	18.827	4.868	
42	2522	5.860	7.950	1.430	0	15.800	13.950	4.289	
43	2035	5.260	7.950	1.430	0	8.990	5.537	2.025	
					0	0	6.990	0	

Table A-III

Properties of Main Hull and Double Bottom, MICHIGAN, Loaded

Station	Main-Hull-Girder Stiffness		Double-Bottom-Girder Stiffness			Buoyancy	Main-Hull Mass	Double-Bottom Mass
	$I_H$	$KA_H$	$I_B$	$KA_B$	S	B	$M_H$	$M_B$
1					0	1.597	6.834	3.247
2	2333	3.014	5.556	0.400	0	1.857	7.337	3.287
3	2833	3.589	5.556	0.400	0	2.749	7.569	3.327
4	3292	4.082	5.556	0.400	0	3.777	7.793	3.353
5	3764	4.575	5.556	0.400	0	6.240	8.142	3.380
6	4208	5.041	5.556	0.400	0	8.283	9.017	3.407
7	4708	5.479	5.556	0.400	0	10.586	10.373	3.433
8	5583	5.890	5.694	0.400	0	13.074	14.959	4.836
9	6264	6.192	6.528	1.000	50,900	15.674	18.537	7.967
10	6944	6.521	7.639	1.000	46,000	18.051	20.653	8.598
11	7236	6.712	10.278	1.000	41,000	20.169	22.765	9.242
12	7347	6.877	13.194	1.000	35,800	22.100	25.012	9.982
13	7208	7.123	17.222	1.000	26,000	24.143	24.363	10.182
14	6931	7.178	20.278	0.650	21,500	26.074	27.011	10.500
15	6819	7.260	23.333	0.650	17,700	27.709	28.563	11.686
16	6806	7.342	26.111	0.650	14,700	29.083	30.749	12.855
17	6875	7.342	29.028	0.650	10,900	29.974	32.573	13.855
18	7056	7.288	30.556	0.650	9,900	30.383	35.687	15.805
19	7250	7.233	32.222	0.650	9,400	30.457	38.489	17.397
20	7403	7.096	33.472	0.650	9,300	30.457	39.269	17.753
21	7458	6.959	33.889	0.650	10,500	30.457	39.432	17.868
22	7472	6.712	34.028	0.650	11,830	30.457	39.446	17.882
23	7444	6.685	34.167	0.650	13,400	30.457	37.643	16.912
24	7333	6.603	33.333	0.650	15,300	30.457	34.270	14.848
25	7069	6.356	31.944	0.650	19,600	30.457	33.731	14.589
26	6681	6.055	30.417	0.650	22,300	30.457	32.940	14.236
27	6569	6.329	28.472	0.650	24,700	30.457	37.777	17.213
28	6611	6.466	25.972	0.650	27,400	30.309	37.808	18.727
29	6806	6.658	22.500	0.650	31,600	29.974	37.138	18.074
30	7355	6.986	18.750	0.650	0	29.491	36.119	17.542
31	8017	7.342	14.583	0.650	0	28.711	34.602	15.433
32	7998	7.589	11.111	1.000	0	27.634	32.435	14.166
33	6770	7.699	17.500	1.000	0	26.186	28.304	11.473
34	5847	7.863	15.000	1.000	0	24.514	24.055	5.204
35	5333	7.808	6.667	0.400	0	22.769	19.188	3.716
36	4958	7.534	5.833	0.400	0	20.800	16.906	3.064
37	4569	7.151	5.556	0.400	0	18.794	12.176	2.025
38	4139	6.438	5.556	0.400	0	16.380	9.833	1.908
39	3792	5.890	5.556	0.400	0	13.520	7.909	2.028
40	3417	5.178	5.556	0.400	0	10.771	6.083	1.923
41	3069	4.411	5.556	0.400	0	7.986	5.449	1.382
42	2764	3.699	5.556	0.400	0	5.460	4.008	1.294
43	2431	2.849	5.556	0.400	0	2.971	1.150	0.468

A-4

Table A-IV

Data for Superstructure - Tank Ship

4 Decks in Superstructure

Superstructure connected to hull girder at nodal points

43 (aft)                      38 (forward)

Distance from elastic axis hull girder to base superstructure

42.600

Distance between forward and aft connection points

75.000

Spring stiffness connecting superstructure to main girder

5.000E+05                      5.000E+05

Masses (vertical) at aft and forward end of superstructure

16.000                      16.410

<u>Deck No.</u>	<u>Distance to Next Deck</u>	<u>Shear Area</u>	<u>Moment of Inertia</u>	<u>Mass</u>
1	14.760	9.500	50000.000	13.670
2	14.100	7.160	22100.000	9.030
3	14.700	4.700	9300.000	5.730
4	14.700	3.400	5100.000	3.980

Data for Propulsion System

Nodal points where couple from eccentric thrust is acting on

main girder                      43 (aft)                      38 (forward)

Nodal points where couple from eccentric thrust is acting on

bottom girder                      49 (aft)                      47 (forward)

Distance from elastic-axis bottom girder to elastic-axis

main girder                      38.000

Distance between nodal points main girder                      125.600

Distance from shaft to elastic-axis bottom girder                      7.500

Distance between nodal points bottom girder                      50.240

	<u>Stiffness (tons/ft)</u>	<u>Mass</u>
Propeller	231120	3.670
Shaft	340960	1.340
Thrust bearing	115179	7.110

Table A-V

Data for Propulsion System - RYERSON

Nodal points where couple from eccentric thrust is acting on  
 main girder            41 (aft)            36 (forward)  
 Nodal points where couple from eccentric thrust is acting on  
 bottom girder        73 (aft)            71 (forward)  
 Distance from elastic-axis bottom girder to elastic-axis  
 main girder            26.000  
 Distance between nodal points main girder            85.000  
 Distance from shaft to elastic-axis bottom girder    8.750  
 Distance between nodal points bottom girder        34.000

	<u>Stiffness (tons/ft)</u>	<u>Mass</u>
Propeller	250000	1.535
Shaft	92100	0.352
Thrust bearing	33380	1.200

Table A-VI

Data for Superstructure - MICHIGAN

4 Decks in Superstructure

Superstructure connected to hull girder at nodal points

34 (aft)            28 (forward)

Distance from elastic axis hull girder to base superstructure

17.000

Distance between forward and aft connection points

45.000

Spring stiffness connecting superstructure to main girder

2.000E+04          1.000E+05

Masses (vertical) at aft and forward end of superstructure

10.120            10.120

<u>Deck No.</u>	<u>Distance to Next Deck</u>	<u>Shear Area</u>	<u>Moment of Inertia</u>	<u>Mass</u>
1	9.000	7.530	4600.000	7.300
2	9.000	4.550	3531.000	4.970
3	9.000	4.180	2300.000	3.970
4	9.000	4.180	1875.000	4.000

Data for Propulsion System

Nodal points where couple from eccentric thrust is acting on  
main girder            34 (aft)            28 (forward)

Nodal points where couple from eccentric thrust is acting on  
bottom girder        34 (aft)            63 (forward)

Distance from elastic-axis bottom girder to elastic-axis  
main girder            32.160

Distance between nodal points main girder            75.000

Distance from shaft to elastic-axis bottom girder    11.100

Distance between nodal points bottom girder        26.000

	<u>Stiffness (tons/ft)</u>	<u>Mass</u>
Propeller	108434	1.882
Shaft	83946	1.006
Thrust bearing	40000	2.331

TABLE A-VII  
A Values, Tank Ship, Ballast

Station	Hull Bending Stiffness, percent				
	60	80	100	120	140
1	0.120	0.110	0.100	0.085	0.070
2	0.300	0.260	0.230	0.200	0.180
3	1.540	1.440	1.360	1.330	1.300
4	3.220	3.320	3.400	3.280	3.140
5	3.800	3.830	3.850	3.700	3.750
6	1.090	0.960	0.860	0.790	0.730
7	0.900	0.780	0.680	0.610	0.540
8	0.800	0.675	0.575	0.500	0.430
9	0.720	0.600	0.500	0.430	0.360
10	0.660	0.550	0.440	0.370	0.300
11	0.600	0.490	0.390	0.320	0.250
12	0.555	0.450	0.350	0.280	0.220
13	0.510	0.410	0.310	0.250	0.190
14	0.480	0.380	0.280	0.220	0.160
15	0.450	0.350	0.260	0.190	0.130
16	0.430	0.330	0.235	0.170	0.110
17	0.405	0.310	0.220	0.160	0.095
18	0.380	0.290	0.200	0.140	0.080
19	0.360	0.270	0.175	0.125	0.070
20	0.340	0.250	0.155	0.110	0.060
21	0.320	0.230	0.140	0.095	0.045
22	0.300	0.210	0.130	0.080	0.040
23	0.275	0.190	0.120	0.070	0.030
24	0.250	0.170	0.100	0.060	0.025
25	0.230	0.160	0.085	0.050	0.020
26	0.220	0.150	0.072	0.045	0.020
27	0.230	0.145	0.060	0.040	0.020
28	0.245	0.155	0.065	0.040	0.030
29	0.275	0.180	0.080	0.060	0.045
30	0.330	0.240	0.150	0.100	0.065
31	0.410	0.310	0.220	0.175	0.130
32	0.500	0.400	0.310	0.260	0.220
33	0.620	0.520	0.430	0.380	0.330
34	0.750	0.670	0.600	0.540	0.480
35	0.870	0.800	0.740	0.690	0.650
36	0.970	0.890	0.820	0.780	0.740
37	1.060	0.970	0.890	0.850	0.810
38	1.160	1.070	0.980	0.940	0.910
39	1.290	1.200	1.130	0.080	1.045
40	1.530	1.410	1.320	1.290	1.260
41	2.600	2.660	2.680	2.660	2.640
42	0.900	0.860	0.830	0.830	0.830
43	0.150	0.120	0.100	0.090	0.080
44	0.020	0.010	0	0	0
45	0	0	0	0	0

Table A-VIII

A Values, Tank Ship, Loaded

Station	Hull Bending Stiffness, percent				
	60	80	100	120	140
1	0.040	0.040	0.040	0.040	0.040
2	0.110	0.105	0.100	0.095	0.090
3	0.200	0.195	0.190	0.185	0.180
4	0.260	0.255	0.250	0.245	0.240
5	0.300	0.295	0.290	0.285	0.280
6	0.230	0.240	0.250	0.255	0.260
7	0.150	0.165	0.180	0.190	0.200
8	0.100	0.115	0.130	0.150	0.160
9	0.060	0.075	0.090	0.100	0.110
10	0.020	0.035	0.050	0.060	0.070
11	0.010	0.010	0.018	0.025	0.030
12	0	0.003	0.005	0.007	0.010
13	0	0	0	0	0
14-31	↓	↓	↓	↓	↓
32	0	0	0	0	0
33	0.010	0.007	0.005	0.002	0
34	0.050	0.040	0.030	0.020	0.010
35	0.170	0.140	0.120	0.100	0.080
36	0.310	0.280	0.260	0.240	0.220
37	0.490	0.460	0.440	0.410	0.390
38	0.720	0.680	0.650	0.610	0.580
39	0.950	0.910	0.870	0.830	0.800
40	1.220	1.170	1.120	1.070	1.030
41	1.520	1.460	1.410	1.360	1.310
42	1.830	1.780	1.730	1.680	1.640
43	2.000	1.960	1.920	1.880	1.840
44	1.760	1.800	1.830	1.870	1.900
45	1.610	1.820	2.040	2.300	2.590

Table A-IX

A Values, RYERSON, Ballast

Station	Hull Bending Stiffness, percent				
	60	80	100	120	140
1	0.800	0.675	0.640	0.620	0.610
2	0.880	0.750	0.680	0.625	0.610
3	0.920	0.800	0.670	0.623	0.600
4	0.930	0.810	0.633	0.610	0.570
5	0.930	0.780	0.557	0.560	0.515
6	0.880	0.680	0.465	0.490	0.420
7	0.810	0.565	0.362	0.380	0.290
8	0.730	0.490	0.300	0.270	0.200
9	0.650	0.430	0.253	0.203	0.137
10	0.590	0.385	0.220	0.153	0.100
11	0.540	0.355	0.195	0.120	0.060
12	0.500	0.320	0.170	0.095	0.038
13	0.470	0.290	0.150	0.076	0.023
14	0.440	0.270	0.128	0.060	0.012
15	0.410	0.245	0.110	0.044	0.006
16	0.380	0.225	0.090	0.030	0.002
17	0.350	0.205	0.072	0.018	0
18	0.330	0.187	0.057	0.010	0
19	0.310	0.170	0.038	0.030	0
20	0.290	0.152	0.023	0	0
21	0.275	0.130	0.010	0	0
22	0.255	0.115	0.003	0	0
23	0.235	0.095	0	0	0
24	0.220	0.075	0	0	0
25	0.200	0.060	0	0	0
26	0.185	0.040	0	0	0
27	0.165	0.025	0	0	0
28	0.150	0.013	0	0	0
29	0.135	0.005	0	0	0
30	0.120	0	0	0	0
31	0.110	0	0	0	0
32	0.100	0.005	0	0	0
33	0.100	0.010	0	0	0
34	0.130	0.023	0.006	0	0
35	0.175	0.050	0.017	0.003	0
36	0.230	0.100	0.050	0.016	0.002
37	0.300	0.170	0.113	0.055	0.010
38	0.365	0.245	0.192	0.128	0.093
39	0.395	0.285	0.230	0.195	0.163
40	0.370	0.245	0.213	0.203	0.190
41	0.230	0.177	0.164	0.150	0.144
42	0.180	0.150	0.138	0.126	0.118
43	0.160	0.140	0.125	0.114	0.107

Table A-X

A Values, RYERSON, Loaded

<u>Station</u>	<u>Hull Bending Stiffness, percent</u>				
	<u>60</u>	<u>80</u>	<u>100</u>	<u>120</u>	<u>140</u>
1	0	0	0	0	0
2	0.325	0.255	0.210	0.190	0.173
3	0.250	0.158	0.110	0.087	0.070
4	0.160	0.070	0.028	0.010	0.003
5	0.080	0.015	0	0	0
6	0.030	0.005	0	0	0
7	0.015	0	0	0	0
8	0.003	0	0	0	0
9	0	0	0	0	0
10-30	↓	↓	↓	↓	↓
31	0	0	0	0	0
32	0.010	0	0	0	0
33	0.035	0	0	0	0
34	0.080	0.010	0	0	0
35	0.143	0.042	0.020	0	0
36	0.225	0.100	0.070	0.040	0.018
37	0.315	0.180	0.147	0.110	0.080
38	0.430	0.290	0.260	0.220	0.190
39	0.560	0.420	0.390	0.360	0.340
40	0.680	0.545	0.520	0.487	0.470
41	0.775	0.687	0.655	0.630	0.610
42	0.860	0.860	0.860	0.840	0.820
43	0.910	1.040	1.130	1.240	1.400

Table A-XI

A Values, MICHIGAN

Station	Hull Bending Stiffness, percent				
	60	80	100	120	140
1	0.130	0.140	0.150	0.160	0.175
2	0.120	0.130	0.140	0.150	0.160
3	0.080	0.095	0.105	0.120	0.130
4	0.050	0.055	0.060	0.065	0.070
5	0.050	0.045	0.040	0.035	0.030
6	0.080	0.070	0.060	0.050	0.040
7	0.150	0.140	0.130	0.120	0.110
8	0.240	0.230	0.215	0.200	0.190
9	0.300	0.290	0.275	0.260	0.250
10	0.330	0.320	0.305	0.290	0.280
11	0.340	0.330	0.315	0.300	0.290
12	0.340	0.330	0.315	0.300	0.290
13	0.320	0.310	0.295	0.280	0.270
14	0.290	0.280	0.265	0.250	0.240
15	0.240	0.230	0.215	0.200	0.190
16	0.170	0.160	0.150	0.140	0.130
17	0.100	0.090	0.080	0.070	0.060
18	0.040	0.030	0.025	0.020	0.010
19	0	0	0	0	0
20-24	↓	↓	↓	↓	↓
25	0	0	0	0	0
26	0.020	0.020	0.020	0.020	0.020
27	0.120	0.115	0.110	0.105	0.100
28	0.300	0.290	0.280	0.270	0.260
29	0.540	0.530	0.520	0.510	0.500
30	0.780	0.770	0.760	0.750	0.740
31	1.020	1.005	0.990	0.980	0.970
32	1.280	1.260	1.245	1.225	1.210
33	1.520	1.500	1.480	1.460	1.440
34	1.720	1.690	1.655	1.630	1.610
35	1.860	1.780	1.700	1.620	1.540
36	1.940	1.905	1.870	1.835	1.800
37	1.960	1.920	1.880	1.840	1.800
38	1.840	1.800	1.770	1.730	1.700
39	1.680	1.665	1.650	1.635	1.620
40	1.580	1.590	1.600	1.610	1.620
41	1.680	1.760	1.840	1.920	2.000
42	2.740	2.860	2.970	3.100	3.200
43	0.820	1.140	1.030	1.140	1.240

FIGURE A-1  
TANK SHIP  
ADDED MASS VS LENGTH  
BALLAST CONDITION

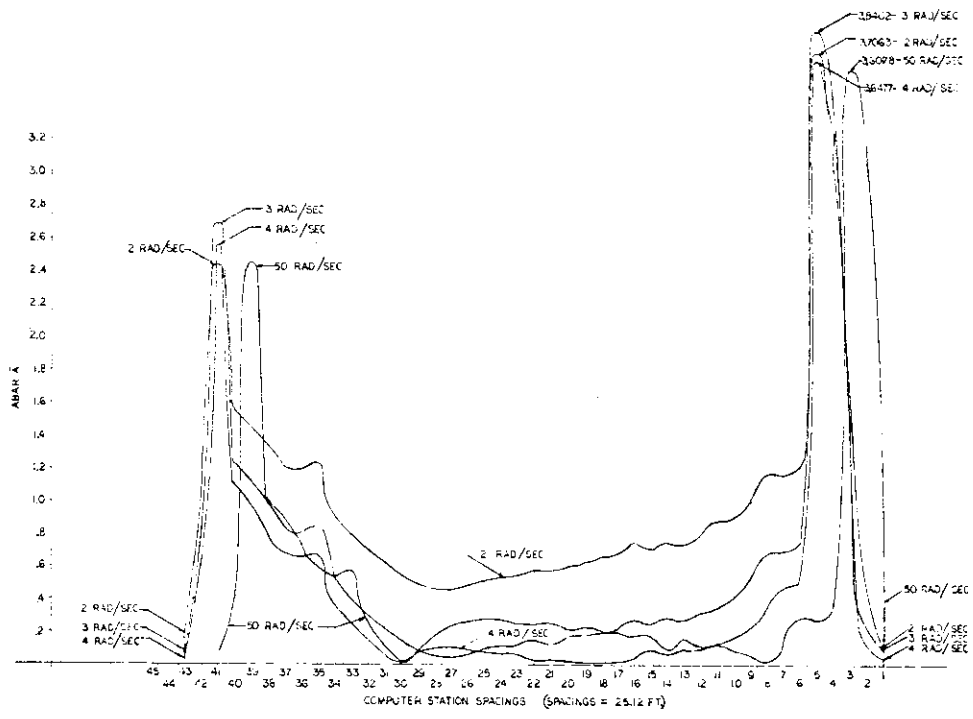
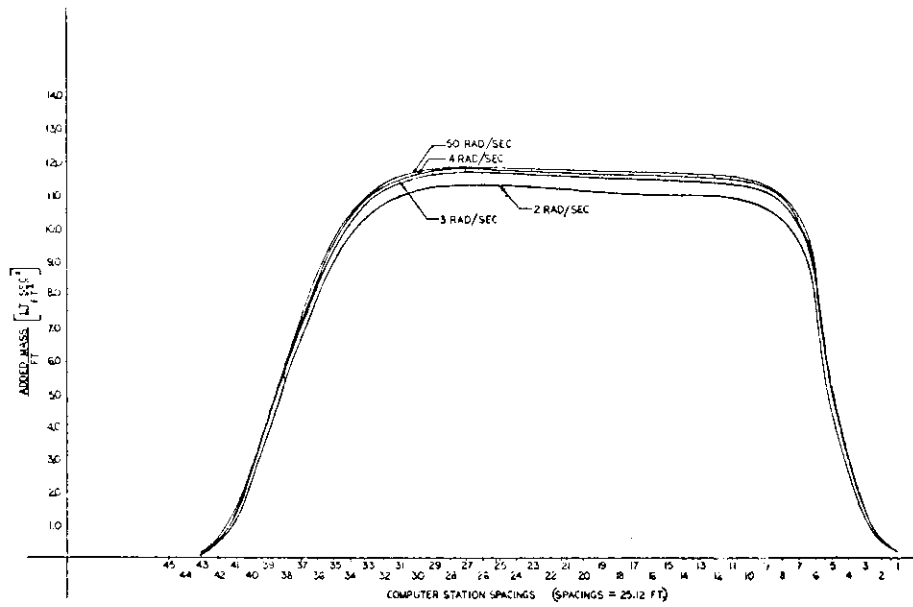


FIGURE A-2  
TANK SHIP  
ABAR X VS LENGTH  
BALLAST CONDITION

FIGURE A-3  
TANK SHIP  
ADDED MASS  
VS LENGTH  
FULL LOAD CONDITION

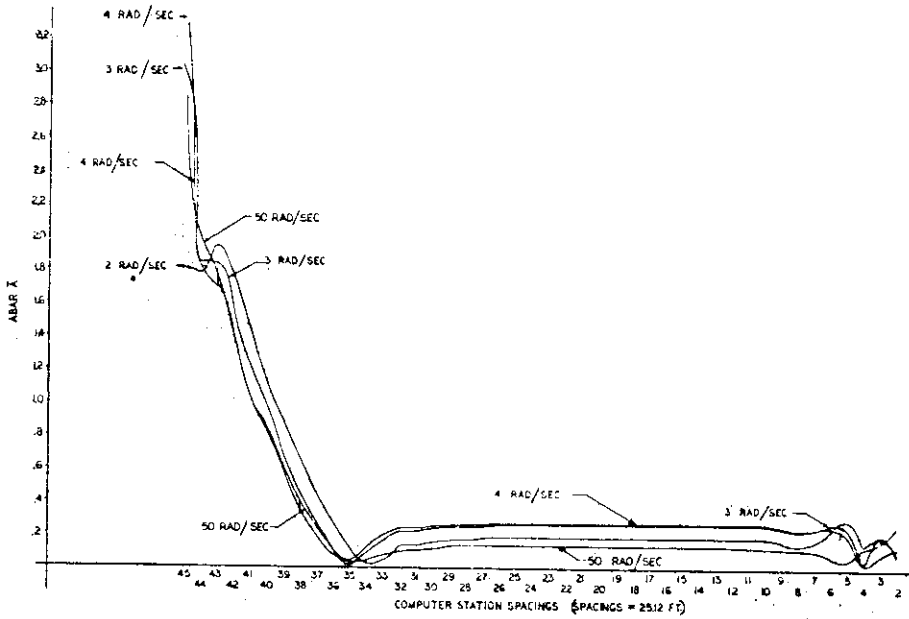
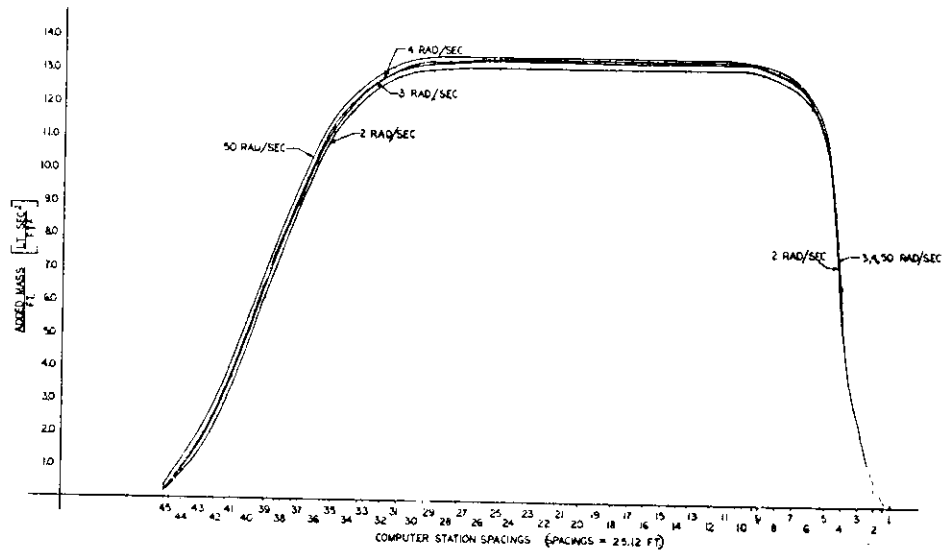


FIGURE A-4  
TANK SHIP  
 $\bar{A}$  vs. LENGTH  
FULL LOAD CONDITION

FIGURE A-5  
 RYERSON BALLAST CONDITION  
 ADDED MASS VS LENGTH

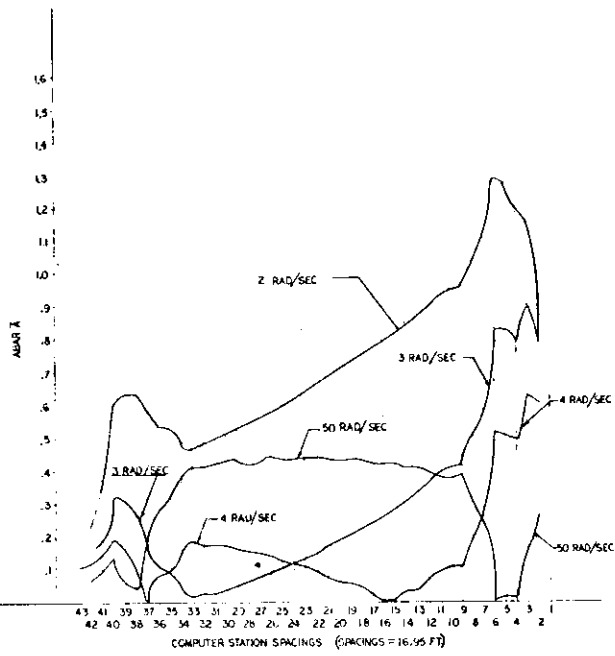
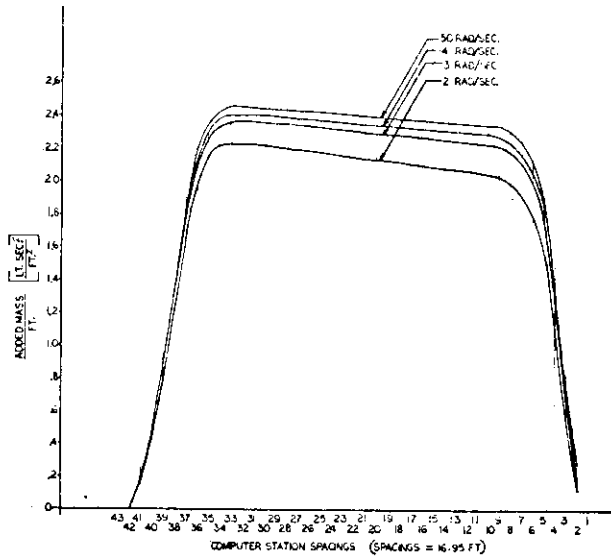


FIGURE A-6  
 RYERSON BALLAST CONDITION  
 $A_{BAR} \bar{X}$  VS. LENGTH

FIGURE A-7  
MICHIGAN  
ADDED MASS VS LENGTH

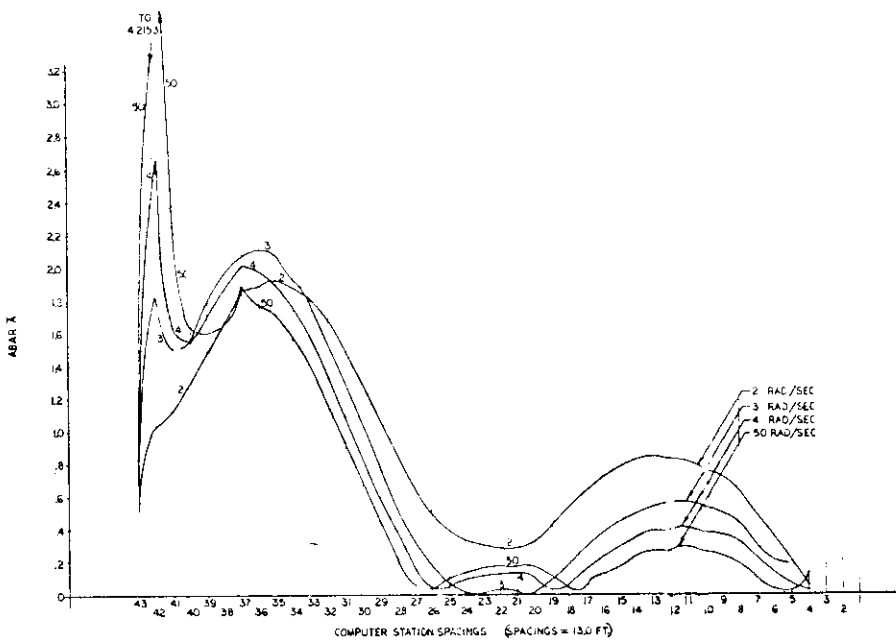
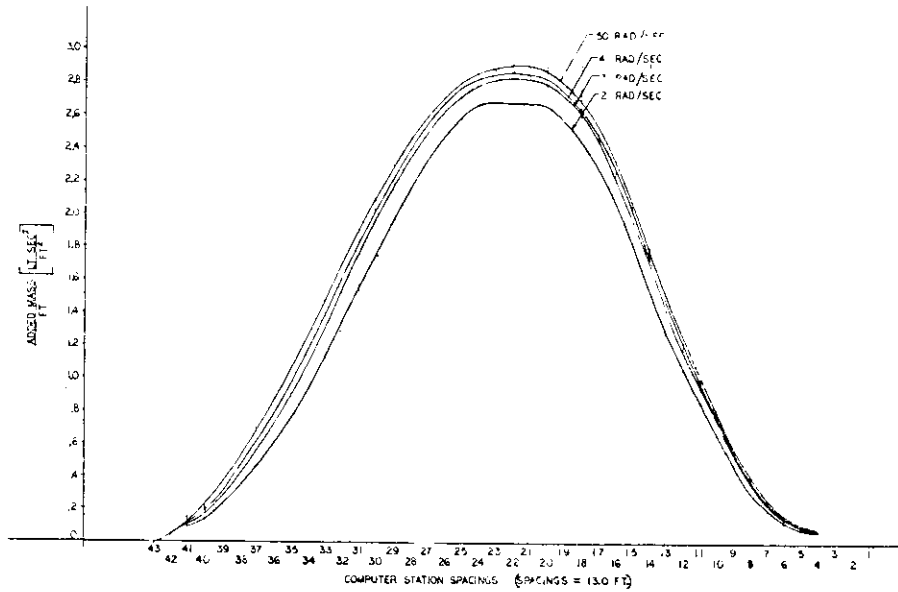


FIGURE A-8  
MICHIGAN  
ABAR A VS LENGTH

APPENDIX B  
PARAMETRIC ANALYSES RESULTS

TABLE B-0

CONVERSION TABLE FOR METRIC UNITS

ITEMS PLOTTED ON CURVES	UNITS USED ON GRAPHS	METRIC EQUIVALENTS	CONVERSION TO METRIC
FREQUENCY OF ENCOUNTER	RAD/SEC	RAD/SEC	Multiply by -
VIBRATION FREQUENCY	CPM	CPM	-
VELOCITY	IN/SEC	MM/SEC	25.4
ACCELERATION	IN/SEC <sup>2</sup>	MM/SEC <sup>2</sup>	25.4
VIBRATION AMPLITUDE	FT	CM	30.48
SHEAR	TONS	METRIC TONS	1.016
SPRINGING FORCE	TONS	METRIC TONS	1.016
STRAIN RATE	IN IN SEC	MM MM SEC	-
$\sqrt{I/\Delta L^3}$	$\sqrt{IN^2/LT-FT}$	$\sqrt{CM^2/MT-M}$	4.564
$\phi_{\zeta\zeta}$	FT <sup>2</sup> -SEC	M <sup>2</sup> -SEC	.093
BENDING MOMENT	FT-TONS	M-MTONS	.310

TABLE B-I  
TANK SHIP (BALLAST)  
PEAK STERN VIBRATORY AMPLITUDE, VELOCITY, AND ACCELERATION (STA. 45)\*\*

SHIP STIFFNESS (%)	AMPLITUDE ( $FT \times 10^{-3}$ ) ( $\omega$ IN CPM)			VELOCITY (IN/SEC $\times 10^3$ )			ACCELERATION (IN/SEC <sup>2</sup> $\times 10^{-3}$ )		
60	.809 (590)	.20 (700)	*	95.46	28.0	*	938.7	326.7	*
80	.543 (624)	.20 (700)	*	67.80	28.0	*	705.4	326.7	*
100	.475 (643)	.217 (700)	*	61.06	30.38	*	654.0	354.4	*
120	.416 (660)	.23 (700)	*	54.91	32.2	*	604.0	375.7	*
140	.327 (680)	.235 (700)	*	44.49	32.9	*	504.3	383.8	*

\* BLANK SPACES INDICATE NO ADDITIONAL SIGNIFICANT PEAKS  
\*\* ALL IN THE VERTICAL DIRECTION

TABLE B-II  
TANK SHIP (BALLAST)  
PEAK THRUST BEARING AMPLITUDE, VELOCITY, AND ACCELERATION\*\*  
(PROP. STA. 1)

SHIP STIFFNESS (%)	AMPLITUDE ( $FT \times 10^{-3}$ ) ( $\omega$ IN CPM)			VELOCITY (IN/SEC $\times 10^3$ )			ACCELERATION (IN/SEC <sup>2</sup> $\times 10^{-3}$ )		
60	.203 (589)	.033 (700)	*	23.92	4.62	*	234.9	53.9	*
80	.183 (613)	.176 (624)		22.44	21.96	6.72	229.4	228.8	78.4
100	.189 (631)	.187 (642)	.091 (700)	23.87	24.03	12.74	251.2	257.3	148.6
120	.195 (655)	.194 (550)	.106 (700)	25.55	25.61	14.84	278.9	281.7	173.1
140	.166 (680)	.114 (700)	*	22.58	15.96	*	255.9	186.2	*

\*BLANK SPACES INDICATE NO ADDITIONAL SIGNIFICANT PEAKS  
\*\*ALL IN THE LONGITUDINAL DIRECTION

TABLE B-III  
TANK SHIP (LOADED)  
PEAK STERN VIBRATORY AMPLITUDE, VELOCITY, AND ACCELERATION (STA 45)\*\*

SHIP STIFFNESS (%)	AMPLITUDE (FT $\times 10^{-3}$ ) ( $\omega$ IN CPM)			VELOCITY (IN/SEC $\times 10^{-3}$ )			ACCELERATION (IN/SEC <sup>2</sup> $\times 10^{-3}$ )		
60	.35 (463)	*	*	32.41	*	*	250.1	*	*
80	.334 (486)	*	*	32.48	*	*	263.2	*	*
100	.297 (500)	*	*	29.7	*	*	247.5	*	*
120	.26 (521)	*	*	27.11	*	*	235.5	*	*
140	.253 (523)	*	*	26.49	*	*	231.1	*	*

\* BLANK SPACES INDICATE NO ADDITIONAL SIGNIFICANT PEAKS

\*\* ALL IN THE VERTICAL DIRECTION

TABLE B-IV  
TANK SHIP (LOADED)  
PEAK THRUST BEARING AMPLITUDE, VELOCITY, AND ACCELERATION\*\*  
(PROP. STA. 1)

SHIP STIFFNESS (%)	AMPLITUDE (FT $\times 10^{-4}$ ) ( $\omega$ IN CPM)			VELOCITY (IN/SEC $\times 10^{-4}$ )			ACCELERATION (IN/SEC <sup>2</sup> $\times 10^{-4}$ )		
60	.261 (403)	.222 (460)	*	21.06	20.45	*	141.6	156.9	*
80	.366 (486)	*	*	35.60	*	*	288.5	*	*
100	.419 (496)	.387 (510)	*	41.53	39.47	*	34.30	335.5	*
120	.497 (520)	.206 (596)	*	51.69	24.57	*	448.0	244.2	*
140	.551 (523)	.462 (537)	.298 (604)	57.69	49.59	36.0	503.3	443.6	362.6

\* BLANK SPACES INDICATE NO ADDITIONAL SIGNIFICANT PEAKS

\*\* ALL IN THE LONGITUDINAL DIRECTION

TABLE B-V  
MICHIGAN (LOADED)  
PEAK STERN VIBRATORY AMPLITUDE, VELOCITY, AND ACCELERATION\*\*  
(STA. 43)

SHIP STIFFNESS (%)	AMPLITUDE (FT x 10 <sup>-3</sup> ) (ω IN CPM)			VELOCITY (IN/SEC x 10 <sup>-3</sup> )			ACCELERATION (IN/SEC <sup>2</sup> x 10 <sup>-3</sup> )		
60	.519 (373)	.34 (536)	*	38.75	36.42	*	241.1	325.1	*
80	***	***	***	***	***	***	***	***	***
100	.497 (395)	.193 (562)	*	39.27	21.70	*	258.6	203.3	*
120	.439 (404)	.258 (420)	.164 (572)	39.79	21.67	18.75	267.7	151.7	178.6
140	.347 (410)	.356 (420)	.146 (580)	28.47	29.88	16.94	194.6	208.9	163.7

\* BLANK SPACES INDICATE NO ADDITIONAL SIGNIFICANT PEAKS

\*\* ALL IN THE VERTICAL DIRECTION

\*\*\* NO DATA AVAILABLE

TABLE B-VI  
MICHIGAN (LOADED)  
PEAK THRUST BEARING AMPLITUDE, VELOCITY, AND ACCELERATION\*\*  
(PROP. STA. 1)

SHIP STIFFNESS (%)	AMPLITUDE (FT x 10 <sup>-3</sup> ) (ω IN CPM)			VELOCITY (IN/SEC x 10 <sup>-3</sup> )			ACCELERATION (IN/SEC <sup>2</sup> x 10 <sup>-3</sup> )		
60	.25 (377)	.254 (601)	*	18.84	30.53	*	118.3	305.8	*
80	***	***	***	***	***	***	***	***	***
100	.426 (395)	.28 (600)	*	33.63	33.60	*	221.2	336	*
120	.461 (402)	.27 (600)	*	37.1	32.4	*	248.8	324	*
140	.456 (410)	.261 (600)	*	37.4	31.32	*	255.9	313.2	*

\* BLANK SPACES INDICATE NO ADDITIONAL SIGNIFICANT PEAKS

\*\* ALL IN THE LONGITUDINAL DIRECTION

\*\*\* NO DATA AVAILABLE

TABLE B-VII  
RYERSON (LOADED)  
PEAK STERN VIBRATORY AMPLITUDE, VELOCITY, AND ACCELERATION (STA. 43)\*\*

SHIP STIFFNESS (%)	AMPLITUDE (FT $\times 10^{-3}$ ) ( $\omega$ IN CPM)			VELOCITY (IN/SEC $\times 10^{-3}$ )			ACCELERATION (IN/SEC <sup>2</sup> $\times 10^{-3}$ )		
60	.35 (360)	.25 (532)	.15 (590)	25.20	26.63	17.70	151.2	236.3	174.1
80	.24 (373)	.235 (382)	.231 (550)	17.91	17.94	25.41	111.4	114.1	232.9
100	.262 (388)	.205 (560)	*	20.31	22.96	*	131.2	214.3	*
120	.251 (393)	.207 (500)	.175 (560)	19.73	20.70	19.60	129.3	172.5	182.9
140	.243 (490)	.235 (500)	.181 (570)	23.81	23.50	20.63	194.5	195.8	196.0

\* BLANK SPACES INDICATE NO ADDITIONAL SIGNIFICANT PEAKS  
\*\* ALL IN THE VERTICAL DIRECTION

TABLE B-VIII  
RYERSON (LOADED)  
PEAK THRUST BEARING AMPLITUDE, VELOCITY, AND ACCELERATION\*\*  
(PROP. STA. 1)

SHIP STIFFNESS (%)	AMPLITUDE (FT $\times 10^{-4}$ ) ( $\omega$ IN CPM)			VELOCITY (IN/SEC $\times 10^{-4}$ )			ACCELERATION (IN/SEC <sup>2</sup> $\times 10^{-4}$ )		
60	.50 (360)	.45 (530)	.33 (582)	36.0	47.7	38.45	216	421.4	373.2
80	.446 (319)	.284 (547)	.253 (600)	28.43	31.06	30.36	151	283	303.6
100	.43 (390)	.278 (476)	.225 (600)	33.54	26.49	27.0	218	210.3	270
120	.432 (393)	.307 (408)	.252 (600)	33.94	25.05	30.24	222.2	170.3	302.4
140	.42 (399)	.37 (600)	*	33.52	44.4	*	223	444	*

\* BLANK SPACES INDICATE NO ADDITIONAL SIGNIFICANT PEAKS

\*\* ALL IN THE LONGITUDINAL DIRECTION

TABLE B-IX  
RYERSON (BALLAST)  
PEAK STERN VIBRATORY AMPLITUDE, VELOCITY, AND ACCELERATION (STA. 43)\*\*

SHIP STIFFNESS (%)	AMPLITUDE (FT $\times 10^{-3}$ ) ( $\omega$ IN CPM)			VELOCITY (IN/SEC $\times 10^{-3}$ )			ACCELERATION (IN/SEC <sup>2</sup> $\times 10^{-3}$ )		
60	.41 (382)	.39 (410)	.251 (600)	31.34	31.98	30.12	199.6	218.5	301.2
80	.401 (430)	.217 (552)	*	34.46	23.95	*	246.8	220.2	*
100	.419 (440)	.222 (560)	*	36.86	24.86	*	270.1	232.1	*
120	.429 (449)	.22 (570)	*	38.50	25.09	*	287.9	238.4	*
140	.473 (307)	.421 (455)	.239 (570)	29.09	38.34	27.27	149.1	290.9	259.3

\* BLANK SPACES INDICATE NO ADDITIONAL SIGNIFICANT PEAKS

\*\* ALL IN THE VERTICAL DIRECTION

TABLE B-X  
RYERSON (BALLAST)  
PEAK THRUST BEARING AMPLITUDE, VELOCITY, AND ACCELERATION \*\*  
(PROP. STA. 1)

SHIP STIFFNESS (%)	AMPLITUDE (FT $\times 10^{-4}$ ) ( $\omega$ IN CPM)			VELOCITY (IN/SEC $\times 10^{-4}$ )			ACCELERATION (IN/SEC <sup>2</sup> $\times 10^{-4}$ )		
60	.68 (340)	.471 (411)	.701 (600)	46.23	38.74	84.12	261.9	265.6	841.2
80	.767 (314)	.549 (430)	.283 (552)	48.17	47.21	31.23	252.1	338.4	287.1
100	.667 (335)	.611 (440)	.327 (600)	44.65	50.83	39.24	249.1	395.2	392.4
120	.685 (450)	.44 (600)	*	61.61	52.8	*	461.8	528	*
140	1.015 (307)	.694 (460)	.652 (600)	62.42	63.90	78.24	319.9	490.4	782.4

\* BLANK SPACES INDICATE NO ADDITIONAL SIGNIFICANT PEAKS

\*\* ALL IN THE LONGITUDINAL DIRECTION

B-6

TABLE B-XI  
CUMULATIVE DAMAGE

SHIP SPEED (KNOTS)	SHIP HEADING	SHIP STIFFNESS (\$)	VLCC LOADED (C.D. x 10 <sup>6</sup> )	VLCC BALLAST (C.D. x 10 <sup>6</sup> )	RYERSON BALLAST (C.D. x 10 <sup>6</sup> )	MICHIGAN LOADED (C.D. x 10 <sup>6</sup> )
0	Head Seas	60	.000117	.00422		
		80	.000028	.0425		
		100	.000012	.03496		
		120	.000021	.00436		
		140	.000023	.00211		
5.92	Head Seas	60	.01577	.0260	.0603	.00127
		80	.00814	.0294	.0489	.03021
		100	.00111	.0590	.1155	.0084
		120	.00091	.0607	.0302	.0864
		140	.00050	.0632	.0066	.0277
11.83	Head Seas	60	.08520	.5370		.11794
		80	.10511	.2532		.09472
		100	.05560	.8722		.0500
		120	.02056	.0387		.0161
		140	.02237	.0243		
11.83	Beam Seas	60	.07582	.0059	.1667	
		80	.00855	.2852	.0586	
		100	.00174	.0108	.0142	
		120	.00050	.0122	.0033	
		140	.00033	.0197	.0084	
17.75	Head Seas	60	4.4174	7.327	5.100	.0553
		80	1.9093	2.781	31.553	.0350
		100	.9000	1.2304	62.153	.5150
		120	.0224	1.747	62.522	.0162
		140	.1891	2.4985	28.233	.0119
17.75	Beam Seas	60				.00015
		80				.00003
		100-140				.00001
23.66	Head Seas	60				.0647
		80				2.608
		100				.380
		120				1.572
		140				.1411

B-7

TABLE B-XII

RYERSON (LOADED) - 140% STIFFNESS  
HEAD SEAS, V = 20 FT/SEC.

Encounter Frequency (Rad/Sec)	Max. Bending Moment	Max. Bending Moment (VdN'/dx = 0)	Max. Bending Moment (A = 0)	Max. Bending Moment (Buoy = 0)
1.273	2,619	2,619	3,449	62.4
1.549	3,200	3,200	3,314	1,148
1.675	2,807	2,807	2,883	2,359
1.736	5,680	5,680	7,809	2,166
1.772	8,307	8,307	5,345	12,560
1.795*	50,276	50,276	40,120	23,013
1.819	9,654	9,654	14,201	5,263
1.854	3,300	3,300	1,687	4,915
1.910	1,205	1,205	1,381	1,609
2.021	989	989	826	575
2.229	207	207	248	137

\*Fundamental Frequency

Encounter Frequency (Rad/Sec)	Head Seas, V = 0.0	
	Max. Bending Moment (25 Modes)	Max. Bending Moment (3 Modes)
1.267	195	211
1.541	3.3	2.9
1.667	252	253
1.728	125	126
1.764	61	61
1.787	75	75
1.811	30	30
1.845	44	43
1.902	13	12
2.012	4.3	4
2.22	2.4	2.1

# PROPELLER COMPUTER OUTPUT

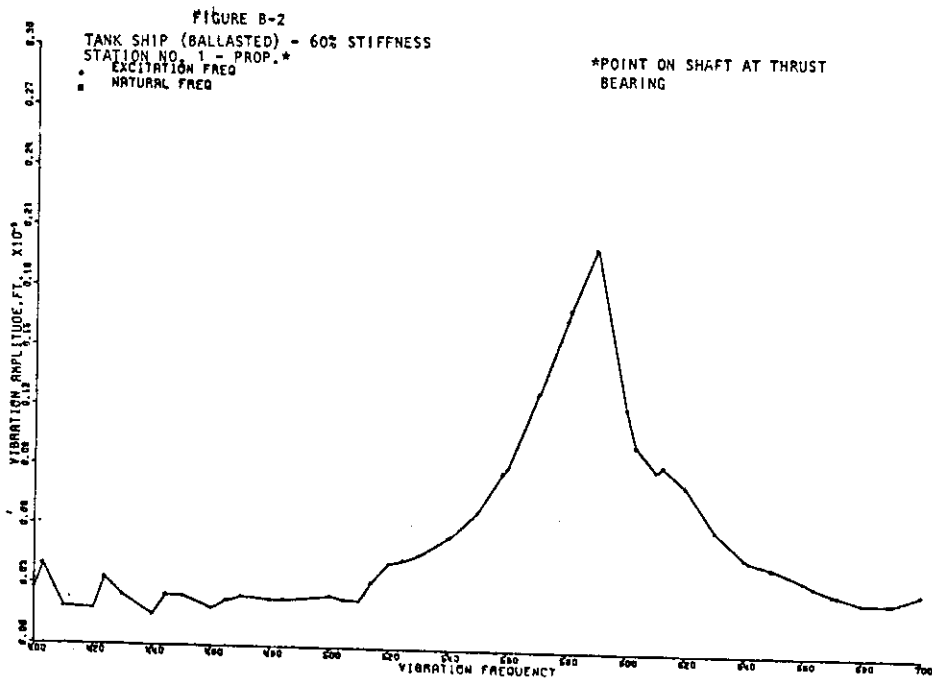
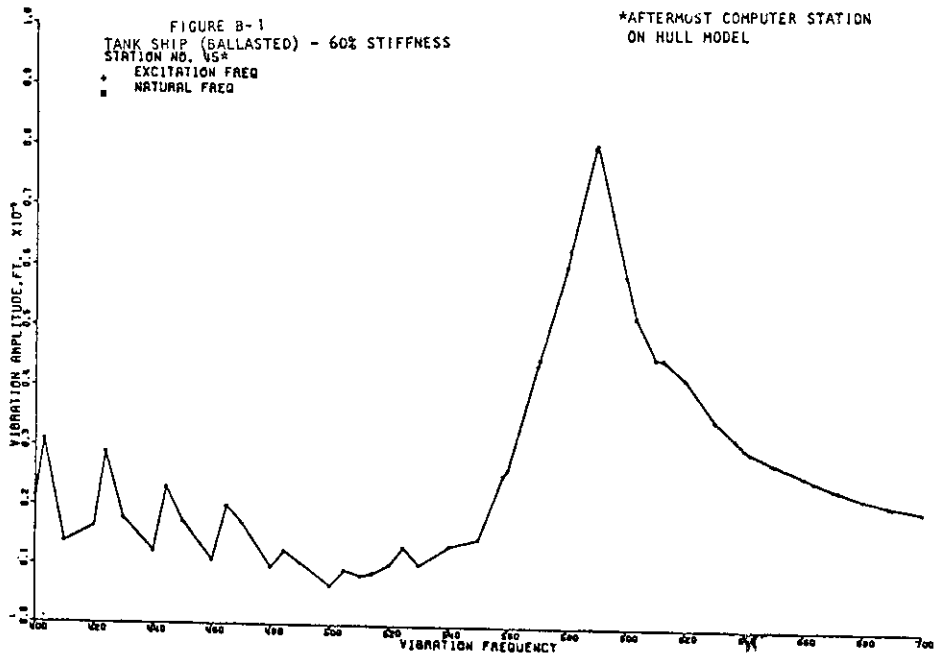


FIGURE B-3  
 TANK SHIP BALLASTED) - 80% STIFFNESS  
 STATION NO. 95 #REQ  
 \* EXCITATION FREQ  
 ■ NATURAL FREQ

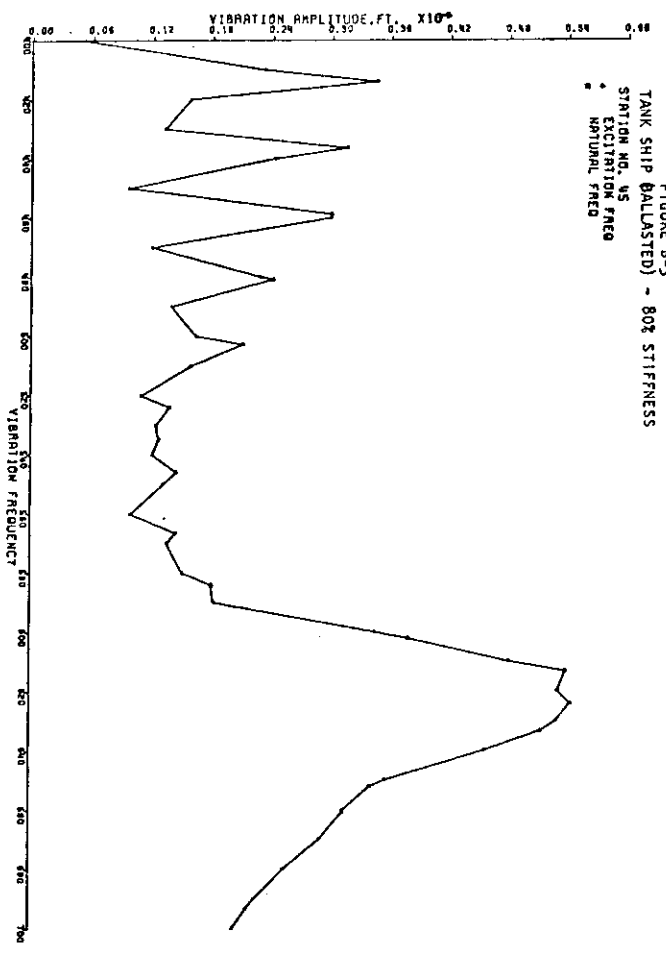
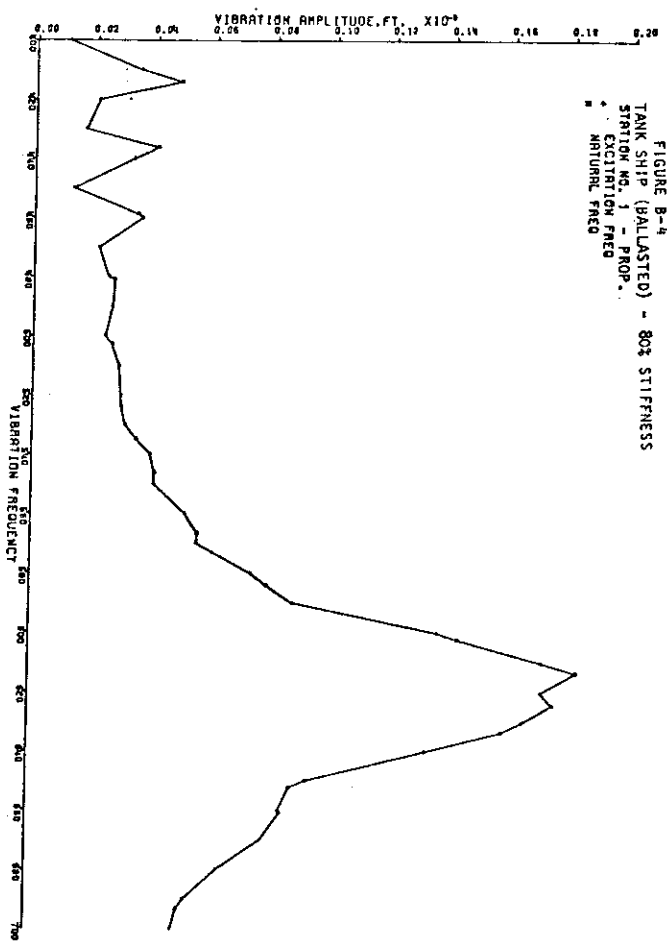
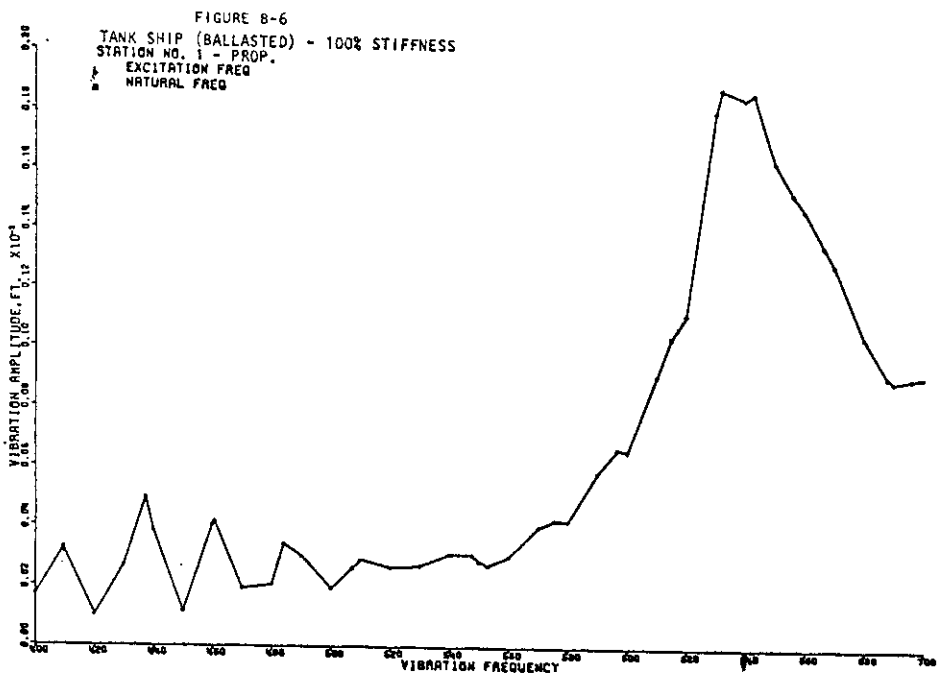
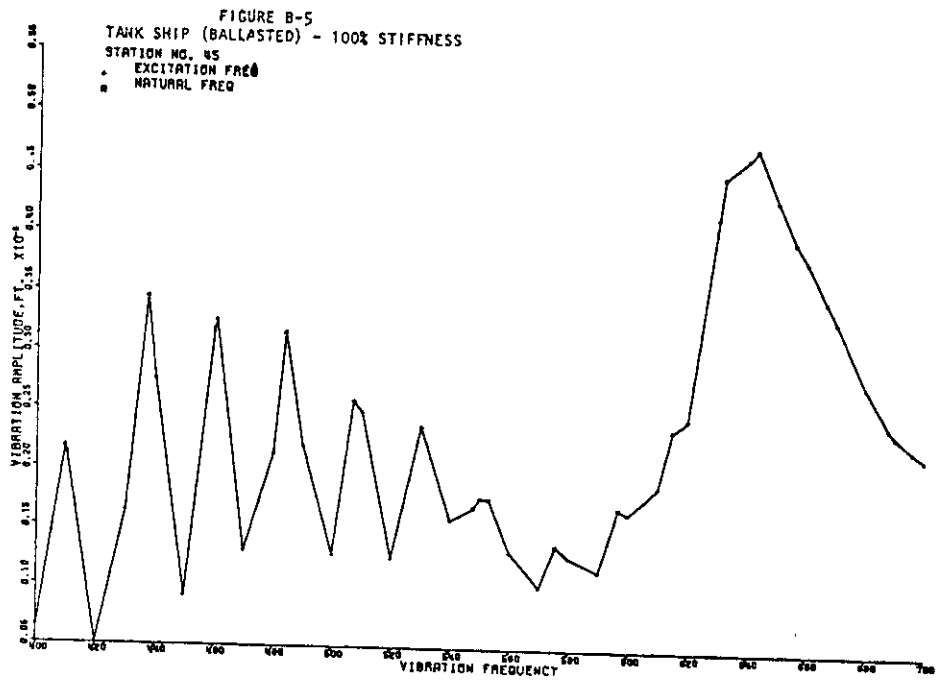
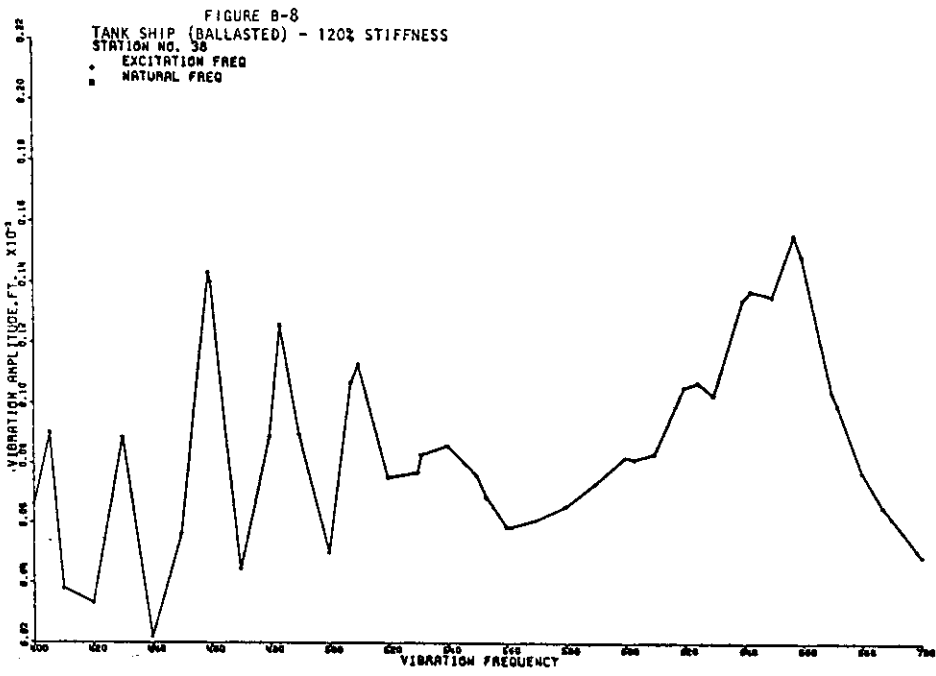
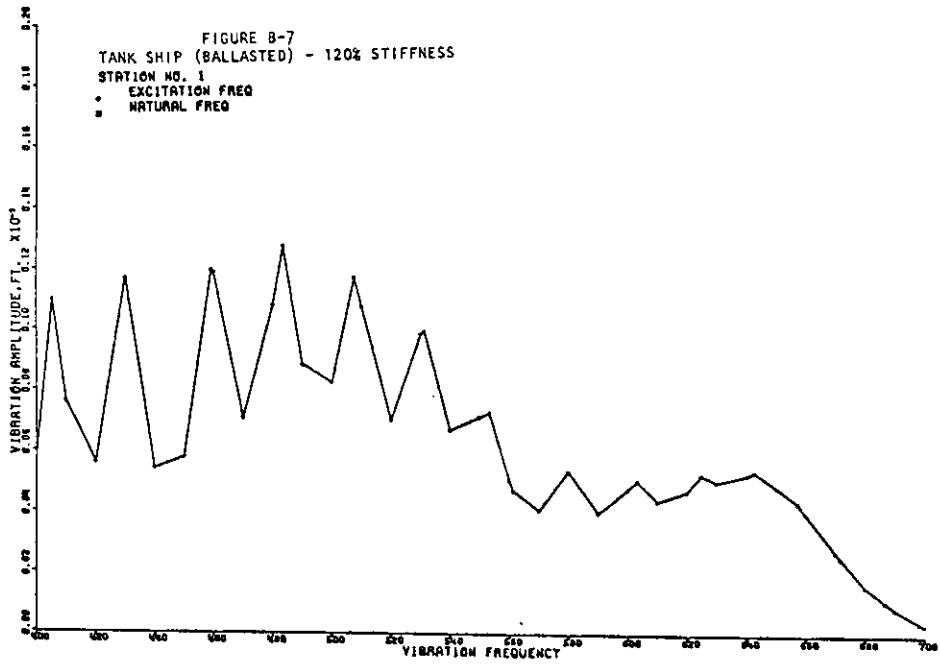
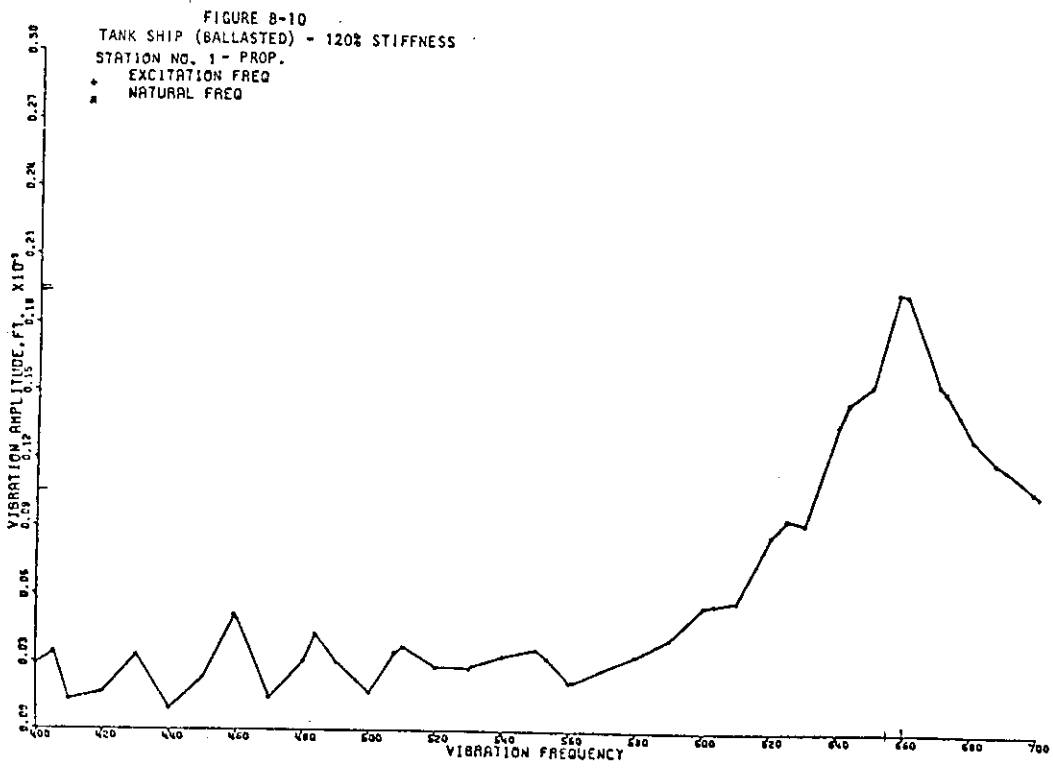
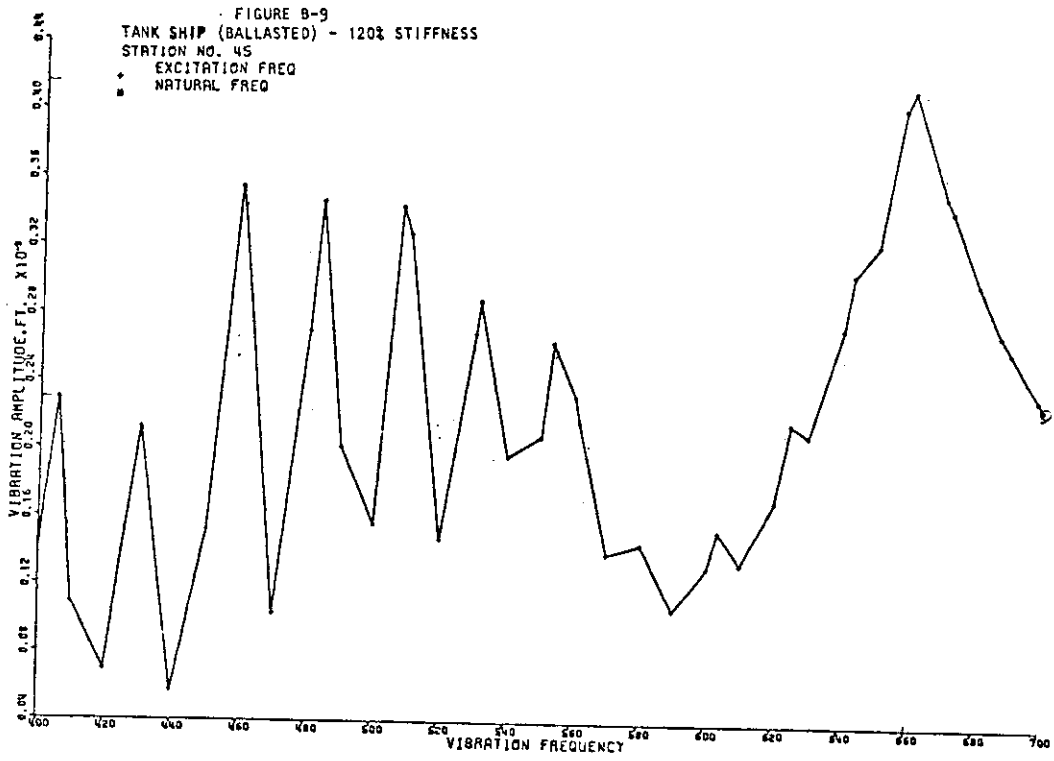


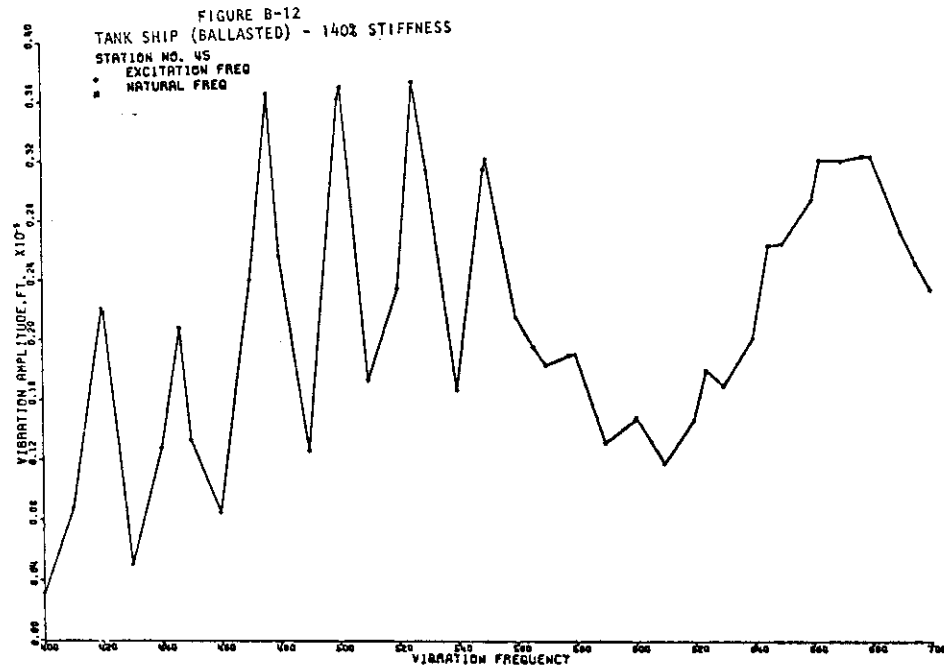
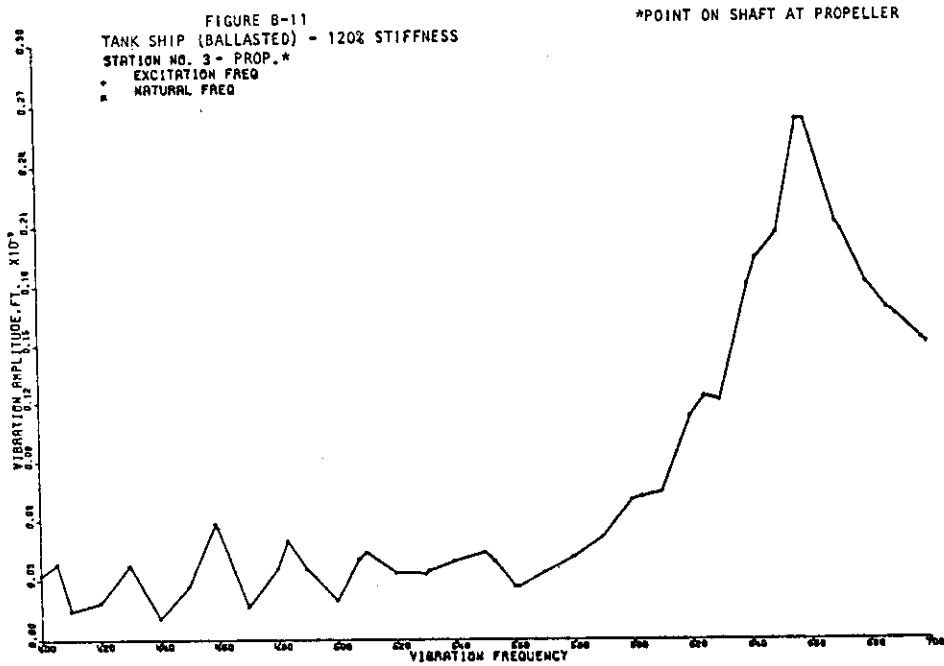
FIGURE B-4  
 TANK SHIP (BALLASTED) - 80% STIFFNESS  
 STATION NO. 1 - PROP.  
 \* EXCITATION FREQ  
 ■ NATURAL FREQ

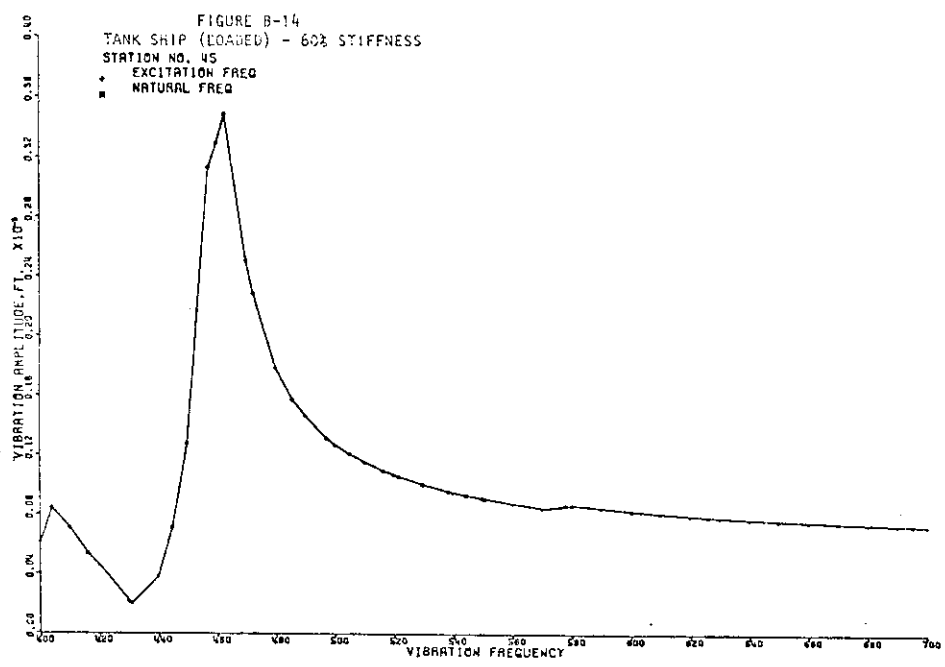
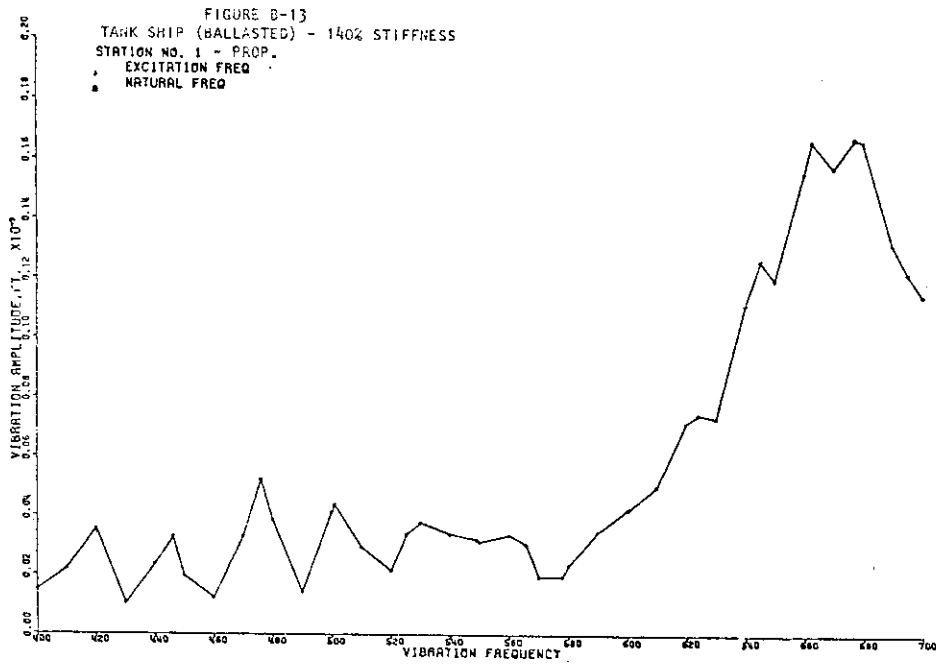


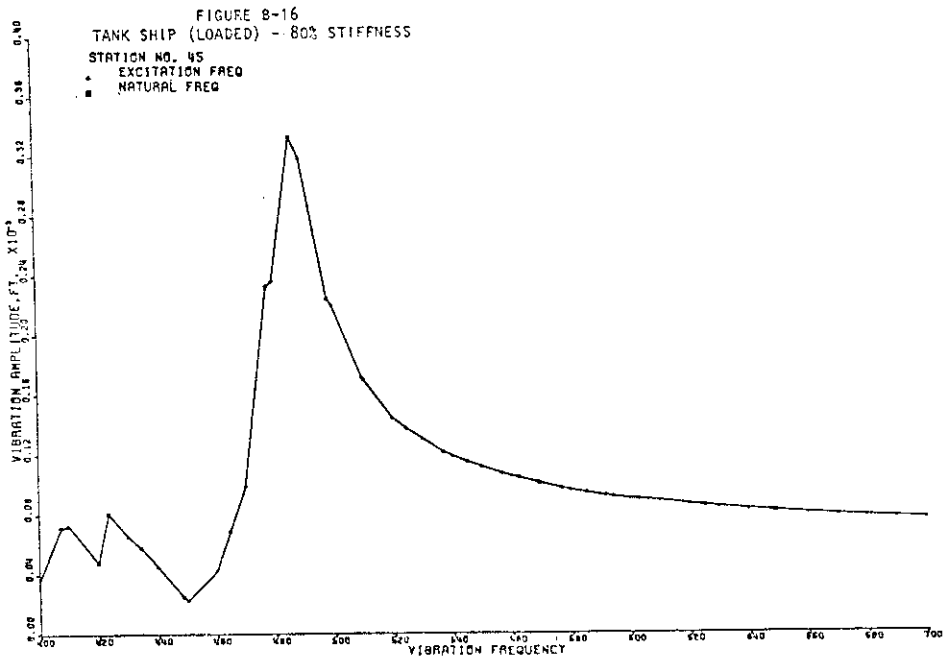
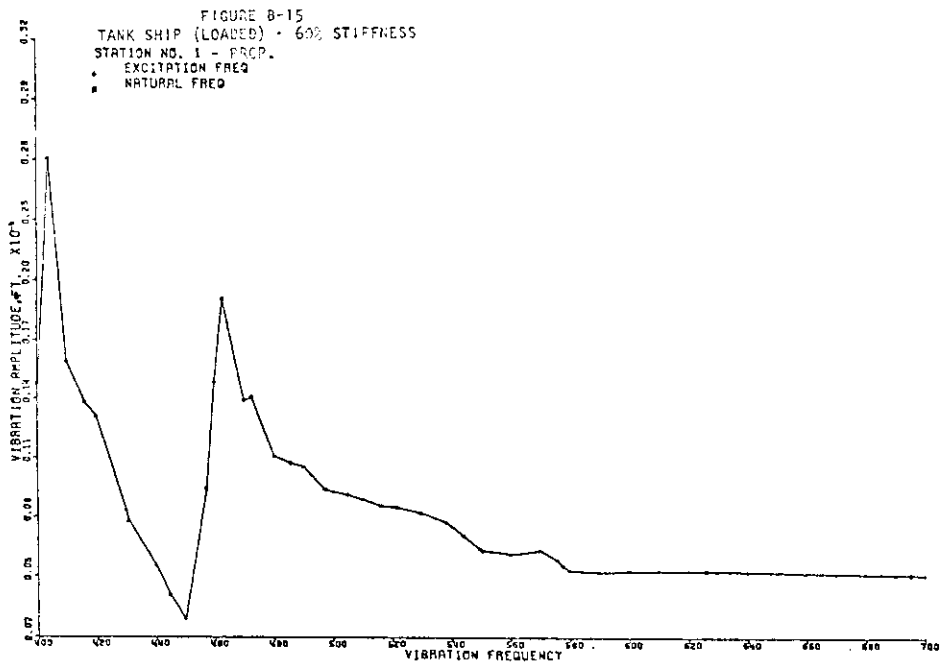












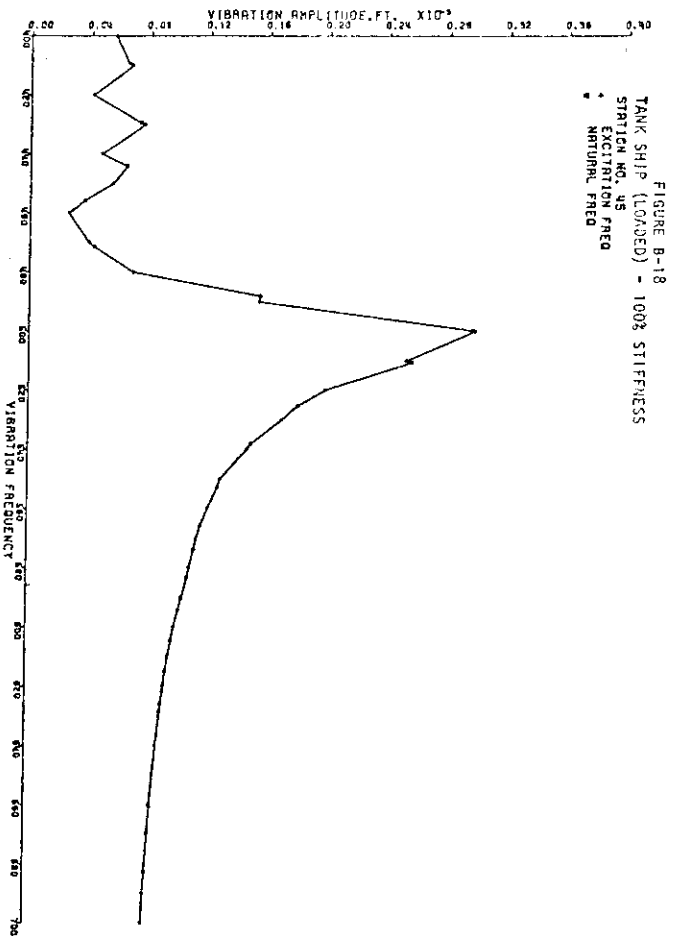
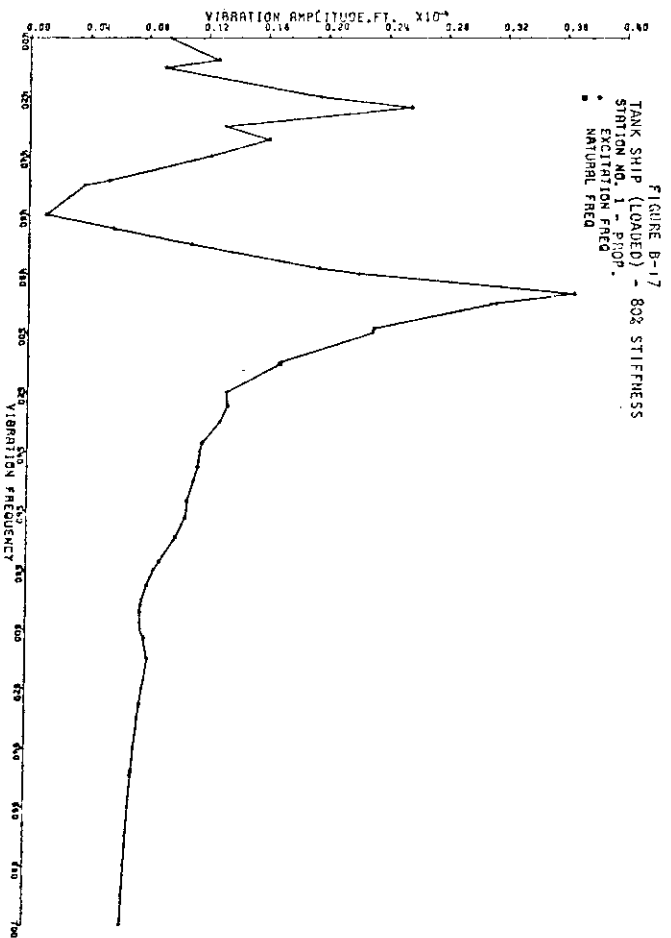


FIGURE B-13  
 TANK SHIP (LOADED) - 100% STIFFNESS  
 STRIP NO. 1 - PROP.  
 \* EXCITATION FREQ  
 ■ NATURAL FREQ

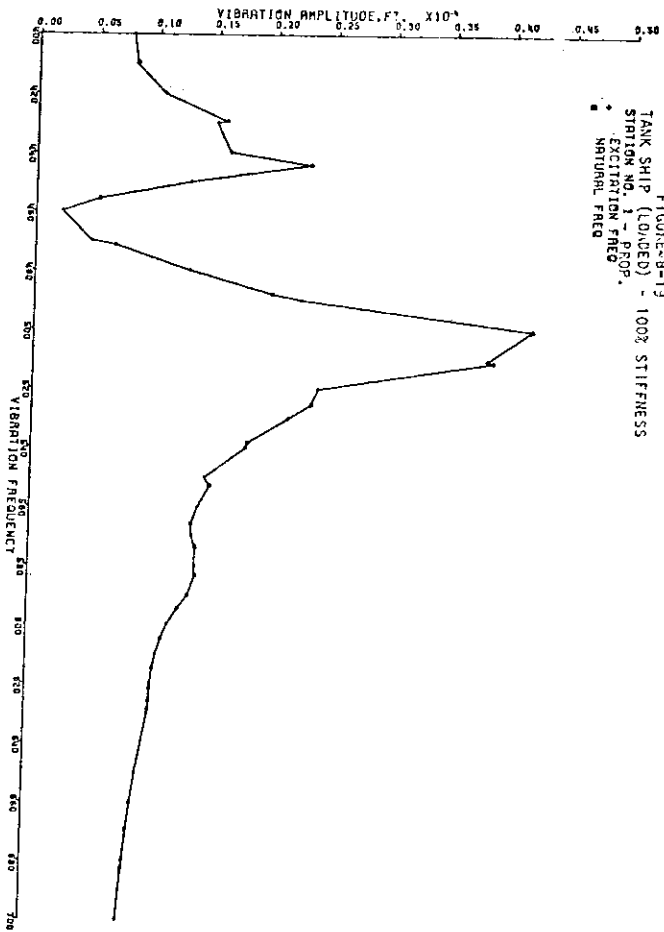
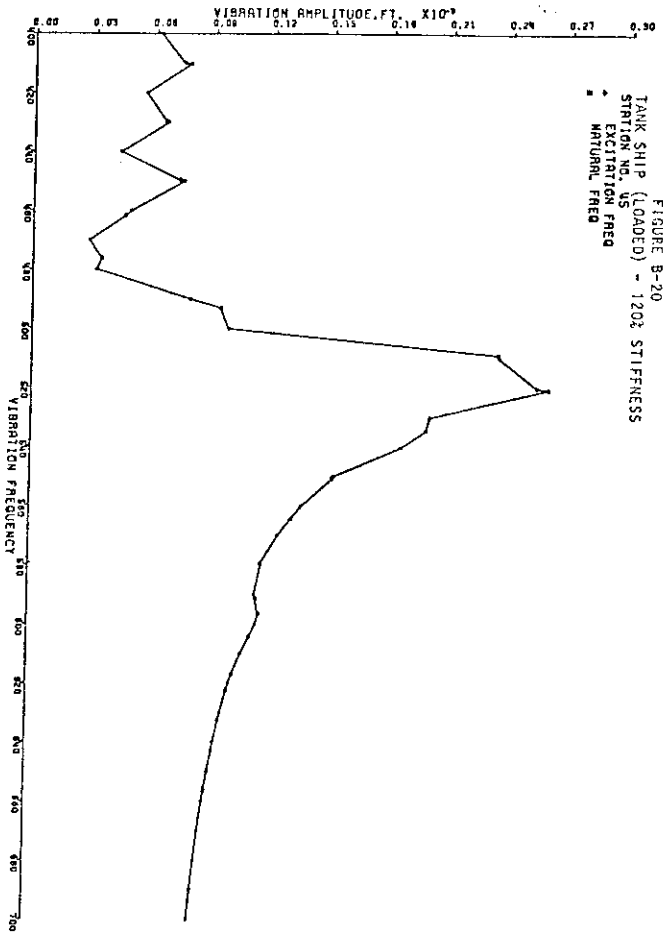
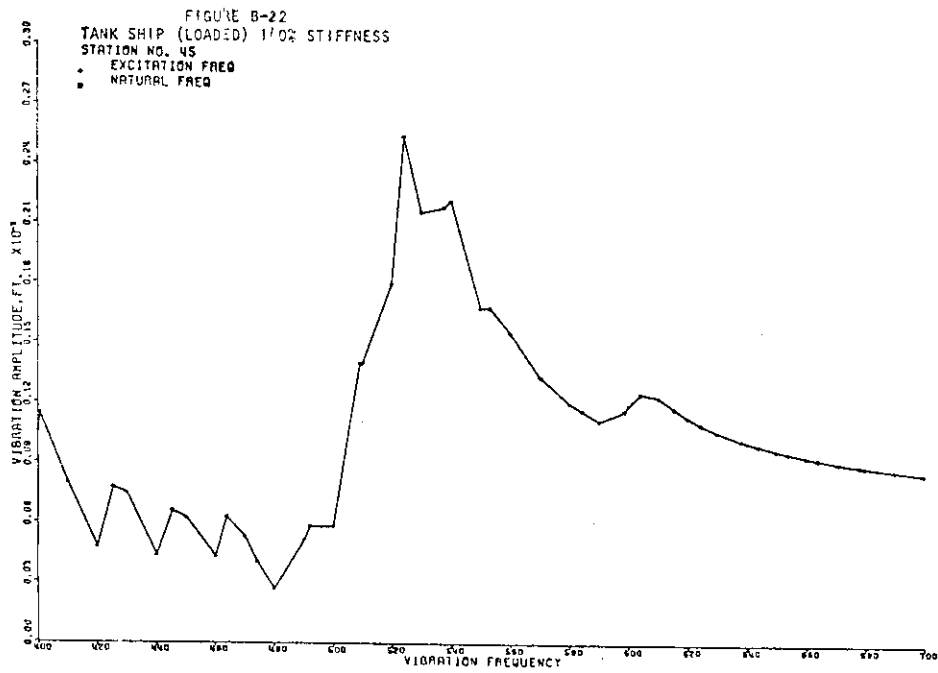
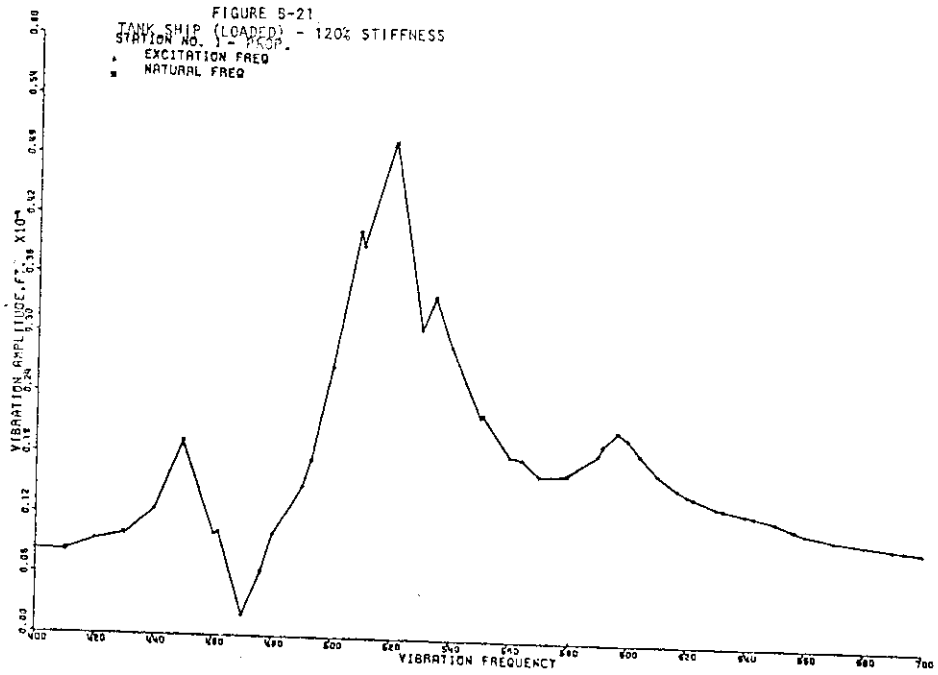


FIGURE B-20  
 TANK SHIP (LOADED) - 120% STIFFNESS  
 STRIP NO. 15  
 \* EXCITATION FREQ  
 ■ NATURAL FREQ





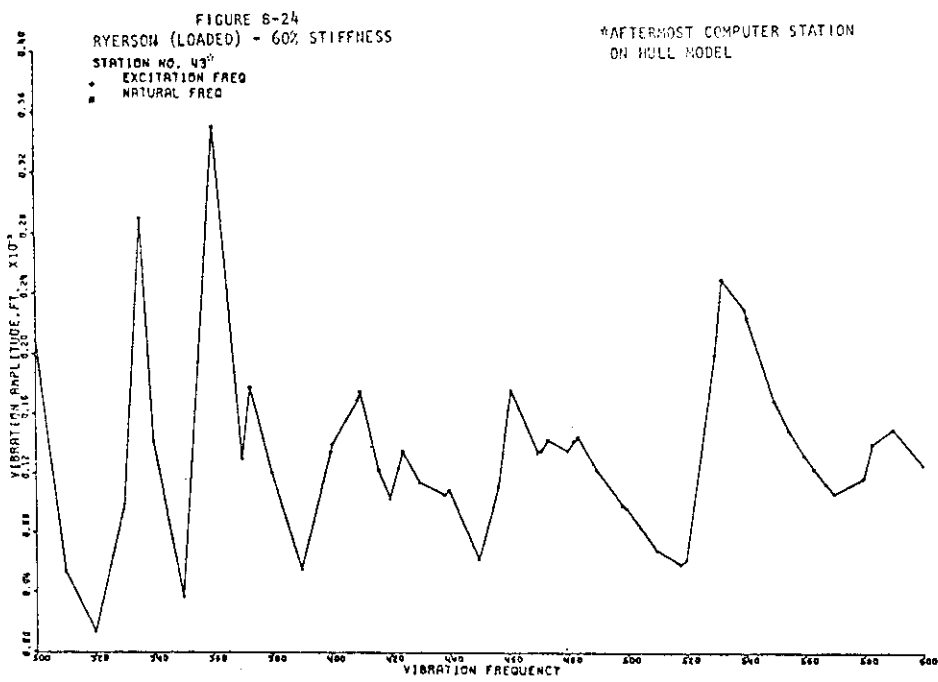
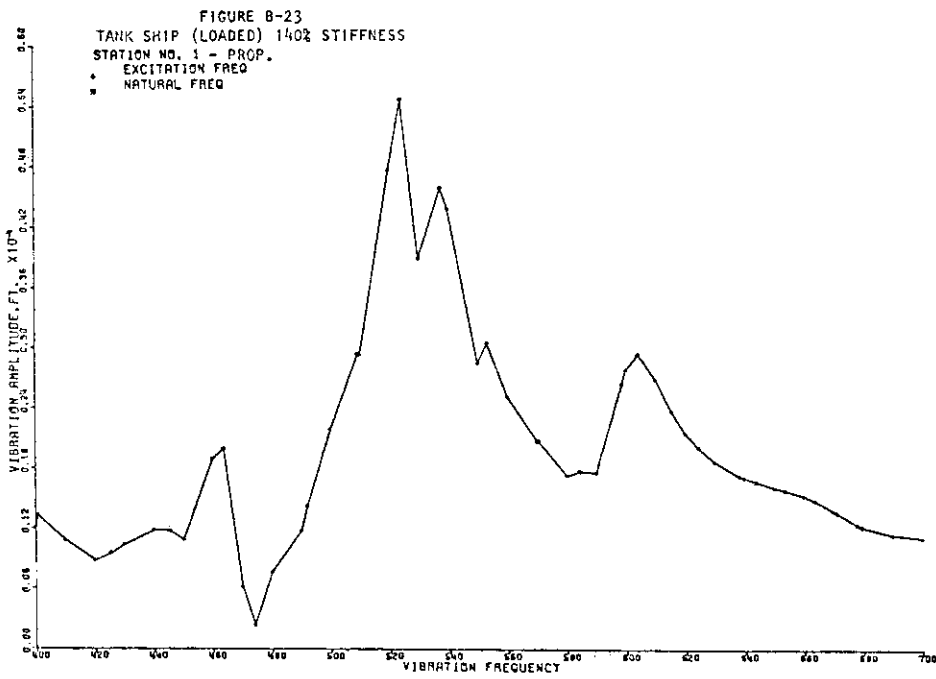


FIGURE B-25  
RYERSON (LOADED) - 80% STIFFNESS  
STATION NO. 1 - PROP.  
• EXCITATION FREQ  
■ NATURAL FREQ

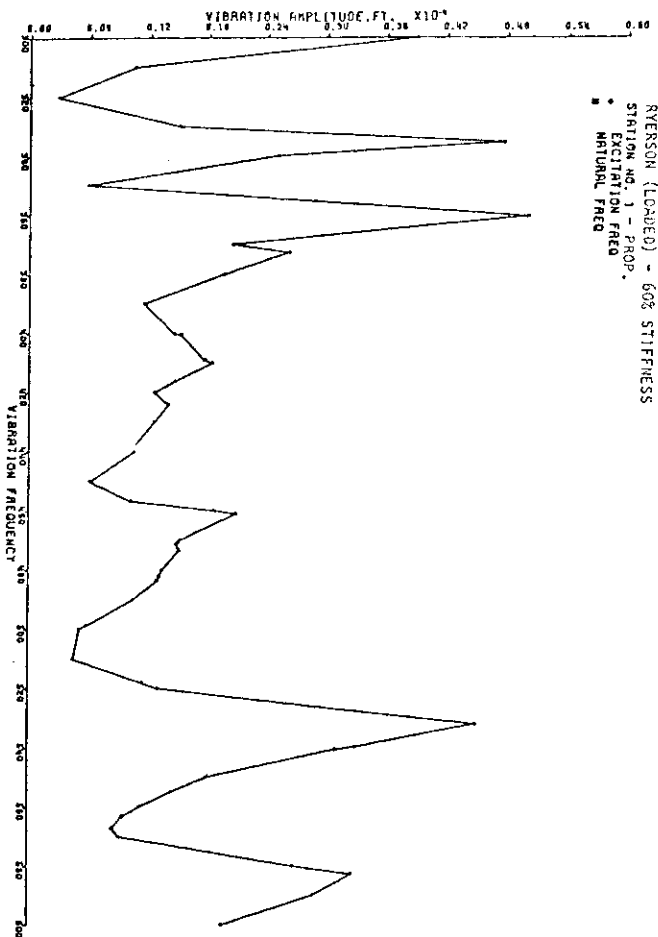
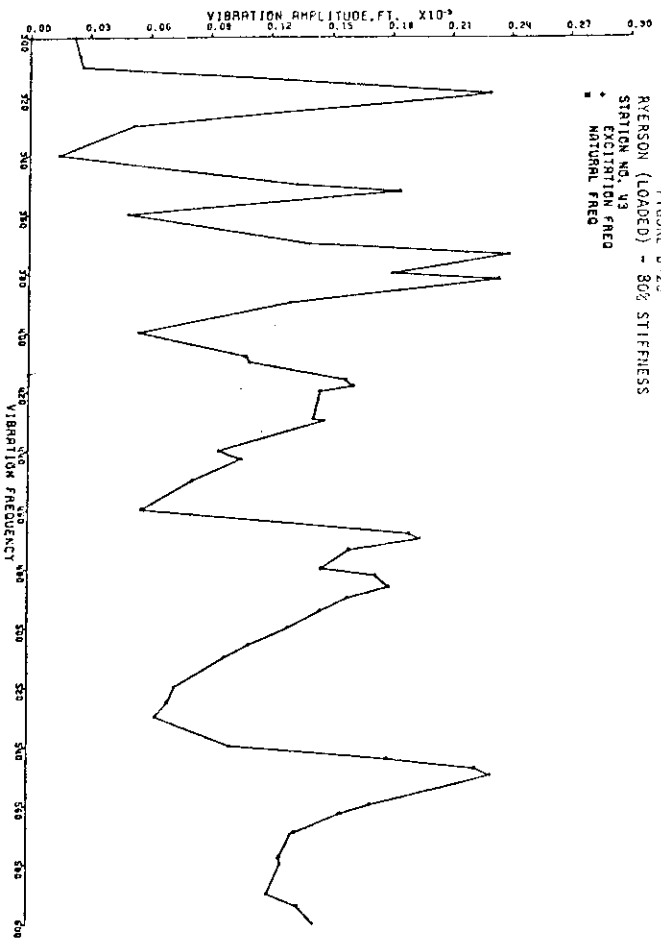
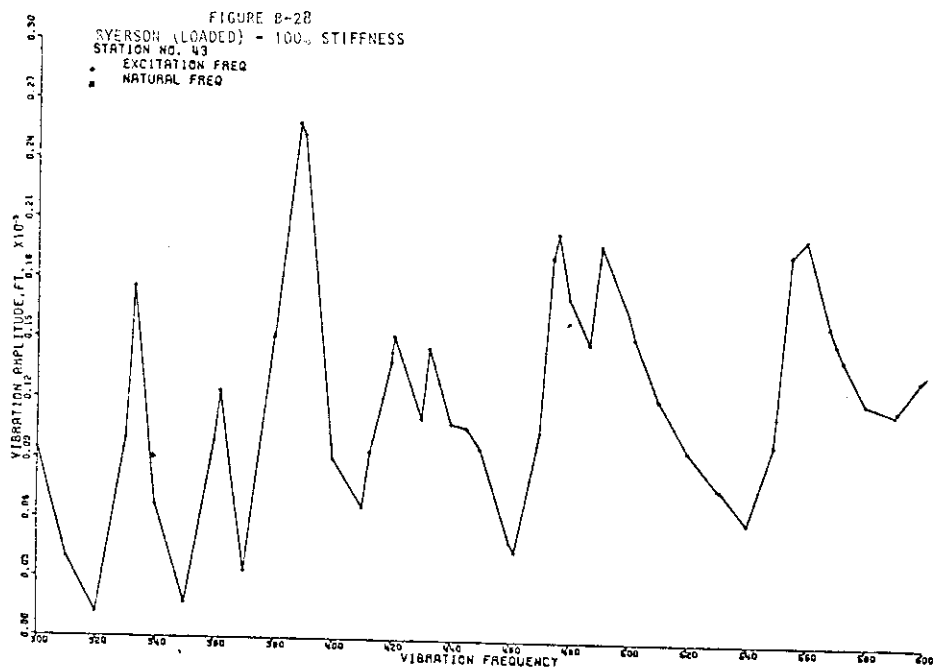
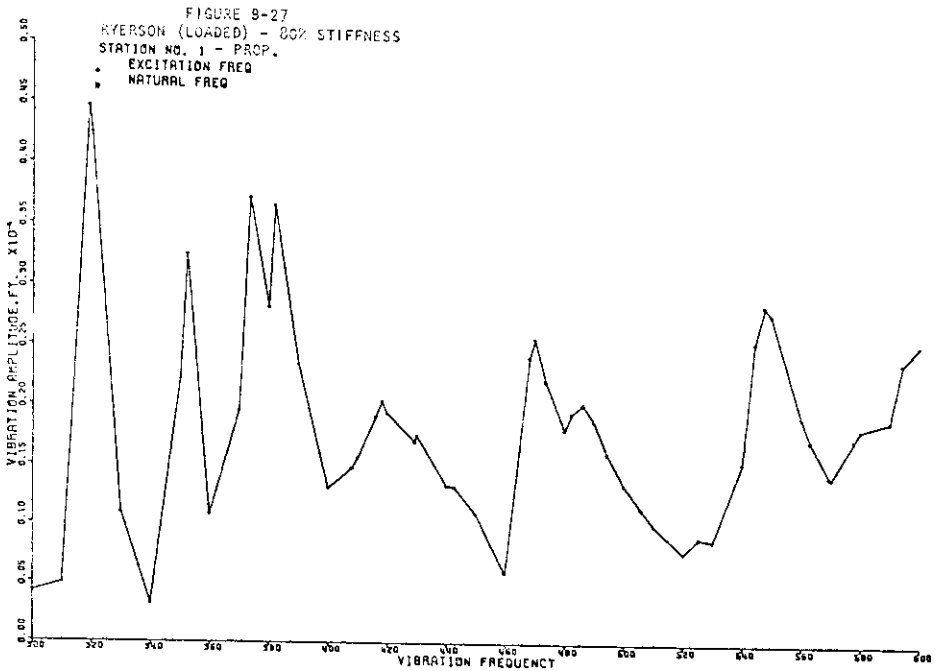
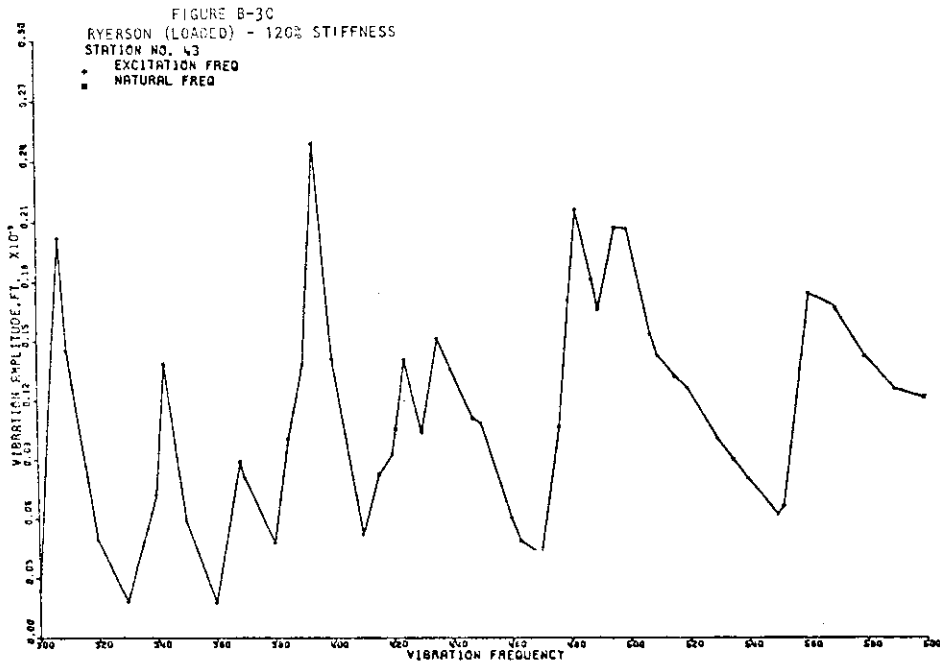
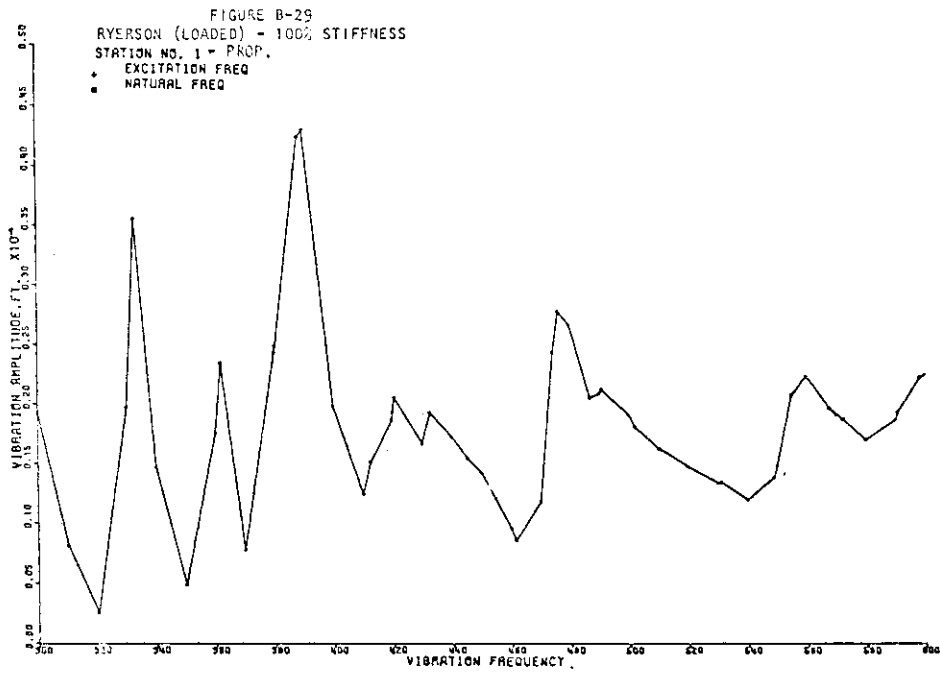
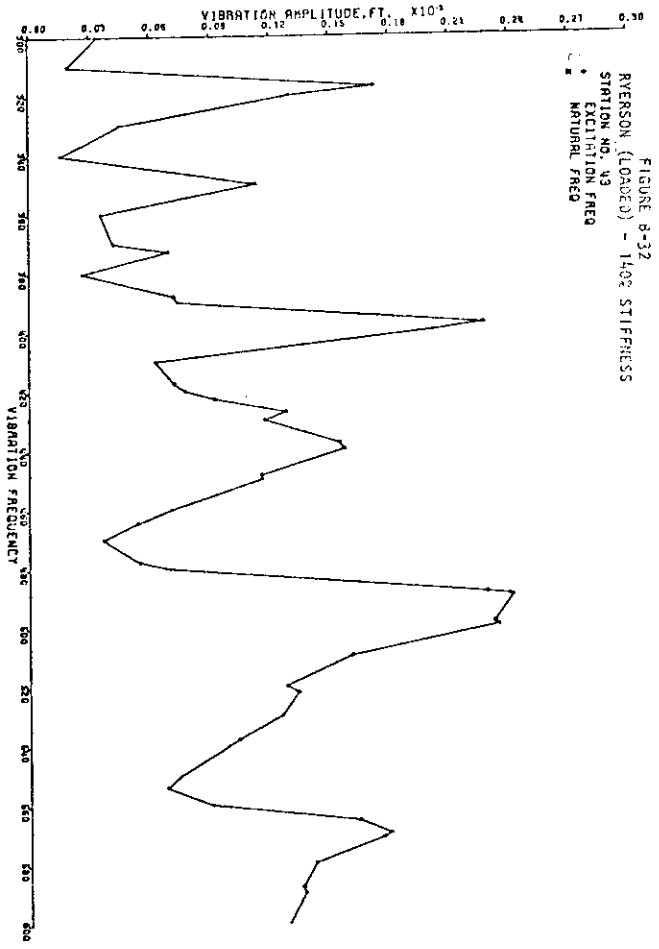
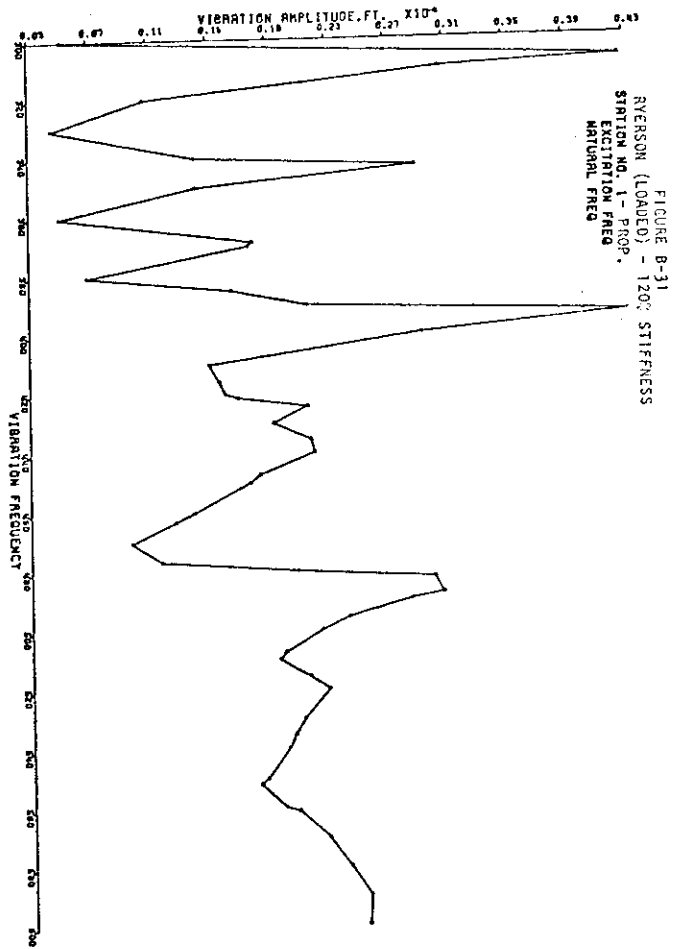


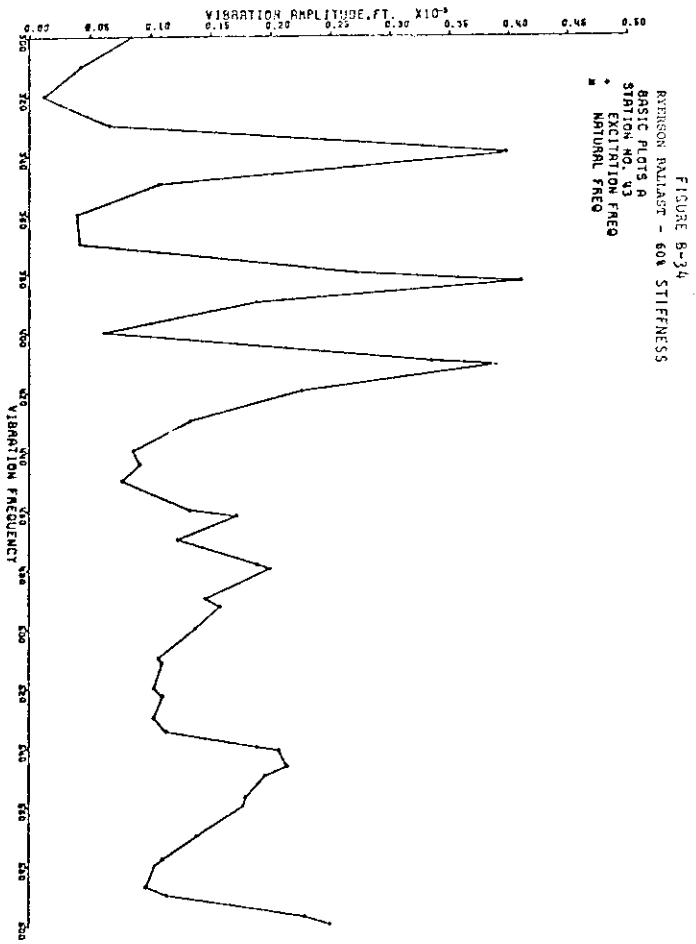
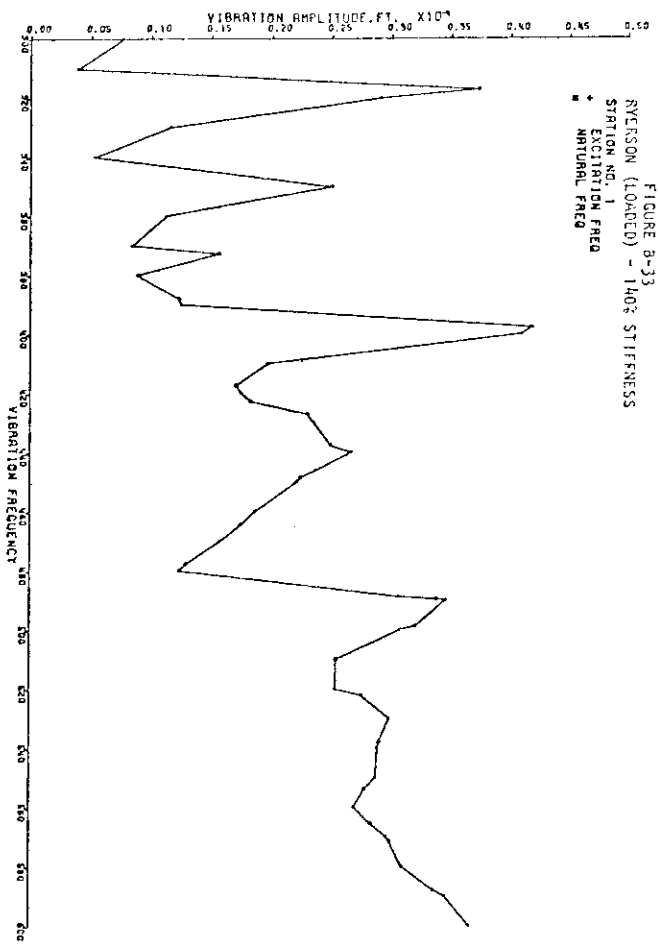
FIGURE B-26  
RYERSON (LOADED) - 80% STIFFNESS  
STATION NO. 19  
• EXCITATION FREQ  
■ NATURAL FREQ

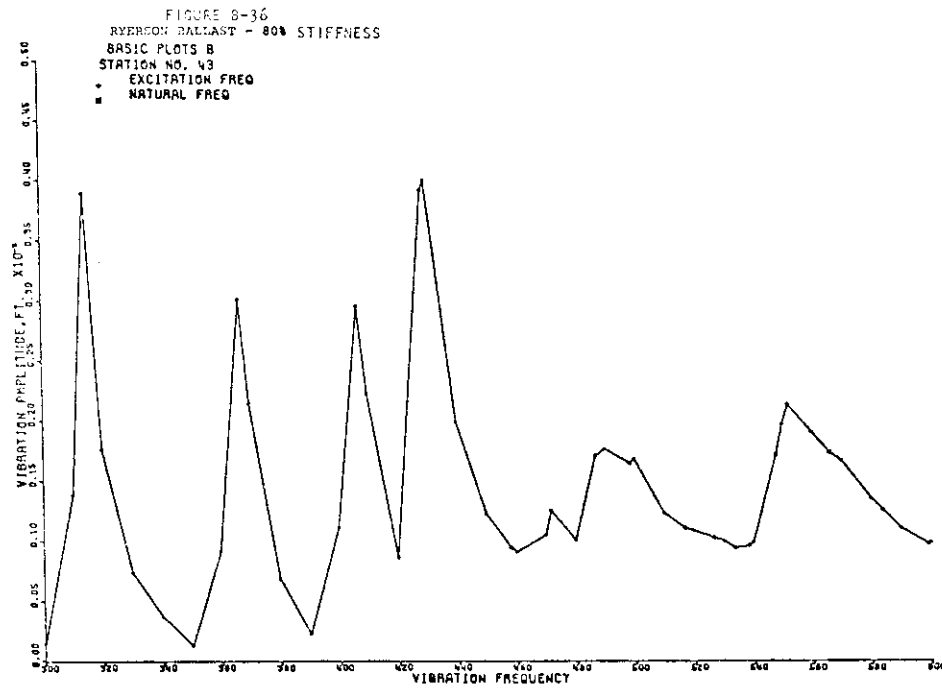
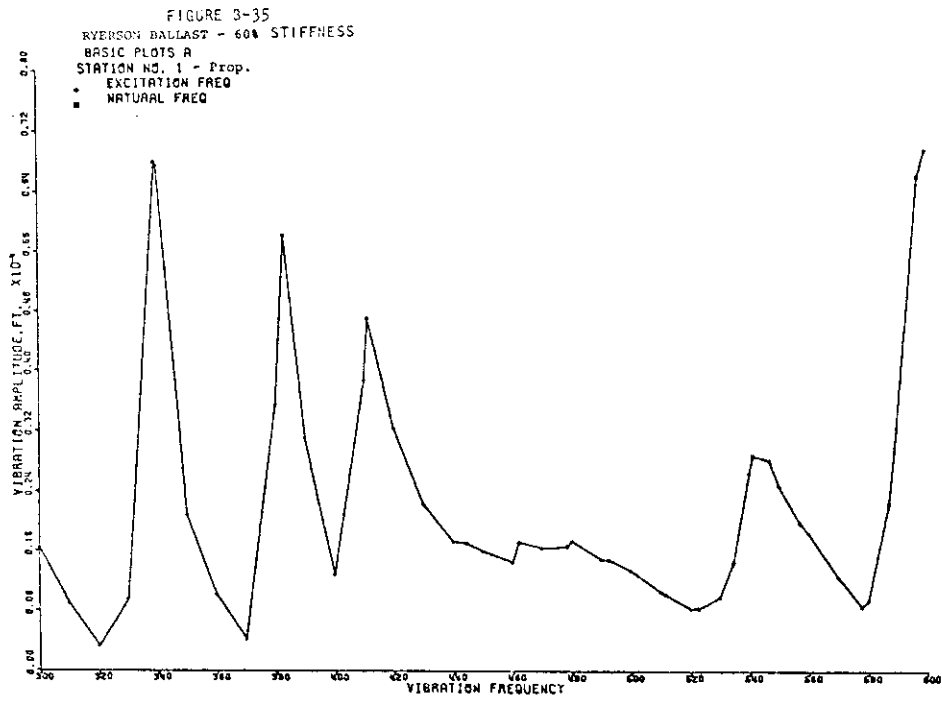












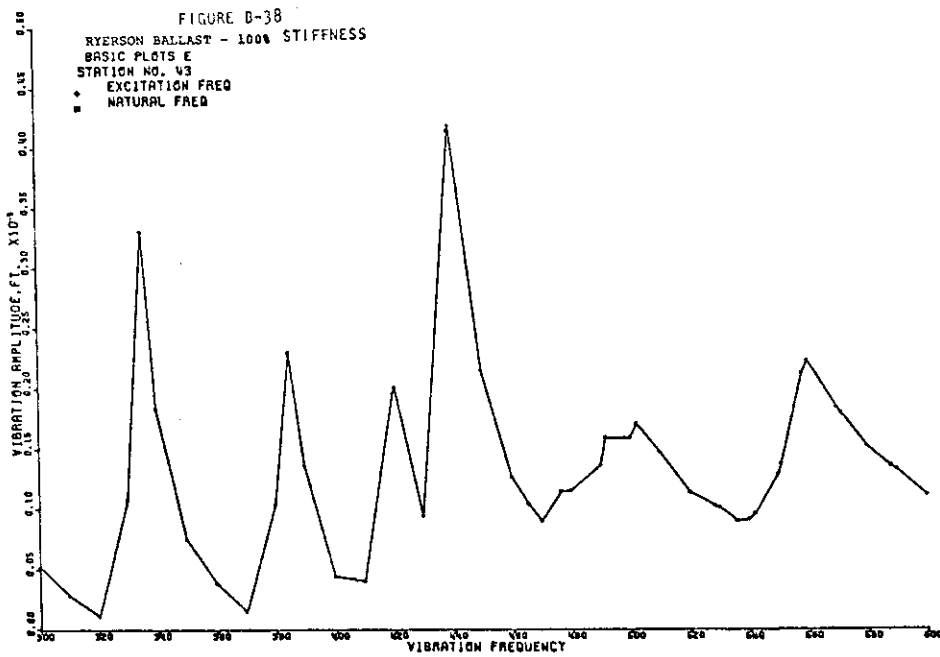
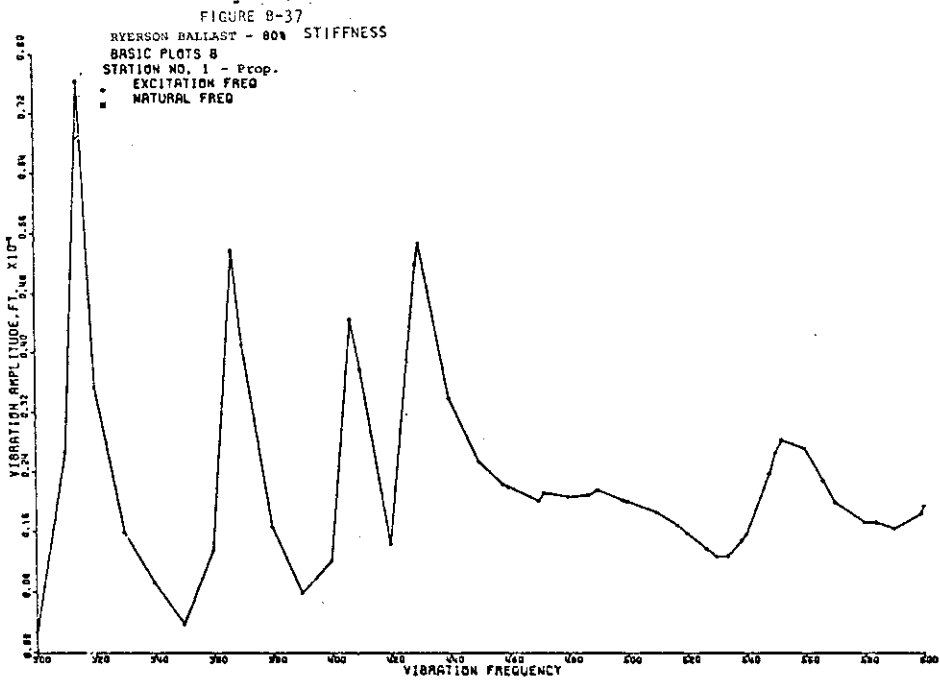


FIGURE D-39  
 RYERSON BALLAST - 100% STIFFNESS  
 BASIC PLOTS E  
 STATION NO. 1 - Prop.

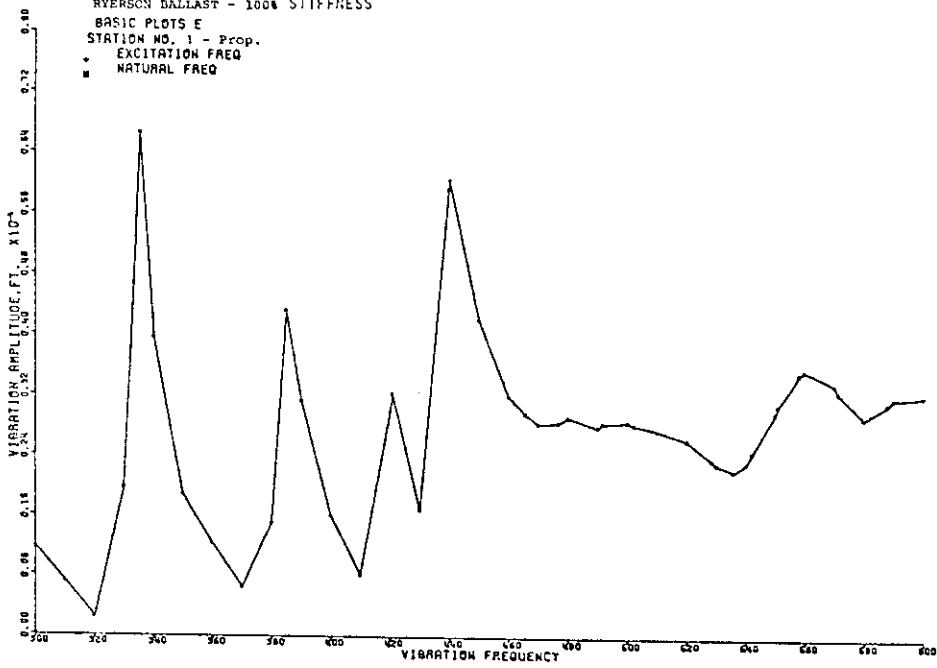
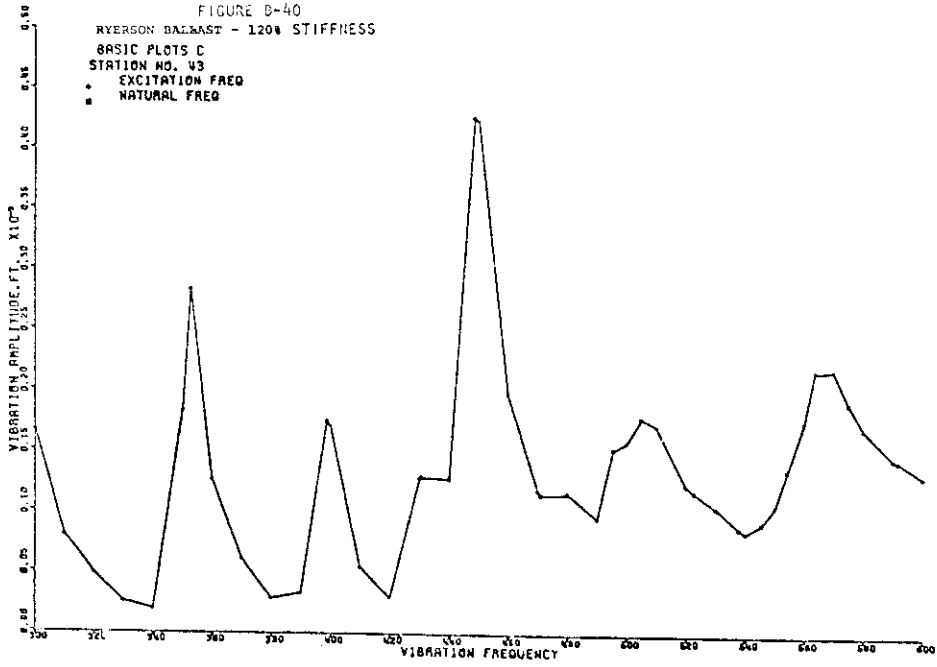
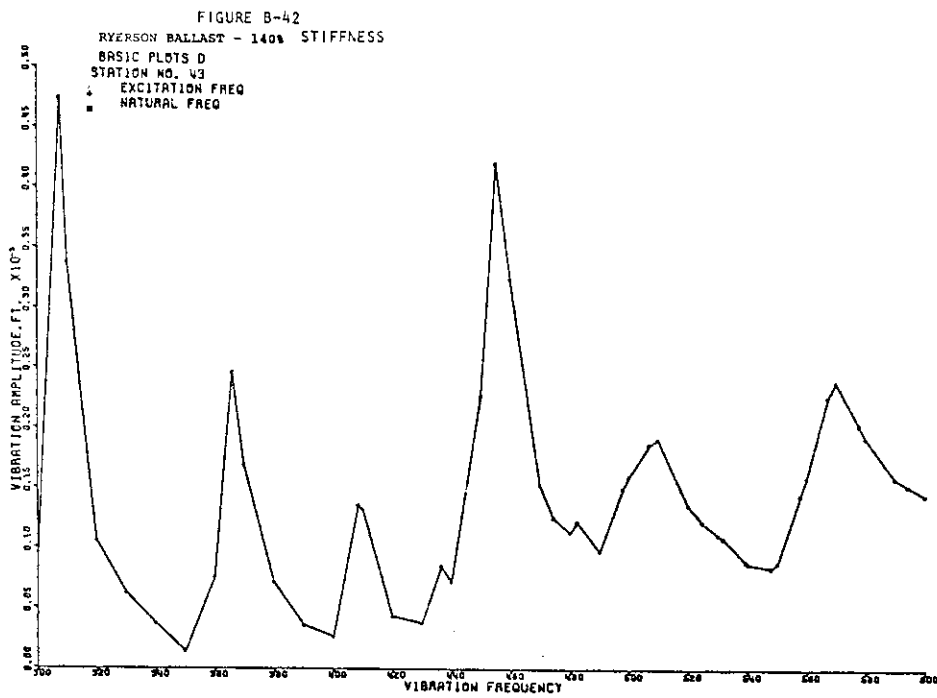
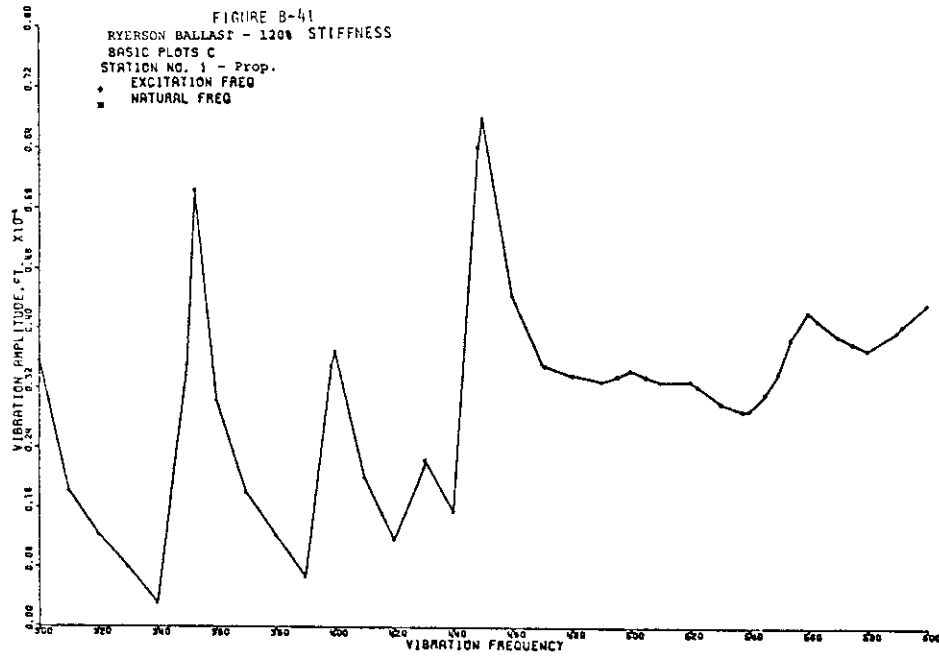
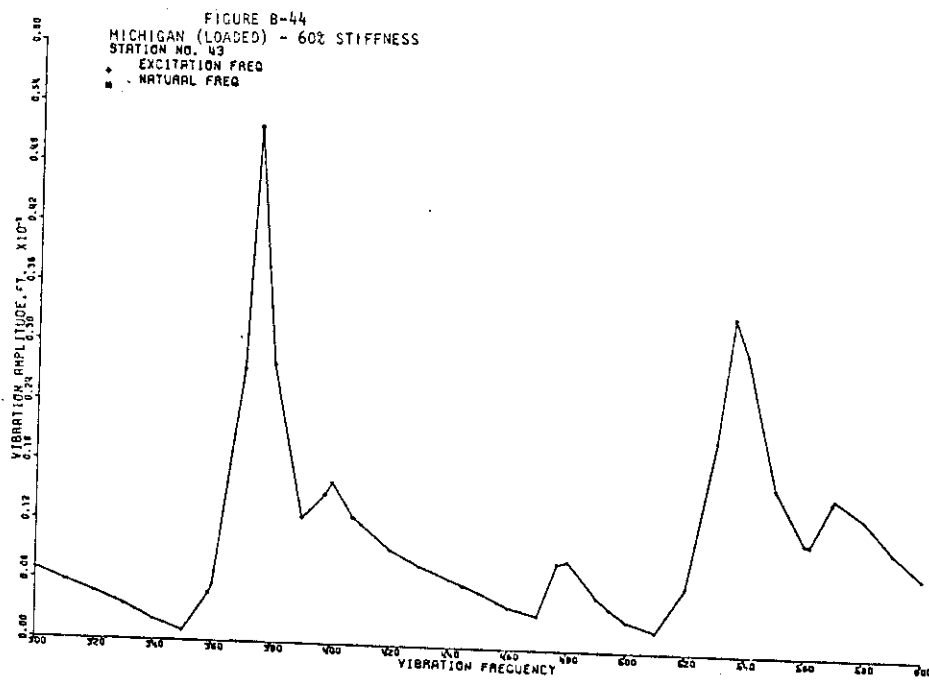
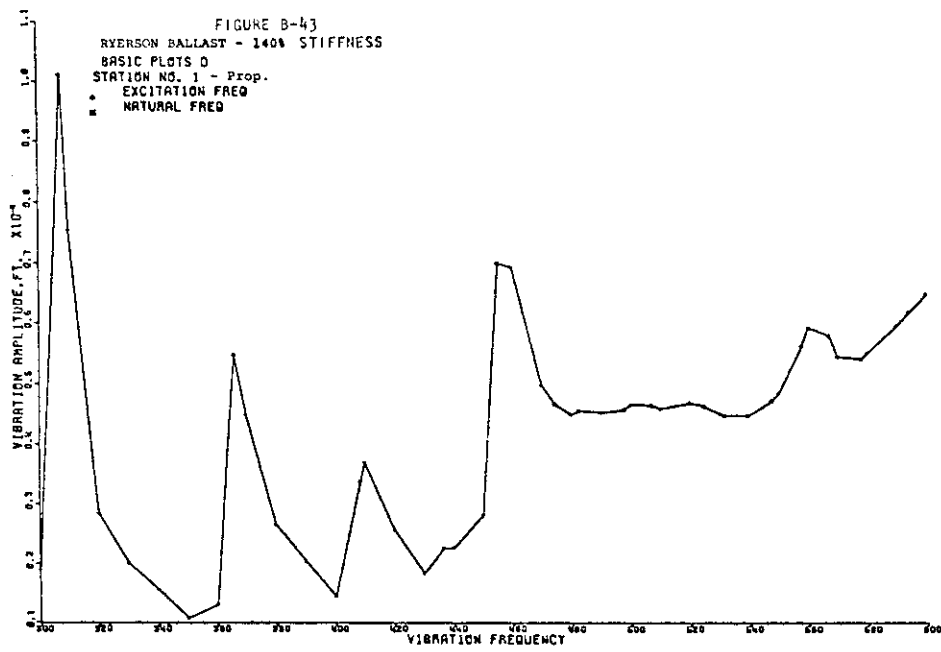
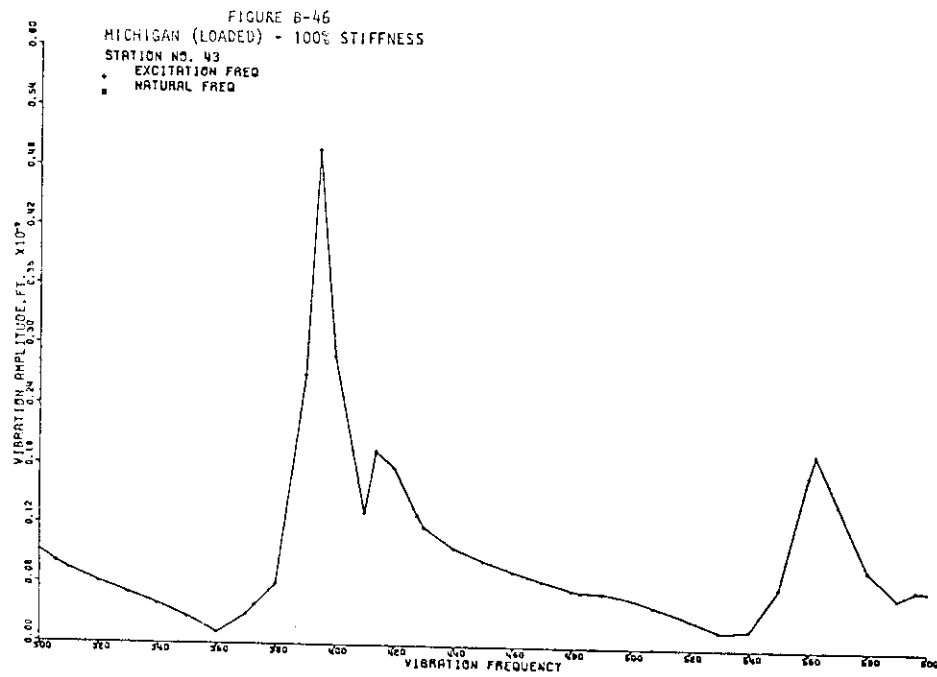
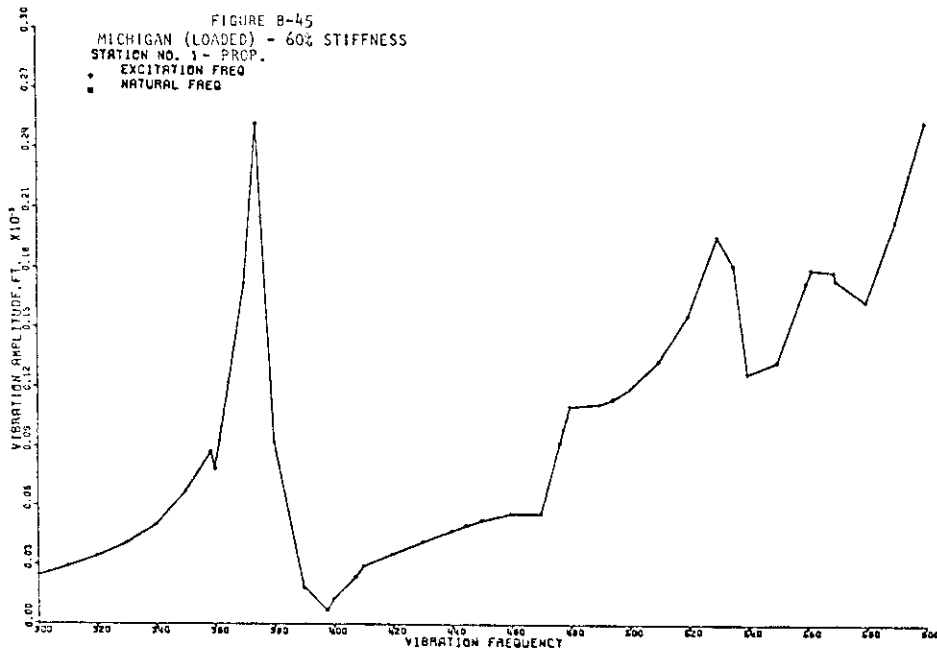


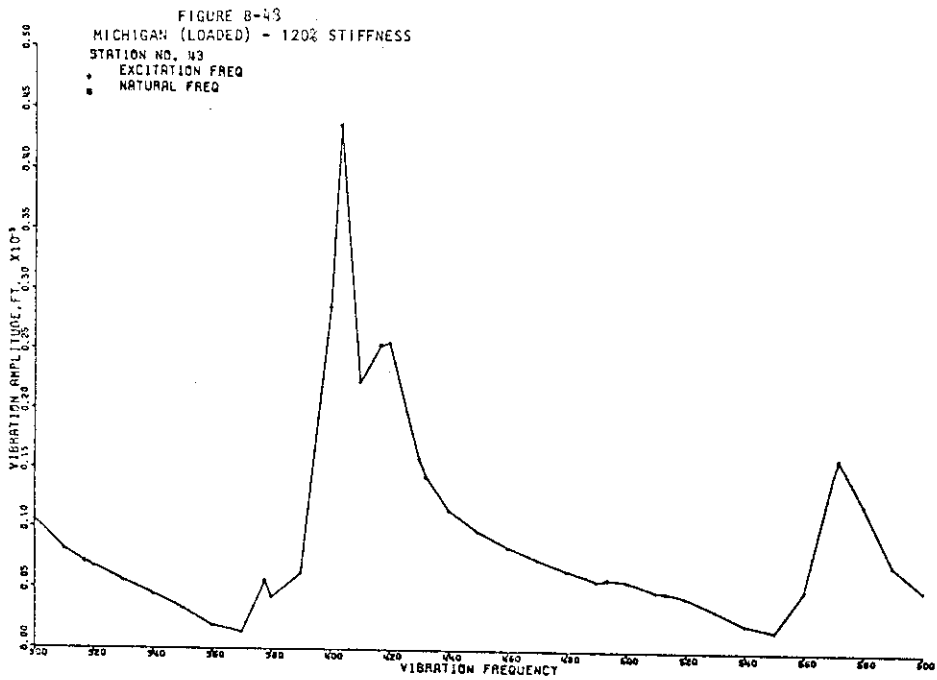
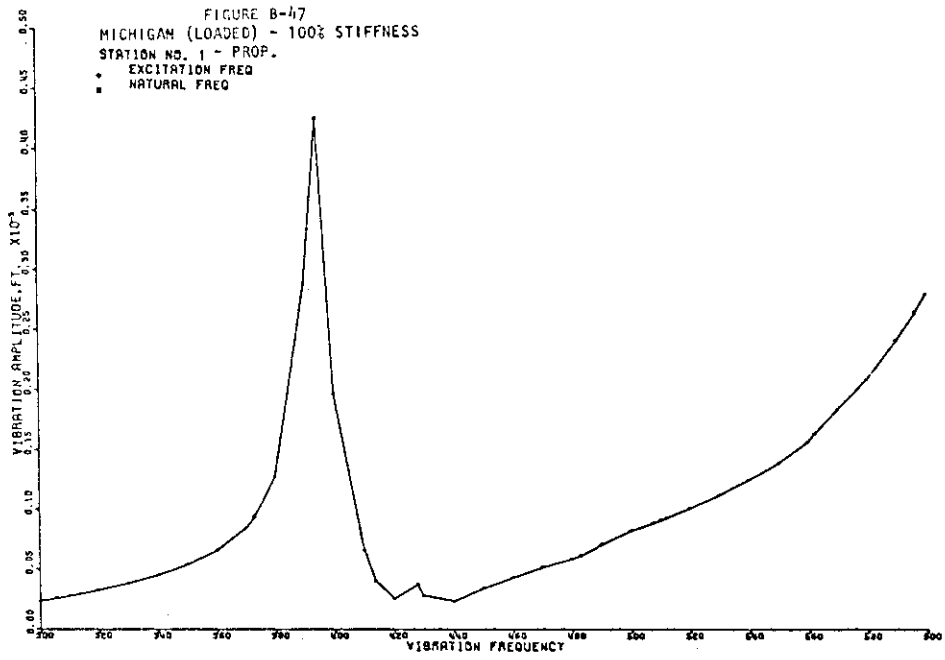
FIGURE D-40  
 RYERSON BALLAST - 120% STIFFNESS  
 BASIC PLOTS C  
 STATION NO. 43

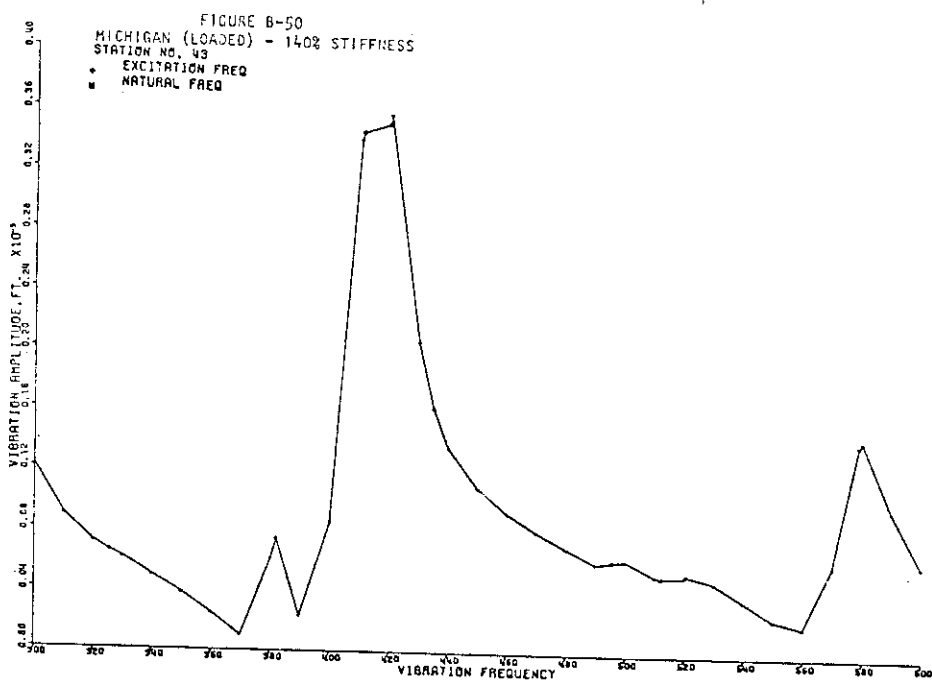
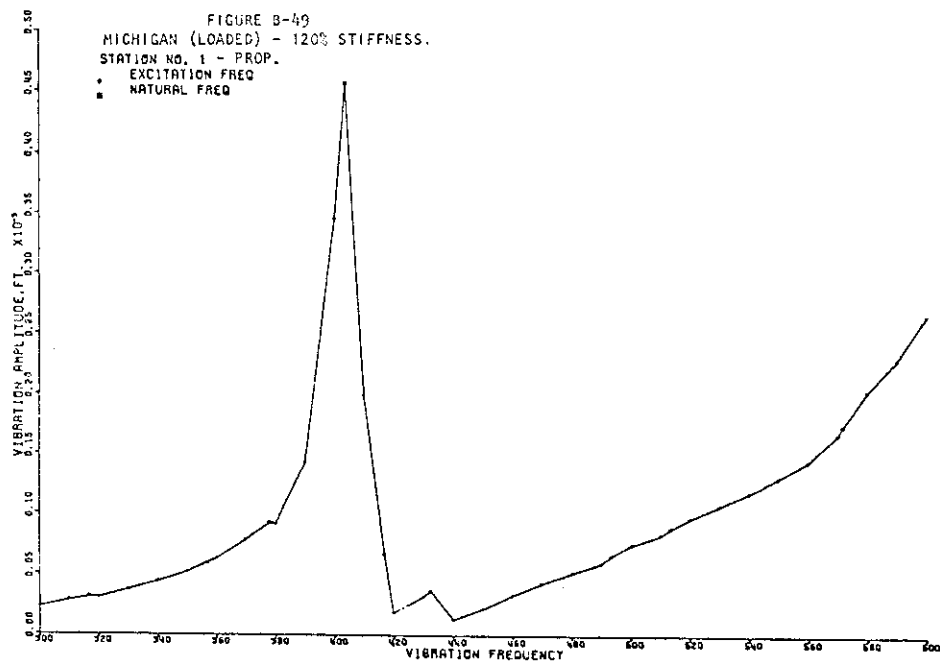


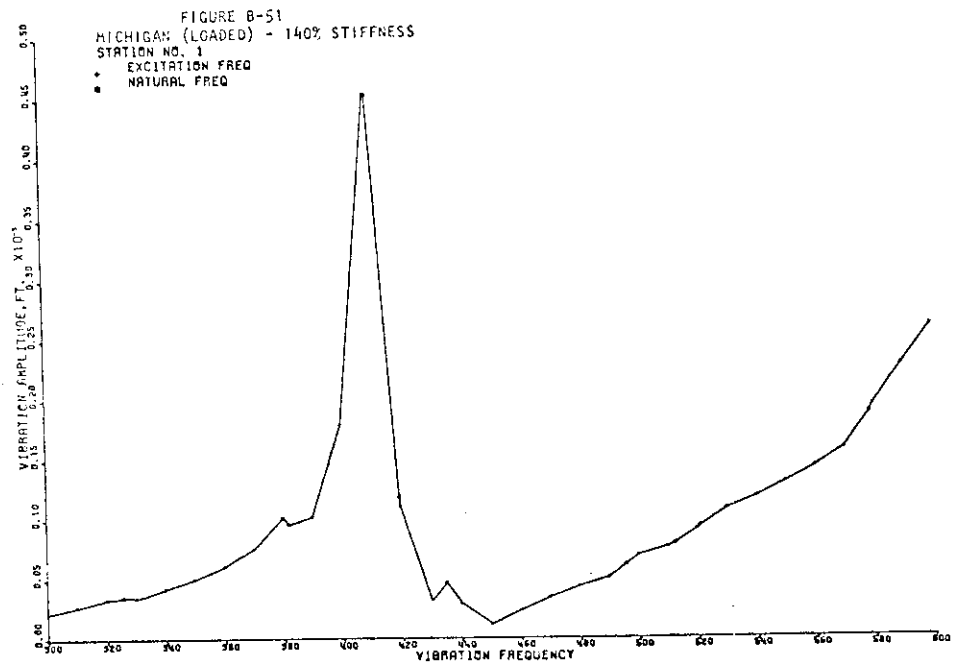












SLAM RESPONSE

- $\tau$  = SLAM DURATION (SEC)
- .125
  - .250
  - △ .500
  - ◇ 1.000
  - 2.000
- NOTE: NUMBERS ABOVE SYMBOLS INDICATE COMPUTER MODEL STATION

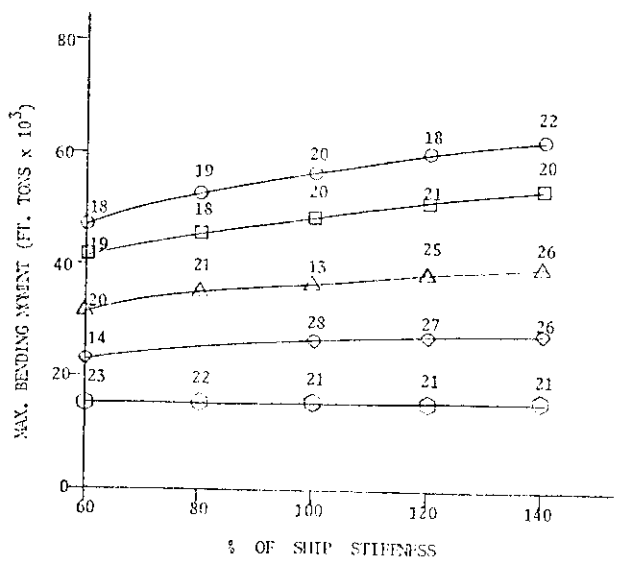
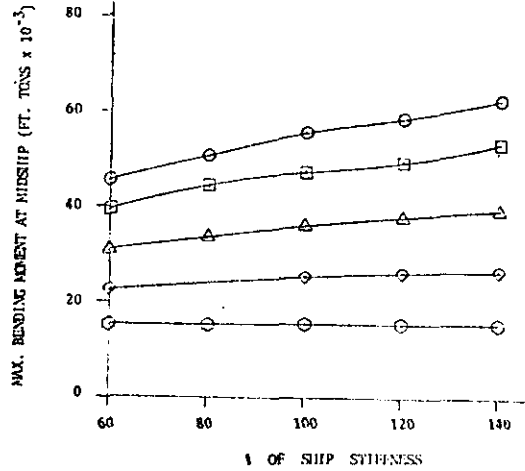


FIGURE B-52  
 MAX. BENDING MOMENT vs. SHIP STIFFNESS  
 TANK SHIP (LOADED)

- τ - SLAM DURATION (SEC)
- .125
  - .250
  - △ .500
  - ◇ 1.000
  - 2.000

FIGURE B-53  
MAX. BENDING MOMENT AT MIDSHIP vs. SHIP STIFFNESS  
TANK SHIP (LOADED)



- τ - SLAM DURATION (SEC)
- .125
  - .250
  - △ .500
  - ◇ 1.000
  - 2.000

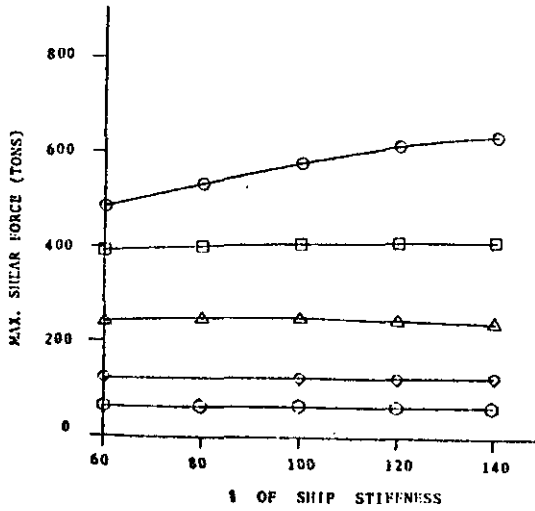


FIGURE B-54  
MAX. SHEAR FORCE vs. SHIP STIFFNESS  
TANK SHIP (LOADED)

$t$  = SLAM DURATION (SEC)

- .125
- .250
- △ .500
- ◇ 1.000
- 2.000

NOTE: NUMBERS ABOVE SYMBOLS INDICATE COMPUTER MODEL STATIONS

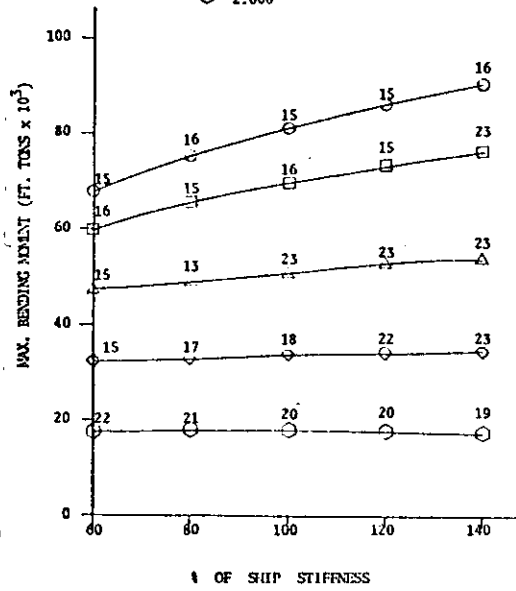


FIGURE B-55  
MAX. BENDING MOMENT vs. SHIP STIFFNESS  
TANK SHIP - BALLAST

- $t$  .125
- .250
- △ .500
- ◇ 1.000
- 2.000

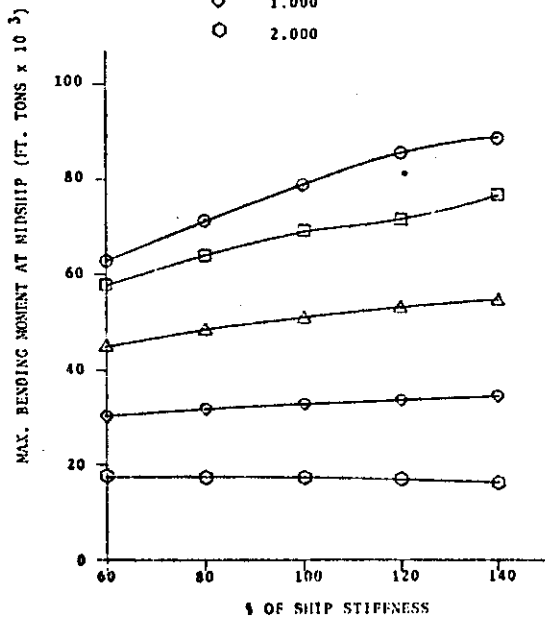


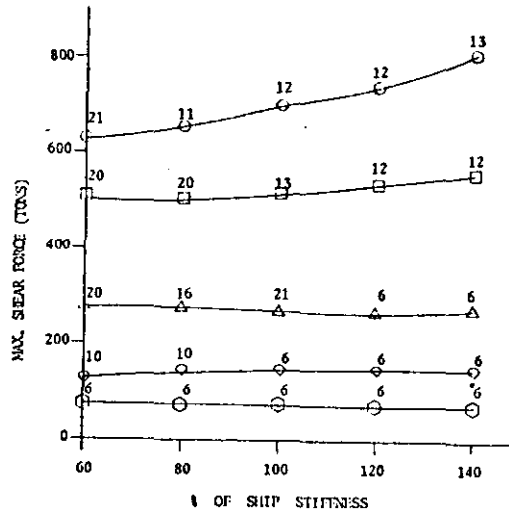
FIGURE B-56  
MAX. BENDING MOMENT AT MIDSHIP vs. SHIP STIFFNESS  
TANK SHIP - BALLAST

$\tau$  = SLAM DURATION (SEC)

- .125
- .250
- △ .500
- ◇ 1.000
- 2.000

NOTE: NUMBERS ABOVE SYMBOLS INDICATE COMPUTER MODEL STATIONS

FIGURE B-57  
MAX. SHEARING FORCE vs. SHIP STIFFNESS  
TANK SHIP - BALLAST



$\tau$  = SLAM DURATION: (SEC)

- .0625
- .125
- △ .250
- ◇ .500
- 1.000

NOTE: NUMBERS ABOVE SYMBOLS INDICATE COMPUTER MODEL STATIONS

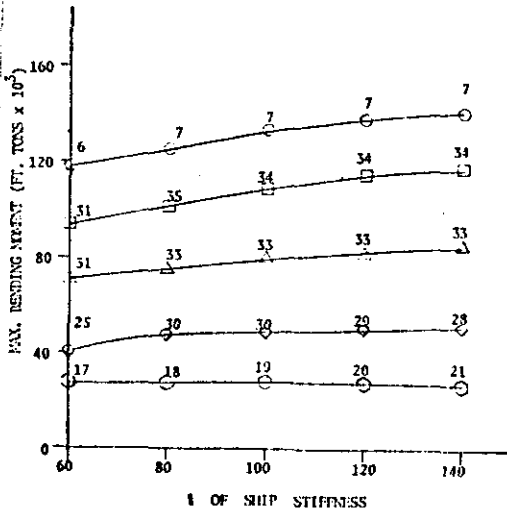


FIGURE B-58  
MAX. BENDING MOMENT vs. SHIP STIFFNESS  
RYERSON - LOADED

τ - SLAM DURATION (SEC)

- .0625
- .125
- △ .250
- ◇ .500
- 1.000

FIGURE B-59  
MAX. BENDING MOMENT AT MIDSHIP vs. SHIP STIFFNESS  
RYERSON - LOADED

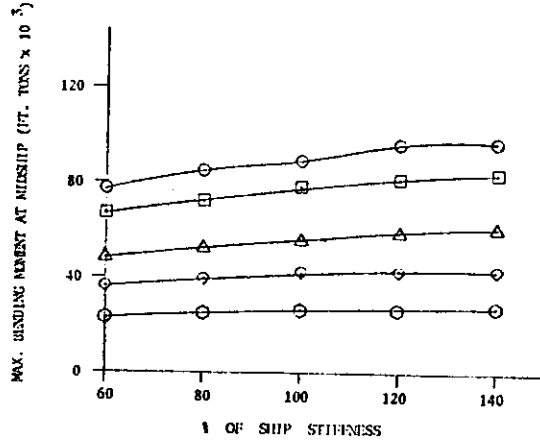
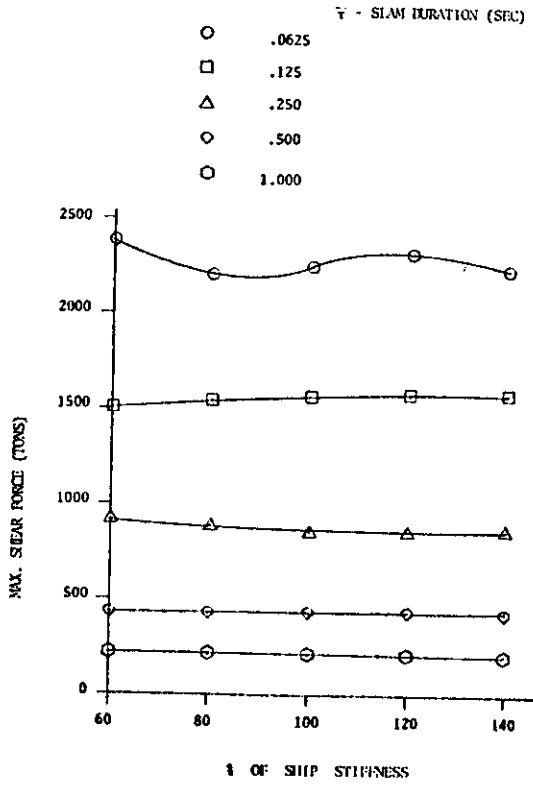


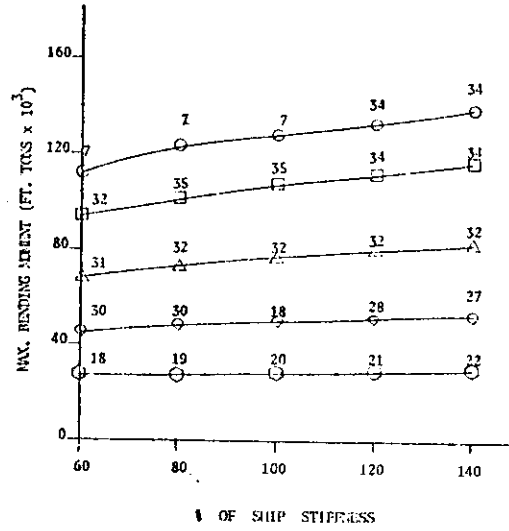
FIGURE B-60  
MAX. SHEARING FORCE vs. SHIP STIFFNESS  
RYERSON - LOADED

$\tau$  = SLAM DURATION (SEC)

- .0625
- .125
- △ .250
- ◇ .500
- 1.000

NOTE: NUMBERS ABOVE SYMBOLS INDICATE COMPUTER MODEL STATIONS

FIGURE B-61  
MAX. BENDING MOMENT vs. SHIP STIFFNESS  
RYERSON - BALLAST



$\tau$  = SLAM DURATION (SEC)

- .0625
- .125
- △ .250
- ◇ .500
- 1.000

MAX. BENDING MOMENT AT MIDSHIP (FT. TONS x 10<sup>3</sup>)

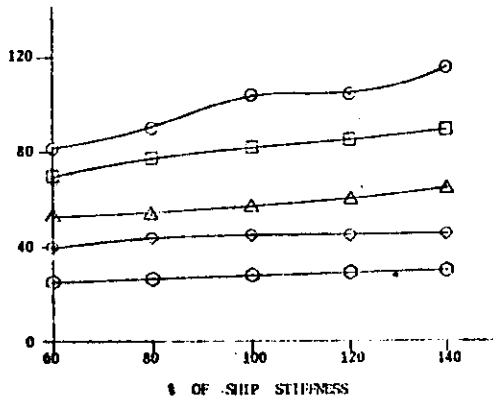
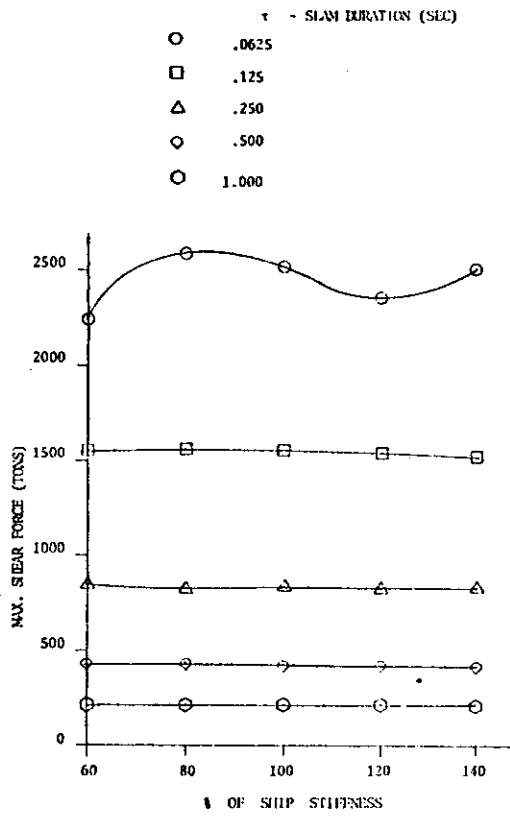


FIGURE B-62  
MAX. BENDING MOMENT AT MIDSHIP vs. SHIP STIFFNESS  
RYERSON - BALLAST

FIGURE B-63  
 MAX. SHEAR FORCE vs SHIP STIFFNESS  
 RYERSON - BALLAST



τ = SLAM DURATION (SEC)

- .04
- .08
- △ .16
- ◇ .32
- .64

NOTE: NUMBERS ABOVE SYMBOLS  
 INDICATE COMPUTER  
 MODEL STATICS

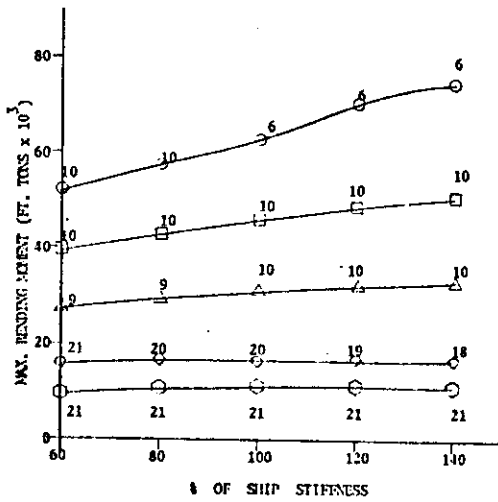


FIGURE B-64  
 MAX. BENDING MOMENT vs. SHIP STIFFNESS  
 MICHIGAN - LOADED

FIGURE B-65  
 MAX. BENDING MOMENT AT MIDSHIP vs SHIP STIFFNESS  
 MICHIGAN - LOADED

τ - SLAM DURATION (SEC)

- .04
- .08
- △ .16
- ◇ .32
- .64

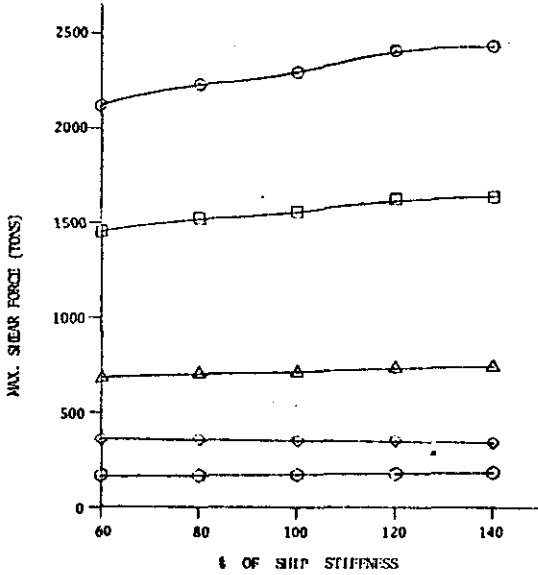
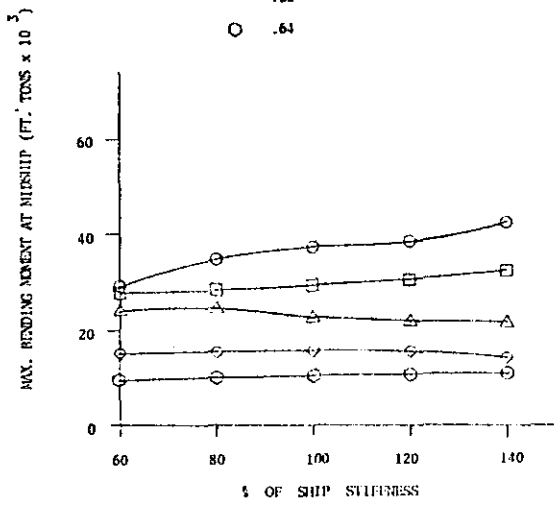
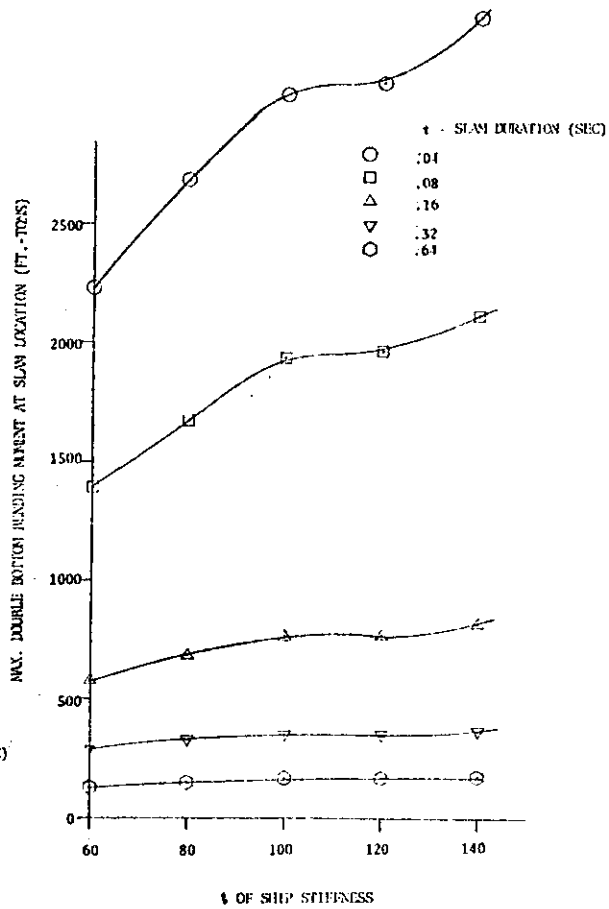


FIGURE B-66  
 MAX. SHEAR FORCE vs SHIP STIFFNESS  
 MICHIGAN - LOADED

FIGURE B-67  
DOUBLE BOTTOM BENDING MOMENT VS  
SHIP STIFFNESS  
MICHIGAN - LOADED



Legend for Figure B-68:

- .04
- .08
- △ .16
- ▽ .32
- .64

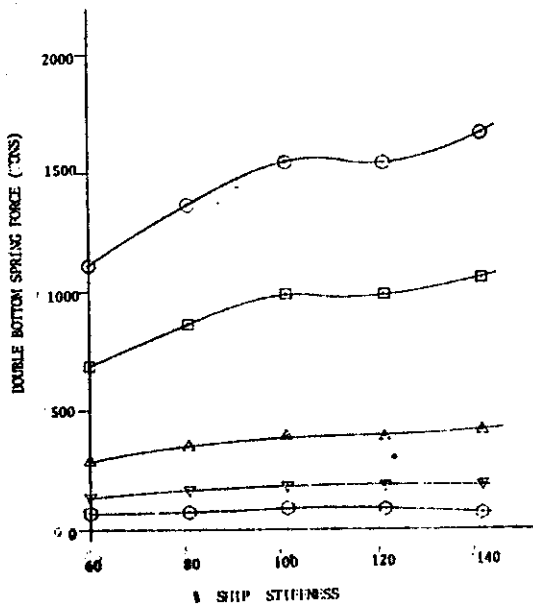


FIGURE B-68  
DOUBLE BOTTOM SPRING FORCE VS SHIP STIFFNESS  
MICHIGAN - LOADED

B-42

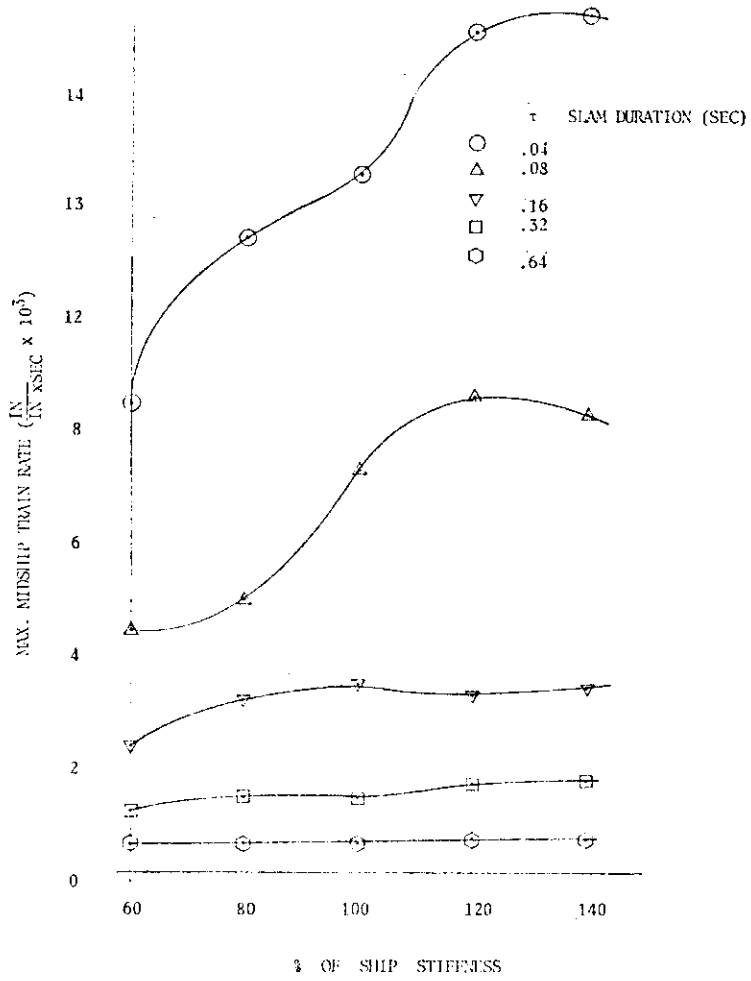


FIGURE B-69  
MAX. MIDSHIP STRAIN RATE  
v.s. SHIP STIFFNESS

MICHIGAN (LOADED)

SLAM COMPUTER OUTPUT

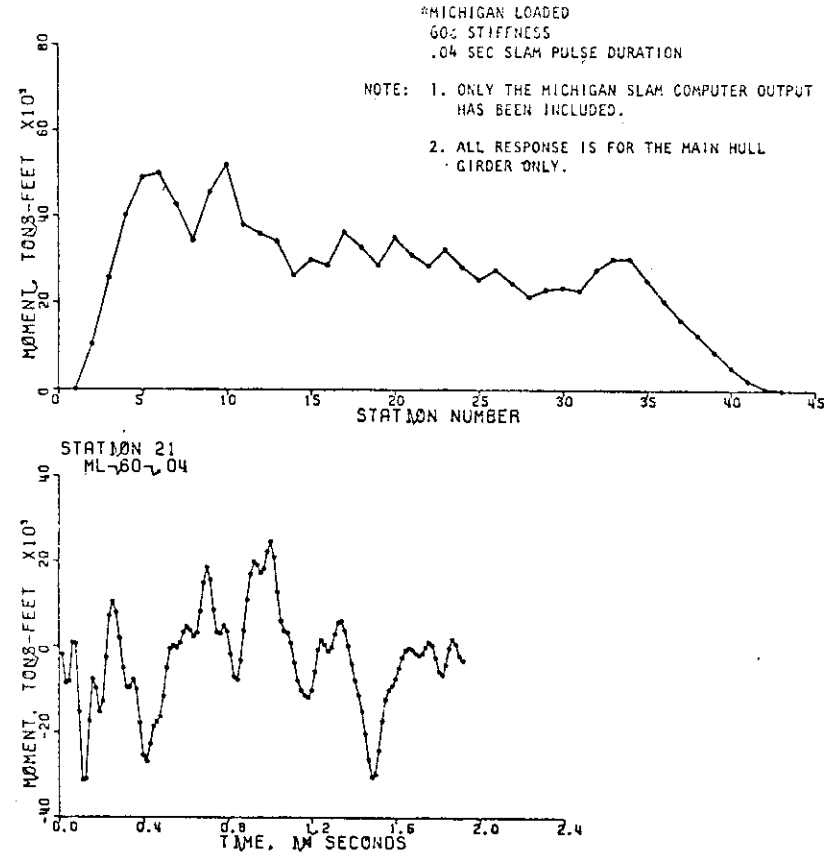


FIGURE B-70  
ML-60-.04"

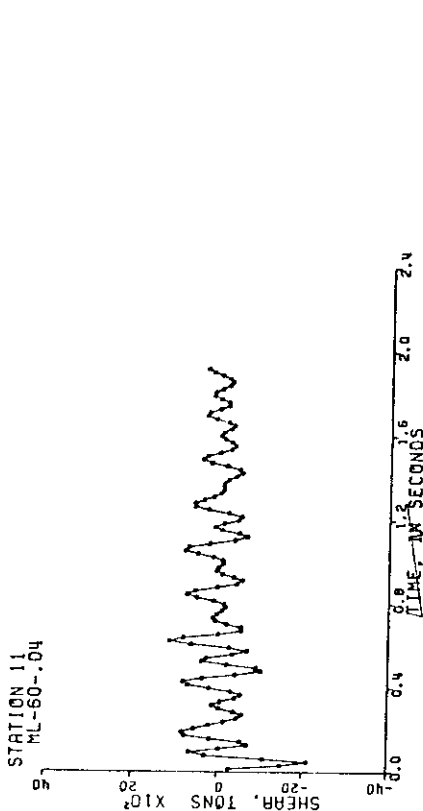
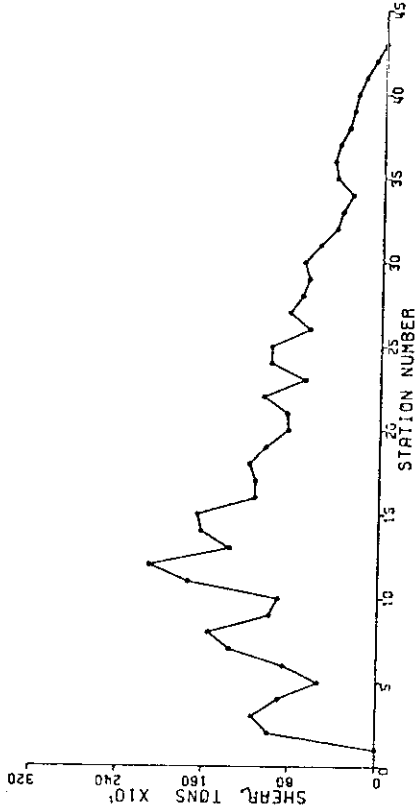


FIGURE 8-72  
ML-60-.04

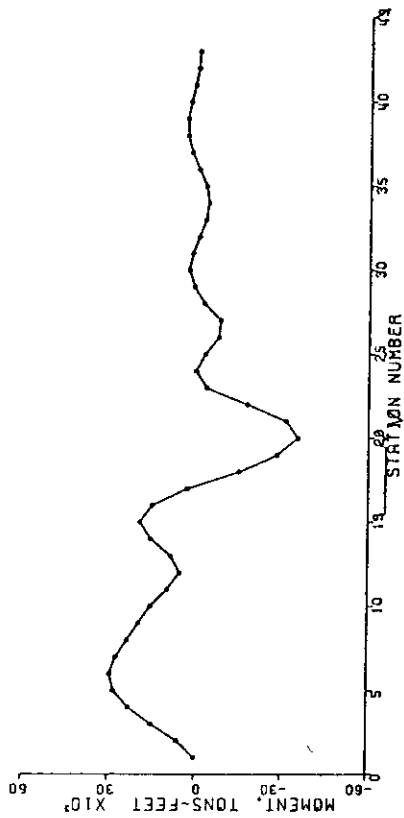


FIGURE 8-71  
AT TIME OF MAX MOMENT FOR STATION 21  
ML-60-.04

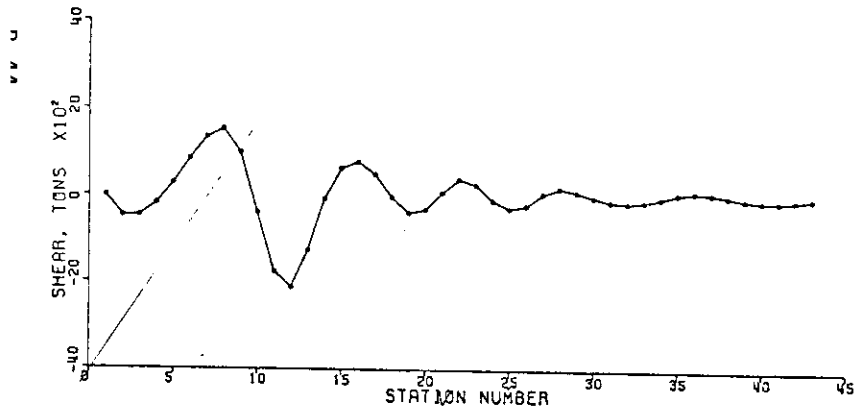


FIGURE 8-73  
AT TIME OF MAX SHEAR FOR STATION 11  
ML-60-.04

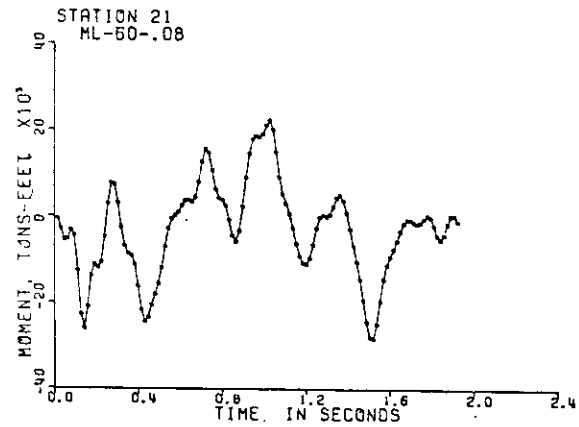
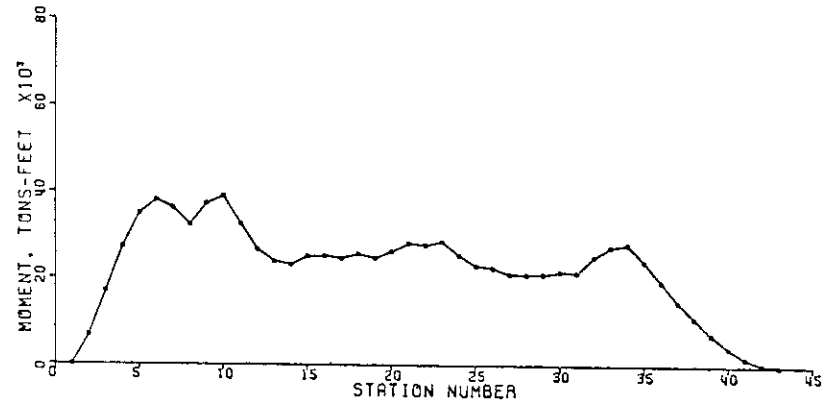


FIGURE 8-74  
ML-60-.08

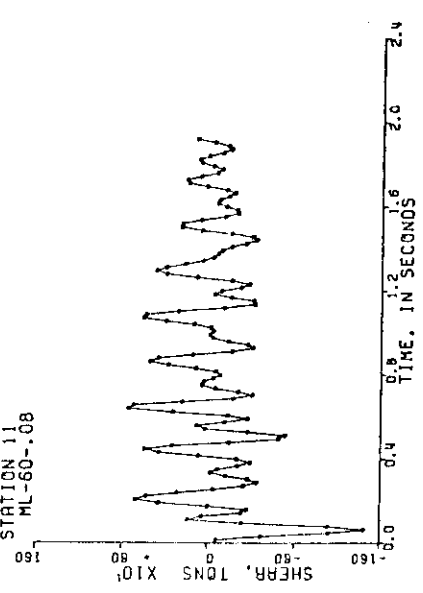
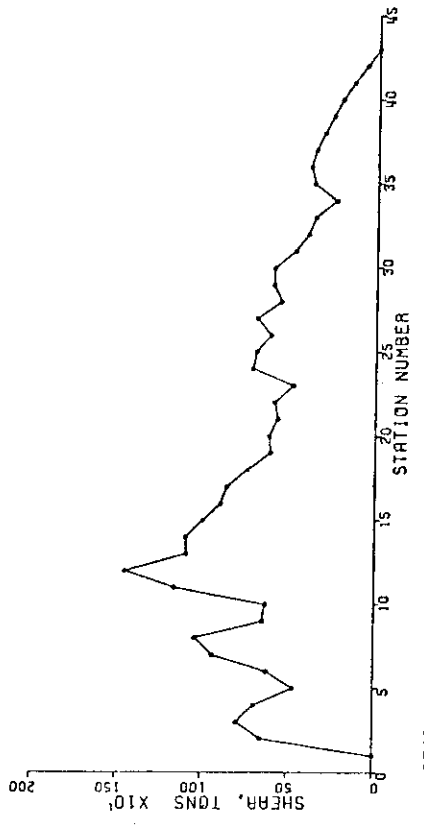


FIGURE 8-76  
ML-60-.08

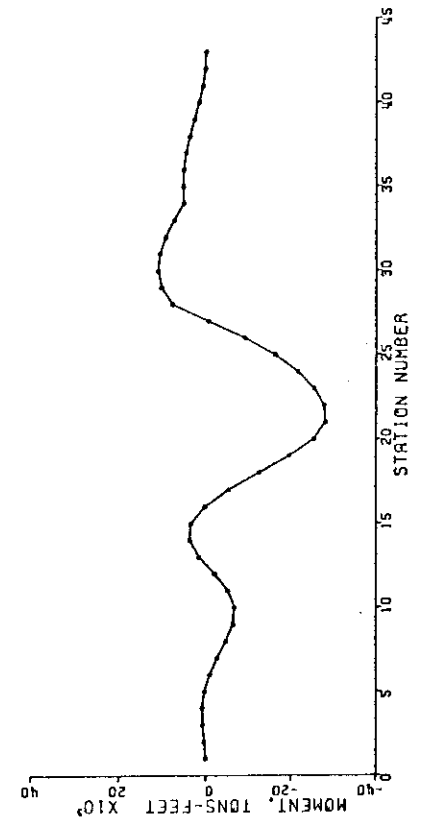
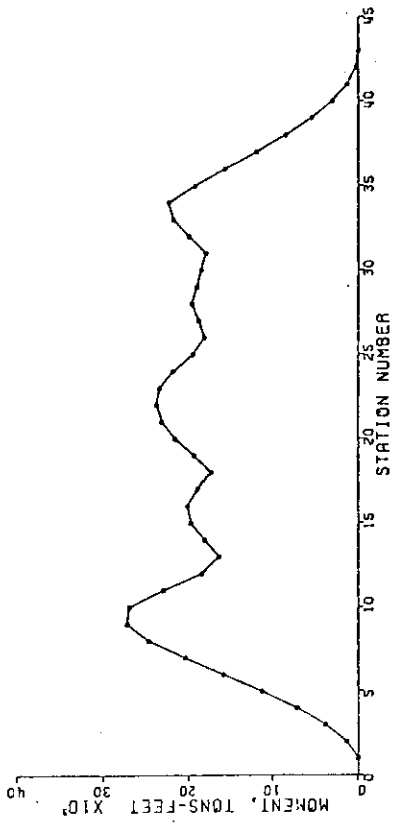


FIGURE 8-75  
AT TIME OF MAX MOMENT FOR STATION 21  
ML-60-.08



STATION 21  
ML-60-.16

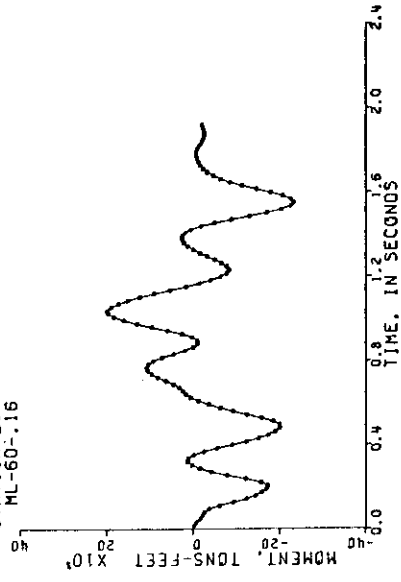


FIGURE B-78  
ML-60-.16

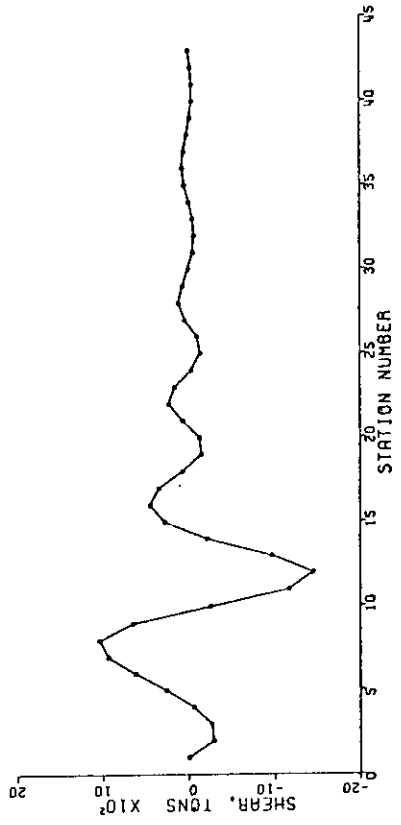


FIGURE B-77  
AT TIME OF MAX SHEAR FOR STATION 11  
ML-60-.08

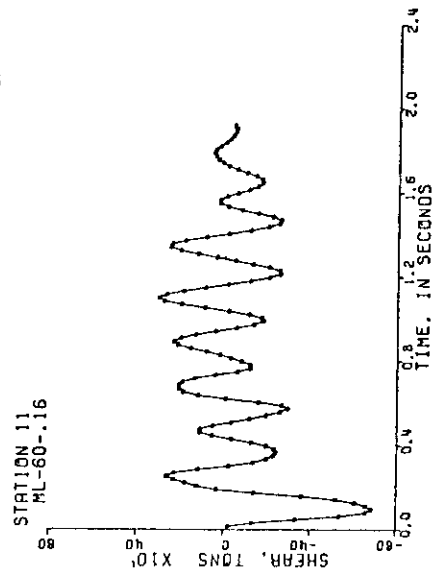
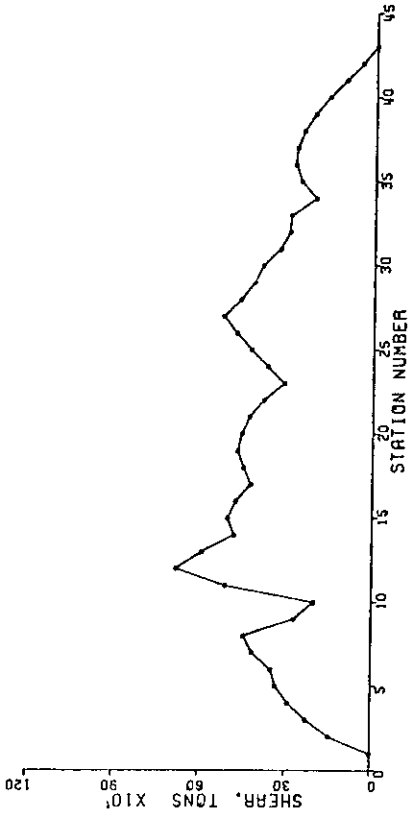


FIGURE B-80  
ML-60-.16

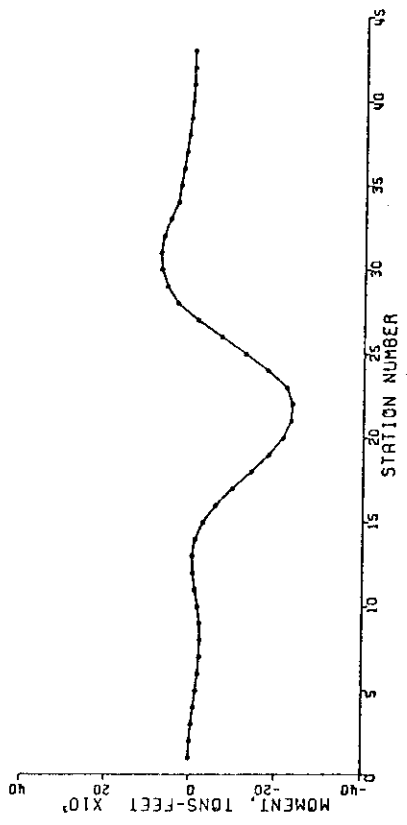
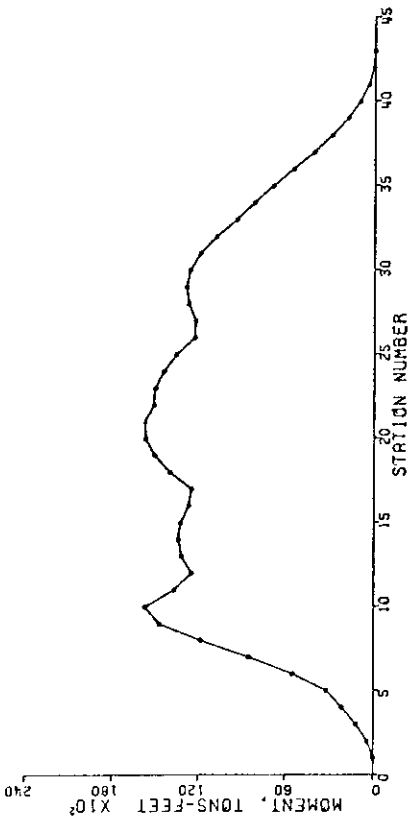


FIGURE B-79  
AT TIME OF MAX MOMENT FOR STATION 21  
ML-60-.16



STATION 21  
ML-60-.32

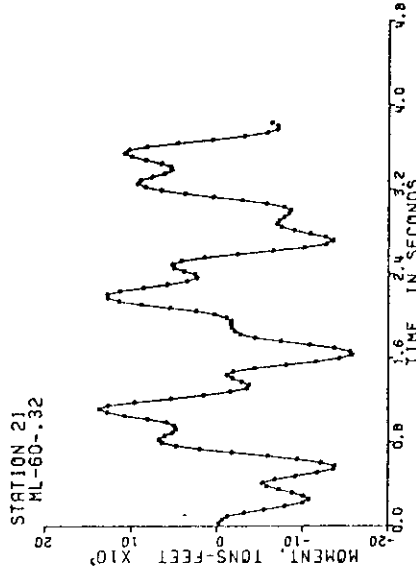
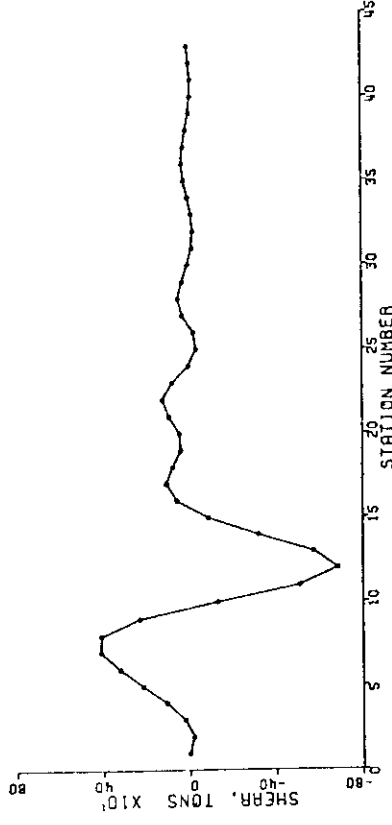


FIGURE B-82  
ML-60-.32



AT TIME OF MAX SHEAR FOR STATION 11  
FIGURE B-81  
ML-60-.16

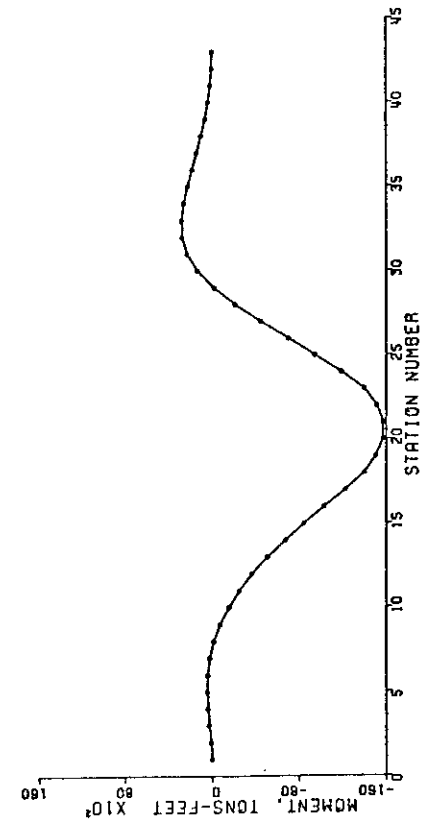
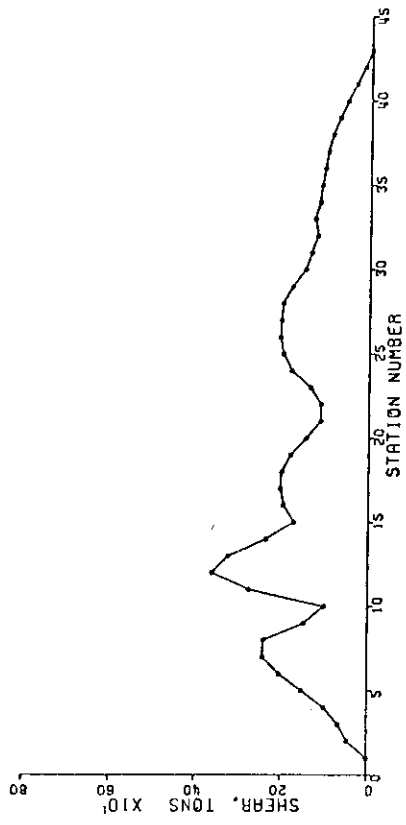


FIGURE 9-83  
AT TIME OF MAX MOMENT FOR STATION 21  
ML-60-.32

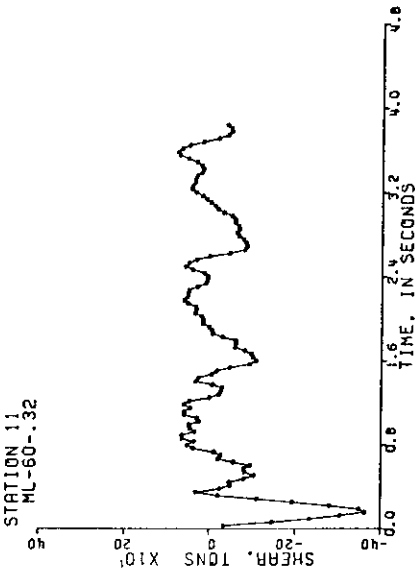


FIGURE 8-84  
ML-60-.32

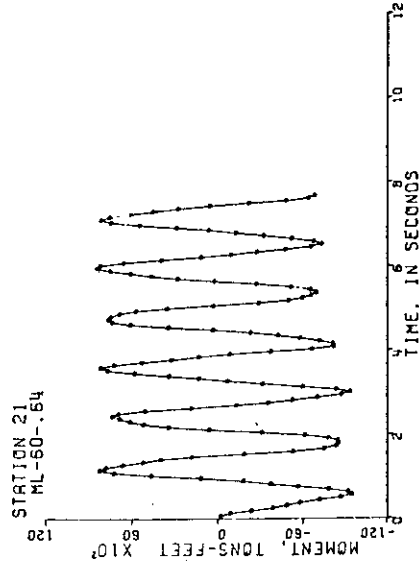
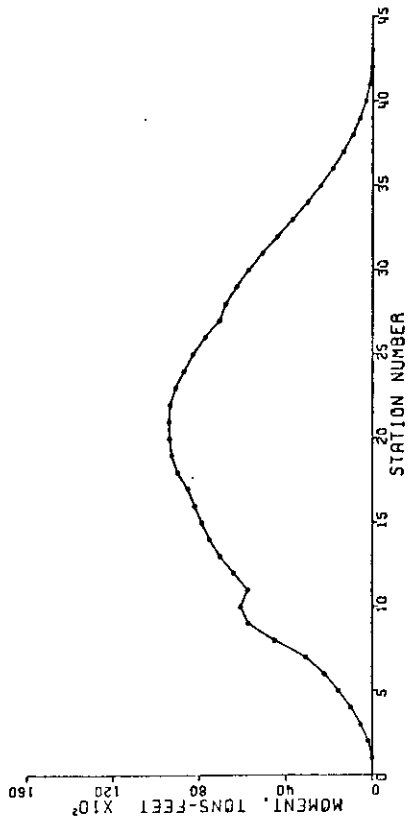


FIGURE B-86  
ML-60-.64

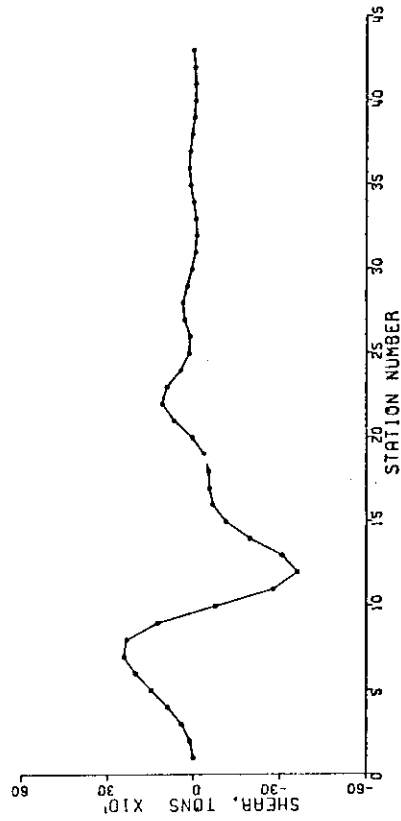


FIGURE B-85  
AT TIME OF MAX SHEAR FOR STATION 11  
ML-60-.32

B-51

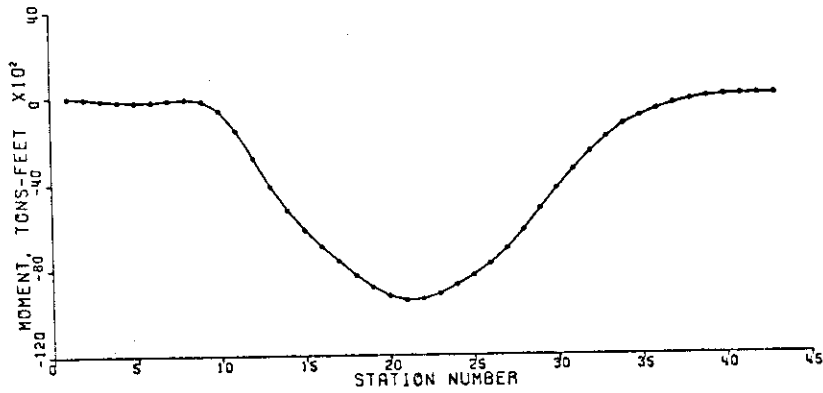


FIGURE B-87  
AT TIME OF MAX MOMENT FOR STATION 21  
ML-60-.64

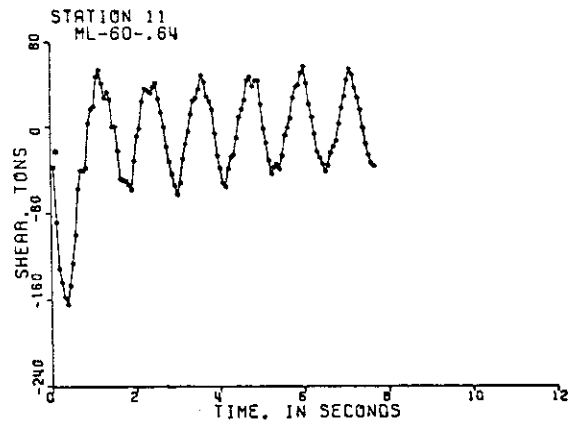
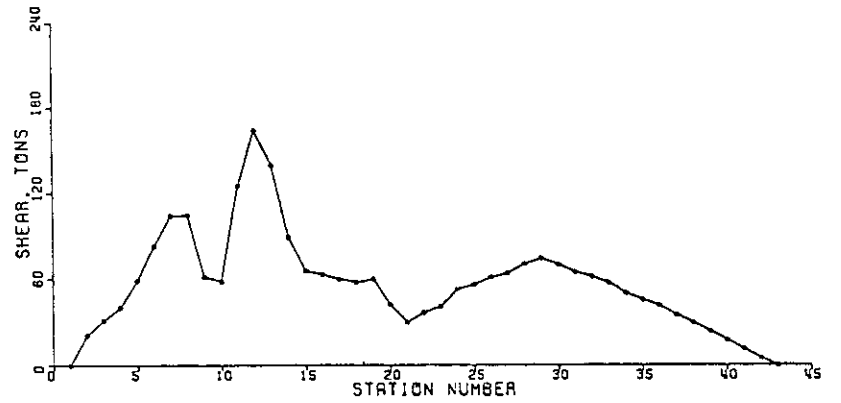


FIGURE B-88  
ML-60-.64

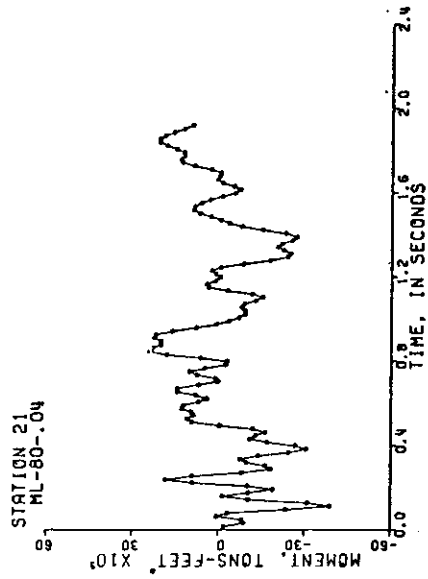
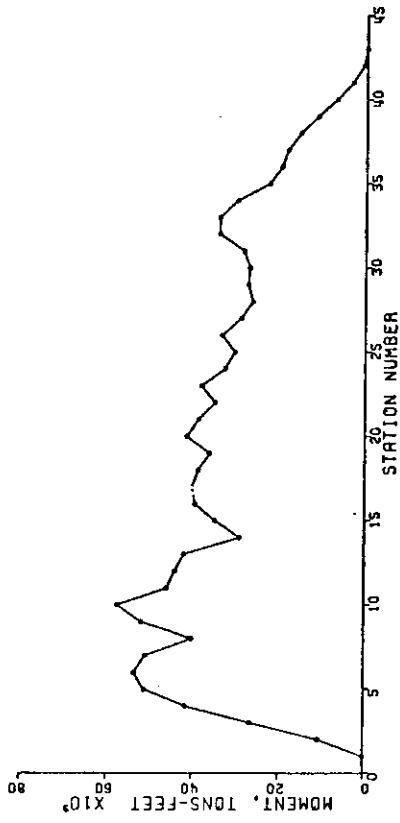


FIGURE B-90  
ML-80-.04

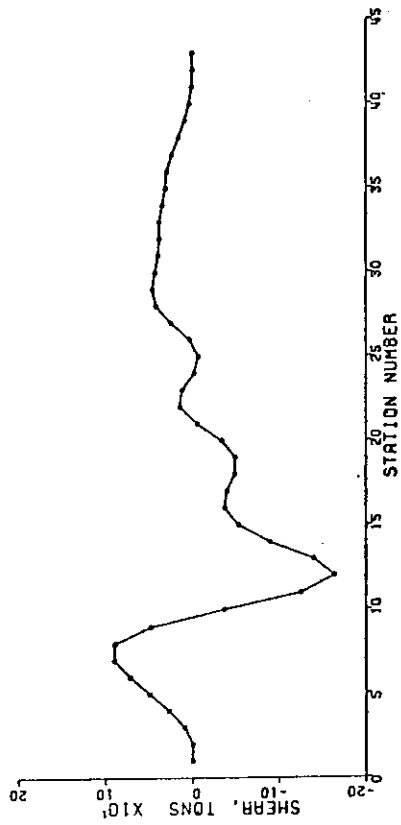


FIGURE B-89  
AT TIME OF MAX SHEAR FOR STATION 11  
ML-80-.04

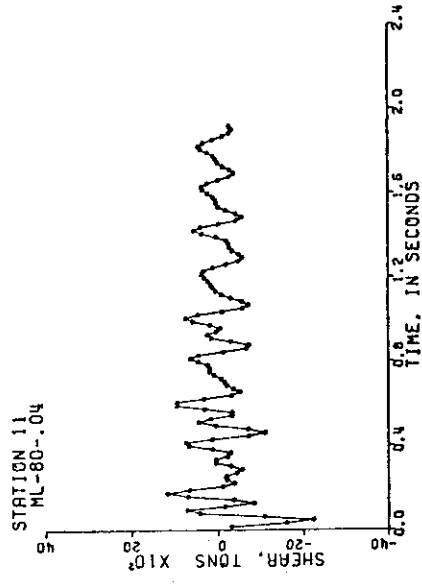
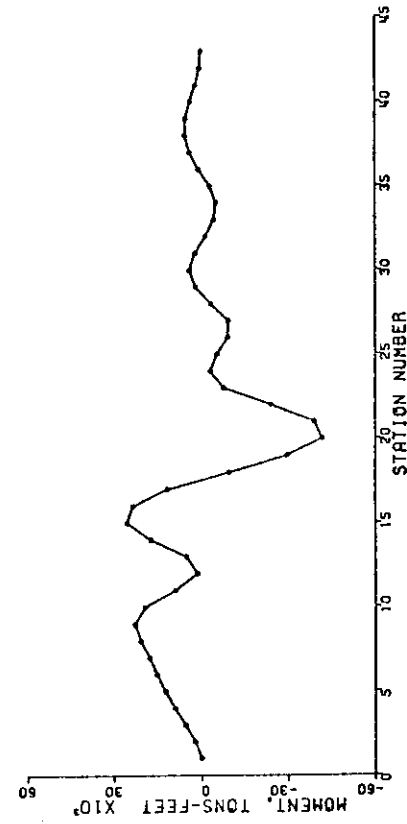
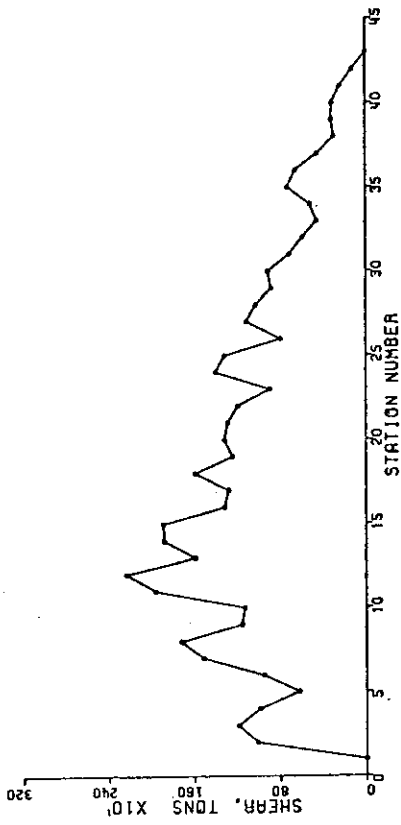


FIGURE 8-91  
AT TIME OF MAX MOMENT FOR STATION 21  
ML-80-.04

FIGURE 8-92  
ENVELOPE  
ML-80-.04

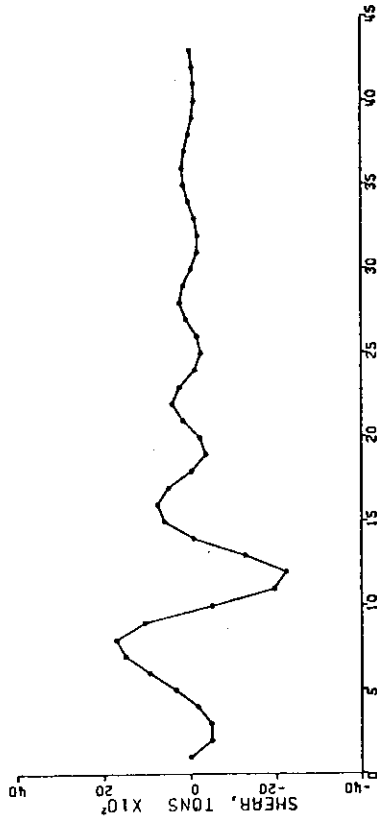
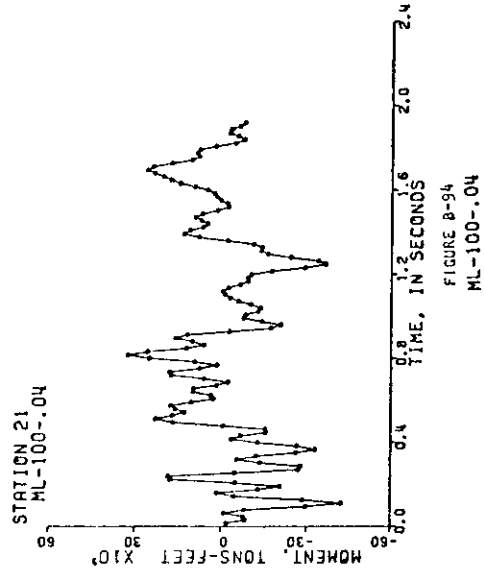
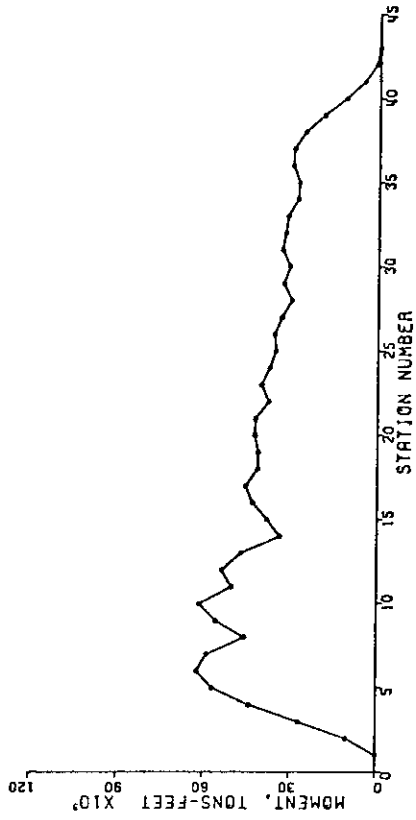


FIGURE B-93  
AT TIME OF MAX SHEAR FOR STATION 11  
HL-80-.04

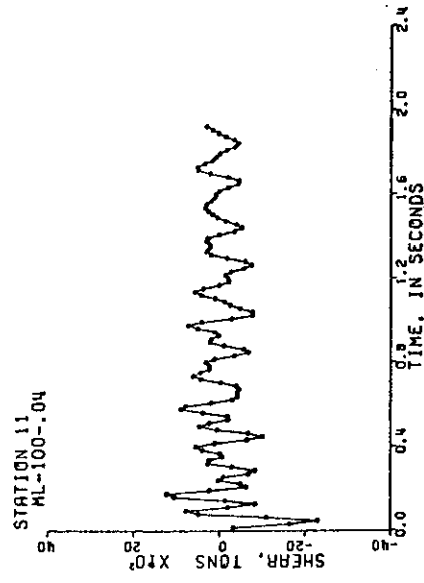
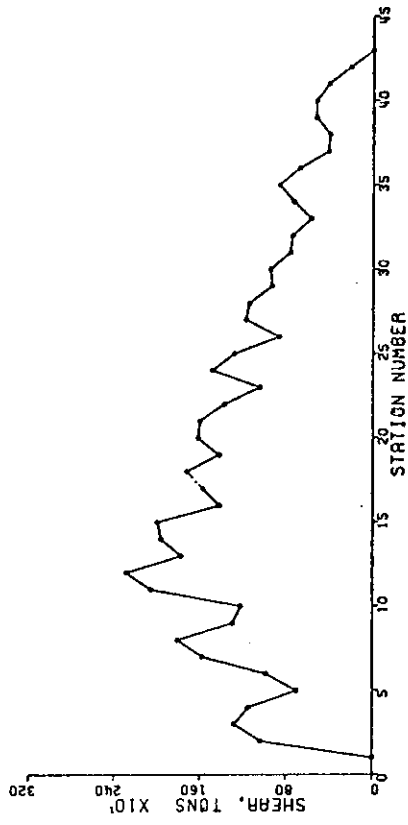


FIGURE 8-96  
ML-100-.04

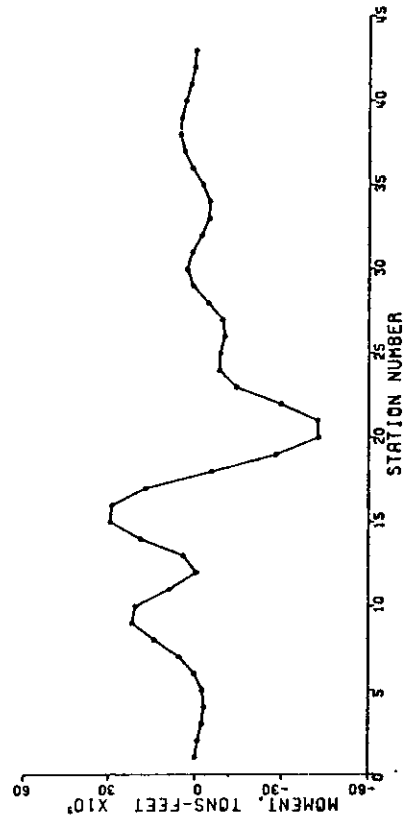


FIGURE 8-95  
AT TIME OF MAX MOMENT FOR STATION 21  
ML-100-.04

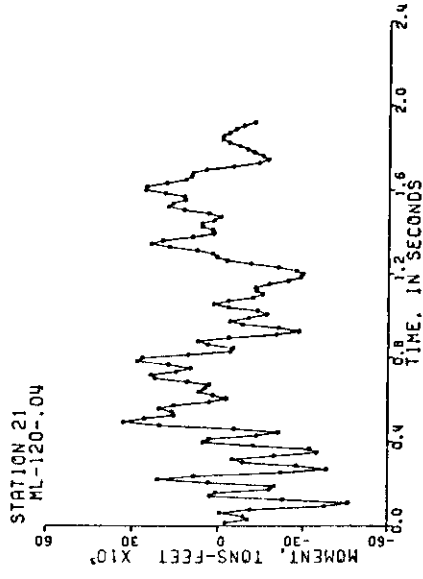
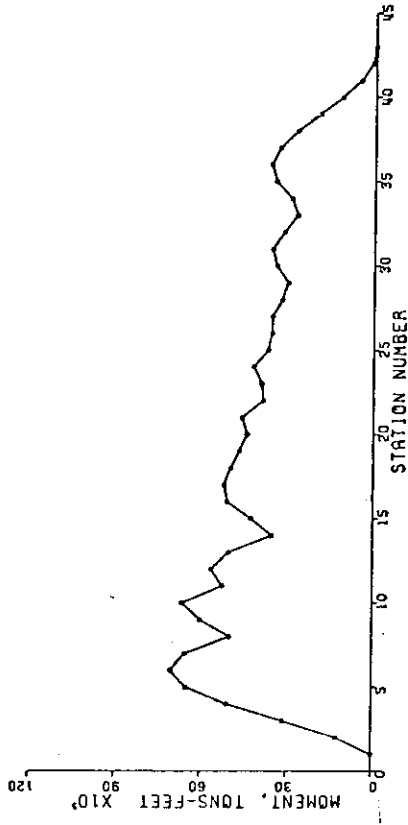


FIGURE B-98  
ML-120-.04

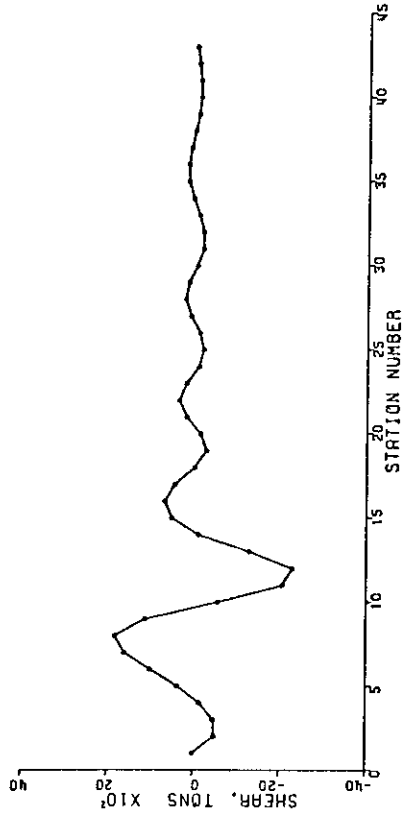


FIGURE B-97  
AT TIME OF MAX SHEAR FOR STATION 11  
ML-100-.04

B-56

B-57

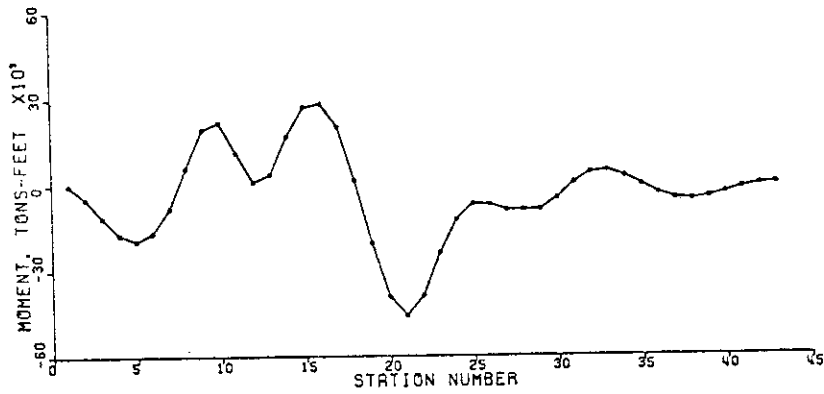


FIGURE B-99  
AT TIME OF MAX MOMENT FOR STATION 21  
ML-120-.04

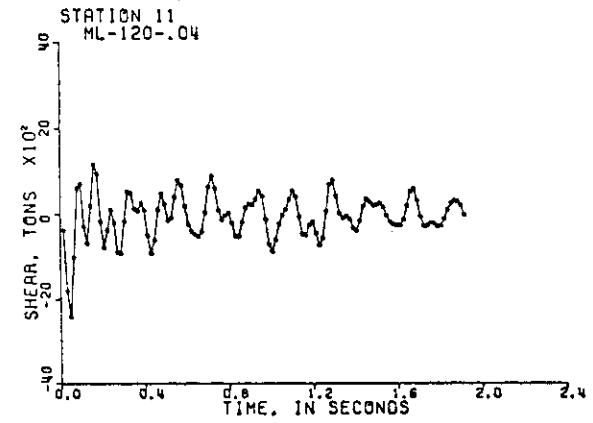
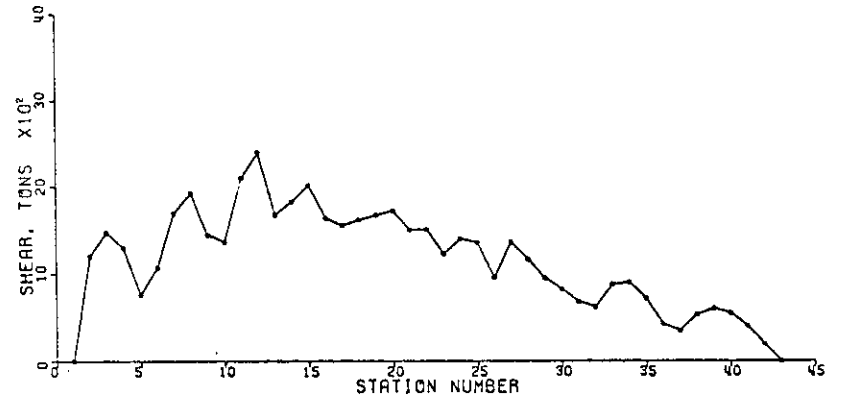


FIGURE B-100  
ML-120-.04

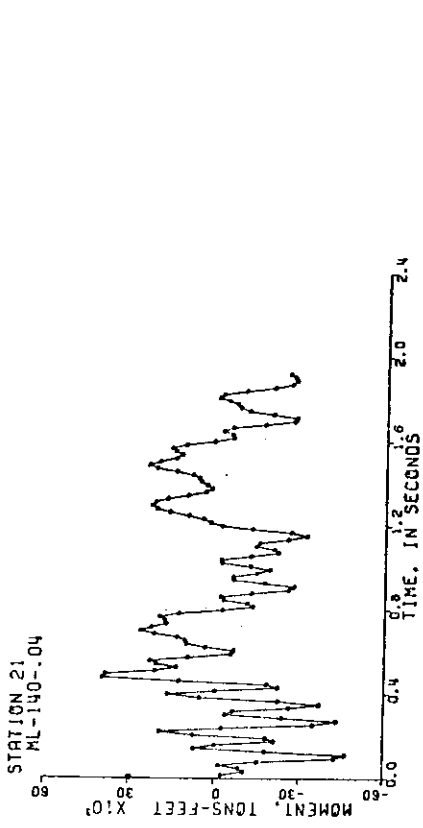
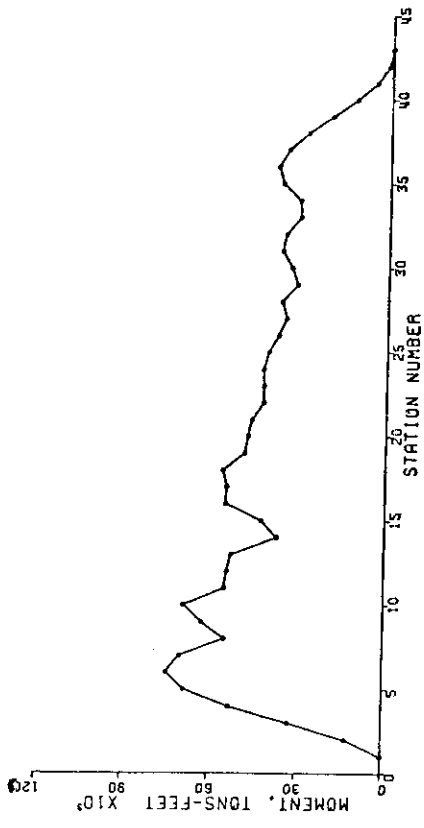


FIGURE B-102  
ML-140-.04

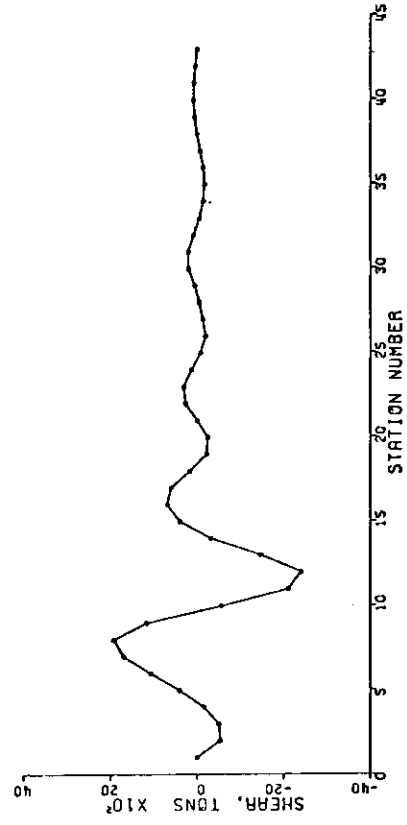


FIGURE B-101  
AT TIME OF MAX SHEAR FOR STATION 11  
ML-120-.04

B-59

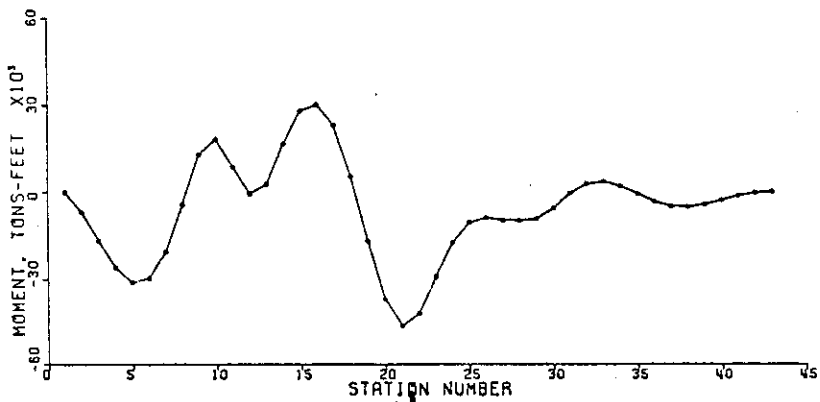


FIGURE B-103  
AT TIME OF MAX MOMENT FOR STATION 21  
ML-140-.04

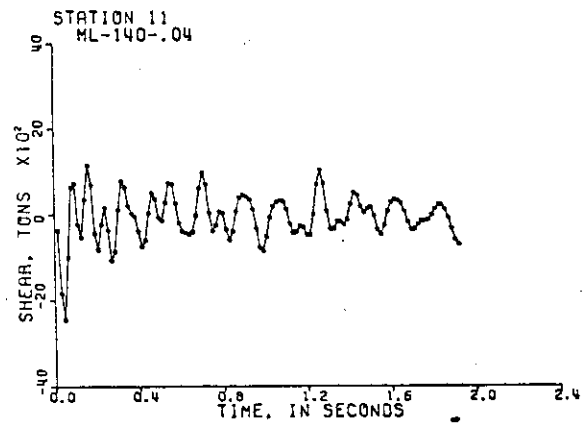
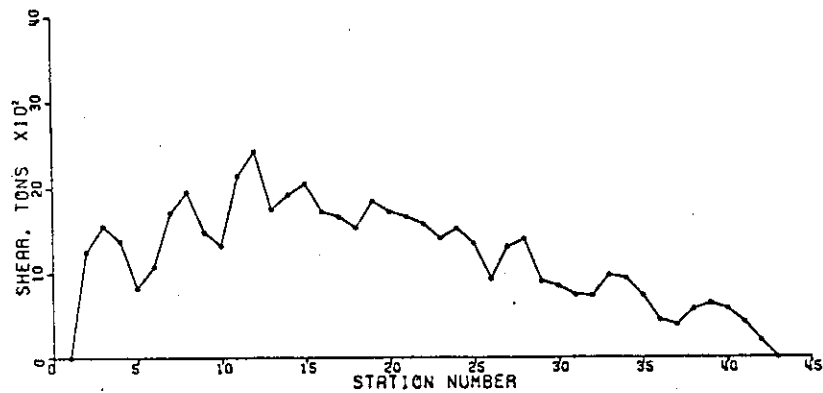


FIGURE B-104  
ML-140-.04

WAVE-EXCITED RESPONSE

- MICHIGAN LOADED
- TANK SHIP LOADED
- △ RYERSON LOADED
- ▽ ODENSE BALLAST
- RYERSON BALLAST

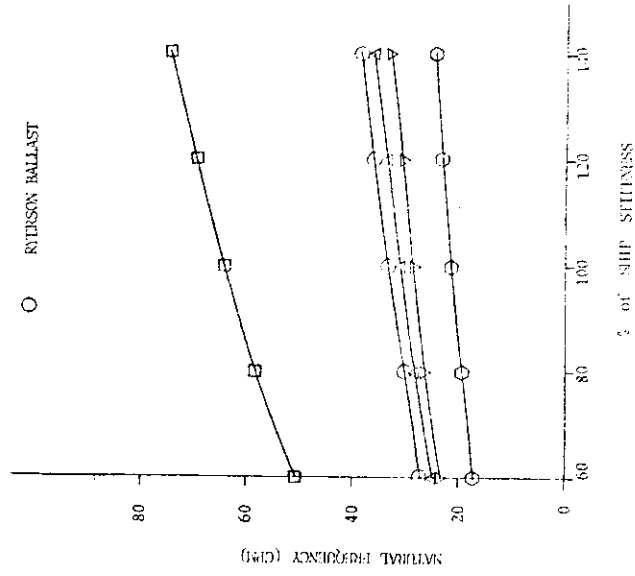


FIGURE B-106

2-NODE NATURAL FREQUENCY V.S. STIFFNESS

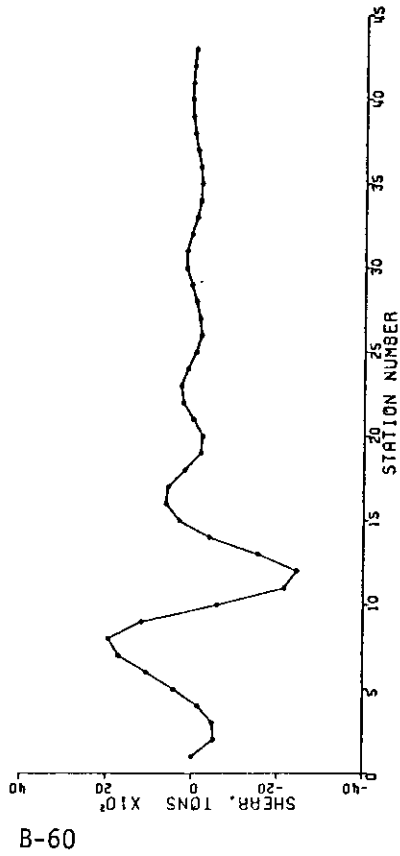


FIGURE B-105  
AT TIME OF MAX SHEAR FOR STATION 11  
ML-140-.04

B-60

B-61

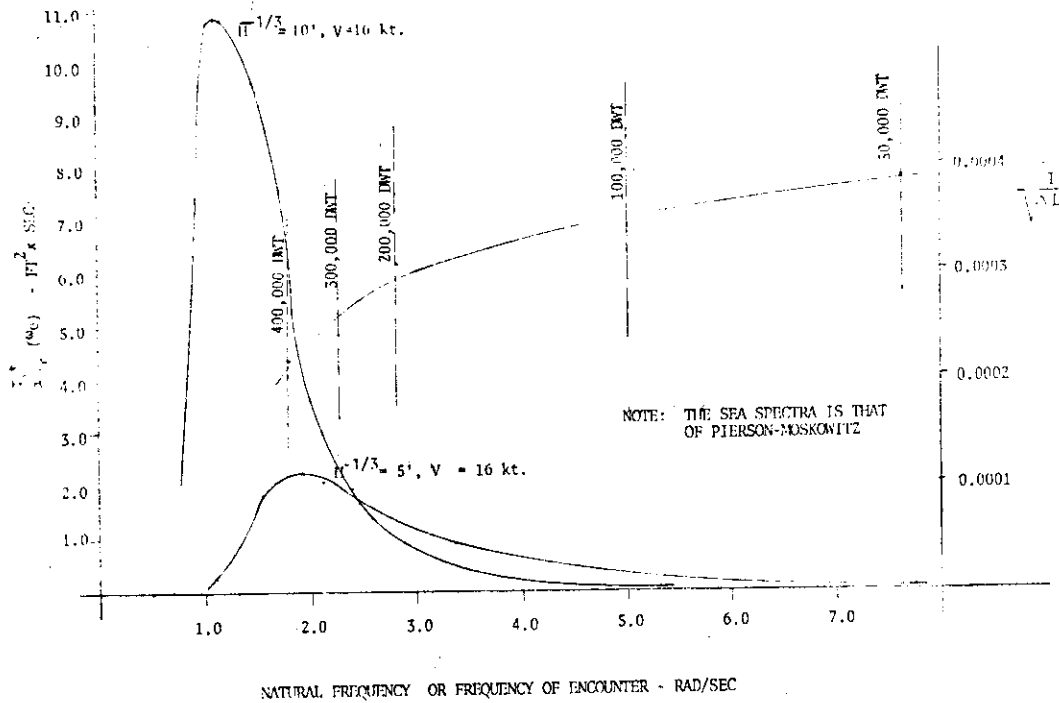


FIGURE B-107  
SPECTRAL DENSITY AND SLICK NUMBER  
vs. NATURAL FREQUENCY AND FREQUENCY OF ENCOUNTER  
OIL TANKERS

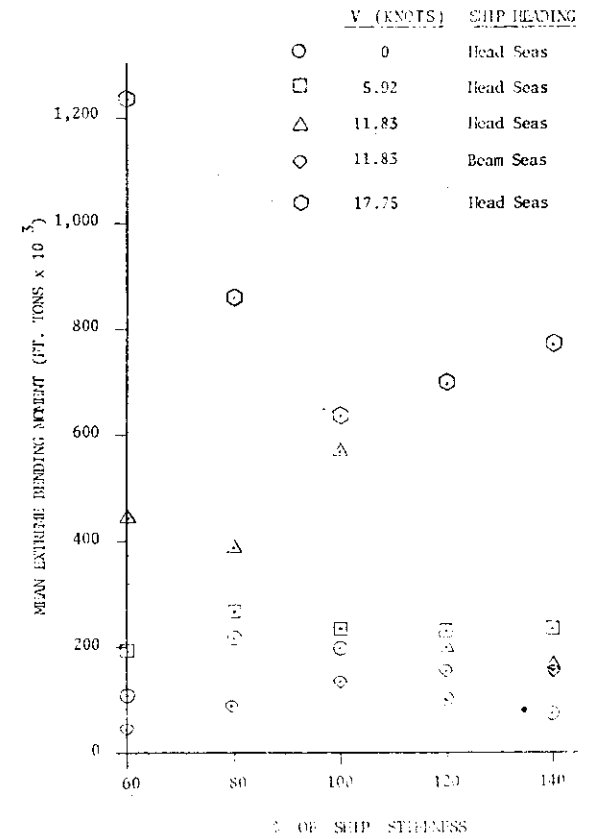
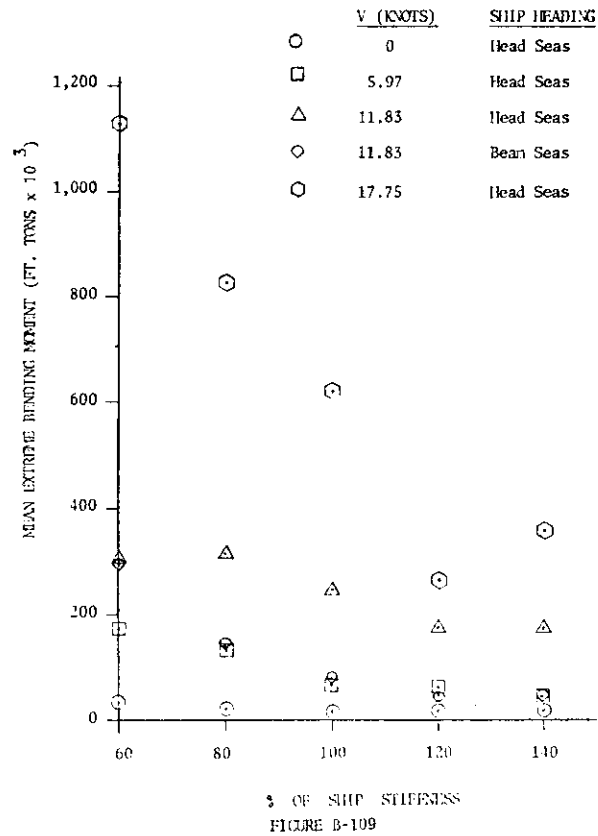
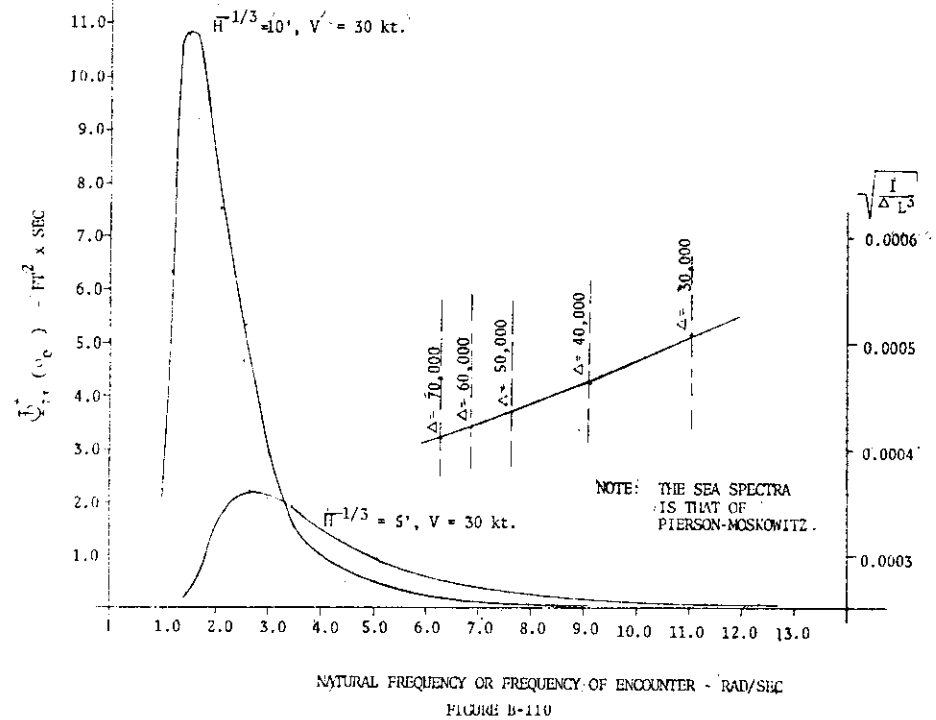


FIGURE B-108  
MEAN EXTREME BENDING MOMENT vs. SHIP STRESSLESS  
T.A.K. SHIP (R.J. LAST)

B-62



MEAN EXTREME BENDING MOMENT vs. SHIP STIFFNESS  
TANK SHIP (LOADED)



SPECTRAL DENSITY AND SLICK NUMBERS  
vs. NATURAL FREQUENCY AND FREQUENCY OF ENCOUNTER  
CONTAINER SHIPS

SHIP HEADING  
 Head Seas  
 Head Seas  
 Head Seas  
 Beam Seas  
 Head Seas

V (KNOTS)  
 5.92  
 11.83  
 17.75  
 17.75  
 23.67

○ □ △ ◇ ○

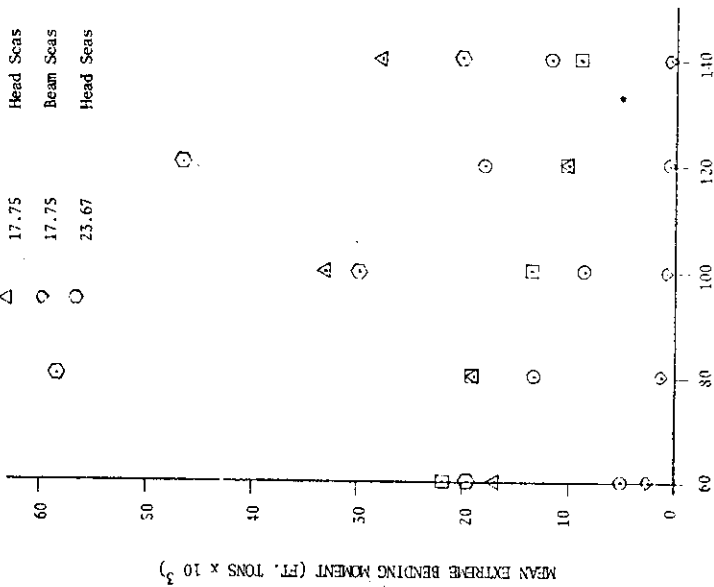


FIGURE B-111  
 MEAN EXTREME BENDING MOMENT vs. SHIP STIFFNESS  
 MICHIGAN (LOADED)

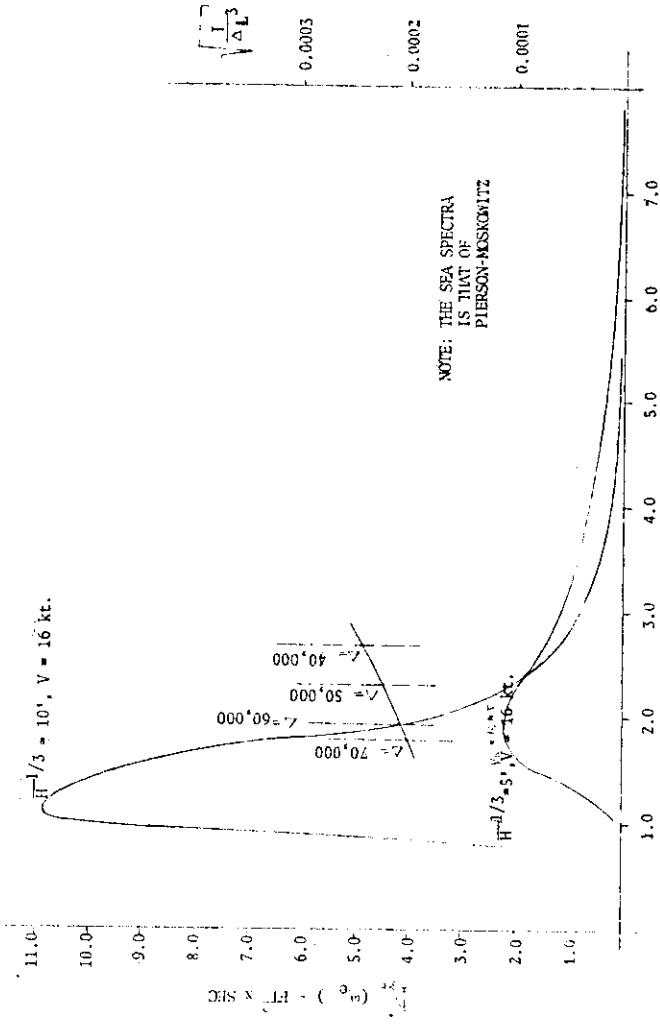


FIGURE B-112  
 SPECTRAL DENSITY AND SCHLICK NUMBERS  
 vs. NATURAL FREQUENCY AND FREQUENCY OF ENCOUNTER  
 GREAT LAKES ORE CARRIERS

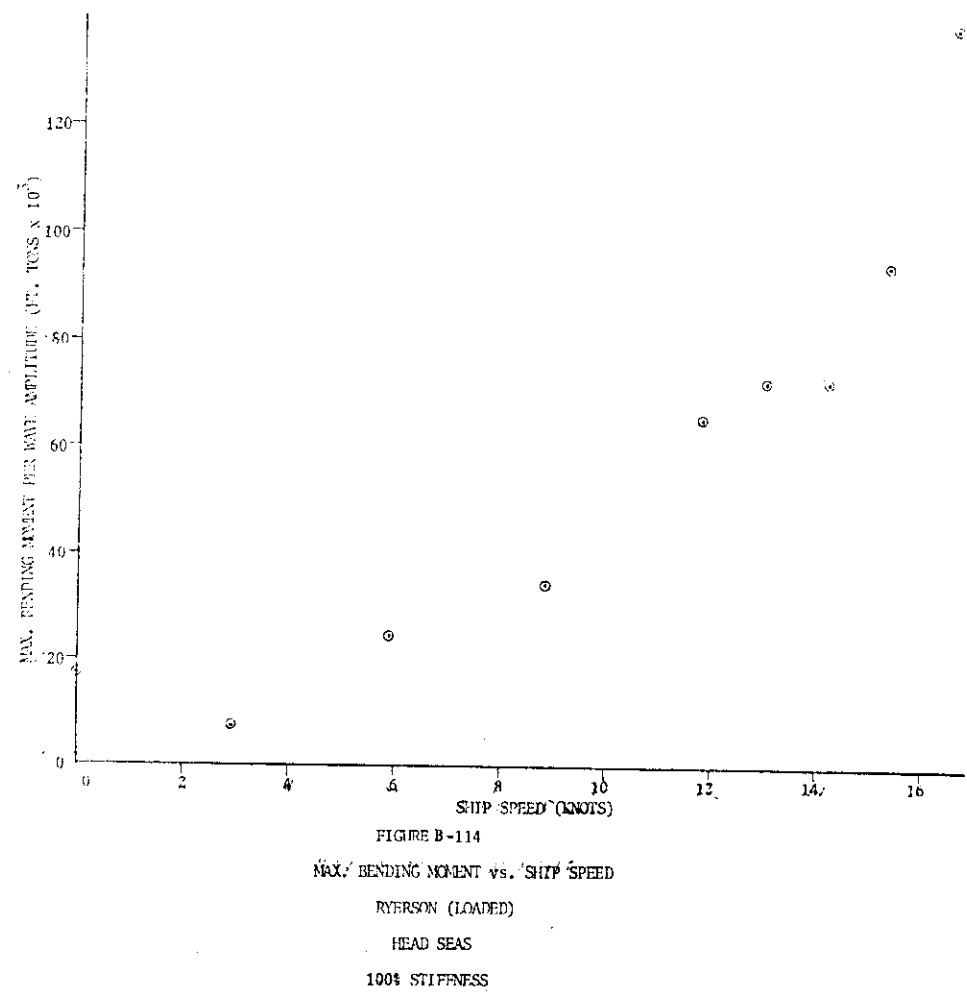
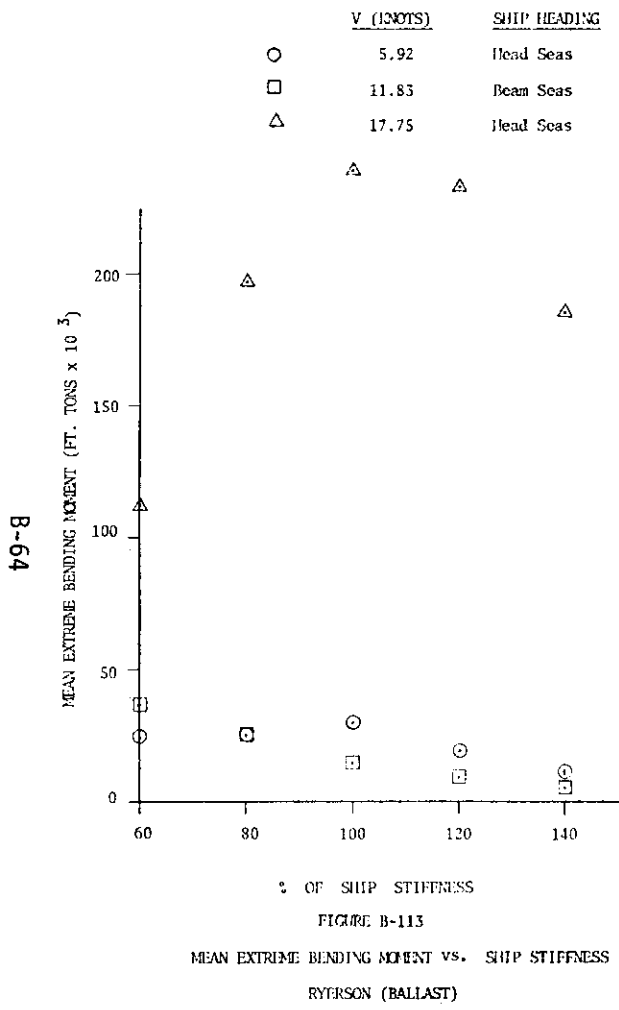


FIGURE B-115  
MAX. BENDING MOMENT vs. LEADING  
RYERSON (LOADED)  
100% STIFFNESS

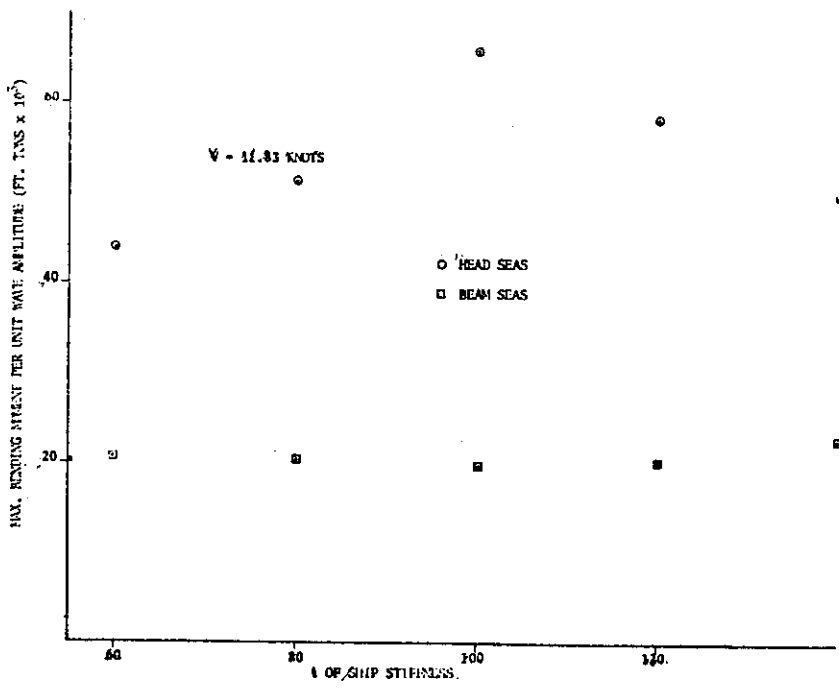
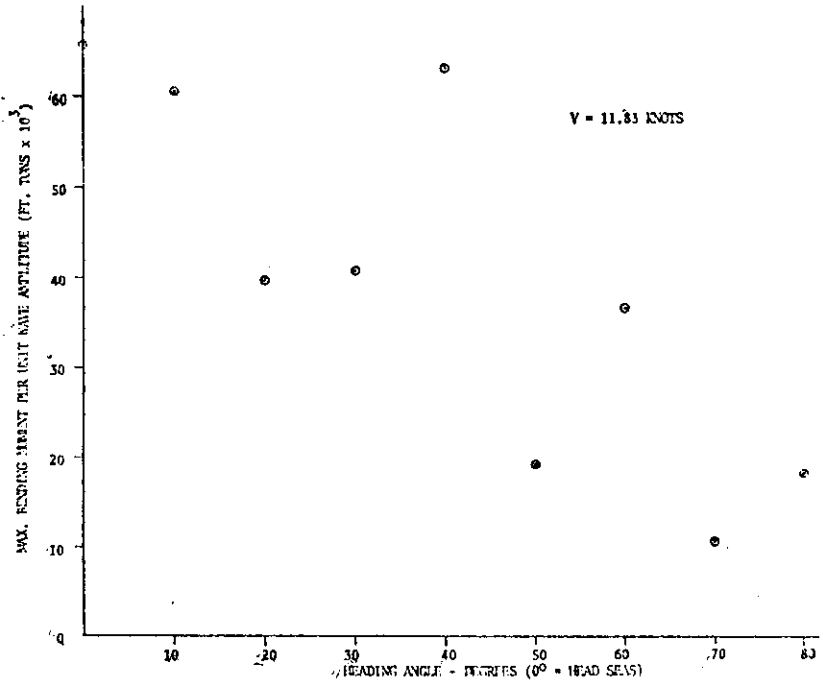


FIGURE B-116  
MAX. BENDING MOMENT vs.  
SHIP STIFFNESS  
RYERSON (LOADED)

## APPENDIX C

## TRENDS

TABLE C-1

CONVERSION TABLE FOR METRIC UNITS

ITEMS PLOTTED ON CURVES	UNITS USED ON GRAPHS	METRIC EQUIVALENTS	CONVERSION TO METRIC
LENGTH	FEET	METERS	x.3048
BEAM	FEET	METERS	x.3048
DRAFT	FEET	METERS	x.3048
DEPTH	FEET	METERS	x.3048
DWT	LONG TONS	METRIC TONS	x1.016
DISPLACEMENT	LONG TONS	METRIC TONS	x1.016
SHP	HORSEPOWER	HORSEPOWER	-
V	KNOTS	KNOTS	-
SM	IN <sup>2</sup> -FT	CM <sup>2</sup> -M	x1.966
EI/L <sup>3</sup>	IN-LB/FT <sup>2</sup>	CM-KG/M <sup>2</sup>	x12.401
EI/L <sup>3</sup>	LB/FT	CM-KG/M <sup>2</sup>	x148.816
I/ΔL <sup>3</sup>	IN <sup>2</sup> /LT-FT	CM <sup>2</sup> /MT-M	x20.832
F <sub>N</sub>	-	-	-
L/B	-	-	-
L/D	-	-	-
B/D	-	-	-
C <sub>B</sub>	-	-	-

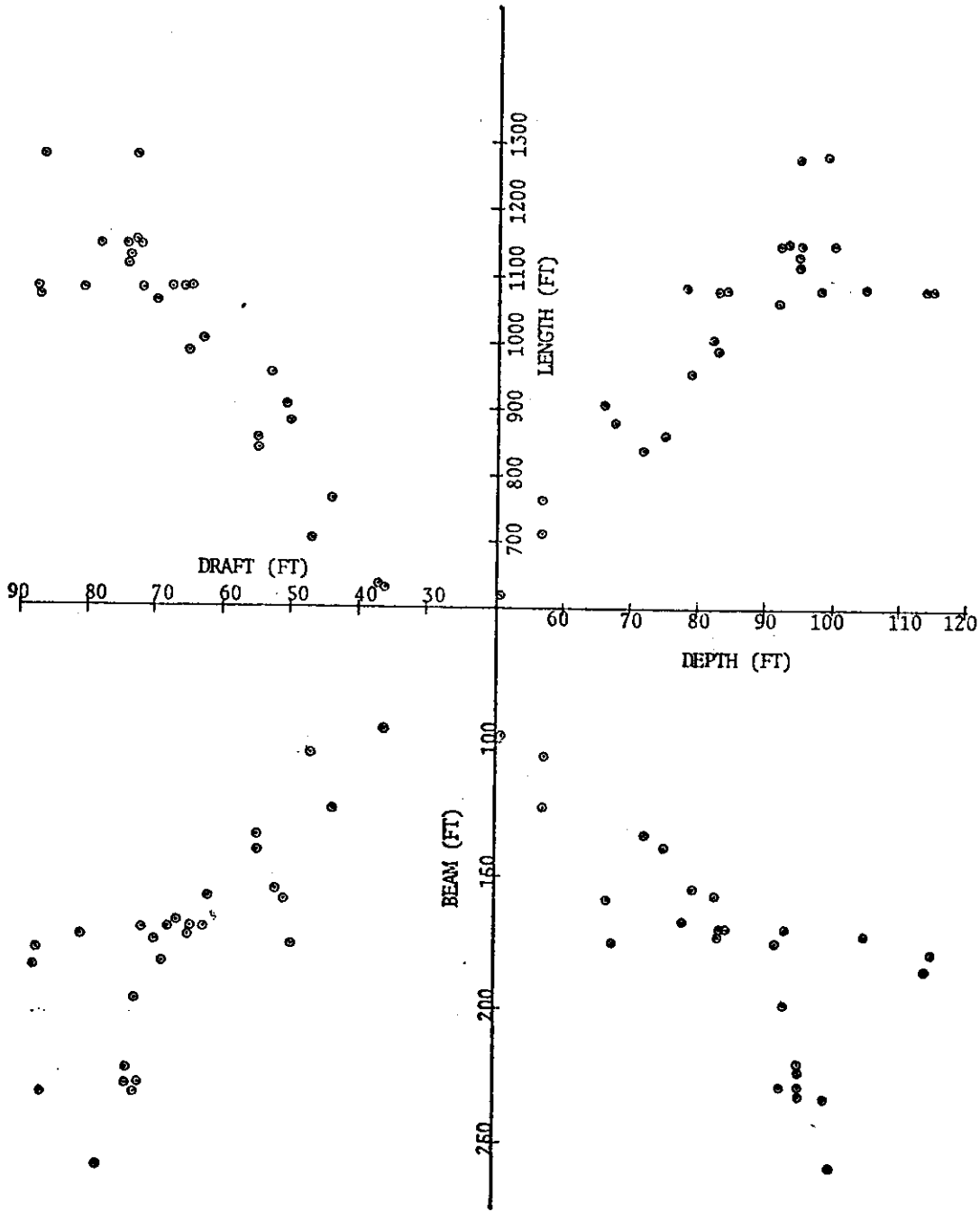
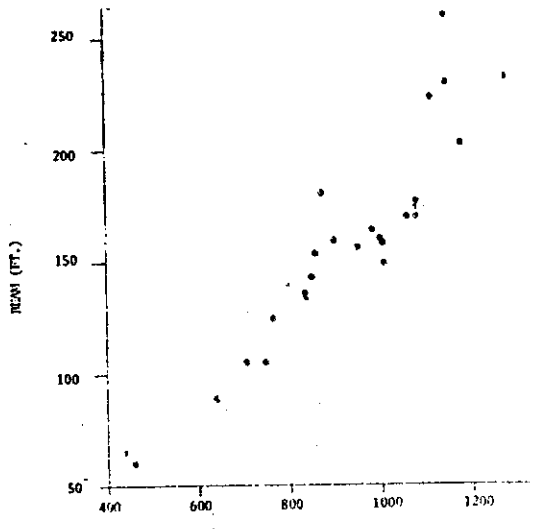
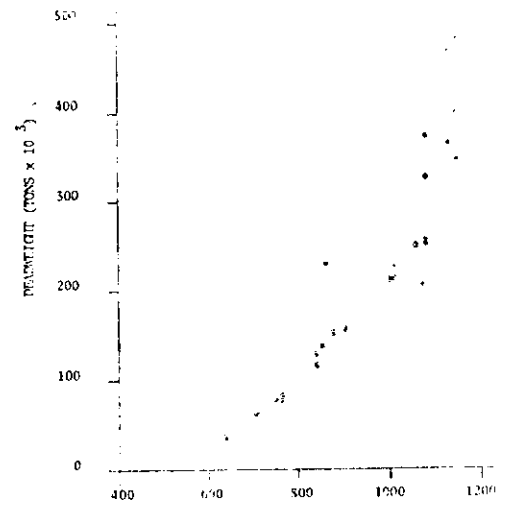


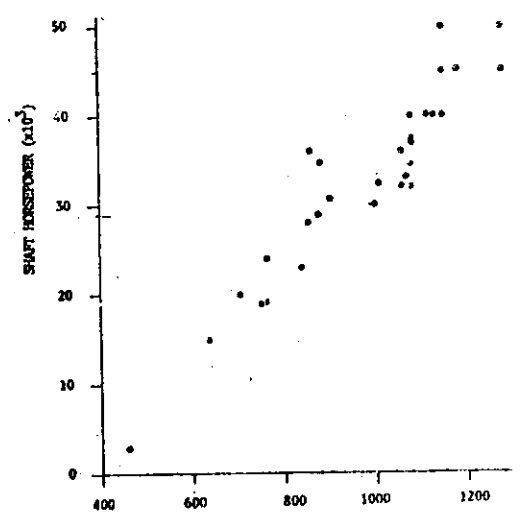
FIGURE C-1 - TANKER PROPORTIONS



LENGTH (FT.)  
 FIGURE C-2  
 BEAM vs. LENGTH  
 TANNERS



LENGTH (FT.)  
 FIGURE C-3  
 DEADWEIGHT vs. LENGTH  
 TANNERS



LENGTH (FT.)  
 FIGURE C-4  
 SHAFT HORSEPOWER vs. LENGTH  
 TANNERS

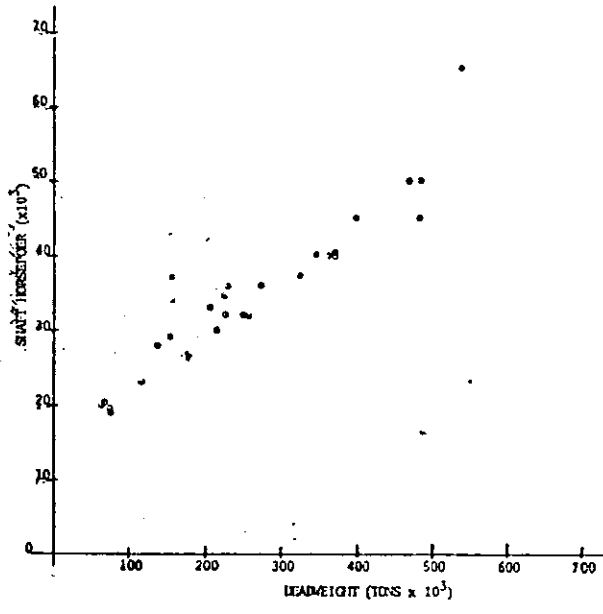
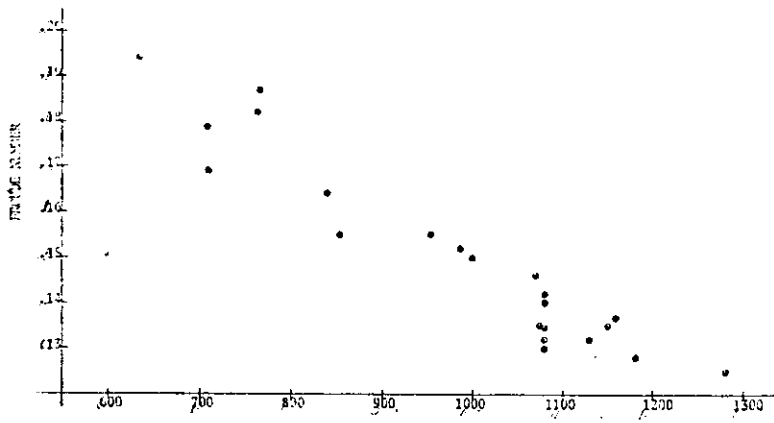
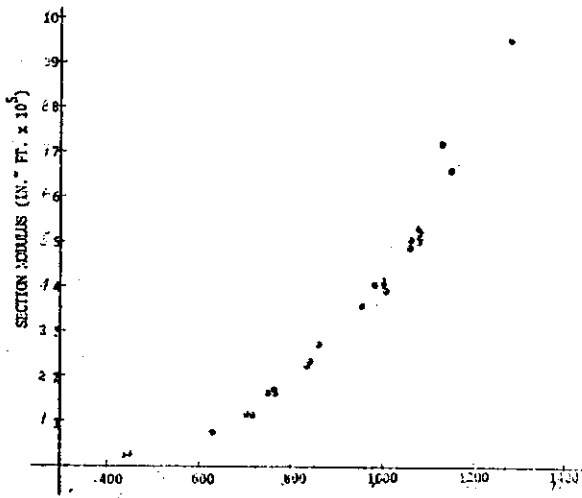


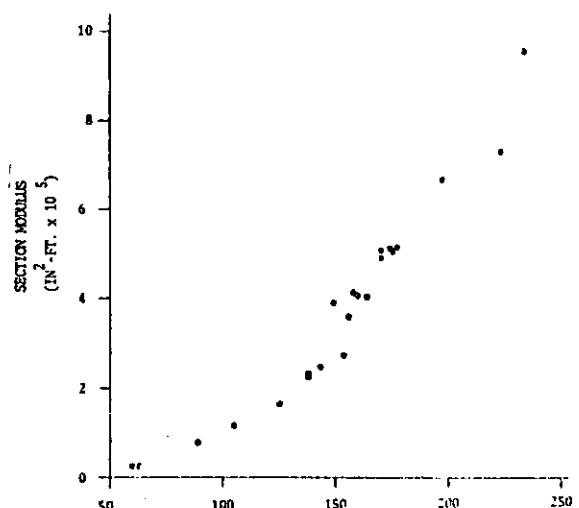
FIGURE C-5  
 SHAFT HORSEPOWER vs. DEADWEIGHT  
 TANNERS



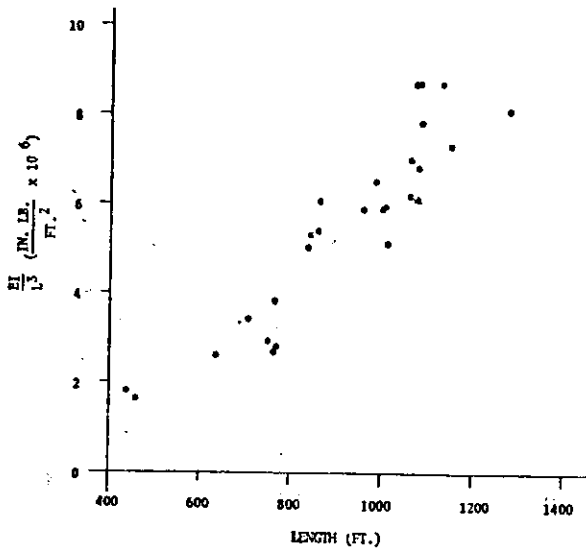
LENGTH (FT.)  
 FIGURE C-6  
 FIBRE NUMBER vs. LENGTH  
 TANKERS



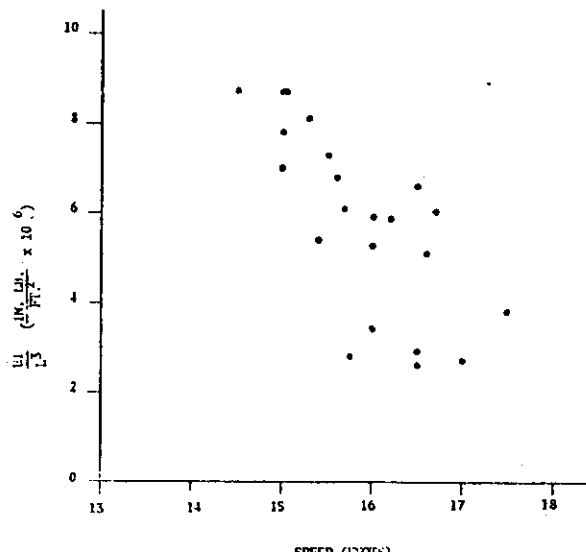
LENGTH (FT.)  
 FIGURE C-7  
 SECTION MODULUS vs. LENGTH  
 TANKERS



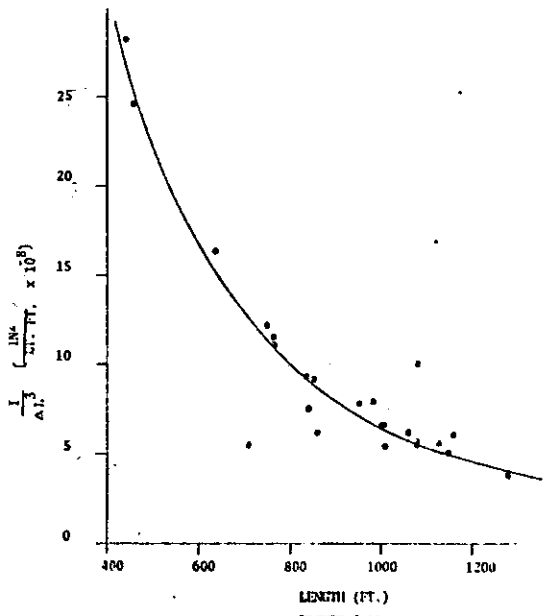
BEAM (FT.)  
 FIGURE C-8  
 SECTION MODULUS vs. BEAM  
 TANKERS



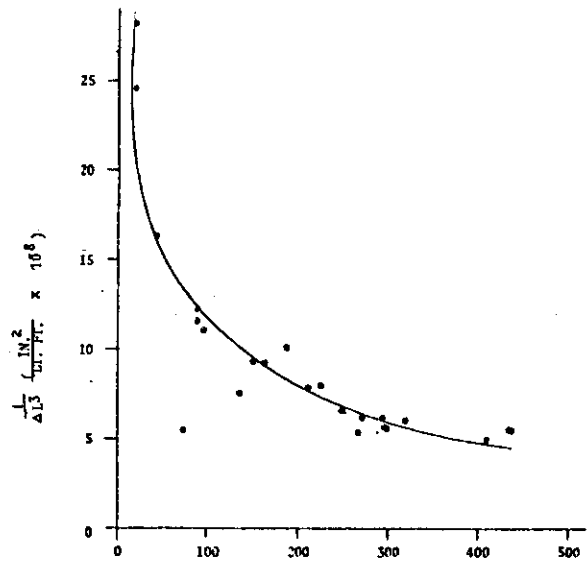
LENGTH (FT.)  
 FIGURE C-9  
 $\frac{EI}{L^3}$  vs. LENGTH - TANKERS



SPEED (KNOTS)  
 FIGURE C-10  
 $\frac{EI}{L^3}$  vs. SPEED - TANKERS



LENGTH (FT.)  
 FIGURE C-11  
 $\frac{I}{AL^3}$  vs. SHIP LENGTH - TANKERS (LOADED)



DEADWEIGHT (TONS x 10<sup>3</sup>)  
 FIGURE C-12  
 $\frac{I}{AL^3}$  vs. DEADWEIGHT - TANKERS

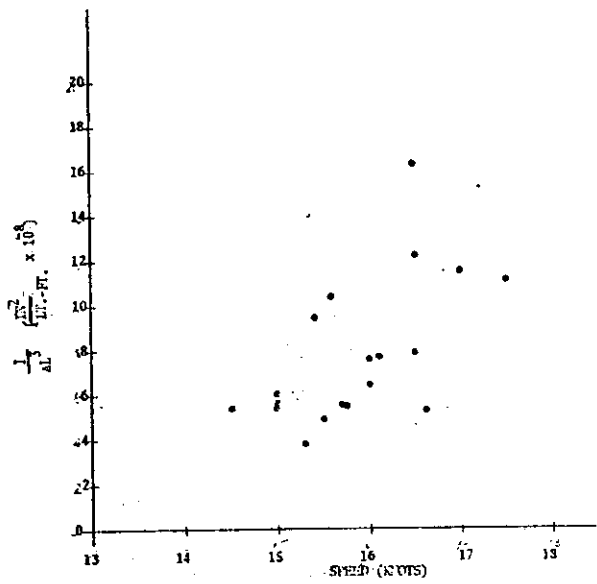


FIGURE C-13  
 $\frac{1}{\Delta L^3}$  vs. SPEED - TANKERS

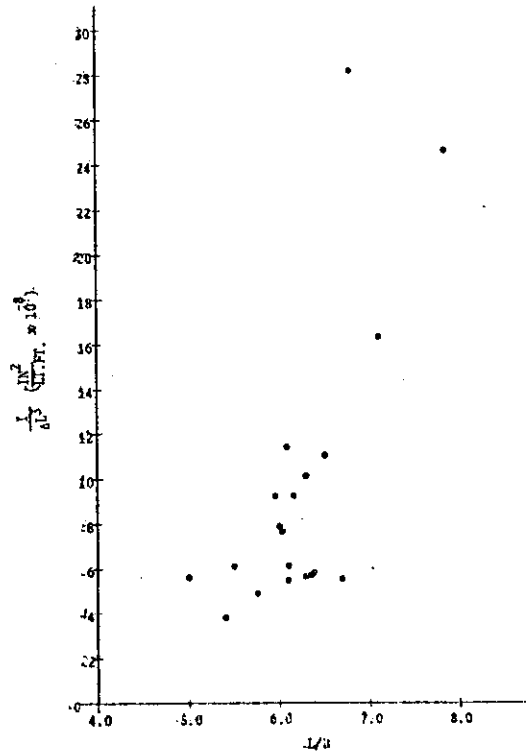


FIGURE C-14  
 $\frac{1}{\Delta L^3}$  vs. L/B - TANKERS

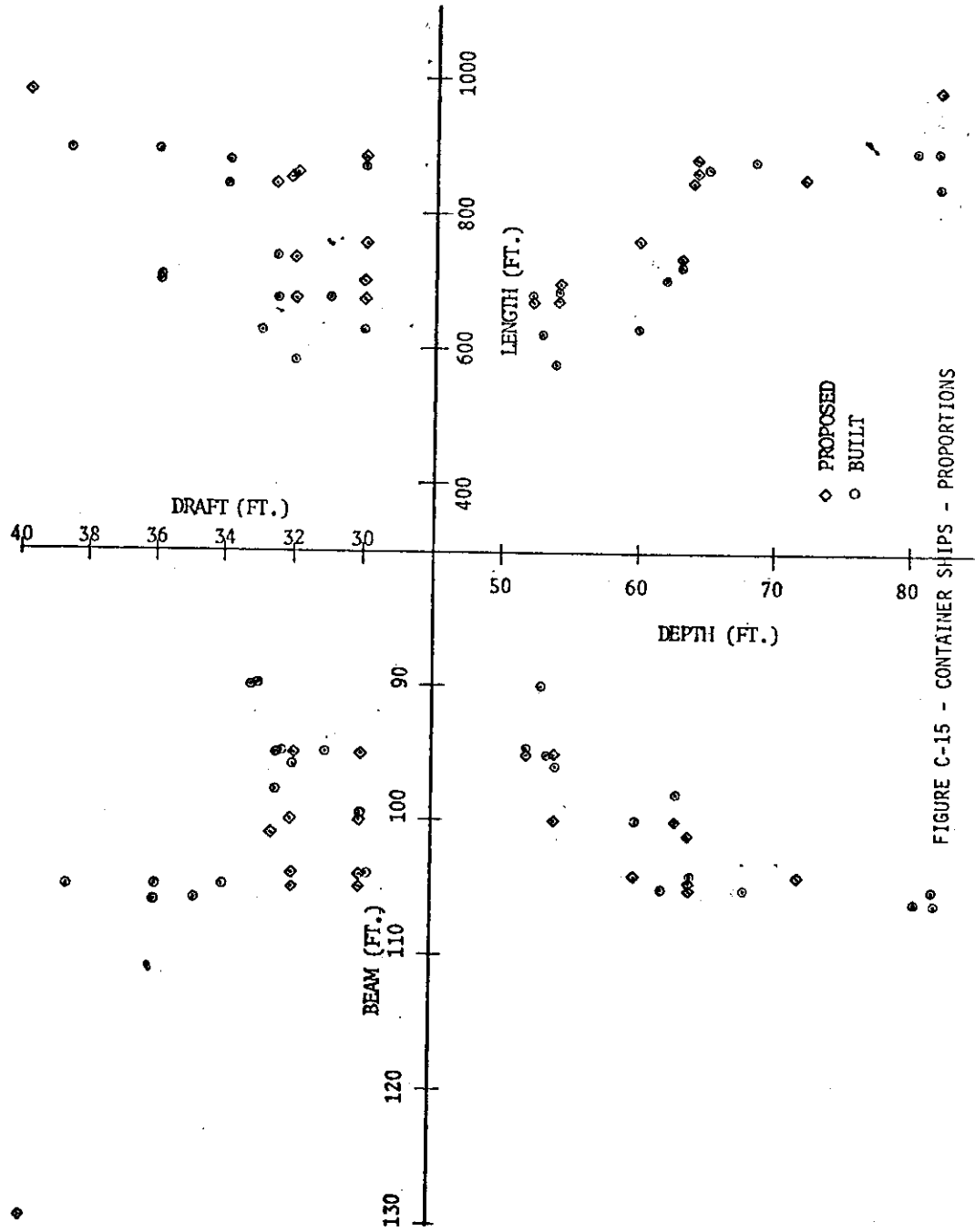
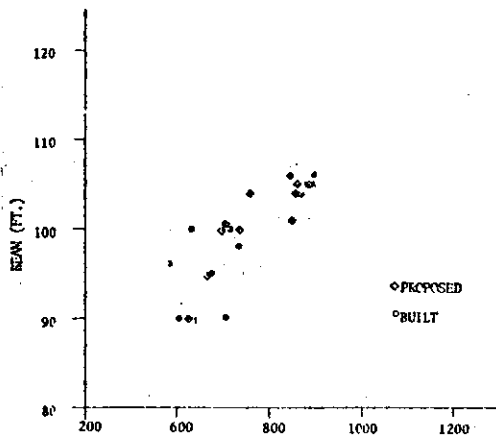
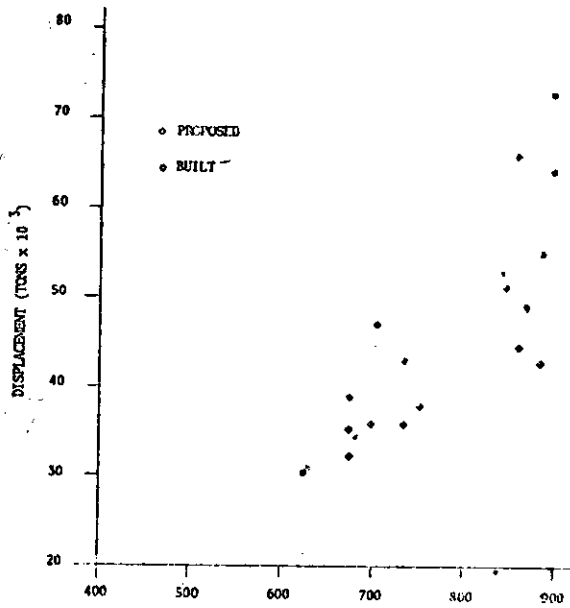


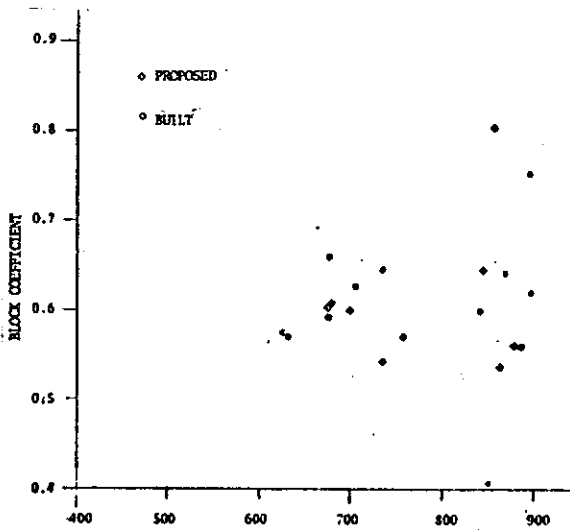
FIGURE C-15 - CONTAINER SHIPS - PROPORTIONS



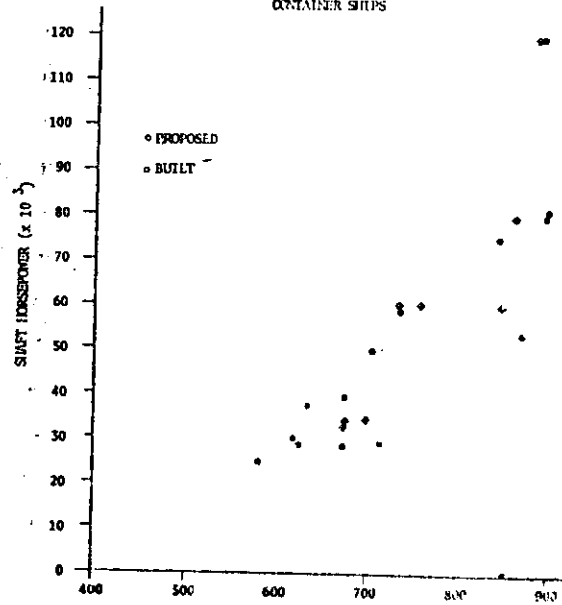
LENGTH (FT.)  
FIGURE C-16  
BEAM vs. LENGTH  
CONTAINER SHIPS



LENGTH (FT.)  
FIGURE C-17  
DISPLACEMENT vs. LENGTH  
CONTAINER SHIPS



LENGTH (FT.)  
FIGURE C-18  
BLOCK COEFFICIENT vs. LENGTH  
CONTAINER SHIPS



LENGTH (FT.)  
FIGURE C-19  
SHAFT HORSEPOWER vs. LENGTH  
CONTAINER SHIPS

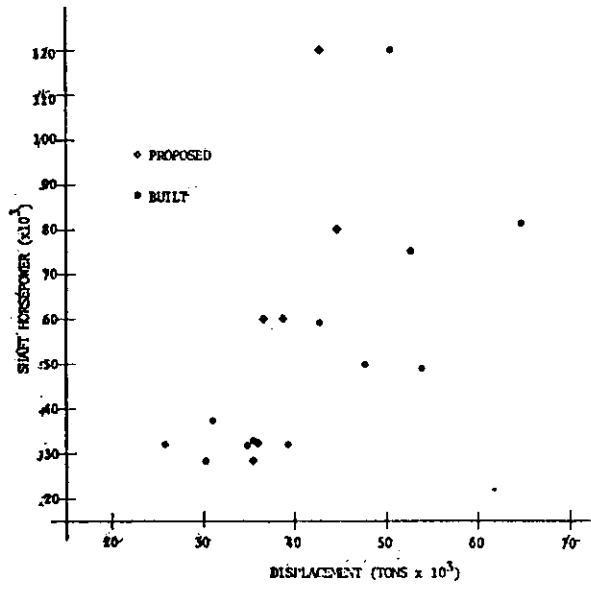


FIGURE C-20  
SHAFT HORSEPOWER vs. DISPLACEMENT  
CONTAINER SHIPS

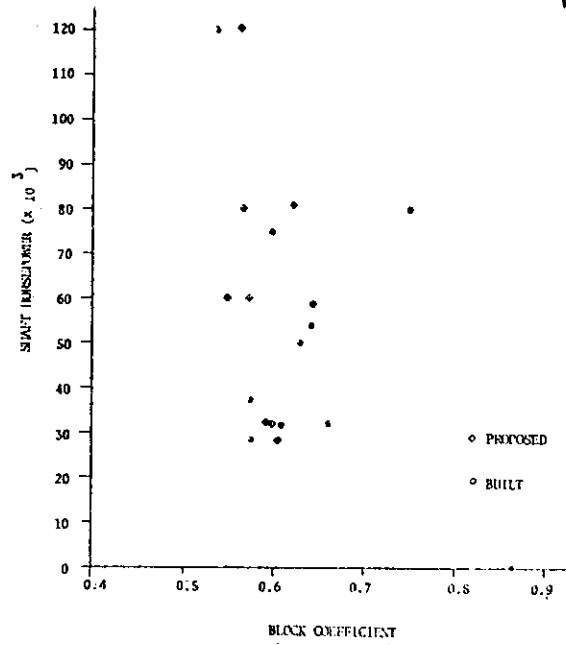
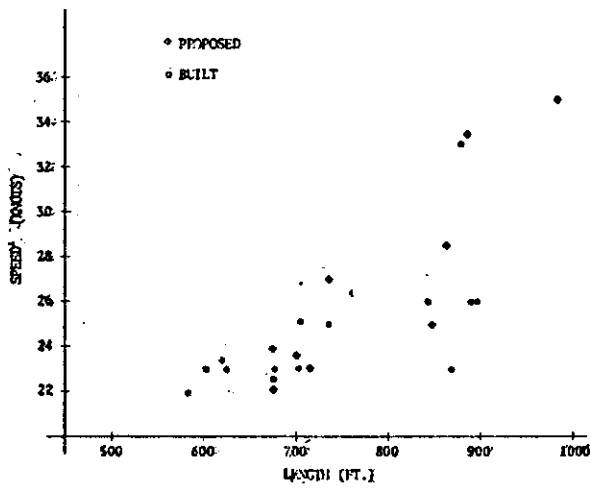


FIGURE C-21  
SHAFT HORSEPOWER vs. BLOCK COEFFICIENT  
CONTAINER SHIPS



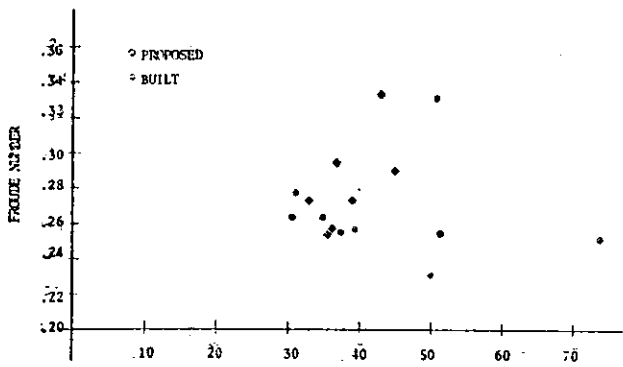


FIGURE C-24  
 FROUDE NUMBER vs. DISPLACEMENT  
 CONTAINER SHIPS

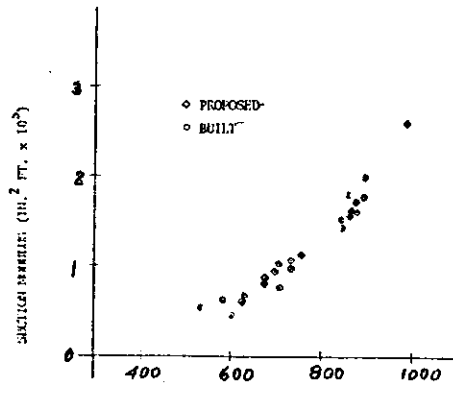


FIGURE C-25  
 SECTION MODULUS vs. LENGTH  
 CONTAINER SHIPS

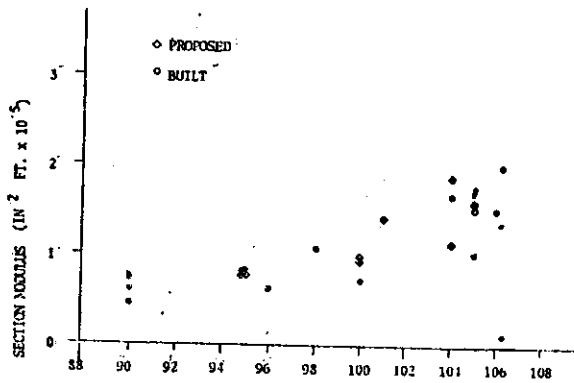


FIGURE C-26  
 SECTION MODULUS vs. BEAM  
 CONTAINER SHIPS

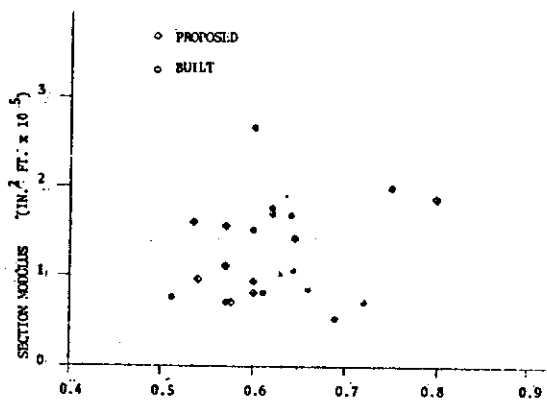
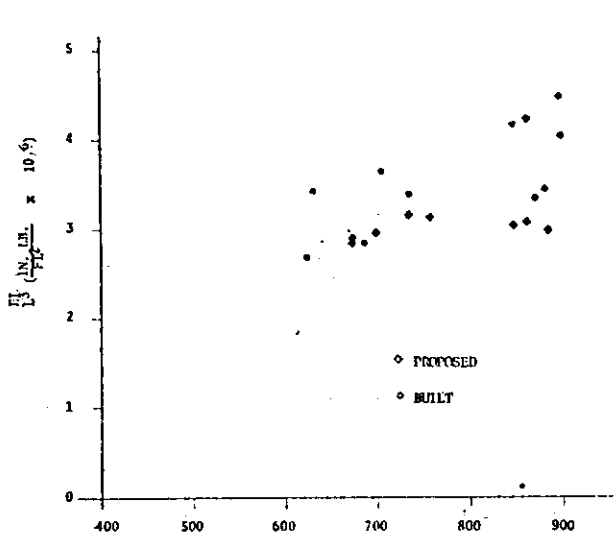
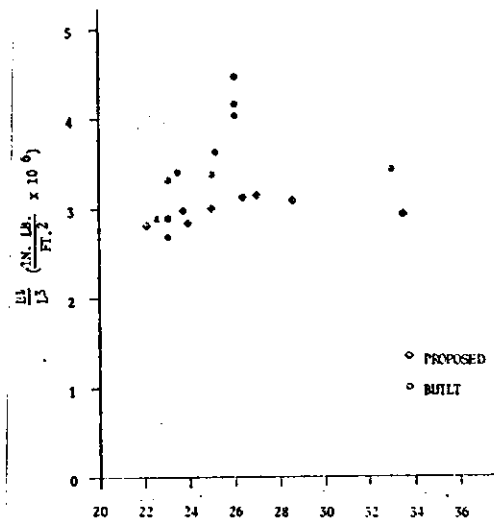


FIGURE C-27  
 SECTION MODULUS vs. BLOCK COEFFICIENT  
 CONTAINER SHIPS



LENGTH (FT.)  
FIGURE C-28



SPEED (KNOTS)  
FIGURE C-29

$\frac{EI}{L^3}$  vs. LENGTH - CONTAINER SHIPS

$\frac{EI}{L^3}$  vs. SPEED - CONTAINER SHIPS

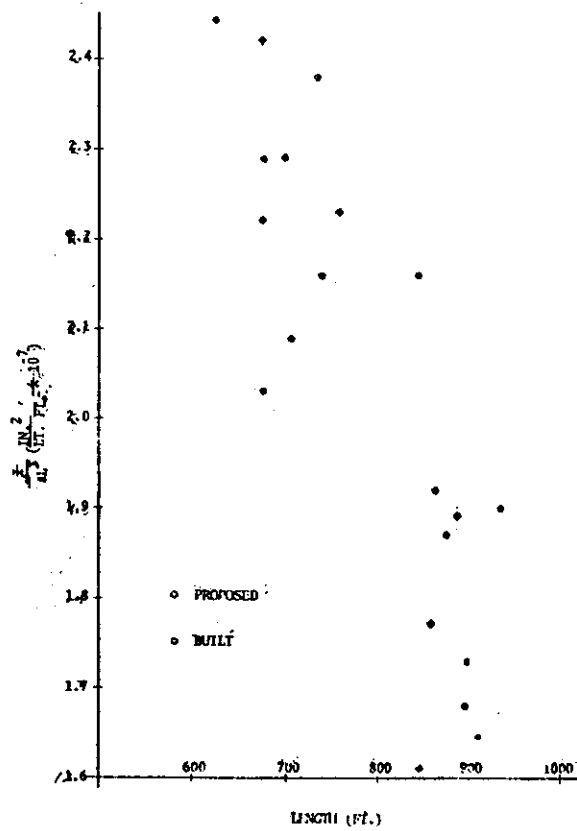
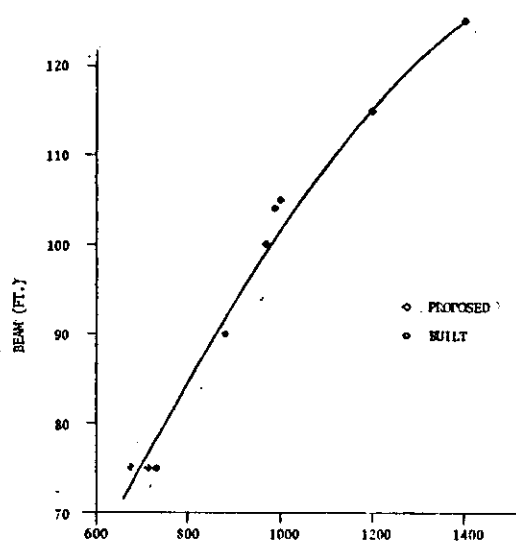


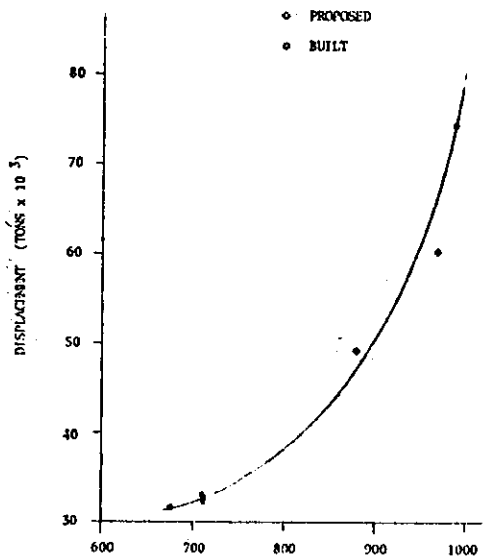
FIGURE C-30  
 $\frac{EI}{L^3}$  vs. LENGTH  
CONTAINER SHIPS







LENGTH (FT.)  
 FIGURE C-36  
 BEAM vs. LENGTH  
 GREAT LAKES BULK CARRIERS



LENGTH (FT.)  
 FIGURE C-37  
 DISPLACEMENT vs. LENGTH  
 GREAT LAKE BULK CARRIERS

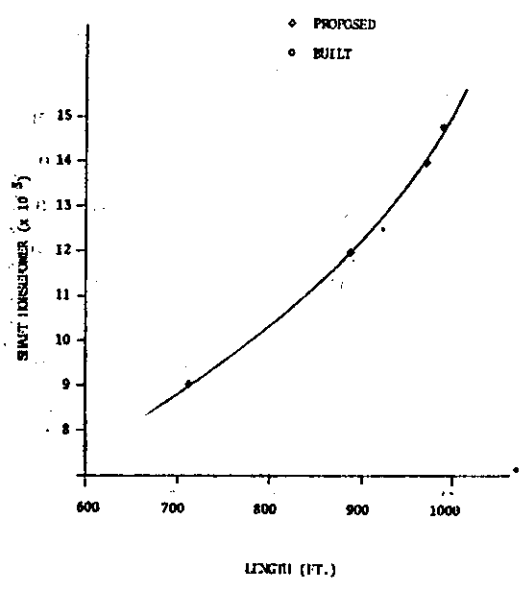


FIGURE C-38  
 SHAFT HORSEPOWER vs. LENGTH  
 GREAT LAKES BULK CARRIERS

FIGURE C-39  
SECTION MODULUS VS. LENGTH  
GREAT LAKES BULK CARRIERS

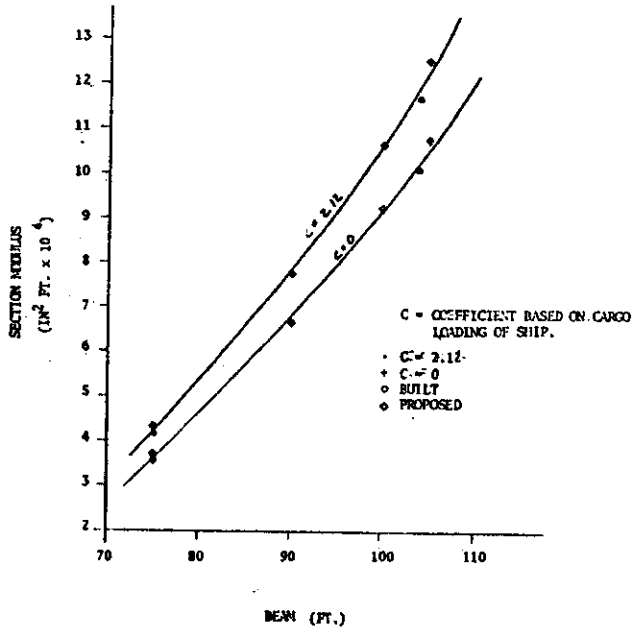
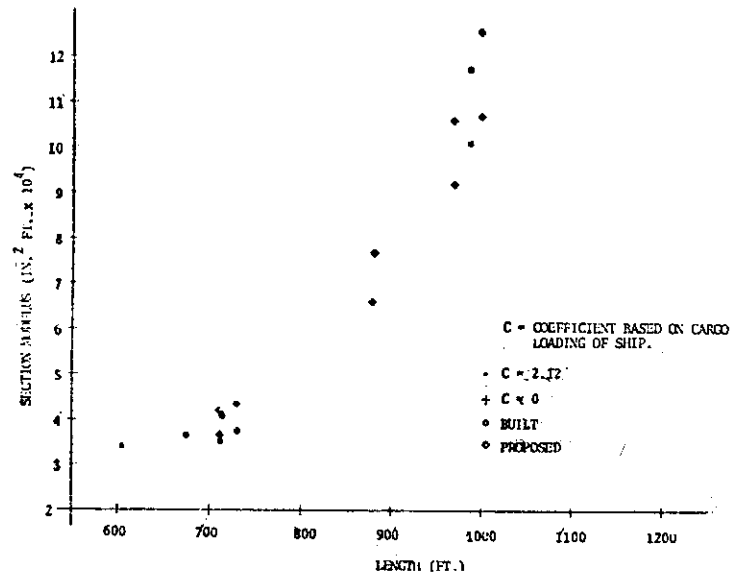


FIGURE C-40  
SECTION MODULUS VS. BEAM  
GREAT LAKES BULK CARRIERS

FIGURE C-41  
L/D vs. LENGTH  
GREAT LAKES BULK CARRIERS

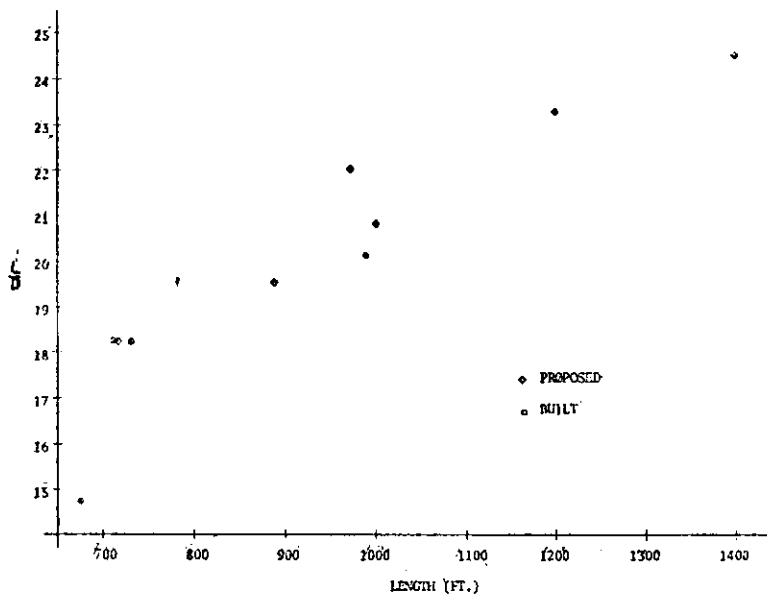


FIGURE C-43  
 $\frac{EI}{L^3}$  vs. LENGTH - GREAT LAKES BULK CARRIERS

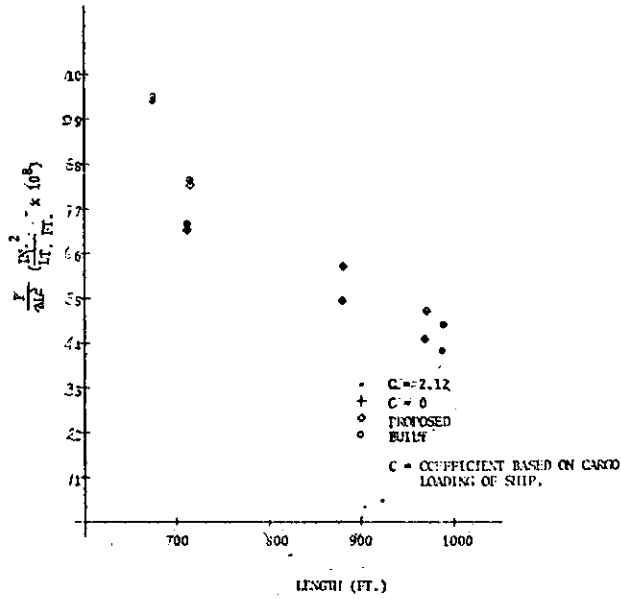
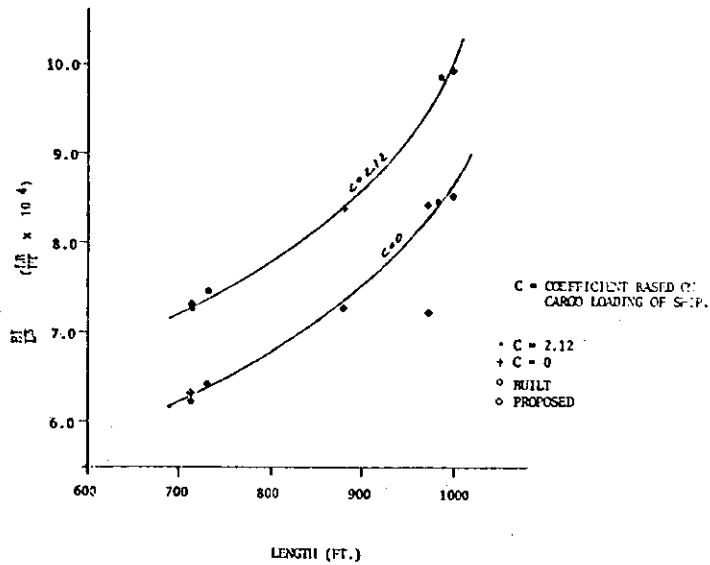
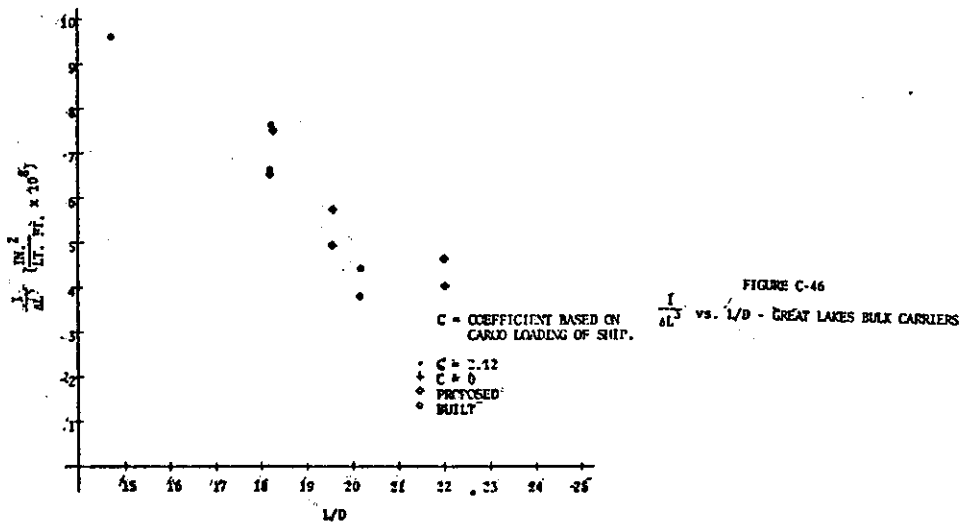
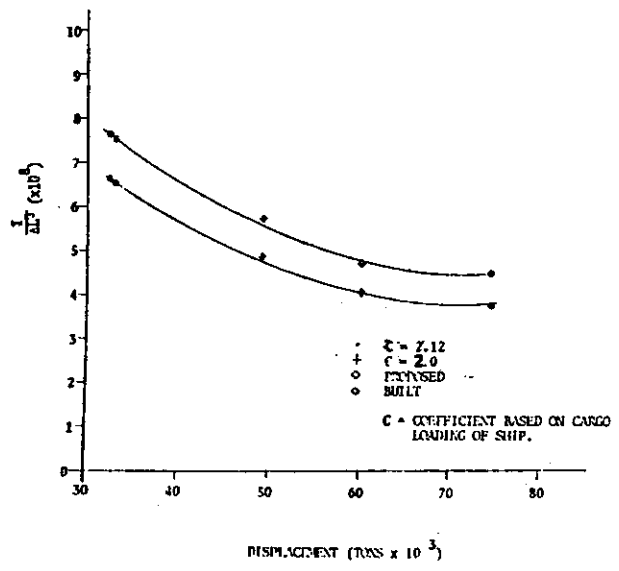


FIGURE C-44  
 $\frac{V}{AL^2}$  vs. LENGTH - GREAT LAKES BULK CARRIERS

FIGURE C-45  
 $\frac{I}{\Delta L^3}$  vs. DISPLACEMENT (LOADED)  
 GREAT LAKE BULK CARRIERS



## DOCUMENT CONTROL DATA - R &amp; D

(Security classification of title, body of abstract and indexing annotation must be entered when the overall report is classified)

1. ORIGINATING ACTIVITY (Corporate author) M. Rosenblatt & Son, Inc. 350 Broadway New York, New York 10013		2a. REPORT SECURITY CLASSIFICATION Unclassified	
		2b. GROUP	
3. REPORT TITLE SHIP VIBRATION PREDICTION METHODS AND EVALUATION OF INFLUENCE OF HULL STIFFNESS VARIATION ON VIBRATORY RESPONSE			
4. DESCRIPTIVE NOTES (Type of report and inclusive dates) Final			
5. AUTHOR(S) (First name, middle initial, last name) Roger G. Kline John C. Daidola			
6. REPORT DATE June 1974	7a. TOTAL NO. OF PAGES 191	7b. NO. OF REFS 79	
8a. CONTRACT OR GRANT NO. NAVSHIPS N00024-73-C-5206	9a. ORIGINATOR'S REPORT NUMBER(S)		
b. PROJECT NO. SF 35.422.306	9b. OTHER REPORT NO(S) (Any other numbers that may be assigned this report) SSC-249		
c. Task 2022, SR-214			
d.			
10. DISTRIBUTION STATEMENT Distribution of this document is unlimited.			
11. SUPPLEMENTARY NOTES		12. SPONSORING MILITARY ACTIVITY Naval Ship Systems Command Department of the Navy Washington, D. C. 20360	
13. ABSTRACT Research is conducted to obtain a greater understanding of induced hull vibrations and, more specifically, to define the role of hull stiffness in such phenomena. Available methods for the prediction of vibratory response to propeller, slam and wave excitations are evaluated. The work scope is limited essentially to the vertical vibration of the main hull. Parametric analyses are presented which include the calculations of the propeller, slam- and wave-induced vibrations of three ships with their hull stiffness varying from 40 percent below to 40 percent above the as-built stiffness. The three ships are a 249,300 DWT tank ship, the Great Lakes ore carrier "STR. EDWARD L. RYERSON" and the 544 ft. general cargo ship "S. S. MICHIGAN." Design trends are developed with respect to characteristics that influence ship stiffness and vibratory response. Propeller-induced main hull vibrations for all three ships do not appear to be effected by variations in hull stiffness. Slam-induced vibrations seem to increase and decrease as stiffness increases and decreases. The tank ship and the Great Lakes ore carrier appear to be prone to wave-induced vibration, and increased hull stiffness has a beneficial effect on limiting the response. Further research is required which would lead to engineering methods for the estimation of propeller excitation forces and slam loads which can be used to predict vibration during the design stages. Literature on wave-induced vibration is			

limited and the subject deserves significant research effort. Particular attention should be

DD FORM 1 NOV 66 1473 paid to the effects of forebody and afterbody shapes Security Classification and damping.

KEY WORDS	LINK A		LINK B		LINK C	
	ROLE	WT	ROLE	WT	ROLE	WT
Ship Vibration Propeller, Slam, Wave, Excitation Prediction Method Hull Stiffness Parametric Analyses						

SHIP RESEARCH COMMITTEE  
Maritime Transportation Research Board  
National Academy of Sciences-National Research Council

The Ship Research Committee has technical cognizance of the inter-agency Ship Structure Committee's research program:

PROF. J. E. GOLDBERG, Chairman, *School of Civil Engineering, Purdue University*  
PROF. R. W. CLOUGH, *Prof. of Civil Engineering, University of California*  
DR. S. R. HELLER, Jr., *C'man, Civil & Mech. Eng. Dept., The Catholic Univ. of America*  
MR. G. E. KAMPSCHAEFER, Jr., *Manager, Technical Services, ARMCO Steel Corporation*  
MR. W. W. OFFNER, *Consulting Engineer, San Francisco*  
MR. D. P. ROSEMAN, *Chief Naval Architect, Hydronautics, Inc.*  
MR. H. S. TOWNSEND, *Vice President, U. S. Salvage Association, Inc.*  
DR. S. YUKAWA, *Consulting Engineer, General Electric Company*  
MR. R. W. RUMKE, *Executive Secretary, Ship Research Committee*

Advisory Group II, "Ship Structural Design Procedures and Analysis", prepared the project prospectus and evaluated the proposals for this project:

DR. S. R. HELLER, Jr., Chairman, *C'man, Civ. & Mech. Eng. Dept., The Catholic University*  
MR. E. R. ASHEY, *Asst. for Advanced Technology, Naval Ship Engineering Center*  
CAPT. J. M. BALLINGER, *USN (Retd.), Manager, Res. & Dev., Sun Shipbuilding & Dry Dock Co.*  
PROF. R. H. GALLAGHER, *School of Civil & Environmental Engrg., Cornell University*  
DR. F. J. HEGER, Jr., *Vice President, Simpson, Gumpertz & Heger*  
DR. D. D. KANA, *Manager, Struct. Dynamics & Acoustics, Southwest Research Institute*  
PROF. J. KEMPNER, *Dept. of Aerospace Engrg. & App. Mechs., Poly. Inst. of New York*  
PROF. E. V. LEWIS, *Director of Research, Webb Institute of Naval Architecture*  
PROF. A. MANSOUR, *Dept. of Ocean Engineering, Massachusetts Institute of Technology*  
PROF. R. H. OWENS, *Dept. of App. Mathematics & Computer Science, Univ. of Virginia*  
DR. P. VAN DYKE, *Principal Research Scientist, Hydronautics, Inc.*  
PROF. G. A. WEMPNER, *School of Engrg. Science & Mechanics, Georgia Inst. of Technology*

The SR-214 Project Advisory Committee provided the liaison technical guidance, and reviewed the project reports with the investigator:

MR. D. P. ROSEMAN, Chairman, *Chief Naval Architect, Hydronautics, Inc.*  
DR. D. D. KANA, *Manager, Struct. Dynamics & Acoustics, Southwest Research Institute*  
PROF. M. SHINOZUKA, *Department of Civil Engineering, Columbia University*

## SHIP STRUCTURE COMMITTEE PUBLICATIONS

*These documents are distributed by the National Technical Information Service, Springfield, Va. 22151. These documents have been announced in the Clearinghouse journal U.S. Government Research & Development Reports (USGRDR) under the indicated AD numbers.*

- SSC-240, *Load Criteria for Ship Structural Design* by E. V. Lewis, R. van Hooff, D. Hoffman, R. B. Zubaly, and W. M. Maclean. 1973. AD 767389.
- SSC-241, *Thermoelastic Model Studies of Cryogenic Tanker Structures* by H. Becker and A. Colao. 1973. AD 771217.
- SSC-242, *Fast Fracture Resistance and Crack Arrest in Structural Steels* by G. T. Hahn, R. G. Hoagland, M. F. Kanninen, A. R. Rosenfield and R. Sejnoha. 1973. AD 775018.
- SSC-243, *Structural Analysis of SL-7 Containership Under Combined Loading of Vertical, Lateral and Torsional Moments Using Finite Element Techniques* by A. M. Elbatouti, D. Liu and H. Y. Jan. 1974. AD A002620.
- SSC-244, *Fracture-Control Guidelines for Welded Steel Ship Hulls* by S. T. Rolfe, D. M. Rhea, and B. O. Kuzmanovic. 1974. AD A004553.
- SSC-245, *A Guide for Inspection of High-Strength Steel Weldments* by The Weld Flaw Evaluation Committee. (To be published).
- SSC-246, *Theoretical Estimates of Wave Loads On the SL-7 Containership In Regular and Irregular Seas* by P. Kaplan, T. P. Sargent and J. Cilmi. 1974. AD A004554.
- SSC-247, *Flame Straightening Quenched-And-Tempered Steels in Ship Construction* by R. L. Rothman. 1974. AD A 002621.
- SSC-248, *Fracture Toughness Characterization of Shipbuilding Steels* by J. R. Hawthorne and F. J. Loss. 1975.

### SL-7 PUBLICATIONS TO DATE

- SL-7-1, (SSC-238) - *Design and Installation of a Ship Response Instrumentation System Aboard the SL-7 Class Containership S.S. SEA-LAND McLEAN* by R. A. Fain. 1973. AD 780090.
- SL-7-2, (SSC-239) - *Wave Loads in a Model of the SL-7 Containership Running at Oblique Headings in Regular Waves* by J. F. Dalzell and M. J. Chiocco. 1973. AD 780065.
- SL-7-3, (SSC-243) - *Structural Analysis of SL-7 Containership Under Combined Loadings of Vertical, Lateral and Torsional Moments Using Finite Element Techniques* by A. M. Elbatouti, D. Liu and H. Y. Jan. 1974.
- SL-7-4, (SSC-246) - *Theoretical Estimates of Wave Loads on the SL-7 Containership in Regular and Irregular Seas* by P. Kaplan, T. P. Sargent and J. Cilmi. 1974.